**Universidade do Minho**
Escola de Medicina

Ana Catarina Barbosa Matos

# Immunoregulatory role of c-MET in pulmonary disease

junho de 2024

Immunoregulatory role of c-MET in pulmonary disease
Ana Catarina Barbosa Matos
UMinho | 2024

**Universidade do Minho**
Escola de Medicina

Ana Catarina Barbosa Matos

# Immunoregulatory role of c-MET in pulmonary disease

Tese de Doutoramento
Doutoramento em Ciências da Saúde

Trabalho efetuado sob a orientação da
**Doutora Sandra Maria Araújo da Costa**
e da
**Doutora Cristina Amorim Cunha**

junho de 2024

DIREITOS DE AUTOR E CONDIÇÕES DE UTILIZAÇÃO DO TRABALHO POR TERCEIROS

Este é um trabalho académico que pode ser utilizado por terceiros desde que respeitadas as regras e boas práticas internacionalmente aceites, no que concerne aos direitos de autor e direitos conexos.
Assim, o presente trabalho pode ser utilizado nos termos previstos na licença abaixo indicada.
Caso o utilizador necessite de permissão para poder fazer um uso do trabalho em condições não previstas no licenciamento indicado, deverá contactar o autor, através do RepositóriUM da Universidade do Minho.



**Atribuição-NãoComercial-SemDerivações**
**CC BY-NC-ND**
https://creativecommons.org/licenses/by-nc-nd/4.0/

## ACKNOWLEGMENTS

Em primeiro lugar, quero agradecer às minhas orientadoras, Sandra Costa e Cristina Cunha, por me terem proporcionado a oportunidade de desenvolver esta tese, pelo apoio, conhecimento transmitido e conselhos científicos ao longo destes anos. Agradeço também aos restantes elementos do grupo, atuais e antigos. Especialmente às incansáveis companheiras de todas as horas, Sofia, Caroline, Raquel, Marcela e também ao Claúdio, não só por toda a ajuda e motivação, mas acima de tudo por se terem tornado pessoas tão especiais na minha vida. Alargo o meu agradecimento a todos os membros do antigo domínio SSRD e da recente equipa i3D por me terem acolhido com carinho ao longo dos últimos anos. Um agradecimento especial às minhas compinchas: Sónia, Joana, Vânia, Raquel, Rafinha, Sara, Viktoriya e Andreia por todos os momentos de descompressão conjunta e às meninas que recentemente tão bem me acolheram e integraram: Consuelo, Frias e Marta.

À minha família, em especial aos meus pais e ao João, agradeço todo a paciência, preocupação e apoio. Ao João agradeço também por ter sido o meu maior pilar, por não me ter deixado baixar os braços nos momentos de inevitável fraqueza e insegurança. E às amigas de longa data, Rita e Ana Isabel, por todo o carinho e preocupação, essenciais para que eu mantivesse a sanidade mental.

Por fim, ao maior amor da minha vida, o meu avô. Se aqui estou foi graças a todas as suas lições e incentivos para "me agarrar aos estudos", dar o melhor de mim e ir sempre mais longe. Finalmente, ao fim de 4 anos, posso dizer que todo o meu percurso académico e em especial esta tese é dedicada a ti, avô!

## FINANCIAL SUPPORT

The work presented in this thesis was performed in the Life and Health Sciences Research Institute (ICVS), University of Minho. Financial support was provided by National funds, through the Foundation for Science and Technology (FCT) (SFRH/BD/145955/2019, COVID/BD/153456/2023, 2022.06674.PTDC, POCI-01-0145-FEDER-028113, UIDB/50026/2020, UIDP/50026/2020); by Programa Operacional Potencial Humano (POPH) and Programa Investigador FCT (IF/00959/2014); by NORTE-01-0145-FEDER-000039, supported by Norte Portugal Regional Operational Programme (NORTE 2020), under the PORTUGAL 2020 Partnership Agreement, through the European Regional Development Fund (ERDF); by Programa Operacional Fatores de Competitividade (COMPETE); by "la Caixa" Foundation and FCT under the agreement LCF/PR/HR17/52190003; and by the ICVS Scientific Microscopy Platform, member of the national infrastructure PPBI - Portuguese Platform of Bioimaging (PPBI-POCI-01-0145-FEDER-022122).

## STATEMENT OF INTEGRITY

I hereby declare having conducted this academic work with integrity. I confirm that I have not used plagiarism or any form of undue use of information or falsification of results along the process leading to its elaboration.

I further declare that I have fully acknowledged the Code of Ethical Conduct of the University of Minho.

## RESUMO

### O papel imunorregulador do c-MET em doenças pulmonares

Uma resposta imunitária rigorosamente coordenada é essencial para preservar a homeostasia tecidual. A inflamação e infeção descontroladas podem levar a complicações graves, incapacidade prolongada e mesmo morte, como acontece na fibrose e aspergilose pulmonar. Uma melhor compreensão dos mecanismos imunorreguladores que controlam as funções efetoras das células imunes em condições inflamatórias associadas à fibrose e em resposta a patógenos é essencial para desenvolver terapias mais eficazes e estratégias preventivas. A via de sinalização c-MET é conhecida por exercer um papel crucial na sobrevivência, motilidade e proliferação celular durante o desenvolvimento e reparação tecidular e em diversas patologias. Embora o c-MET tenha sido reconhecido como elemento-chave na modulação da resposta imune em doenças inflamatórias, o seu papel nas células imunes em doenças inflamatórias e infeciosas pulmonares permanece desconhecido. Assim, o principal objetivo desta Tese de Doutoramento foi investigar como é que a via de sinalização c-MET nas células imunes modula a inflamação em doenças pulmonares, fornecendo conhecimentos sobre a interação entre o c-MET e a imunidade pulmonar. Utilizando um modelo de fibrose pulmonar (FP) em murganho, demonstramos que a população de macrófagos mais abundante é a dos macrófagos intersticiais (IMs), estes exibem um fenótipo anti-inflamatório durante a fase inflamatória (ifFP), e induzem a ativação de fibroblastos e a diferenciação em miofibroblastos *in vitro*. Além disso, na ifFP a expressão de c-MET é induzida em células imunes pulmonares, especificamente IMs, células T e neutrófilos. Mais importante, o nosso estudo demonstra que a deleção de *c-Met* em células imunes melhora a FP, associada ao recrutamento precoce de células imunes que expressam c-MET e subsequente atenuação do ambiente pró-inflamatório. Utilizando um modelo de aspergilose pulmonar em murganho, descobrimos que a expressão de c-MET é também induzida em células imunes pulmonares, principalmente neutrófilos, IMs, macrófagos alveolares e células T. Além disso, a deleção de *c-Met* em células imunes exacerba a carga fúngica e inflamação pulmonar, associada ao aumento de IMs e neutrófilos no pulmão infetado. Mais importante, a deleção de *c-Met* compromete a função imune antifúngica, aumentando a suscetibilidade à infeção. Esta tese de Doutoramento destaca a contribuição fundamental da via de sinalização c-MET para potenciar a ativação pró-inflamatória das células imunes, prejudicial à lesão e fibrose pulmonar, mas que proporciona uma resposta protetora à infeção por *Aspergillus fumigatus*. Estes resultados destacam o potencial de terapias moduladoras da expressão de c-MET para direcionar a ativação e função de células imunes, oferecendo uma abordagem inovadora para gerir a resposta imune pulmonar a lesões e agentes infeciosos.

**Palavras-chave:** *Aspergillus fumigatus*, Aspergilose, c-MET, Fibrose Pulmonar, Inflamação

## ABSTRACT

### Immunoregulatory role of c-MET in pulmonary disease

A well-coordinated immune response is essential for the maintenance of tissue homeostasis. Uncontrolled inflammation and infection can lead to severe complications, prolonged disability and even death, as seen in pulmonary fibrosis and aspergillosis, respectively. A deeper understanding of the immunoregulatory mechanisms that control effector functions of immune cells in fibrotic-associated inflammatory conditions and in response to pathogens is critical to develop more effective therapies and preemptive strategies. The c-MET signaling is known to exert a crucial role in modulating cell survival, motility, and proliferation during tissue development and repair and in several pathologic contexts. Although c-MET has been recognized as a key player in modulating the immune response in inflammatory and autoimmune diseases, its role on immune cells in inflammatory and infectious lung diseases remains unknown. Therefore, the central purpose of this Doctoral Thesis was to investigate how c-MET signaling in immune cells modulates the progression of inflammation in lung disease, providing critical insights into the crosstalk between c-MET and lung immunity. Using a mouse model of pulmonary fibrosis (PF), we demonstrated that the most abundant macrophage population is interstitial macrophages (IMs), which present an anti-inflammatory phenotype during the inflammatory phase (ipPF) and induce fibroblast activation and differentiation into myofibroblasts *in vitro*. Furthermore, during ipPF, c-MET expression is induced in lung immune cells, specifically IMs, T cells, and neutrophils. More importantly, our study demonstrates that *c-Met* deletion in immune cells ameliorates the severity of PF, associated with early recruitment of c-MET-expressing immune cell populations and subsequent attenuation of proinflammatory environment, resulting in less severe fibrotic lesions. In addition, using a mouse model of pulmonary aspergillosis, we found that c-MET expression is also induced in lung immune cells, particularly neutrophils, IMs, alveolar macrophages and T cells. Furthermore, *c-Met* deletion in immune cells exacerbates fungal burden and lung inflammation, associated with increased numbers of IMs and neutrophils in infected lung. More importantly, our study shows that *c-Met* deletion compromised their antifungal effector functions, increasing susceptibility to infection. Overall, this Doctoral thesis highlights the pivotal contribution of c-MET signaling in immune cells to enhance their proinflammatory activation, with detrimental consequences for lung injury and fibrosis, while providing a protective response to *Aspergillus fumigatus* infection. These findings highlight the potential of targeted therapies that modulate c-MET expression to redirect the activation and effector functions of immune cells, offering an innovative approach to manage lung immune responses to injuries and infectious agents.

**Keywords:** Aspergillosis, *Aspergillus fumigatus*, c-MET, Inflammation, Pulmonary Fibrosis

## TABLE OF CONTENTS

Direitos de autor e condições de utilização do trabalho por terceiros ..... ii
Acknowlegments ..... iii
Financial support ..... iii
Statement of integrity ..... iv
Resumo ..... v
Abstract ..... vi
List of abbreviations ..... ix
List of figures ..... xiii
List of tables ..... xv
Chapter I – General Introduction ..... 1
1. c-MET signaling pathway: Modulation of immune response and pathogen recognition ..... 2
1.1. c-MET signaling pathway ..... 2
1.2. c-MET signaling pathway in inflammatory-related diseases ..... 5
1.2.1. Cancer ..... 5
1.2.2. Intestinal inflammation ..... 8
1.2.3. Autoimmune neuroinflammation ..... 9
1.2.4. Skeletal muscle inflammation ..... 12
1.3. c-MET signaling pathway in infectious diseases ..... 12
1.3.1. *Helicobacter pylori* infection ..... 12
1.3.2. *Listeria monocytogenes* infection ..... 13
1.3.3. *Salmonella typhi* infection ..... 15
1.3.4. *Pseudomonas aeruginosa* infection ..... 15
1.3.5. *Plasmodium* spp. infection ..... 16
1.3.6. *Leishmania mexicana* infection ..... 17
1.3.7. *Candida albicans* infection ..... 18
1.4. General overview ..... 20
2. Lung diseases: fibrosis and aspergillosis ..... 20
2.1. Idiopathic pulmonary fibrosis and progressive pulmonary fibrosis ..... 22
2.1.1. Immune cells in pulmonary fibrosis ..... 25
2.2. *Aspergillus fumigatus* and pulmonary aspergillosis ..... 28
2.2.1. Invasive pulmonary aspergillosis ..... 30

2.2.2 Recognition of *Aspergillus fumigatus* by pattern recognition receptors and antifungal immune response ..... 31
3. Aims ..... 37
4. References ..... 38
Chapter II – Interstitial Macrophages Lead Early Stages of Bleomycin-Induced Lung Fibrosis and Induce Fibroblasts Activation ..... 54
1. Introduction ..... 56
2. Materials and Methods ..... 58
3. Results ..... 64
4. Discussion ..... 71
5. References ..... 75
Chapter III – c-MET Exacerbates Pulmonary Fibrosis via Deregulation of Immune Cell Recruitment and Activation ..... 77
1. Introduction ..... 79
2. Materials and Methods ..... 81
3. Results ..... 89
4. Discussion ..... 99
5. References ..... 104
Chapter IV – Recognition of *Aspergillus fumigatus* by c-MET is required for protective immunity against infection ..... 108
1. Introduction ..... 110
2. Materials and Methods ..... 112
3. Results ..... 117
4. Discussion ..... 122
5. References ..... 124
Chapter V – General Discussion and Future Perspectives ..... 126
1. General Discussion and Future Perspectives ..... 127
2. References ..... 131

## LIST OF ABBREVIATIONS

| | |
|---|---|
| **ABPA** | Allergic bronchopulmonary aspergillosis |
| **AMs** | Alveolar macrophages |
| **APCs** | Antigen-presenting cells |
| **Arg1** | Arginase 1 |
| **ATC** | Adoptive T cell transfer |
| **BAL** | Bronchoalveolar lavage |
| **BALF** | BAL fluid |
| **BLM** | Bleomycin |
| **BM** | Bone marrow |
| **BMDMs** | Bone marrow-derived macrophages |
| **CagA** | Cytotoxin associated gene A |
| **Cag-PAI** | CagA pathogenicity island |
| **CAPA** | COVID-19-associated pulmonary aspergillosis |
| **cDCs** | Classical DCs |
| **CFUs** | Colony-forming units |
| **cKO** | Conditional knockout mice |
| **CLRs** | C-type lectin receptors |
| **CM** | Conditioned medium |
| **COPD** | Chronic obstructive pulmonary disease |
| **COVID-19** | Coronavirus disease of 2019 |
| **CPA** | Chronic pulmonary aspergillosis |
| **CTD-ILD** | Connective tissue disease ILD |
| **CTDs** | Connective tissue diseases |
| **Ctgf** | Connective tissue growth factor |
| **DCs** | Dendritic cells |
| **DC-SIGN** | DC–specific ICAM3–grabbing non–integrin |
| **Dpi** | Days post-infection |
| **EAE** | Experimental autoimmune encephalomyelitis |
| **ECM** | Extracellular matrix |
| **EGFR** | Epidermal growth factor receptor |
| **ERK** | Extracellular-signal-regulated kinase |

| | |
|---|---|
| **FACS** | Fluorescence-associated cell-sorting |
| **FAK** | Focal adhesion kinase |
| **Gab1** | Grb2-associated binding protein 1 |
| **Gapdh** | Glyceraldehyde-3-phosphate dehydrogenase |
| **G-CSF** | Granulocyte colony-stimulating factor |
| **GrB** | Granzyme B |
| **Grb2** | Growth factor receptor-bound protein 2 |
| **GSK3β** | Glycogen synthase kinase 3 beta |
| **HGF** | Hepatocyte growth factor |
| **HP** | Hypersensitivity pneumonitis |
| **HRCT** | High-resolution computed tomography |
| **IBD** | Inflammatory bowel diseases |
| **ICU** | Intensive care units |
| **IFN** | Interferon |
| **IGF** | Insulin-like growth factor |
| **IIP** | Idiopathic interstitial pneumonias |
| **IL** | Interleukin |
| **ILDs** | Interstitial lung diseases |
| **IMs** | Interstitial macrophages |
| **Inl** | Internalin |
| **IPA** | Invasive pulmonary aspergillosis |
| **IPF** | Idiopathic pulmonary fibrosis |
| **IPT** | Immunoglobulin-plexin-transcription |
| **JAK** | Janus kinase |
| **LAP** | LC3-associated phagocytosis |
| **LC3** | Microtubule-associated protein 1 light chain 3 |
| **LDH** | Lactate Dehydrogenase |
| **LLC** | Lewis lung carcinoma cells |
| **LRR** | Leucine-rich repeat |
| **LR-MSCs** | Lung-resident mesenchymal stem cells |
| **MACS** | Magnetic-activated cell sorting |
| **MAPK** | Mitogen-activated protein kinase |

| | |
|---|---|
| **MBL** | Mannose-binding lectin |
| **MEK** | MAPK effector kinase |
| **MelLec** | Melanin-sensing CLR |
| **MFI** | Mean fluorescence intensity |
| **MHC** | Major histocompatibility complex |
| **MMPs** | Matrix metalloproteinases |
| **MS** | Multiple sclerosis |
| **NADPH** | Nicotinamide adenine dinucleotide phosphate hydrogen |
| **NE** | Neutrophil elastase |
| **NETs** | Neutrophil extracellular traps |
| **NF** | Nuclear factor |
| **NLRs** | NOD-like receptors |
| **NLRP3** | NLR family pyrin domain-containing 3 |
| **NOD** | Nucleotide-binding oligomerization domain |
| **NOX** | NADPH oxidase |
| **PAMPs** | Pathogen-associated molecular patterns |
| **pDCs** | Plasmacytoid DCs |
| **PDGF** | Platelet-derived growth factor |
| **PF** | Pulmonary fibrosis |
| **PI3K** | Phosphatidylinositol 3-kinase |
| **PRRs** | Pattern recognition receptors |
| **PSI** | Plexin-semaphorin-integrin |
| **ROS** | Reactive oxygen species |
| **RT-qPCR** | Reverse transcription quantitative PCR |
| **SEMA** | Semaphorin |
| **Shc** | Src homology 2 domain-containing |
| **SMA** | Smooth muscle actin |
| **SOS** | Son of sevenless |
| **SP** | Surfactant protein |
| **SPH** | Serine protease homology |
| **STAT** | Signal transducer and activator of transcription |
| **STIV** | *Salmonella typhi* invasin |

| | |
|---|---|
| **T4SS** | Type IV secretion system |
| **TCR** | T cell receptor |
| **TGF** | Transforming growth factor |
| **Th** | T helper |
| **TLRs** | Toll-like receptors |
| **TNF** | Tumor necrosis factor |
| **Treg** | Regulatory T |
| **TRIF** | Toll/interleukin-1 receptor domain-containing adaptor inducing IFN-β |
| **Tyr** | Tyrosine |
| **UC** | Ulcerative colitis |
| **UIP** | Usual interstitial pneumonia |
| **VacA** | Vacuolar cytotoxin A |
| **WT** | Wild-type |

## LIST OF FIGURES

### Chapter I – General Introduction

Figure 1. Structure of the c-MET receptor and HGF. ..... 3
Figure 2. Schematic representation of HGF/c-MET signaling pathway. ..... 4
Figure 3. Pathogenic activation of HGF/c-MET signaling pathway. ..... 19
Figure 4. Types of ILDs. ..... 21
Figure 5. Pathogenesis of pulmonary fibrosis. ..... 23
Figure 6. Effect of innate and adaptive immune response in fibrogenesis. ..... 28
Figure 7. *Aspergillus fumigatus* dynamic conidia and hyphae cell wall. ..... 29
Figure 8. Pattern recognition receptors involved or potentially involved in the innate immune detection of *Aspergillus fumigatus*. ..... 34
Figure 9. Innate and adaptive immune responses to *Aspergillus fumigatus* infection. ..... 36

### Chapter II – Interstitial Macrophages Lead Early Stages of Bleomycin-Induced Lung Fibrosis and Induce Fibroblasts Activation

Figure 1. Macrophage populations in the lung during the inflammatory phase of BLM-induced pulmonary fibrosis mouse model. ..... 65
Figure 2. Macrophage populations phenotype in the lung during the inflammatory phase of BLM-induced pulmonary fibrosis mouse model. ..... 67
Figure 3. IMs are activated towards an anti-inflammatory phenotype, and AMs are in a transient activation state at day 7 after BLM-induced pulmonary fibrosis. ..... 68
Figure 4. Conditioned medium from BLM-sorted IMs induced fibroblasts proliferation and differentiation into myofibroblasts. ..... 70

### Chapter III – c-MET Exacerbates Pulmonary Fibrosis via Deregulation of Immune Cell Recruitment and Activation

Figure 1. Gating strategy for the identification of myeloid and lymphoid cell populations in dissociated mice lung by flow cytometry. ..... 84
Figure 2. Gating strategy for the identification of T lymphocytes in dissociated human lung by flow cytometry. ..... 85
Figure 3. c-MET expression is enhanced in immune cells during BLM-induced lung inflammation. ..... 90
Figure 4. Deletion of *c-Met* from immune cells attenuates lung injury following BLM administration. ..... 92

Figure 5. *c-Met* deletion in immune cells promotes early inflammatory cells recruitment after BLM administration. ..... 93
Figure 6. Boosted leukocyte chemoattraction and retrained proinflammatory milieu in cKO mice lung mainly on day 5 following BLM administration. ..... 94
Figure 7. Attenuated lung fibrosis in cKO mice on day 14 following BLM administration. ..... 95
Figure 8. c-MET expression is augmented in T cells in fibrosis-related ILD. ..... 96
Figure 9. Profile of c-MET expression in neutrophils and macrophages among distinct interstitial lung diseases. ..... 97
Figure 10. Profile of c-MET expression in T cells, neutrophils and macrophages among distinct interstitial lung diseases. ..... 98
Figure 11. Schematic illustration of the importance of c-MET in immune cells during BLM-induced PF progression. ..... 102

**Chapter IV – Recognition of *Aspergillus fumigatus* by c-MET is required for protective immunity against infection**

Figure 1. Gating strategy for the identification of immune cell populations in dissociated mice lung by flow cytometry. ..... 114
Figure 2. c-MET expression is induced in immune cells in the lungs of mice infected with *Aspergillus fumigatus*. ..... 117
Figure 3. c-MET expression in immune cells is required to control *A. fumigatus* infection in the lung. 118
Figure 4. c-MET expression in immune cells is required for *A. fumigatus*-induced antifungal effector functions. ..... 119
Figure 5. c-MET is required for effector functions of macrophages after *A. fumigatus* infection..... 120
Figure 6. c-MET is required for the activation of the glycolytic pathway in macrophages after *A. fumigatus* infection. ..... 121

## LIST OF TABLES

### Chapter I – General Introduction

Table 1. Findings of HGF levels in tumors and impact of c-MET signaling pathway in tumor-associated immune cells. 7

Table 2. Findings of HGF and c-MET levels in intestinal inflammation and impact of c-MET signaling pathway in intestinal inflammation-associated neutrophils. 9

Table 3. Findings of HGF and c-MET levels in autoimmune neuroinflammation and impact of c-MET signaling pathway in autoimmune neuroinflammation-associated T lymphocytes. 11

Table 4. Activation of c-MET signaling pathway in pathogen recognition and internalization. 19

### Chapter III – c-MET Exacerbates Pulmonary Fibrosis via Deregulation of Immune Cell Recruitment and Activation

Table 1. Demographics of patients who performed lung biopsy. 81

Table 2. Demographics of patients who performed bronchoalveolar lavage collection. 82

Table 3. Antibodies used for flow cytometry staining of mouse samples. 83

Table 4. Antibodies used for flow cytometry staining of human samples. 84

# CHAPTER I

## General Introduction

Literature review in preparation:

Catarina Barbosa-Matos, Agostinho Carvalho, Cristina Cunha, Sandra Costa. c-MET signaling pathway: Modulation of immune response and pathogen recognition.

## 1. c-MET signaling pathway: Modulation of immune response and pathogen recognition

The role of c-MET, a tyrosine kinase receptor, and its ligand, hepatocyte growth factor (HGF), has been extensively studied during organ development. This signaling pathway culminates in essential cues for the correct organ growth and development, such as the epithelial-to-mesenchymal transition of myogenic progenitor cells, growth and survival of hepatocytes and placental trophoblast cells, and proliferation and motility of muscle progenitors (1–8). Furthermore, the HGF/c-MET signaling pathway has been demonstrated to be critical to the malignant features of tumor cells, inducing similar cellular properties, such as transformation, survival, proliferation, migration, among others (9). Moreover, the HGF/c-MET signaling pathway is crucial for the control of tissue homeostasis, supported by its involvement in the regeneration of several organs, mainly through induction of re-epithelization processes, as in renal fibrosis (10–12), liver cirrhosis and injury (13,14), lung fibrosis (15) and ischemia-reperfusion injury (16).

Recently, evidence has emerged supporting the role of c-MET signaling pathway in regulating the immune response, including phenotype and effector function of immune cells, with the subsequent impact on the outcome of multiple immune-mediated diseases in various organs. These include prototypical inflammatory conditions, such as inflammatory bowel disease and skeletal muscle inflammation, and classical autoimmune diseases, such as autoimmune neuroinflammation, in which HGF/c-MET signaling pathway differently impacts inflammatory processes depending on the pathological condition, as described in the following subsections.

Moreover, many pathogens seize the host's HGF/c-MET signaling pathway to provide a more favorable environment for the spread of infection, actively activating and deregulating the signaling pathway through their pathogenic factors. The activation of this signaling pathway exacerbates infection extent, mainly via phosphatidylinositol 3-kinase (PI3K) and actin reorganization, favoring pathogens internalization.

This section will be focused on the mechanisms by which HGF/c-MET signaling pathway modulates the recruitment, phenotype, and function of immune cells in inflammatory conditions, as well as the role of this signaling pathway in pathogen recognition and associated immune response.

### 1.1. c-MET signaling pathway

c-MET is a tyrosine kinase receptor, abundantly expressed in epithelial cells during organ development and tissue repair, as well as in cancer cells and immune cells. This receptor comprises a small and completely extracellular α-chain (50 kDa) and a more extensive single-pass transmembrane β-chain (145kDa). Structurally, the extracellular domain of the c-MET receptor consists of a semaphorin (SEMA) domain, a plexin-semaphorin-integrin (PSI) domain, and four immunoglobulin-plexin-transcription (IPT) factors 1-4. Intracellularly, the cytoplasmic tail contains the juxtamembrane domain which has two

phosphorylation sites (Serine 985 and tyrosine (Tyr)1003), the catalytic tyrosine kinase comprising two phosphorylation sites (Tyr1234 and Tyr1235) and the C-terminal tail, a multi-protein docking site containing two phosphorylation sites (Tyr1349 and Tyr1356) (Figure 1A) (17). The primary c-MET ligand, HGF, can bind to c-MET via two binding sites. One possibility is to bind to the IPT3 and IPT4 domains of the receptor, and the other is to bind to the SEMA domain, which is only exposed after proteolytic processing, and, to date, is the only one able to activate c-MET signaling pathway. Structurally, HGF consists of an N-terminal domain, four consecutive kringle domains, and a serine protease homology domain (Figure 1B) (17).

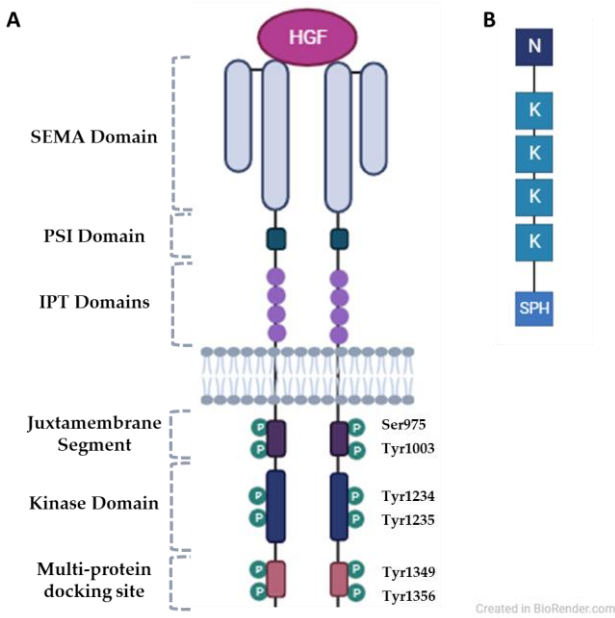



**Figure 1. Structure of the c-MET receptor and HGF.** (A) c-MET extracellular domain contains a SEMA domain, a PSI domain, and four IPT domains. The intracellular domain contains the tyrosine kinase domain flanked by a juxtamembrane regulatory segment and a multi-protein docking site at the C-terminal. Upon HGF binding, c-MET undergoes dimerization and phosphorylation. The cytoplasmic segments of the receptor have critical amino acid residues that, once phosphorylated, serve as activators and regulators of varying biological activities by recruiting signaling effector proteins. (B) HGF consists of an N-terminal domain (N), four consecutive kringle domains (K), and a serine protease homology (SPH) domain.

The binding of HGF to c-MET promotes c-MET dimerization and phosphorylation of two critical tyrosine residues (Tyr1234 and Tyr1235), recruitment of cytosolic effector proteins, subsequent activation of downstream signaling pathways and respective biological activities. Due to the diversity of downstream signaling mediators, c-MET can trigger various biological activities, for example, in tumor cells PI3K/AKT/mTOR, PI3K/AKT/nuclear factor (NF)-κB, PI3K/AKT/Wnt/β-catenin, PI3K/focal adhesion kinase (FAK), Janus kinase (JAK)/signal transducer and activator of transcription (STAT), RAS/RAF/mitogen-activated protein kinase (MAPK) effector kinase (MEK)/extracellular-signal-regulated kinase (ERK) pathways, can impact cell proliferation, invasion, migration, survival and epithelial-mesenchymal transition (Figure 2) (18–27).

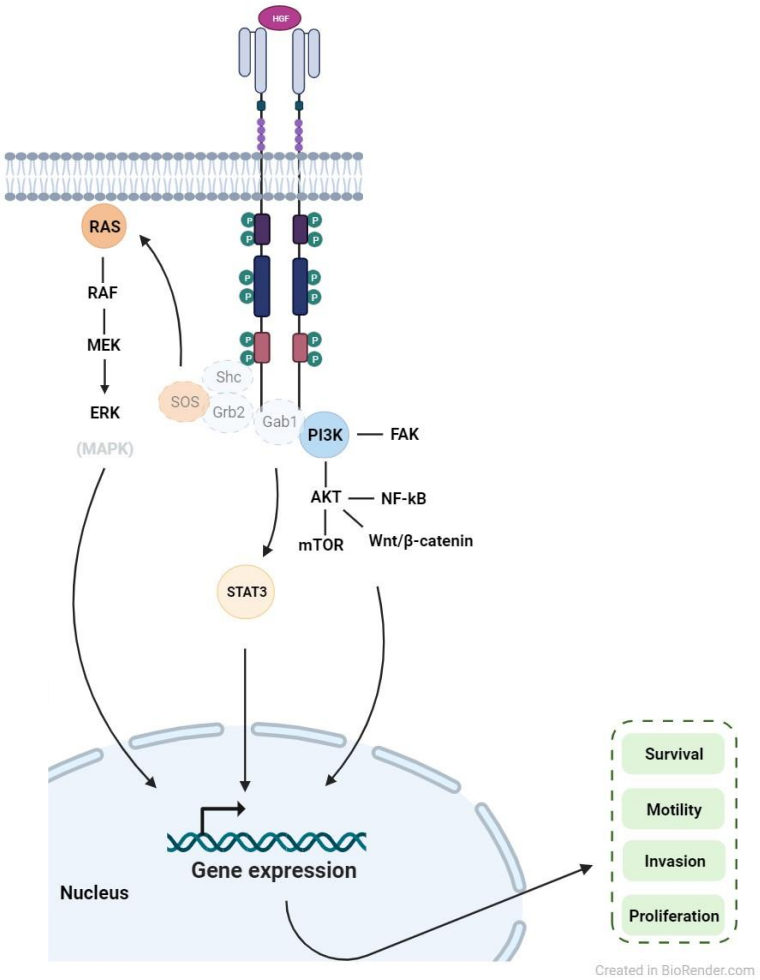



**Figure 2. Schematic representation of HGF/c-MET signaling pathway.** Upon HGF binding, c-MET undergoes phosphorylation in the tyrosine kinase domain, recruiting signaling effector proteins, including adaptor proteins and effector molecules. Among adaptor proteins are growth factor receptor-bound protein 2 (Grb2), src homology 2 domain-containing (Shc) and a multi-adaptor protein Grb2-associated binding protein 1 (Gab1) that creates binding sites for more downstream adaptors. Among effector molecules are PI3K and the signal transducer and activator of transcription STAT3. The activation of the MAPK cascades is initiated by the binding of the adaptor proteins Shc and Grb2 to RAS guanine nucleotide exchanger son of sevenless (SOS) that activates RAS, which subsequently activates MEK, and finally ERK. Subsequent translocation of ERK to the nucleus activates transcription factors involved in the expression of various genes, such as genes associated with cell motility and proliferation. PI3K can signal through FAK or AKT, PI3K/AKT may activate different downstream intermediates, such as mTOR, NF-κB, Wnt/β-catenin, ultimately activating transcription of various genes, such as genes associated with cell survival, motility, invasion and proliferation. c-MET activation can also activate STAT3 which translocates to the nucleus controlling the transcription of genes mainly involved with cell invasion.

Furthermore, the c-MET-induced PI3K signaling cascade has also been described to shape the activation profile and function of macrophages. In fact, HGF treatment of bone marrow-derived macrophages (BMDMs) differentiated with M-CSF (M0), interferon (IFN)-γ and lipopolysaccharide (M1) or IL-4 (M2), induced c-MET activation, especially in M1 macrophages. The signaling pathway activation was concomitant with the downregulation of M1 markers expression, including *iNos*, *tumor necrosis factor* (*Tnf*), and *Il-6*, and the upregulation of *Arg-1*, IL-10 and transforming growth factor (TGF)-β1. The phenotypic alteration of HGF-treated M1 macrophages occurred via activation of PI3K pathway by phosphorylation of AKT, cyclic AMP-response element-binding protein 1, and C/EBPβ and inactivation of

NF-κB (28, 29). In conclusion, HGF/c-MET signaling pathway seems to shift M1 macrophages toward a M2-like phenotype and sustain an M2-like phenotype through the PI3K signaling pathway. Moreover, in animals receiving stress signals, such as granulocyte colony-stimulating factor (G-CSF) injection, higher c-MET levels were found on the surface of bone marrow cells, polymorphonuclear cells, immature c-Kit$^+$/Lin$^-$ cells, and primitive CD34$^-$Sca-1$^+$/c-Kit$^+$/Lin (SKL) cells (30). c-MET activation enhanced mTOR signaling pathway, down-regulated FOXO3a expression, and ultimately increased ROS production, which enhances cell motility upon stress stimuli (30). Furthermore, c-MET blockage in mice injected with G-CSF resulted in fewer progenitors circulating. Overall, these results demonstrated that activation of c-MET induces the mTOR/FOXO3a/ROS signaling cascade, enhancing the acquisition of migratory capacity in BM hematopoietic progenitor cells that allows their recruitment in the context of host defense and repair mechanisms (30).

The activation of the HGF/c-MET signaling pathway via PI3K clearly modulates the activation phenotype of macrophages and the migratory of BM hematopoietic progenitor cells in inflammatory conditions, highlighting the involvement of the c-MET signaling pathway in immunity.

## 1.2. c-MET signaling pathway in inflammatory-related diseases

### 1.2.1. Cancer

Aberrant c-MET signaling pathway activation in cancer cells contributes to tumor progression in multiple cancer types and enhances aggressive cellular invasiveness. However, the activation of c-MET signaling pathway in immune cells was recently described to have the opposite role in tumor progression by enhancing immune cells' recruitment and antitumoral effector functions.

Interestingly, in patients with metastatic melanoma undergoing anti-PD-1 immunotherapy, serum HGF levels were increased in a subset of non-responder patients (31). HGF levels in mice were increased in lymph nodes and tumor tissues upon adoptive T cell transfer (ATC) (31). The efficacy of ATC was enhanced by co-treatment with a c-MET inhibitor, capmatinib, which concordantly decreased the levels of HGF (31). These results suggest that decreased HGF levels may indicate a better response to immunotherapy (Table 1).

Finisguerra *et al.* showed that c-MET expression was increased in circulating neutrophils from Lewis lung carcinoma cells (LLC)-tumor-bearing mice and respective tumor-associated neutrophils, as well as in tumor-associated neutrophils from non-small-cell lung tumors (32). Moreover, the deletion of *c-Met* in immune cells increased the growth and metastatic burden of subcutaneous LLC-induced tumors and inhibited neutrophil recruitment to the tumor site (32). Moreover, similar results were obtained in other tumor types, namely orthotopic fibrosarcomas and melanomas, spontaneous mammary tumors,

hepatocellular carcinomas, and chemically induced colorectal cancers (32). Interestingly, through *in vitro* approaches, the authors proved that neutrophil capacity to adhere and transmigrate through an activated endothelium was dependent on c-MET expression since c-*Met* deficient neutrophils lost this capacity. Furthermore, *nitric oxide synthase* expression, nitric oxide production, and 3-nitrotyrosine formation were decreased in *c-Met* deficient tumor-associated neutrophils (32). Interestingly, tumor conditioned media induced c-MET expression in bone marrow neutrophils which was abolished by the blockage of TNF-α, suggesting TNF-α as a main potentiator of c-MET signaling activation (32). Together, these data demonstrate that c-MET is induced by inflammatory stimuli, which is required for neutrophil extravasation to inflamed tissues and for their production of cytotoxic nitric oxide (Table 1).

In contrast, Glodde *et al.* showed that c-MET inhibition with capmatinib in mice bearing melanomas improved the effectiveness of ATC immunotherapy by promoting prolonged survival and higher tumor eradication (31). Moreover, this *in vivo* c-MET inhibition increased the proportion of T cells in the blood and tumor-infiltrating T cells. ATC-treated mice without capmatinib co-treatment showed an increased frequency of neutrophils in the peripheral blood, mature neutrophils in bone marrow mononuclear cells, a reactive influx of c-MET$^+$ neutrophils into tumor tissues, along with suppression of T cell proliferation and IFN-γ secretion. Co-treatment with capmatinib resulted in an additional increase of mature neutrophils in the bone marrow. However, it inhibited their accumulation in the peripheral blood, their influx to tumor tissue and tumor-draining lymph nodes, along with a reciprocal increase of T cell numbers in the tumor-draining lymph nodes with higher proliferative capacity (31). In mice with mammary cancer, anti-PD-1+anti-CD137 immunotherapy alone highly increased the recruitment of c-MET$^+$ neutrophils into tumors and draining lymph nodes, which was abolished by co-treatment with capmatinib (31). Overall, this study shows that c-MET induces neutrophils recruitment from the bone-marrow and favors their migration into inflamed tissues in response to ATC immunotherapy. Moreover, c-MET-dependent reactive neutrophil infiltration into lymph nodes restrained anti-tumor T cell expansion. Therefore, c-MET inhibition improved the effect of immunotherapies through reduced recruitment of neutrophils and potentiated T-cell anti-tumor immunity (Table 1).

Besides neutrophils, the expression of c-MET has also been described in CD8$^+$ tumor-infiltrating lymphocytes. A significant proportion of CD8$^+$ tumor-infiltrating lymphocytes expresses c-MET in mouse models of colon carcinoma and thymoma, and human malignant melanoma samples (33). Furthermore, upon *in vitro* differentiation of highly purified splenic cells into CD8$^+$ cytotoxic T lymphocytes using melanoma-associated antigen, a significant proportion presented enhancement of c-MET expression. These c-MET$^+$CD8$^+$ cytotoxic T lymphocytes showed higher intracellular levels of the cytolytic effector

molecules granzyme B (GrB), and perforin, and higher expression levels of executioner molecules, TNF, IFN-γ, Fas ligand, lymphocyte function-associated antigen 1, and CD107a compared to the c-MET negative counterparts (33). Curiously, overstimulation of these cells with HGF attenuated these characteristics, increased CD8 expression intensity, and reduced their cytotoxic function. Furthermore, c-MET$^{+}$CD8$^{+}$ cytotoxic T lymphocytes were adoptively transferred into mice injected with mouse melanoma cells, which showed a reduction in metastatic lung foci formation due to an increase in their tumor-specific cytotoxic activity, and increased production of IFN-γ and GrB (33). Of note, HGF-pretreatment before the adoptive transference reverted this phenotype (33). Together, these data suggest that CD8$^{+}$ cytotoxic T lymphocytes that express c-MET have enhanced cytolytic capacities, which are directly restrained by HGF overstimulation, ultimately favoring tumor outgrowth, suggesting a specific threshold of c-MET activation in CD8 T lymphocytes for protection against tumors (Table 1).

These studies indicate that c-MET is required for neutrophil transmigration and nitric oxide production, and enhanced CD8 T cell cytotoxicity, pointing to c-MET expression in immune cells as a tumor growth restrictor. In contrast, c-MET-dependent reactive neutrophil infiltration into lymph nodes is also detrimental to the effectiveness of ATC immunotherapy through restraining of anti-tumor T cell expansion.

**Table 1. Findings of HGF levels in tumors and impact of c-MET signaling pathway in tumor-associated immune cells.**

| | Feature | Tumor type | Finding |
|---|---|---|---|
| Human | Serum HGF | Metastatic melanoma | Increased in non-responder patients undergoing immunotherapy |
| Mouse | Lymph node and tumor tissues HGF | Melanoma | Decreased in more efficient immunotherapy (upon c-MET inhibition by capmatinib) |
| | *c-Met* deletion in immune cells | Carcinoma | ↓Tumor-infiltrating neutrophils<br>Increased tumor growth and metastatic burden |
| | c-MET inhibition with capmatinib | Melanoma | Improved the effectiveness of ATC immunotherapy<br>↑ T cells in the blood and tumor<br>↑ Mature neutrophils in bone marrow<br>↓ Neutrophils in the blood and tumor |
| | | Mammary tumor | Co-treatment with anti-PD-1+anti-CD137 immunotherapy:<br>↓ c-MET$^{+}$ neutrophils in tumor and draining lymph nodes |
| | c-MET$^{+}$CD8$^{+}$ cytotoxic tumor-infiltrating T lymphocytes | Carcinoma<br>Lymphoma | Higher intracellular levels of the cytolytic effector molecules (compared to c-METCD8$^{-}$ cytotoxic tumor-infiltrating T lymphocytes) |
| | Adoptive transfer of c-MET$^{-}$CD8$^{+}$ lymphocytes | Melanoma | ↑Tumor-specific cytotoxicity<br>Decreased tumor metastatic burden |

Symbols indicate the frequency of the immune population: ↑ higher frequency and ↓ lower frequency.

### 1.2.2. Intestinal inflammation

Inflammatory bowel diseases (IBD), Crohn's disease and ulcerative colitis (UC), are chronic inflammatory gastrointestinal diseases distinguished by the location and extent of the bowel wall involvement (34–37). UC is associated with excessive neutrophil infiltration, which correlates with the disease severity (38,39). Although crucial for host protection, neutrophil effector mechanisms can lead to extensive tissue damage, as in many chronic inflammatory conditions (40,41).

Interestingly, in IBD patients, the serum levels of HGF were increased comparatively to patients with gastrointestinal diseases other than IBD and healthy controls (42,43). Moreover, serum levels of HGF positively correlated with disease activity, which means that the severe active form has the highest levels of HGF compared to the inactive and mild form of the disease (42,43), suggesting high HGF levels in the serum as a predictor of worse prognosis (Table 2). Recently, Stakenborg *et al.* reported that patients with active UC present increased expression levels of *HGF* and *c-Met* in colonic biopsies compared to patients with inactive disease and healthy individuals (42). Moreover, by performing a cellular deconvolution analysis, the authors reported that neutrophilic gene enrichment signature positively correlated with *HGF* and *c-Met* expression (42). A dextran sulfate sodium-induced colitis mouse model recapitulates the HGF expression pattern observed in UC patients, with HGF expression increasing in the blood and colon throughout the progression of the disease with a peak at the acute inflammatory phase (42). Moreover, the percentage of c-MET$^{+}$ blood and colonic neutrophils was significantly increased during the acute inflammatory phase of the disease. Furthermore, the role of c-MET$^{+}$ neutrophils in this model was further corroborated by taking advantage of a conditional knockout (cKO) mouse for *c-Met* in neutrophils, which showed reduced body weight loss and improved disease activity index during dextran sulfate sodium-induced colitis (42). These results were associated with reduced proportion of immune cells in the colonic lamina propria during the acute phase, specifically neutrophils, Ly6C$^{hi}$ monocytes, and CD4 T cells, specifically Th17. This decrease in Th17 resulted from less production of IL-1β, which regulates the differentiation of naïve T cells into Th17 during inflammation (42).

In sum, increased levels of serum HGF and colonic *HGF* and *c-MET* are associated with active and more severe UC and c-MET expression in neutrophils exacerbates colonic inflammation in a mouse model through uncontrolled and unresolved inflammatory processes (Table 2).

**Table 2. Findings of HGF and c-MET levels in intestinal inflammation and impact of c-MET signaling pathway in intestinal inflammation-associated neutrophils.**

| | Feature | Finding |
|---|---|---|
| Human | Serum HGF | Increased compared to other gastrointestinal disease patients and healthy volunteers |
| | | Increases with disease severity |
| | Colonic *HGF* and *c-MET* | Increased compared to healthy volunteers |
| | | Increased upon disease active status |
| Mouse | Colonic and serum HGF | Increased compared to healthy mice |
| | | Increases with disease progression |
| | Colonic and blood c-MET$^+$ neutrophils | Increased compared to healthy mice |
| | | Increases with disease progression |
| | *c-Met* deletion in neutrophils | Decreases disease severity<br>↓ neutrophils, monocytes and CD4 T cells, Th17 |

Symbols indicate the frequency of the immune population: ↓ lower frequency

### 1.2.3. Autoimmune neuroinflammation

Multiple sclerosis (MS) is an autoimmune inflammatory and demyelinating disease of the central nervous system, characterized by inflammatory infiltrates, progressive demyelination, and damage of the surrounding axons (44–46). In rodents, the most appropriate model for immune studies in MS is the experimental autoimmune encephalomyelitis (EAE), which mimics the pathologic and clinical characteristics of human MS (46). EAE can be induced by immunization of mice with central nervous system antigens triggering autoimmune activation or by adoptive transfer of myelin antigen-specific CD4$^+$ T cells that infiltrate the central nervous system (46).

Müller *et al.* described a decrease in the HGF concentration in the cerebrospinal fluid in MS patients compared to patients with other neurological diseases (47). Furthermore, in patients with active MS, the levels of HGF in the cerebrospinal fluid were decreased comparatively to patients with inactive disease. MS patients treated with Natalizumab, a widely used and highly effective treatment, showed an increased concentration of HGF in the cerebrospinal fluid compared to untreated patients (47). Thus, suggesting that high HGF levels in the cerebrospinal fluid may indicate a better prognosis and response to therapy. In contrast, HGF levels in mice are elevated in both spinal cord and serum at the peak of EAE (48). Afterwards, in the remission phase, serum HGF levels returned to baseline, while HGF levels persisted

slightly high in the spinal cord. Importantly, c-MET expression in the spinal cord was found to be significantly increased at peak and remission of EAE. At the peak of the disease, c-MET expression in the spinal cord was restricted to large clusters of infiltrating leukocytes, particularly $CD11b^+$ macrophages (48).

Bai *et al.* reported that systemic administration of HGF improved functional recovery and enhanced spinal cord remyelination in mice with EAE (49). Concordantly, Benkhoucha *et al.* further explored how the systemic administration of HGF and the selective overexpression of HGF in mice neurons ameliorated EAE (50,51). HGF systemically treated or HGF transgenic animals showed increased $CD4^+CD25^+Foxp3^+$ regulatory T (Treg) cells and IL-10-producing Treg cells and reduced IFN-$\gamma^+$ and IL-$17^+$ splenic $CD4^+$ T cells (50,51). These results suggest that the elevation of Treg cells and the suppression of Th1 and Th17 are associated with the clinical benefit of HGF on EAE pathogenesis. Furthermore, dendritic cells stimulated with recombinant HGF exhibited a tolerogenic phenotype, characterized by reduced production of the proinflammatory-polarizing Th1 cytokines IL-12p70, IFN-γ and IL-12/IL-23p40 and increased production of the Th17 cell-inhibiting cytokine, IL-27 (50). Upon co-cultured with $TCR^{MOG}$ T cells, HGF-treated dendritic cells were able to inhibit T cells proliferation, activation, production of TNF-α, IFN-γ, and IL-12p70, and induced the production of IL-4, IL-10, and TGF-β (50,51). Overall, these studies suggest HGF as a potent immunomodulator capable of inhibiting EAE, by promoting the tolerization of dendritic cells, which restrains T cells activation and induces an anti-inflammatory (Th2 and Tregs) pattern.

More recently, Benkhoucha *et al.* verified the expression of c-MET in $CD8^+$ and $CD4^+$ T cells in an EAE model, conferring specific proinflammatory properties (52). The authors verified that c-MET expression was induced at the peak of EAE in $CD8^+$ T cells from the spleen and central nervous system, and these c-$MET^+CD8^+$ T cells display high expression of T cell activation markers. Moreover, increased cell proliferation and higher release of GrB and IFN-γ by c-$MET^+CD8^+$ T cells were found *ex vivo* in MOG-induced EAE. After HGF treatment, the cytotoxic function of EAE-isolated c-$MET^+CD8^+$ T cells was reduced, as was their ability to lyse their target cells by inhibiting the production of GrB and IFN-γ (52). Together, these data suggest that $CD8^+$ cytotoxic T lymphocytes that express c-MET have enhanced cytolytic capacities, which are directly restrained by HGF overstimulation, ultimately preventing EAE. Interestingly, c-MET expression has also been detected in $CD4^+$ T cells in the brain and peripheral blood mononuclear cells of MS patients (53,54). Furthermore, MS patients had increased proportion of $CD4^+$c-$MET^+$ T lymphocytes in the peripheral blood compared with patients with other neurological diseases, and these $CD4^+$c-$MET^+$ T lymphocytes expressed higher levels of an adhesion molecule integrin α4, which is essential for adhesion capacity (53). Similarly, c-MET expression was induced at the peak of

EAE in $CD4^+$ T cells from the spleen, lymph nodes, and central nervous system, and these c-$MET^+CD4^+$ T cells display high expression of T cell activation markers and increased pro-migratory profile, associated with overexpression of the same adhesion molecule, integrin α4 (53). Besides the enhancement of adhesion capacity, c-MET also up-regulated pathways of Th1 and Th17 signature genes in EAE-isolated $CD4^+$ T cells. Among Th subsets differentiated from peripheral blood mononuclear cells from healthy donors, the highest levels of *c-Met* mRNA and c-MET protein were found in Th17 and Th17.1 (54). Activated c-$MET^+$ Th17 and Th17.1 cells showed increased production of IL-17 alone or in combination with IFN-γ, suggesting that c-MET induces higher production of proinflammatory cytokines by these activated cells (54). These studies demonstrate that c-MET expression in CD4 T cells confers a proinflammatory phenotype, Th1 and Th17, and migratory properties through integrin α4 expression (53).

In sum, decreased levels of HGF in cerebrospinal fluid are associated with the active status of MS. Overall, in EAE c-MET expression in CD8 and CD4 T cells confers them higher cytolytic, and pro-migratory and proinflammatory capacities, respectively. However, HGF/c-MET signaling pathway overactivation restrained T cell activation, enhanced Treg cells differentiation and IL-10 production, and reduced IL-17 production suggesting HGF overexpression as an inducer of anti-inflammatory pattern preventing EAE progression (Table 3).

**Table 3. Findings of HGF and c-MET levels in autoimmune neuroinflammation and impact of c-MET signaling pathway in autoimmune neuroinflammation-associated T lymphocytes.**

| | Feature | Finding |
|---|---|---|
| Human | HGF in cerebrospinal fluid | Decreased compared to other neurological disease patients |
| | | Decreased upon disease active status |
| | | Increased upon treatment |
| | c-$MET^+$ $CD4^+$ T cells in blood | Increased compared to other neurological disease patients |
| Mouse | HGF in serum and spinal cord | Increased at the peak of EAE compared to healthy mice |
| | c-$MET^+$ macrophages in the spinal cord | Increased compared to healthy mice |
| | HGF administration | Decreases disease severity<br>↓ Th17 and Th1 cells<br>↑ Th2 and Tregs cells |
| | c-$MET^+CD8^+$ T cells | Increased proliferation<br>Increased cytolytic function<br>(compared to c-$METCD8^-$ T cells) |
| | c-$MET^+CD4^+$ T cells | Increased pro-migratory capacity<br>Increased proinflammatory profile<br>(compared to c-$METCD4^-$ T cells) |

Symbols indicate the frequency of the immune population: ↓ lower frequency.

### 1.2.4. Skeletal muscle inflammation

Skeletal muscle is relatively superficial, so injuries often occur in daily life in response to physiological and pathological environments. Skeletal muscle injuries imply highly regulated regeneration processes to guarantee functional maintenance. Regeneration processes comprise immune cell infiltration, clearance of the damaged myofibers, activation of satellite cells, myofiber formation and maturation, and subsequent muscle reconstruction.

Choi *et al.* implemented a cardiotoxin-induced muscle injury mouse model and verified high HGF production and c-MET activation, mainly in macrophages at the injury site (55). Delivery of HGF *in vivo* facilitated the restoration of muscle weight and regeneration by reducing proinflammatory mediators and promoting the transition of macrophage to the M2 phenotype (55). After muscle injury, the c-MET pharmacological inhibition with PHA-665752 deregulated the population of macrophages and delayed muscle mass re-establishment and muscle fiber regeneration (55). These results were accompanied by increased levels of proinflammatory mediators, IL-1β, iNOS, and CCL2, and reduced levels of anti-inflammatory and pro-regenerative mediators, IL-10, TGF-β, arginase 1 (Arg1), CD163, and resistin-like alpha, in an AMPK-dependent manner (55). These data suggest that c-MET signaling pathway regulates muscle repair by inducing macrophage transition towards an anti-inflammatory, M2-like phenotype through AMPK activation.

## 1.3. c-MET signaling pathway in infectious diseases

### 1.3.1. *Helicobacter pylori* infection

*Helicobacter pylori* is a gram-negative human microbial pathogen that persistently colonizes the stomach. Infection by *H. pylori* is associated with chronic gastritis, peptic ulcers, and dyspepsia and contributes to an enhanced risk of developing gastric adenocarcinoma and lymphoma of the gastric mucosal-associated lymphoid tissue (56,57). Several virulence factors produced by *H. pylori* can differently modulate signaling pathways in gastric epithelial cells. Among them are cytotoxin-associated gene A (CagA), CagA pathogenicity island (Cag-PAI), and vacuolar cytotoxin A (VacA) (58–60). The Cag-PAI contains genes encoding cagA and components of a multi-molecular complex, type IV secretion system (T4SS), that facilitates the delivery of bacterial factors, including CagA effector protein, into the host cells (59).

c-MET was described to be induced in a gastric adenocarcinoma epithelial-like, AGS, cell line upon *H. pylori* infection (61–64), particularly in *H. pylori* strains with a functional T4SS (65). c-MET inhibition, either with an HGF antagonist or AGS cells transfection with siRNA for *c-Met*, inhibited c-MET phosphorylation in AGS cells and restricted their invasion capacity normally induced by *H. pylori* infection (64,65). Also, the activity of MMP-2 and MMP-9 was decreased in *c-Met* siRNA transfected cells, in

contrast to the usual increase after *H. pylori* infection. Moreover, siRNA for *c-Met* decreased the p-AKT, p-mTOR, and p-S6 levels, and reversed the proinflammatory cytokines production during *H. pylori* infection (64).

Oliveira *et al.* found that CagA partially colocalizes with c-MET, E-cadherin and p120-catenin, and more importantly, they found that silencing of *c-Met* abolished these interactions (62). A direct intracellular interaction between *H. pylori* effector protein, CagA, and phosphorylated c-MET was found (63). Importantly, this interaction deregulates downstream effector molecules, leading to the modulation of specific cellular functions, namely the promotion of motogenic response (61). In particular, the activation of c-MET by CagA led to the activation of β-catenin and NF-κB, known to enhance proliferation and inflammation, respectively (63). More recently, Li *et al.* showed that negative regulation of autophagy usually triggered by CagA depends on the activation of c-MET signaling pathway, via AKT, and enhances the production of proinflammatory cytokines (64). Interestingly, *H. pylori* mutant strains *cagA*Δ/Δ and *virB11*Δ/Δ induced lower levels of c-MET expression, while *H. pylori vacA*Δ/Δ mutant strain induced similar levels compared to the wild-type strain (61,65,66). *H. pylori cagA*Δ/Δ mutant strain also induced less cell invasion and lower MMP-2 and MMP-9 activity (65).

The *H. pylori* effector protein, CagA, interacts directly with c-MET, activating the signaling pathway, which enhances the extracellular matrix degradation and subsequent capacity for cell invasion (Figure 3 and Table 4).

### 1.3.2. *Listeria monocytogenes* infection

*Listeria monocytogenes* is a human foodborne pathogen, a ubiquitous gram-positive bacterium, that can cause a systemic infection, listeriosis (67). *Listeria* infections show several intensities of clinical presentations, from asymptomatic or mild gastroenteritis in healthy individuals to sepsis, meningoencephalitis, or abortions, in immunocompromised individuals (68). After ingestion, *L. monocytogenes* has the capacity to cross the host's epithelial barriers, relying on the fact that invasion factors, such as internalin (Inl) A and InlB, facilitate the infection of nonphagocytic cells (69–71).

Several studies described that InlB binds to the extracellular domain of c-MET and induces c-MET phosphorylation in several mammalian cell lines, while InlA protein did not (71–73). InlB shows phylogenetically defined isoforms with varying virulence potential. More specifically, isoforms of the phylogenetic lineage I strongly bound and activated c-MET than isoforms of the phylogenetic lineage II (72,73). InlB protein can be divided as follows: N-terminal cap region, leucine-rich repeat (LRR) domain, inter-repeat Ig-like, b-repeat, and a carboxyl-terminal cell surface-anchoring. Notably, the LRR domain of InlB protein is required for the binding to c-MET. This interaction subsequently activates the signaling

pathway and mediates bacteria invasion into the human epithelial HEp-2 cell line (71–73). Niemann *et al.* found that InlB is structurally different from HGF and bind to different c-MET sites (74). In fact, the authors explored the binding structure in more detail, and the proposed structure consists of a high-affinity binding between the LRR domain of InlB and the first Ig-like domain of c-MET, followed by inter-repeat binding of InlB to c-MET SEMA domain and finally receptor oligomerisation via the carboxyl-terminal cell surface-anchoring domain (74). Notably, through manipulation of host cell energy metabolism towards enhanced mitochondrial respiratory activity, a reduction in the entry of *L. monocytogenes* bacteria was verified, due to the slower endocytic recycling of c-MET, which causes a decrease in the availability of cell surface receptors so that bacteria can engage for their entry (75).

The interaction of InlB with the c-MET and subsequent enabling of *L. monocytogenes* uptake has been shown to happen through the activation of PI3K which is involved in the enhancement of cytoskeletal remodeling (76). Gessain *et al.* demonstrated that intestinal cells have a constitutive PI3K activation, so InlB is dispensable for *L. monocytogenes* internalization. However, placental cells which do not exhibit constitutive PI3K activity, render on InlB for signaling activation and bacteria internalization (77). Interestingly, Mungunsukh *et al.* and Kolditz *et al.* engineered alterations to InlB to potentiate c-MET signaling pathway activation. Mungunsukh *et al.* tested their tandem dimmer in pulmonary arterial endothelial cells and observed induced ERK1/2, PI3K/AKT, and STAT3 pathways, along with increased migration and proliferation (78). Kolditz *et al.* tested their constitutively dimeric truncated variant of InlB in human keratinocytes and observed an increase in migration and proliferation, similar in magnitude to that of HGF (79).

Furthermore, Chalenko *et al.* reported that InlB improved the efficiency of *L. monocytogenes* captured by M1 macrophages differentiated from peripheral blood monocytes of healthy donors while inhibiting the intracellular multiplication of bacteria in these cells (80). Moreover, pretreatment of macrophages with a hypervirulent lineage I InlB isoform reduced the capacity of *L. monocytogenes* uptake and augmented their capacity to support the intracellular multiplication of bacteria (73). These results correlated with the efficiency of InlB interactions with c-MET, which could explain the observed enhancement in bacteria uptake by macrophages, reversed by the stronger binding of c-MET to the hypervirulent lineage I isoform of InlB resulting in decreased bactericidal activity in macrophages.

Together, these studies show that *L. monocytogenes* relies on c-MET receptor binding to achieve maximum signaling pathway activation, allowing for efficient bacterial uptake during invasion (Table 4).

### 1.3.3. *Salmonella typhi* infection

*Salmonella typhi* is a gram-negative bacterium, mainly transmitted in food or water contaminated by the feces or urine of subjects excreting the bacteria, that causes severe systemic infection and typhoid fever. After ingestion, bacteria reach the intestinal epithelium and infect macrophages and dendritic cells, which fail to kill the bacteria. Subsequently, the bacteria spreads and originates a systemic infection, which spreads to several organs (81). *S. typhi* constitutively expresses the virulence factor *S. typhi* invasin (STIV) in the outer membrane, which is required for intestinal epithelial cell invasion.

Chowdhury *et al.* treated a human colorectal adenocarcinoma cell line with recombinant STIV and found the coexistence of STIV and c-MET (82). The authors further explored the possibility of direct binding of STIV to c-MET, and effectively confirmed their direct interaction and its dependence to bacteria invasion. Moreover, this interaction resulted in c-MET phosphorylation early after infection and weak persistence afterwards. This phosphorylation led to the activation of downstream signaling pathway involving Src, PI3K/AKT, and Rac1, subsequent actin polymerization around the attached bacterial, and internalization in the cell (82). Additionally, inhibition of c-MET *in vivo* limited the invasion of intestinal epithelial cells and systemic infection by *S. Typhi* (82).

This study evidence that *S. Typhi* seizes c-MET signaling pathway to enhance internalization (Figure 3 and Table 4).

### 1.3.4. *Pseudomonas aeruginosa* infection

*Pseudomonas aeruginosa* is a gram-negative bacterium known to induce keratitis, an inflammation of the cornea. *P. aeruginosa* releases lipopolysaccharide, which causes an acute inflammation that, once deregulated, can escalate to stromal destruction and loss of vision.

Jiang *et al.* reported that *Hgf* expression was increased in mice's cornea post-infection with *P. aeruginosa* (83). Additionally, infected mice treated with recombinant HGF demonstrated more severe infection, lower levels of total *c-Met, mTOR, IL-10,* and increased levels of phosphorylated c-MET, *PI3KCa, Akt*, and proinflammatory cytokines, namely IL-12p40 and IL-18, in the cornea (83). *In vitro*, the authors verified higher levels of *mTOR* in LPS-stimulated macrophage cell line, RAW 264.7, and peritoneal macrophages upon treatment with a c-MET inhibitor, thus confirming c-MET signaling pathway activation acts by downregulating *mTOR* (83).

This study shows that HGF induces c-MET signaling pathway activation with downstream downregulation of mTOR, enhancing proinflammatory cytokines production and ultimately exacerbating *P. aeruginosa* infection (Table 4).

### 1.3.5. *Plasmodium* spp. infection

Infected female *Anopheles* mosquitoes transmit the *Plasmodium* spp. parasite by injecting sporozoites, which enter the bloodstream and are transferred to the hepatocytes. Within these cells, the parasite matures, then it is released into the bloodstream, and replicates in human erythrocytes. Human malaria infection can be caused by five different *Plasmodium* spp., namely *P. falciparum, P. vivax, P. ovale, P. malariae*, and *P. knowlesi*, while *P. berghei* can cause mouse malaria infection.

Interestingly, pretreatment of human hepatoma cells, HepG2, with HGF prior to infection with *P. berghei* sporozoites increased the infection extent and apoptosis protection of *P. berghei*-infected cells (84–87). Moreover, HGF is secreted by sporozoite-wounded HepG2 cells (84). Importantly, HepG2 cells treated with HGF showed actin reorganization required for sporozoite development inside host cells (84).

After the culture of mouse hepatoma cells Hepa1-6 with *P. berghei* sporozoites, c-MET phosphorylation was induced (84). Kaushansky and Kappe found that other *Plasmodium* spp. did not activate c-MET, neither *Plasmodium yoelii* nor *Plasmodium falciparum* sporozoites (86). The c-MET activation facilitates *P. berghei* invasion and early development, which failed in the other species, possibly due to the requirement for more specialized molecules, including CD81, among others (86,87).

Moreover, transfection of HepG2 cells with constitutive active *c-MET* led to enhanced infection with *P. berghei*. Concordantly, the downregulation of *c-MET* in these cells resulted in complete resistance to infection (84). Selective inhibitors against human c-MET, Crizotinib and PHA-665752, and B-Raf, SB-590885, reduced *in vitro* proliferation of *P. falciparum* and *P. knowlesi,* and reduced the parasitemia of *P. falciparum* prior to the schizont stage. Moreover, in a murine model of malaria, a c-MET inhibitor, PHA-665752, reduced *P. berghei* blood infection (88). Similarly, the use of genistein, a broad inhibitor of receptors tyrosine kinase, inhibited c-MET phosphorylation and reduced the extent of *P. berghei* infection in human hepatoma cell lines, HepG2 and Huh7, and mouse hepatoma cell line, Hepa1-6 cells (89). However, the authors reported that the treatment with genistein does not affect cell invasion, but it inhibits the initial development of the parasites once inside the host cells (89). Interestingly, genistein treatment of mice infected with *P. berghei* or *P. yoelii* sporozoites reduced the extent of liver infection (89). Moreover, mice that ingested genistein in their diet maintained a low percentage of parasitized red cells during the infection, and in these animals the development of experimental cerebral malaria was prevented (89).

Overall, c-MET activation allows the infection and boosts intracellular development of *Plasmodium* spp. sporozoites through induction of the actin cytoskeleton reorganization, thus increasing the extent of infection of malaria infection (Table 4).

### 1.3.6. *Leishmania mexicana* infection

The *Leishmania* parasite is deposited in the host skin by a female sandfly in the infective stage, metacyclic promastigotes. Then, macrophages phagocytosed promastigotes and, once inside the macrophage, can differentiate into amastigotes and replicate (90). More than 20 *Leishmania* parasite species are pathogenic to mammalians. Depending on the clinical manifestations, Leishmaniasis can be categorized as tegumentary (cutaneous, mucosal, or cutaneous-diffuse forms) and visceral (91). The development of Leishmaniasis depends not only on the capacity of the host's immune response but also on the species of the parasite and its virulence factors (92). Examples known as primary causatives of cutaneous form are *L. major, L. mexicana, L. amazonensis,* and *L. braziliensis,* while *L. donovani* and *L. infantum* cause the visceral form, the most severe form of the disease that is frequently fatal without treatment (91). Although macrophages are the primary infected cells, other immune cells recruited to the site of the infection, such as monocytes, dendritic cells, and neutrophils, can become infected. Upon *Leishmania* spp. infection, neutrophils are rapidly recruited. Their role might be microbicidal, protective, or detrimental, depending on the parasite species and host factors, such as the genetic background and immune status (93).

Passelli *et al.* found that HGF levels increased in mice ears after *L. mexicana* infection. Moreover, the highest c-MET expression in these infected mice was detected in neutrophils from infected ears, comparatively to monocytes and dendritic cells (94). *In vitro* infection of bone marrow neutrophils with *L. mexicana* metacyclic promastigotes, the infective form of the parasite, or with amastigotes, the replicative form of the parasite, which is present during the chronic phase of the disease, induced a significant increase of *c-Met* mRNA (94). Moreover, using a fluorescent *L. mexicana* parasite, the authors verified a significant increase in c-MET expression in infected bone marrow neutrophils (94). Treatment of *L. mexicana* infected mice with established cutaneous lesions with c-MET inhibitor, capmatinib, resulted in decreased ear lesion size, significantly reduced infiltration of neutrophils at the site of infection, and significantly increased intracellular IFN-γ expression in ear $CD4^+$ T cells (94). Moreover, mice deficient for *c-Met* in neutrophils better controlled *L. mexicana* infection and exhibited significantly smaller ear lesions, along with reduced recruitment of neutrophils and reduced percentage of infected neutrophils, monocytes, and dendritic cells in the ear. Furthermore, $CD4^+$IFN-$\gamma^+$ T cells' frequency was increased in the draining lymph node of mice deficient for *c-Met* in neutrophils, while the frequency of $CD4^+$IL-$4^+$ T cells was lower (94). Interestingly, the infection of bone marrow neutrophils deficient for *c-Met* with metacyclic *L. mexicana* parasites increased the levels of ROS and slightly decreased parasite survival compared to wild-type bone marrow neutrophils (94).

This study shows that *L. mexicana*-induced c-MET activation in neutrophils has a negative impact on cutaneous lesions caused by *Leishmania* spp. since its expression increases neutrophils recruitment to the infection site, but decreases their ability to produce ROS, providing a niche for further expansion of the pathogen in the host (Figure 3 and Table 4).

### 1.3.7. *Candida albicans* infection

Although *Candida* species can exist in the mucosal surfaces of the host as harmless commensals, they emerged as agents of opportunistic infections. Under specific conditions that increase host predisposition, they can become harmful pathogens that can cause from superficial infections, such as oral or vaginal candidiasis, to invasive and life-threatening infections in debilitating patients.

Amongst *Candida* species, *C. albicans* is the most frequently isolated from the oral cavity (95). *C. albicans* can invade the host cell by endocytosis through the interaction of an adhesin of the cell wall, Als3, with host cadherins (96). Cell surface glycosyl phosphatidylinositol-anchored-proteins are critical for host-pathogen interactions. Besides Als3, also Hyr1, a cell surface protein expressed in *C. albicans* hyphae, is crucial for neutrophil evasion (97).

Very recently, Phan *et al.* infected an oral epithelial cell line with *C. albicans* hyphae and observed that c-MET expression accumulated around the hyphae (98). Moreover, siRNA knockdown of *c-Met* and treatment with a c-MET inhibitor, SGX523, decreased the endocytosis of *C. albicans* (98). Concordantly, *c-MET* transfection increased the endocytic capacity of the cells. In fact, in response to *C. albicans* infection, c-MET forms a multi-protein complex with E-cadherin and EGFR that mediates endocytosis of *C. albicans* in epithelial cells (98). Interestingly, in mice infected with *C. albicans*, treatment with a combination of EGFR and c-MET inhibitors, gefitinib and SGX523, reduced the oral fungal burden (98).

The hyphal component, Als3, was found to be required to induce both endocytosis and active penetration of *C. albicans* (98). Infection of oral epithelial cells with *C. albicans* mutant *als3*Δ/Δ showed that this hyphae component is required to activate EGFR and c-MET and that epithelial cells infected with this mutant released significantly less proinflammatory cytokines. Although *hyr1*Δ/Δ mutant also reduced the phosphorylation of c-MET and EGFR and the endocytose of *C. albicans*, Hyr1 is dispensable for active penetration and proinflammatory response by oral epithelial cells (98).

In short, this study described c-MET as a novel receptor for *C. albicans* endocytosis through a multiprotein complex with EGFR and E-cadherin in oral epithelial cell. The interaction of this complex with Als3 and Hyr1 contributes to maximal epithelial cell invasion (Figure 3 and Table 4).

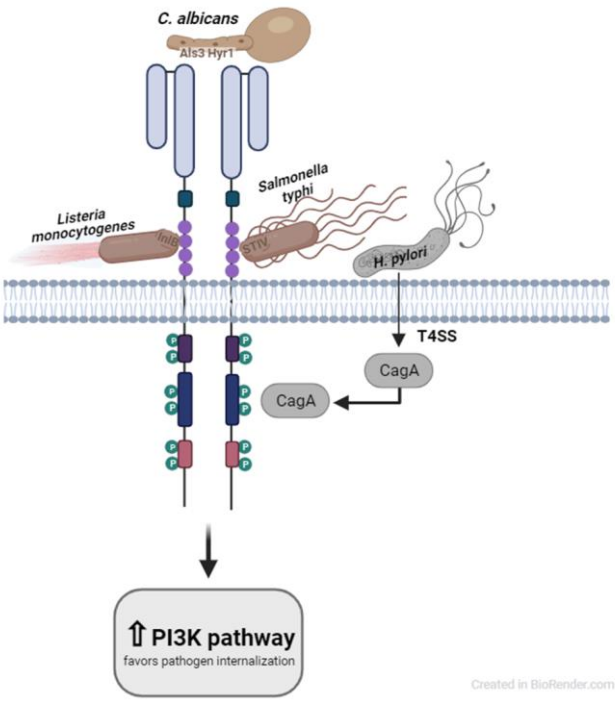



**Figure 3. Pathogenic activation of HGF/c-MET signaling pathway.** Bacterial proteins, namely CagA from *Helicobacter pylori*, InlB from *Listeria monocytogenes*, or STIV from *Salmonella typhi* and fungal proteins, namely Als3 and Hyr1 from *Candida albicans* deregulate c-MET signaling pathway towards a more suitable environment for infection.

**Table 4. Activation of c-MET signaling pathway in pathogen recognition and internalization.**

| | Infectious agent | Recognized protein | Effect | Involved downstream signaling mediators |
|---|---|---|---|---|
| Bacteria | *Helicobacter pylori* | cagA | Induction of motogenic response<br>Decreases autophagy<br>Increases production of proinflammatory cytokines | PI3K/AKT |
| | *Listeria monocytogenes* | InlB | Enhances cytoskeleton remodeling<br>Favors bacteria internalization<br>Increases bacteria phagocytosis<br>Decreases intracellular multiplication of bacteria | PI3K/AKT |
| | *Salmonella typhi* | STIV | Enhances cytoskeleton remodeling<br>Favors bacteria internalization | PI3K/AKT |
| | *Pseudomonas aeruginosa* | | Increases severity of *P. aeruginosa*-induced keratitis<br>Increases production of proinflammatory cytokines | PI3K/AKT/mTOR |
| Parasite | *Plasmodium* spp. | | Enhances actin cytoskeleton reorganization<br>Favors parasite internalization and development | |
| | *Leishmania mexicana* | | Increases severity of *L. mexicana*-induced ear lesion<br>Increases recruitment of neutrophils<br>Decreases neutrophilic ROS production | |
| Fungi | *Candida albicans* | Als3 and Hyr1 | Favors fungi internalization | |

### 1.4. General overview

The c-MET signaling pathway has been associated with the modulation of the immune response and the subsequent outcome of inflammatory-related conditions. The mechanisms by which the HGF/c-MET signaling pathway modulates the recruitment, phenotype, or functions of immune cells in inflammatory conditions, as well as its role in the recognition of pathogens and the associated immune response, have been reviewed in this section. As evident from the above discussion, several studies have tested the therapeutic effect of HGF systemic administration and inhibitors for c-MET or tyrosine kinases in general. Nevertheless, these approaches can also act on epithelial or cancer cells, which affects tissue repair and tumor growth, so the effects observed may not be directly associated with the impact on immune cells.

Increasing evidence indicates that c-MET signaling pathway stimulates antitumor immunity by exacerbating the effector cytotoxic functions of neutrophils and CD8 T cells (32,33). Unfortunately, only a few studies have employed lineage-specific deletion of the *c-Met* in immune cells in other inflammatory and infectious disease contexts. Particularly, c-MET expression in neutrophils was recently found to exacerbate inflammatory bowel disease through intensified tissue inflammation and increase *Leishmania mexicana* infection's extent through inhibition of ROS production by infected neutrophils (42,94).

Besides, many pathogens seize host's HGF/c-MET signaling pathway, mainly via the overactivation of PI3K cascade and actin reorganization, to favor their internalization and the spread of infection.

Undoubtedly, further research is required to fully clarify the impact of the HGF/c-MET signaling pathway in pathogen recognition and immune response and apply these findings in the clinic. Unfortunately, inflammatory and infectious diseases have a significant impact on patients' quality of life and even survival. So, relevant discoveries about the involvement of HGF/c-MET signaling pathway in lung immunity could improve patients' well-being and average life expectancy.

## 2. Lung diseases: fibrosis and aspergillosis

The lungs are undoubtedly crucial for sustaining general health and well-being, as they are involved in gas exchange and provide a protective barrier against inhaled harmful substances such as dust, allergens, and pathogens. Indeed, the lung epithelium is the first line of defense in the lung, providing a mucosal barrier that contributes to the mucociliary clearance function that ultimately results in the extrusion of inhaled materials and prevents inhaled toxins and pathogens from contacting the subepithelial tissue. When inhaled particles overcome the anatomical barriers and reach the respiratory alveoli, they are confronted with cells of the innate immune system, which may ultimately lead to disease, depending on the immune status of the host and the type of particle inhaled. In fact, the complete re-establishment of tissue homeostasis in response to a threat or injury would require a rapid, well-coordinated and effective

immune response in order to eliminate foreign particles and prevent acute exacerbations. Unfortunately, uncontrolled or inefficient inflammatory processes can lead to severe complications in the lung, associated with a poor prognosis and even death, as seen in pulmonary fibrosis and invasive pulmonary aspergillosis.

A broad group of respiratory disorders that affect the lung interstitium, designated as interstitial lung diseases (ILDs), are associated with varying degrees of lung inflammation and fibrosis (99). ILDs present significant morbidity, mortality, and financial burden (100,101). Major ILDs categories include environmental exposures-related ILDs, such as hypersensitivity pneumonitis, asbestosis and silicosis; autoimmune connective tissue disease-associated ILDs, particularly rheumatoid arthritis and systemic sclerosis; sarcoidosis; and idiopathic interstitial pneumonias (IIP) (Figure 4) (102). Idiopathic pulmonary fibrosis (IPF) is the most frequent IIP, and it represents a prototypical fibroproliferative disorder with an unknown cause. IPF is characterized by a progressive and irreversible loss of respiratory function, ultimately leading to respiratory failure and early mortality (99,103–105). Moreover, patients with other ILDs can develop a progressive fibrosing phenotype, thus presenting a faster progression, a worse prognosis, and early mortality, similar to patients with IPF (106–114).

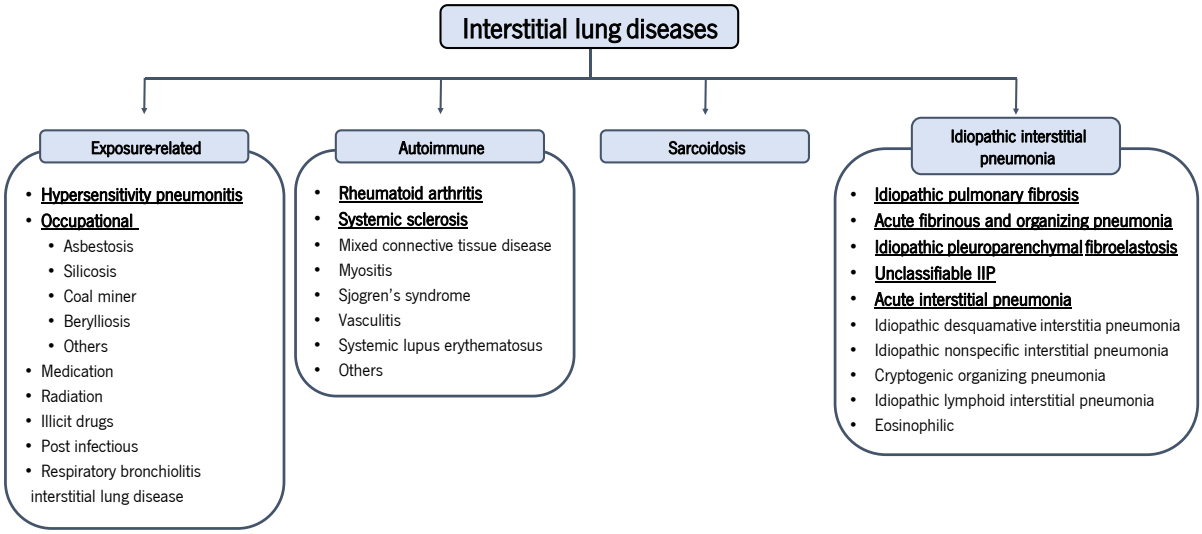



**Figure 4. Types of ILDs.** Types of ILDs most likely to have a progressive-fibrosing phenotype are underlined.

Invasive fungal infections represent a critical health issue, particularly in immunocompromised patients, as they are responsible for high economic costs, morbidity and mortality (115,116). Although most inhaled fungal pathogens are easily eliminated by the host's cells without manifesting symptoms, a small subset of fungal species can cause disease (117,118). Among these fungal species are *Aspergillus* spp., *Pneumocystis jirovecii, Cryptococcus neoformans, Candida* spp., non-*Aspergillus* filamentous fungi (*Fusarium* spp., *Rhizopus* spp. and *Mucor* spp.) and endemic fungi (*Blastomyces dermatitidis*,

*Coccidioides immitis*, *Coccidioides posadasii* and *Histoplasma capsulatum*) (118–129). *Aspergillus* infection covers a broad clinical spectrum of disease, with invasive pulmonary aspergillosis (IPA) being a leading cause of morbidity and mortality, particularly in immunocompromised patients (130).

### 2.1. Idiopathic pulmonary fibrosis and progressive pulmonary fibrosis

ILDs constitute a heterogeneous group of lung diseases classified together due to their invariable interstitial inflammation and fibrosis (99,110). IPF is the prototypical fibroproliferative ILD, but a significant proportion of patients with other interstitial lung disease (ILD) subtypes, 10.4% to 60.6%, can develop a progressive fibrosing phenotype (Figure 4), which significantly contributes to a decline in lung function, poor response to treatment, increased morbidity and mortality (106,109–112,131). Among the most common progressive fibrosing ILD subtypes are fibrotic hypersensitivity pneumonitis (HP) (1.6–40.0%), autoimmune connective tissue diseases (CTDs)-associated ILD (CTD-ILD) (16.6–46.7%), particularly rheumatoid arthritis-associated ILD and systemic sclerosis-associated ILD, and unclassifiable ILD (17.2–71.4%) (Figure 4) (113,131–133).

In Europe and the United States, the estimated annual incidence of IPF ranges from 2.8 to 19.0 *per* 100,000 persons, and that of non-IPF progressive fibrosing ILDs from 2.1 to 32.6 *per* 100,000 persons (131,134). IPF patients' mortality rate is very high, and these patients present an estimated survival of 3–5 years after diagnosis due to respiratory failure, frequently precipitated by acute disease exacerbations (135–137). Similarly, the survival of patients with progressive fibrosing ILDs is estimated to be only 4–5 years from diagnosis, and their mortality is also precipitated by acute exacerbations (138,139).

While IPF is a predominantly fibroproliferative interstitial pneumonia, the progressive fibrosing phenotype in ILDs other than IPF can be preceded or associated with persistent inflammation, such as HP and CTD-ILD (104,140). HP is a complex syndrome caused by chronic exposure to environmental antigens which, in susceptible individuals, trigger an exaggerated immune response in the lung (141,142). The development of fibrosis in these patients occurs due to a combination of features, including the development of autoimmune characteristics, T helper (Th) type 1 switching to Th2 cells and the release of pro-fibrotic factors by immune cells (142–144). CTDs are systemic autoimmune diseases characterized by circulating autoantibodies and systemic manifestations associated with autoimmune-mediated organ injury, such as ILD (145). Similar to HP, T lymphocytes and other immune cells, stimulated by the severely dysregulated immune system, release pro-fibrotic cytokines, chemokines and growth factors that promote fibroblast proliferation and differentiation into myofibroblasts contributing to the progression towards a fibrotic phenotype (145).

Although triggered by different pathophysiological mechanisms, either repeated epithelial damage or exaggerated inflammation, pulmonary fibrosis (PF) is the ultimate common denominator of IPF and non-IPF progressive fibrosing ILD. These triggers ultimately culminate in aberrant wound healing processes, namely the induction of fibroblast proliferation and differentiation into myofibroblasts (108). Myofibroblasts are responsible for excessive production of extracellular matrix (ECM), which contributes to thickening of alveolar walls, destroying the lung architecture with irreversible loss of respiratory function (Figure 5) (146,147).

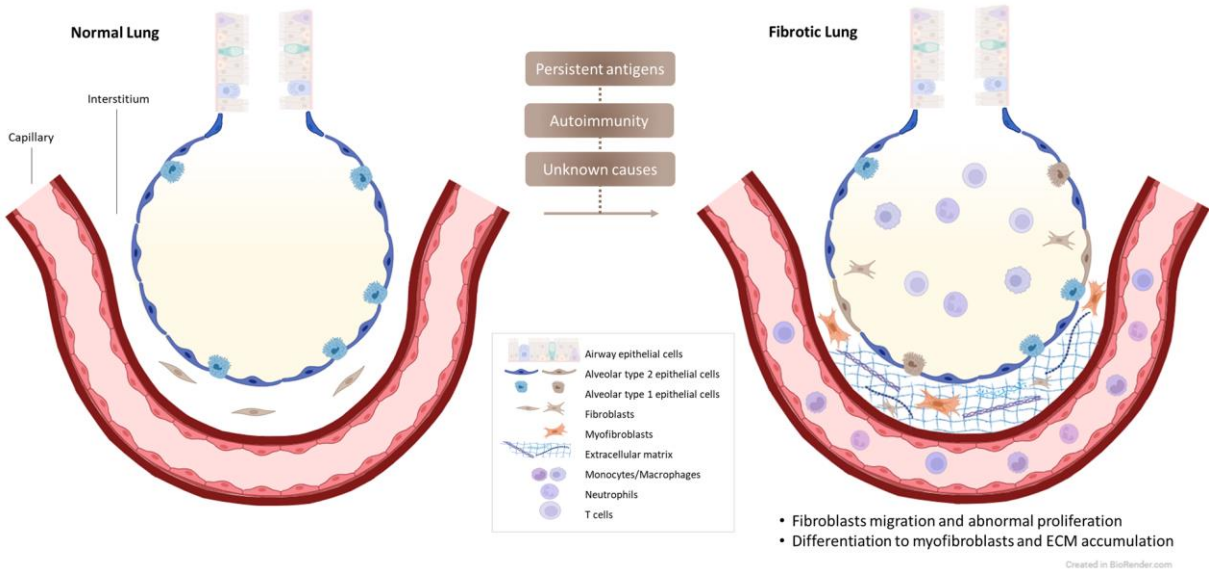



**Figure 5. Pathogenesis of pulmonary fibrosis.** Pulmonary fibrosis is the final common denominator of different ILDs, but it originates from distinct pathophysiological mechanisms, including those of unknown etiology (IPF), autoimmunity (CTD-ILD), granulomatous inflammation caused by persistent inhalation of antigens (HP, sarcoidosis, drug-induced ILD) or other insults. Repeated injury to alveolar epithelial cells or excessive immune activation and inflammation trigger fibroblast activation, proliferation and differentiation into myofibroblasts. The subsequent phase of fibrogenesis, common to all diseases, regardless of the initial cause or triggering factor, consists of the aberrant production of the extracellular matrix that leads to remodeling and destruction of the lung architecture with irreversible loss of respiratory function.

IPF and progressive PF ILDs diagnosis rely on a combination of clinical and radiological criteria and may also require cellular or histopathological findings (114). Firstly, clinical findings and the known potential causes of ILDs should be carefully evaluated. In some cases, this would be sufficient information to make a definitive diagnosis of specific ILDs with known causes. Otherwise, the patient should undergo high-resolution computed tomography (HRCT) imaging of the chest to identify ILD patterns, including patterns of usual interstitial pneumonia (UIP), non-specific interstitial pneumonia, or other patterns specific to the respective ILDs (99,104,144,148,149). In most ILDs patients, the HRCT pattern and relevant clinical information enable a definite diagnosis at the ILDs multidisciplinary team discussion (110). The diagnostic approach to IPF relies on HRCT patterns of UIP, recognized by traction bronchiectasis/bronchiolectasis and/or honeycombing (104). UIP is the radiologic hallmark pattern of

IPF but can also be identified in patients with fibrotic HP and fibrotic CTD-ILD (104). In these ILDs patients that exhibit progressive fibrosing phenotype, the UIP pattern is usually accompanied by fast worsening respiratory symptoms, decline of lung function, and radiological evidence of disease progression (113,114). In patients with clinical and HRCT findings that are not conclusive enough to establish a definitive diagnosis, bronchoalveolar lavage (BAL), transbronchial cryobiopsy, or surgical lung biopsy may be useful. BAL is a very safe procedure and allows an analysis of immune cells which, although not required in typical IPF, can be valuable in the definitive diagnosis of some ILDs; for example, BAL lymphocytosis is indicative of HP rather than IPF or sarcoidosis (140,150). Moreover, BAL analysis allows the exclusion of infections or other malignancies in patients with suspected ILDs (151). When the previous findings remain inconclusive, bronchoscopy and lung biopsy should be performed if it is worth the risk of complications and mortality (152,153). Fortunately, novel methods can be employed, namely transbronchial cryobiopsy, which is also invasive but carries fewer risks (154,155). Therefore, when absolutely necessary, the diagnosis made by histopathological analysis of lung biopsies is based on a combination of patchy dense fibrosis with architectural distortion, honeycombing and fibroblast foci (104). In some patients, the diagnosis of ILDs is a challenging process. Even after exhaustive evaluation of all the relevant parameters, 10-20% of the cases are still diagnosed as unclassifiable ILDs. Several factors contribute to this uncertainty in diagnosis, such as unusual or overlapping radiological or histopathological patterns and heterogeneity in the evolution of the disease (156,157).

Non-pharmacologic and supportive care strategies are transversal to all patients with fibrotic ILDs, and they are essential for successfully improving patients' quality of life. These strategies include smoking cessation, protection from risky exposures, avoidance of medications that can trigger ILDs, pulmonary rehabilitation to reduce dyspnea and improve exercise capacity, and, in particular cases, long-term oxygen therapy can prevent pulmonary hypertension due to hypoxemia (158–161). Concerning pharmacological strategies, immunosuppressive treatment is potentially beneficial for non-IPF patients despite not demonstrating any clear benefit for IPF patients (162–164). The first line of immunosuppressive therapy is generally based on the use of corticosteroids, which should preferably be replaced by non-steroidal agents to avoid the side effects of prolonged steroid use (138,165). Currently, only two approved antifibrotic drugs, Nintedanib and Pirfenidone, have demonstrated efficacy in delaying the progression of IPF (166–168). Nintedanib inhibits multiple signaling pathways through the binding to the intracellular adenosine triphosphate binding site domain of the tyrosine kinase receptors, namely vascular endothelial growth factor, fibroblast growth factor and platelet-derived growth factor (PDGF) receptors. The suppression of these signaling pathways decreases fibroblast activity by inhibiting the production of

fibrogenic growth factors, thus slowing the progression of IPF (167,169,170). Pirfenidone is a modified pyridine molecule that reduces the TGF-β-induced collagen synthesis, as so slowing the fibrotic process in IPF patients (171–173). However, these antifibrotic treatments can only delay disease progression rather than provide a cure. Lung transplantation would be the only option to improve survival time (174–176). However, the decision to select patients with IPF for lung transplantation is challenging and requires the balancing of critical aspects, namely the risk of mortality due to the existence of other comorbidities and the probability of survival after transplantation. Despite all the efforts to develop foolproof therapies, pulmonary fibrosis remains a severe and irreversibly fatal health problem. Therefore, the identification of novel effective therapeutic strategies would benefit from a better understanding of the cellular and molecular mechanisms that modulate the progression of pulmonary fibrosis.

### 2.1.1. Immune cells in pulmonary fibrosis

As already mentioned, acute exacerbations in patients with IPF and progressive fibrosing ILDs are clinically meaningful events associated with a rapid deterioration in respiratory function that worsens prognosis and precipitates their mortality (135–137,139). Interestingly, extensive innate and adaptive inflammatory infiltrates were detected in IPF patients experiencing acute exacerbation, predominantly in those exhibiting rapid rather than slow disease progression (177). Moreover, the proportion of macrophages and neutrophils was increased in the BAL fluid of IPF patients experiencing acute exacerbation (178). As such, indicating that the inflammatory infiltration accelerates the disease progression, at least in acute exacerbation conditions.

Moreover, damaged end-stage alveolar epithelial cells, such as those found in IPF, actively release proinflammatory mediators, such as chemokines, cytokines and cytoplasmic elements, which trigger an innate immune response and ultimately contribute to uncontrolled tissue remodeling (179–181). Neutrophils migrate into the lung-injured sites during the early alveolar epithelial cells' injury stage. Neutrophils can be recruited and/or activated by several receptors and proteins, including IL-8, granulocyte-macrophage colony-stimulating factor and G-CSF (182). IL-8, also called CXCL8, is the predominant neutrophilic chemoattractant. Notably, this cytokine and G-CSF are increased in BAL and sputum from IPF patients, indicating neutrophil infiltration and activation (183–185). Neutrophils are characterized by the production of neutrophil elastase (NE), which can have profibrotic or antifibrotic properties. On the one hand, NE degrades ECM components, alleviating PF, and on the other hand, NE aggravates PF by promoting fibroblast proliferation and differentiation into myofibroblast (186). The use of NE inhibitors attenuated the progression of PF in a mouse model via suppression of lung inflammation in early stages and TGF-β1 activation in later stages (187,188). Interestingly, these studies point toward

a more profibrotic role of NE in IPF. Moreover, neutrophils can directly induce endothelial and epithelial cell death and tissue injury through neutrophil extracellular traps (NETs) formation and secretion of toxic mediators, such as reactive oxygen species (ROS) (189). ROS have also been described to induce lung fibroblast activation, their differentiation into the myofibroblast, and collagen production via IL-17, a well-known inducer of inflammation and fibrosis (190). Overall, these studies in mouse models confirm that neutrophil functions are altered in fibrogenesis, which contributes to the intensification of an environment more propitious to persistent tissue inflammation, and, consequently, progression to fibrosis (Figure 6) (191).

Macrophages are highly plastic cells that modulate their phenotype according to the tissue environment. These cells may exhibit antifibrotic, profibrotic, or tissue-regenerating functions. “Classically” activated, M1-like, macrophages are well known for producing proinflammatory cytokines, such as TNF, IL-1β, and IL-6, thereby maintaining tissue inflammation. “Alternatively” activated, M2-like, macrophages are characterized by releasing anti-inflammatory cytokines, such as IL-4 and TGF-β, and they are the most represented phenotype during IPF progression (192–198). M2-like macrophages induce fibroblast proliferation, activation, and differentiation, mainly via secretion of several profibrotic growth factors, including TGF-β, PDGF-α, insulin-like growth factor (IGF)-1 and CCL18 (Figure 6) (192–198). Although at lower proportion, M1-like macrophages can attenuate fibrosis by matrix metalloproteinases (MMPs)-dependent ECM degradation (Figure 6) (199–202).

T cells were identified in the lungs of IPF patients in organized lymphoid structures and zones of active disease with epithelial cell regeneration and fibrosis, T cells accumulation can persist and potentially sustain chronic inflammation (203–205). In a study based on the establishment of a PF mouse model in athymic mice, the authors found that T cells were enhancers of fibroblasts proliferation and ECM production since athymic mice presented attenuation of these fibrogenic processes (206). T cells, including CD8 cytotoxic T lymphocytes, Treg cells, and CD4 Th cells have been described to differently impact fibrosis progression. Most importantly, the paradoxical functions of the different Th cells subsets directly impact on fibrogenesis. Th1 cells are characterized by the production of proinflammatory cytokines, such as IFN-γ, TNF, and IL-12, and their response limits tissue fibrosis progression since IFN-γ and IL-12 suppress collagen synthesis (Figure 6) (207–209). Furthermore, IFN-γ increases the expression of MMPs in fibrotic tissues, and these proteolytic enzymes degrade ECM components, thus ameliorating fibrosis (207–209). In contrast to Th1 cells, Th2 cells are characterized by the production of anti-inflammatory cytokines, such as IL-4, IL-13, IL-5, and IL-10, and their response is known to exaggerate fibrosis in chronic inflammatory diseases (207). IL-4 and IL-13 promote fibroblast activation,

proliferation, and differentiation into myofibroblasts, and these effects are attenuated by the co-stimulation with IFN-γ (Figure 6) (210,211). Additionally, IL-4 and IL-13, stimulate the expression and secretion of a potent profibrotic mediator, IGF-1, by macrophages (212). IL-5 also accentuates alveolitis and fibrosis in mouse lungs by inducing massive recruitment of eosinophils, which directly stimulate myofibroblast differentiation and collagen synthesis *in vitro* (213). New evidence has emerged about the involvement of other Th cells, such as Th17 and Treg cells, in the pathogenesis of IPF. Type-17 immunity involves not only the several subtypes of IL-17 but also IL-22 and IL-23. IL-17A levels were elevated in the BAL of IPF patients (214). In contrast, although IL-22 levels were decreased in the plasma of IPF patients, they negatively correlated with the severity of the disease (215). Moreover, a study based on the establishment of PF in IL-23p19 or IL-17A knockout mice found that both interleukins induced TGF-β1 production, collagen deposition, and fibrosis progression (Figure 6) (216). Furthermore, IL-17A mediates the recruitment of neutrophils, and its neutralization promotes the resolution of acute inflammation and delays the progression of PF in mouse models (217–220). Therefore, these data suggest a profibrotic role for type-17 immunity by initiating and sustaining inflammation in the first stages of tissue injury. The role of Treg cells in IPF remains controversial, appearing to exert anti- or profibrotic roles, depending on the stage of the disease. An increased proportion of Treg cells was found in the blood of IPF patients (221). In mouse models of PF, Treg cells enhanced the production of TGF-β and increased lung collagen deposition (Figure 6) (222,223). Furthermore, the adoptive transfer of Treg cells exacerbated PF in mouse models and deviated the balance towards a Th2 response (223,225). Concordantly, Treg cells depletion ameliorated the progression of PF in a mouse model, due to a shift in the balance between Th1 and Th2 towards Th1 dominance (224). Therefore, these data suggest a profibrotic role for Treg cells by sustaining TGF-β-induced collagen deposition and a Th2 response.

While CD4 T cells tend to accumulate in organized lymphoid structures in the lungs, CD8 T cells are more dispersed in the lung parenchyma of patients with IPF (226). An increased proportion of CD8 T cells in the lungs of IPF patients was found to correlate with decreased lung capacity (226). Moreover, a subset of CD8 T cells negative for CD28 was found to be increased in lung explants from IPF patients and these cells exhibited enrichment in profibrotic and proinflammatory transcriptional profiles (227). In a mouse model of PF, CD8 T cells secrete a profibrotic mediator, IL-13 (Figure 6) (228). Overall, these studies point to CD8 T cells presence as indicative of more severe lung injury, with a detrimental contribution to the progression of pulmonary fibrosis.

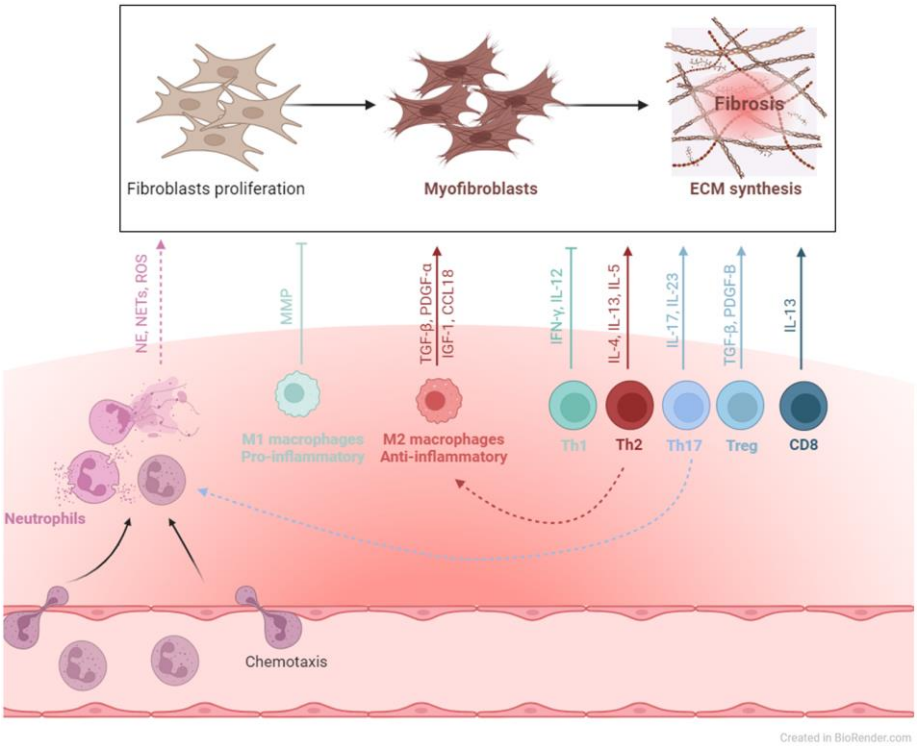



**Figure 6. Effect of innate and adaptive immune response in fibrogenesis.** After damage to the alveolar epithelial cells, immune cells are recruited to the injured lung and can acquire a functional phenotype depending on microenvironmental signals. Both innate (macrophages and neutrophils) and adaptive (T cells) immune cells can modulate fibrogenesis through different mechanisms. Innate immunity: Neutrophils produce several serine proteases, such as NE, which degrade matrix components but can also activate TGF-β thereby promoting ECM accumulation. Macrophages can differentiate into M1 and M2 macrophages. M1 macrophages ameliorate PF by enhancing ECM degradation through MMPs activities and M2 macrophages enhance PF through the production of TGF-β, PDGF, IGF-1 and CCL18. Adaptive immunity: Th1 inhibits fibrogenesis, while Th2, Th17, Treg and CD8 T cells promote PF.

## 2.2. *Aspergillus fumigatus* and pulmonary aspergillosis

*Aspergillus* genus is divided into subgenera, sections and species (229). The most clinically relevant section is the Fumigati, which includes *Aspergillus fumigatus, Aspergillus lentulus, Aspergillus udagawae, Aspergillus thermomutatus,* and *Aspergillus fischeri.* Regarding the most relevant species from the non-Fumigati section, this includes *Aspergillus flavus, Aspergillus nidulans, Aspergillus niger,* and *Aspergillus terreus* (230,231). Although these notable non-*fumigatus* species are also implicated in IPA, the most common causative species is *Aspergillus fumigatus* (232,233).

Asexual *Aspergillus* spores, conidia, are characterized by small size (2-3 μm) and easily disperse in the atmosphere, thus being inhaled in the range of one hundred to one thousand *per* day and swiftly reaching the alveolar spaces of the lung (122,234). The first protective mechanism of *A. fumigatus* against the threatening conditions of the surrounding environment is the fungal cell wall, consisting in a polysaccharide barrier. *A. fumigatus* conidium inner cell wall is composed of a fibrillar β-(1,3)-glucan core linked to chitin, galactomannan and β-(1,3)-glucans/β-(1,4)-glucans, which is surrounded by α-(1,3)-glucans and galactomannan (Figure 7) (235,236). This polysaccharide skeleton is covered up by a

dihydroxynaphthalene-melanin pigment followed by a rodlet layer responsible for the conidia's hydrophobicity. These outer components mask pathogen-associated molecular patterns (PAMPs) that are present in the inner conidia cell wall, thereby avoiding the recognition by the host's immune system and conferring resistance to elimination. During the swelling of fungal cells, melanin and rodlet layers are shed, and germination occurs, along with a remodeling in the distribution of carbohydrates, exposing PAMPs (235).

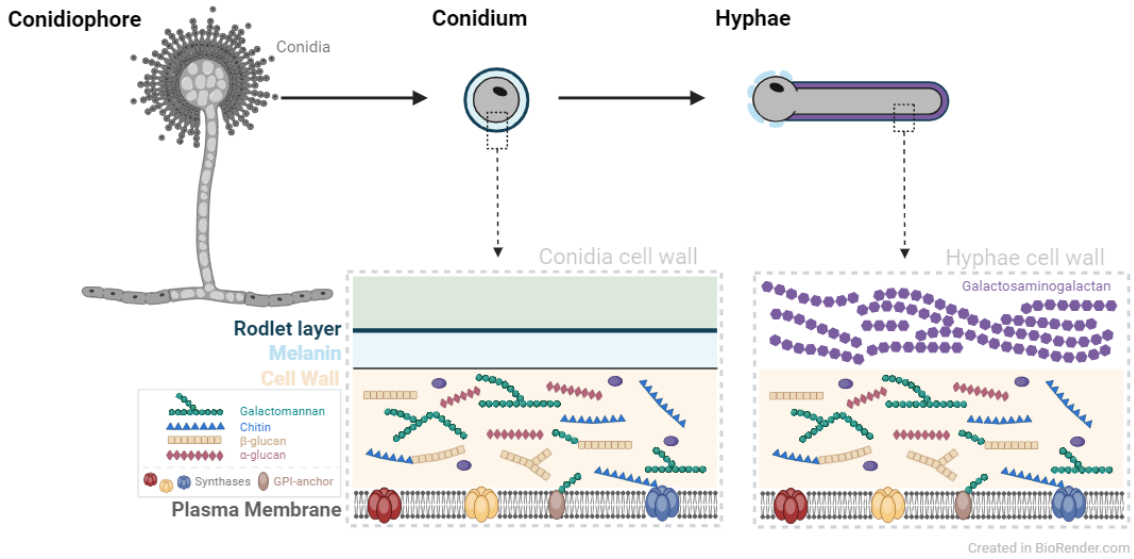



**Figure 7. *Aspergillus fumigatus* dynamic conidia and hyphae cell wall.** Conidiophore, the reproductive hyphal structure, produces and disseminates asexual spores, the conidia. The cell walls of conidia and hyphae of *Aspergillus fumigatus* contain PAMPs, namely β-glucan, α-glucan, galactomannan, and chitin. The surface of the conidia comprises a rodlet layer that confers hydrophobicity and a layer of melanin covering the cell wall carbohydrate structure, conferring protection against environmental stress and immune recognition. These conidia unique external layers are shed once conidia are swollen and germinate, forming hyphal structures, which contain a unique cell wall component, galactosaminogalactan.

Inhalation of *Aspergillus* spores is common and inert in immunocompetent individuals, as the conidia are rapidly eliminated. However, upon compromised immune system or underlying lung conditions, *Aspergillus* conidia inhalation can lead to three broad categories of pulmonary aspergillosis, namely allergic bronchopulmonary aspergillosis (ABPA), chronic pulmonary aspergillosis (CPA) and IPA (235,237–239). Although these diseases have some overlapping features, they are established in different clinical contexts, and the pathogenetic mechanisms and clinical manifestations are also distinct. The non-invasive form of pulmonary aspergillosis, namely ABPA, is mainly developed by patients with a history of asthma and cystic fibrosis (240–242). CPA generally affects patients who are not suffering from general immunodeficiency status but have an underlying lung condition, such as tuberculosis, chronic obstructive pulmonary disease (COPD), or sarcoidosis (239,243). IPA is the most severe form of pulmonary aspergillosis and occurs in severely immunocompromised hosts, which present an estimated mortality rate between 30% and 80% (244–247).

### 2.2.1. Invasive pulmonary aspergillosis

The annual incidence of IPA is more than 300,000 cases among around 10 million at-risk patients (248). The groups of patients at risk of developing IPA includes patients with profound or prolonged neutropenia post-chemotherapy or as a result of allogeneic hematopoietic stem cell transplant (249). In these patients, *Aspergillus* growth results in the spread of the infection, angioinvasion, galactomannan in circulation, and, in some cases, hemoptysis. Furthermore, in non-neutropenic patient populations, IPA is more likely to develop in solid organ transplant recipients (250,251), in critically ill patients in intensive care units (ICU) (252–255), in patients undergoing prolonged corticosteroid therapy (256), as well as in individuals with comorbidities such as COPD and human immunodeficiency virus (257–260). Critically ill hospitalized patients are becoming increasingly relevant due to the increasing incidence of *Aspergillus* co-infection in patients with severe respiratory viral infections, namely influenza and coronavirus disease of 2019 (COVID-19) (261–265). Since the recent COVID-19 pandemic, IPA emerged as one major complication in these patients, designated as COVID-19-associated pulmonary aspergillosis (CAPA). CAPA affected 10-15% of ICU-admitted COVID-19 patients with 50-55% estimated mortality (262–265).

The diagnosis of pulmonary fungal diseases is usually based on clinical and radiological features accompanied by serological or microbiological evidence (266). The gold standard for diagnosing IPA remains the detection of tissue invasion by *Aspergillus* hyphae through histopathological analysis, together with the detection of *Aspergillus* after culturing the patient BAL. The classic radiologic characteristics associated with IPA include the halo sign, an area of hemorrhagic pulmonary nodules, and a late appearance of the air crescent sign (267). Despite being the most reliable diagnostic criteria, sample collection for histopathology analysis requires invasive procedures and in many cases is hampered by host factors or clinical instability. Therefore, less invasive methods are increasingly being used, such galactomannan antigen detection in plasma, serum, BAL fluid, or cerebrospinal fluid (268).

Early initiation of IPA treatment is crucial for positive patient outcomes since it attenuates disease progression and decreases mortality (269). Indeed, if IPA is strongly suspected, antifungal therapy should begin even while the diagnosis is being confirmed (270). The primary treatment for IPA is a triazole antifungal agent, voriconazole, if a resistant pathogen is not suspected (270,271). This therapeutic agent integrates the class of azoles, which interfere in the synthesis of a fungal membrane component, the ergosterol (272,273). Another class of antifungal drugs is echinocandins, like caspofungin, which are β-(1,3)-glucans-synthesis inhibitors that can be used in combination with voriconazole to mitigate the fungal resistance (272,274,275). In case patients do not tolerate voriconazole or when it is advisable to avoid its side effects, alternative triazoles can be used, namely isavuconazole and posaconazole

(276,277). The first antifungal agent to show activity against *Aspergillus* was deoxycholate amphotericin B. This drug belongs to the class of polyenes antifungal drugs, which interact with fungal membrane sterols (272). Although this drug is still used in low-resource settings, which do not have alternative agents available, recommendations against its use emerged due to its poor safety profile (278,279). Lipid formulations of amphotericin B significantly improved this therapeutic option, specifically liposomal amphotericin B, amphotericin B lipid complex and colloidal dispersion. These lipid formulations are advantageous if there is a risk of drug interactions with azoles, severe hepatotoxicity, or if triazole-resistant pathogen is suspected (280). Despite the availability of antifungal treatment, mortality rates in immunocompromised patients with IPA remain high. Moreover, despite all the efforts to develop foolproof therapies, drug resistance remains a severe, unavoidable, difficult-to-overcome, and ever-increasing problem (281). Therefore, a better understanding of the mechanisms of pulmonary fungal recognition and subsequent host defense against *Aspergillus* remains required for identifying novel effective therapeutic strategies.

### 2.2.2 Recognition of *Aspergillus fumigatus* by pattern recognition receptors and antifungal immune response

Invading fungi are recognized by host immune cells through innate immune receptors termed pattern recognition receptors (PRRs), namely Toll-like receptors (TLRs), C-type lectin receptors (CLRs), nucleotide-binding oligomerization domain (NOD)-like receptors (NLRs) and/or retinoic acid-inducible gene-I-like receptors (Figure 8) (282,283). The PRRs on the cell surface directly recognize the respective PAMPs on the fungal cell wall and induce an innate antifungal response for immediate protection through fungal engulfment, production of cytokines and ROS or to further activate adaptive immunity. *Aspergillus fumigatus* recognition occurs mostly via the TLRs, TLR1, TLR2, TLR4 and TLR6, the CLRs, dectin-1, dectin-2, melanin-sensing C-type lectin receptor (MelLec), mannose receptor and DC-specific ICAM3-grabbing non–integrin (DC-SIGN) and the NLRs, NOD1, NOD2 and NLR family pyrin domain-containing 3 (NLRP3) (284). Additionally, extracellular proteins, such as pentraxins, ficolins, collectins and complement system proteins can act as opsonins that bind to *Aspergillus fumigatus*, facilitating its phagocytosis and elimination by the phagocytes through activation of the complement cascade (285).

The best characterized family of PRRs are TLRs, found at the cell surface (TLR1, TLR2, TLR4, TLR6) or in endocytic compartments (TLR3, TLR7, TLR9). TLRs are mostly expressed in monocytes, macrophages, dendritic cells (DCs) and neutrophils. Engagement of TLRs initiates signaling cascades, TLR4 in particular activates a signaling pathway from the cell surface through the adaptor protein myeloid differentiation

marker 88 (MyD88) (286). This adaptor protein mediates the translocation of NF-κB to the nucleus with subsequent production of proinflammatory cytokines. Furthermore, following ligand binding to TLR4, this receptor also undergoes endocytosis and engages Toll/interleukin-1 receptor domain-containing adaptor inducing IFN-β (TRIF)-dependent signaling from endosomes which induces the translocation of IFN regulatory factor 3 to the nucleus and transcription of type I IFN genes (287). TLR4 is the only that utilizes both adaptor proteins, the remaining transmembrane TLRs use MyD88 for signal transduction, while the intracellular TLRs use TRIF (Figure 8).

Members of the CLRs family involved in the recognition of *Aspergillus fumigatus* are the transmembrane receptors Dectin-1, Dectin-2, mannose receptor, DC-SIGN, MelLec and the soluble collectins mannose-binding lectin (MBL) and the lung surfactant proteins (SP) SP-A and SP-D (288) (Figure 8). The most studied *Aspergillus fumigatus* receptor is Dectin-1, which recognizes fungal β-(1,3)-glucans from several fungal pathogens and it is highly expressed in monocytes, macrophages, DCs and neutrophils (289,290). Several mice and human studies highlight the crucial role of this receptor for multiple antifungal defense mechanisms, including phagocytosis, ROS production, cytokine production, inflammasome activation and adaptive immunity response (289,290). Upon ligand binding, Dectin-1 promotes fungal uptake by phagocytosis and the initiation of a signaling cascade through the spleen tyrosine kinase (Syk)/caspase recruitment domain-containing protein 9 (CARD9) that regulates gene expression and cytokine production (Figure 8) (291,292). Dectin-2 is mainly expressed by alveolar macrophages (AMs) and DCs in response to *A. fumigatus* (293). Dectin-2 recognizes mannans of fungal cell walls and *A. fumigatus* galactomannan (293–296). Similarly to Dectin-1, Dectin-2 mediates NF-κB activation via Syk-CARD9 with subsequent cytokine production, as well as phagocytosis, ROS production and induction of adaptive immunity responses (Figure 8) (293). Recently, the MelLec CLR was reported to recognize dihydroxynaphthalene-melanin in the cell wall of *A. fumigatus* conidia, being essential for antifungal immunity and subsequent protection against the dissemination of *A. fumigatus* infection in mice (297). In mice MelLec expression is limited to endothelial cells, while in humans it is also expressed by myeloid cells (297). Another transmembrane receptor of the CLRs family, DC-SIGN, is expressed on the surface of macrophages and DCs (298–300). Galactomannans are suggested to be the main *A. fumigatus* conidia cell wall component recognized by DC-SIGN (301). Additionally, the mannose receptor recognizes N-linked mannan and it is mostly expressed in macrophages. Both CLRs, DC-SIGN and mannose receptor, can mediate endocytosis of fungal antigens, processing in DCs and subsequent presentation to T cells (302,303). Pulmonary collectins, SP-A, SP-D, and MBL serve as opsonins in response to *A. fumigatus* (304,305). *A. fumigatus* conidia opsonization by SP-A and SP-D enhances

conidia phagocytosis and elimination by AMs and neutrophils (306). Additionally, treatment of polymorphonuclear neutrophil with human recombinant MBL enhanced phagocytosis of *A. fumigatus* conidia, through MBL-mediated activation of the lectin pathway of the complement system (307,308). NLRs are cytoplasmatic PRRs which have been shown to be triggered by internalized pathogen components or by other PRRs. NLRs are divided into two major subsets, one composed by NOD1 and NOD2 and the other consists of inflammasome-forming NLRs. NOD1 and NOD2 are expressed in monocytes, macrophages, DCs, T and B lymphocytes. Although these non-inflammasome forming NLRs have not been thoroughly investigated, their recognition of *A. fumigatus* is known to mediate the release of proinflammatory cytokines (Figure 8) (309,310). More recently, a hyphal component of *A. fumigatus,* galactosaminogalactan, was reported to activate the NLRP3 inflammasome which leads to pro-IL-1β cleavage by caspase-1 and subsequent secretion of mature IL-1β, which has a central role in driving inflammation and mediating effective effector functions of immune cells (311,312).

The humoral innate immunity involves soluble pattern recognition molecules including complement components, ficolins, collectins, and pentraxins. Regarding the complement system, upon activation it acts by opsonization of the pathogen and by contributing to the recruitment and activation of immune cells (313,314). Moreover, the pentraxins family, which comprises multifunctional multimeric proteins, also act as opsonins, facilitating *A. fumigatus* phagocytosis. Particularly, pentraxin-3 is secreted by various types of cells, including monocytes, macrophages, neutrophils and DCs (315). Besides the well-recognized role as opsonins, the members of the pentraxin family, including pentraxin-3 and serum amyloid P component (SAP), can also promote protective innate effector functions against *A. fumigatus* through the activation of the classical complement system pathway (316–318).

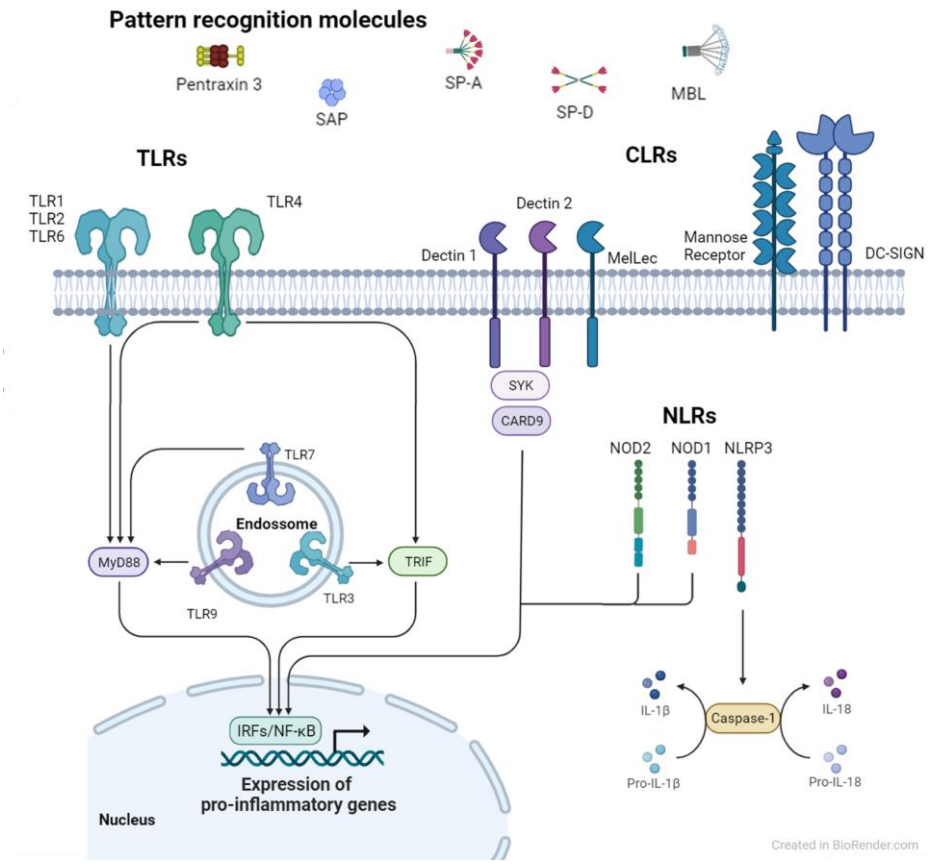



**Figure 8. Pattern recognition receptors involved or potentially involved in the innate immune detection of *Aspergillus fumigatus*.** *A. fumigatus* conidia can be sensed by the humoral system, namely soluble PPRs, as PTX3, SAP, SP-A, SP-D or MBL, which opsonize the conidia and facilitate the phagocytosis. Besides, PAMPs from the fungal cell wall can be recognized by transmembrane PRRs, such as TLR1, 2, 4, 6, and Dectin-1, Dectin-2, MelLec, DC-sign and Mannose receptor, activating signal-transducing pathways and subsequent production of cytokines. Response to *A. fumigatus* can also occur through intracellular receptors, such as TLR3 and NOD2. The sensing and internalization of the *A. fumigatus* conidia trigger the production of proinflammatory cytokines and chemokines, necessary for the activation of fungal elimination mechanisms in the own cell and for cell-to-cell communication. IRFs, Interferon regulatory factors.

PRRs are crucial mediators for initiating the innate antifungal response, both for immediate protection and to ultimately modulating the adaptive response. AMs are recognized as the first line of defense against *A. fumigatus* infection. Within 2 hours after macrophages infection with *A. fumigatus*, engulfment of the conidia occurs with concomitant release of cytokines and chemokines, responsible for further recruitment of innate effector cells (319–321). The pathogen recognition by macrophages also promotes phagolysosome acidification (322) and induces the production of ROS, with a maximum 3 hours after phagocytosis, as so inhibiting fungal germination (Figure 9) (319).

Early after infection by *A. fumigatus*, neutrophils are recruited to the lungs, serving a crucial role in the effective elimination of germinating conidia and extracellular hyphae through several mechanisms, including aggregation, phagocytosis, oxidative killing by nicotinamide adenine dinucleotide phosphate hydrogen (NADPH)-oxidase-mediated ROS production and non-oxidative killing by degranulation which releases proteins with antimicrobial activity, as defensins, serine proteases and lysozyme (Figure 9)

(323,324). Another neutrophil-mediated antimicrobial defense relies on their capacity to release NETs, which immobilize the pathogens, restricting the spread of the infection (Figure 9) (325). Moreover, neutrophils in the lung also act by lactoferrin-mediated iron sequestration or through lipocalin-1-mediated fungal siderophores sequestration, inhibiting conidial germination and fungal growth, respectively (326,327).

DCs are antigen-presenting cells (APCs) that act as the bridge between the innate and adaptive immune response. DCs derived from DCs progenitors can be categorized into plasmacytoid (pDCs) and classical (cDCs). pDCs contribute to the antifungal response by type I IFN, IFN-α, production and cDCs which undergo functional maturation at the infection site (328,329). Interestingly, immature DCs can directly phagocytose *A. fumigatus* conidia and hyphae, maturate at the site of the infection and then transport fungal antigens from the lung to draining lymph nodes and spleen, cross-presenting antigens to naïve T cells, activating the CD4 Th cells differentiation (Figure 9) (330–332). DCs trigger T cell proliferation and activation by binding their major histocompatibility complex (MHC) II to the T cell receptor (TCR), followed by the interaction of co-stimulatory molecules present on their surface (Figure 9) (330,331,333–336). Interestingly, Th1 cells are essential for the resistance to *Aspergillus* infection and to promote efficient IFN-γ- and TNF-mediated antifungal response of macrophages and neutrophils at the site of infection (284,337–340). Several studies highlight the crucial role of the Th1 response in protective immunity against *Aspergillus fumigatus*, but not all Th responses contribute to fungus elimination. In fact, Th2 response is known to mediate anti-inflammatory processes, protective immunity suppression and allergic disease associated with fungal persistence (284,337–339,341,342). In agreement, the blockage of the IL-4 receptor, which induces the differentiation into Th2 cells, resulted in increased survival of infected mice and these animals' acquired resistance against lethal reinfection (343). Thus, confirming that Th2 response is detrimental in fighting lung infection by *A. fumigatus*. Th17 cells contribute to potentiating antifungal response against *A. fumigatus* (290,344). Th17 cells are well-known for their secretion of IL-17A and IL-17F that trigger neutrophils chemoattraction to the site of infection and subsequent enhancement of their secretion of ROS, proteolytic enzymes and antimicrobial peptides (290,344–347). Despite the involvement of Th17 in enhanced fungal clearance, prolonged Th17 activation can cause pulmonary damage due to the induction of massive inflammation (348,349). Treg cells provide tolerance at the onset of infection, limit inflammation and prevent allergies associated with fungal persistence (350–352).

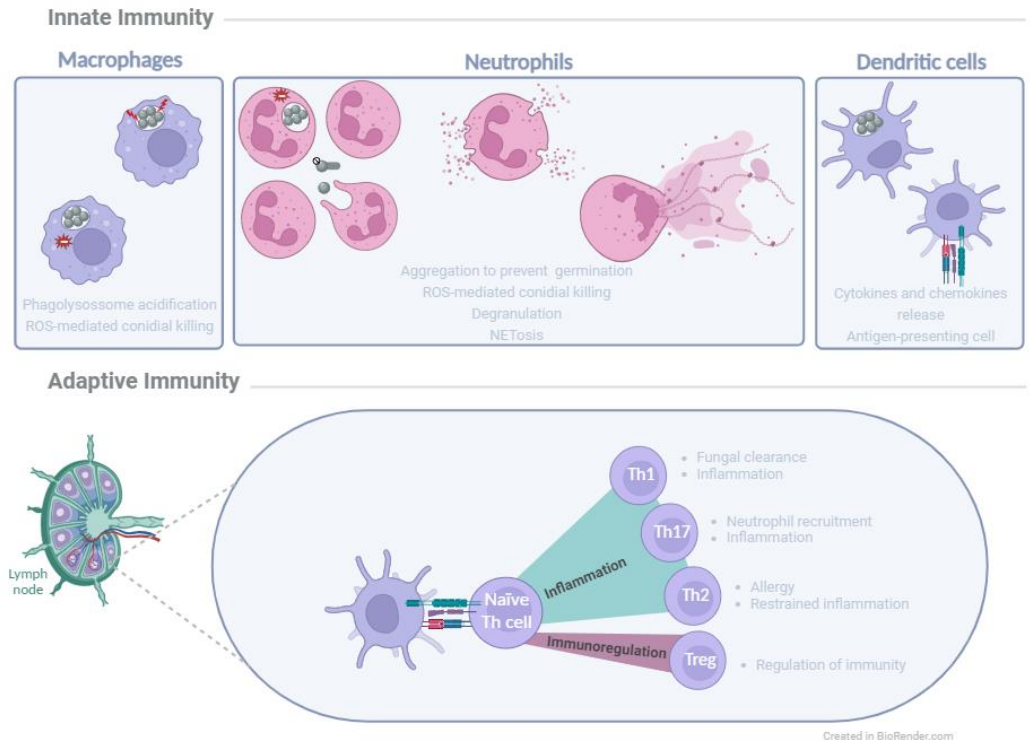



**Figure 9. Innate and adaptive immune responses to *Aspergillus fumigatus* infection.** Once *Aspergillus* conidia starts to germinate, the cells from the innate immune system, as macrophages, neutrophils and DCs, are able to recognize PAMPs in the fungal cell wall. Fungal germination is avoided by several effector processes, including phagocytosis, ROS production, degranulation, NETosis and antigen presentation. DCs are the bridge to adaptive immunity since they migrate to the lymph nodes and trigger T cells differentiation into Th1, Th2, Th17 and Treg, with distinct contributions to the antifungal response.

## 3. Aims

Recent studies have highlighted the crucial role of c-MET signaling in immune cells in inflammatory and infectious diseases, modulating the outcome of the respective pathological condition. However, nothing is known about the impact of c-MET signaling in immune cells in both lung inflammatory and infectious diseases. Therefore, the central purpose of this Doctoral Thesis was to investigate how c-MET signaling in immune cells modulates the progression of lung fibrosis-associated inflammation and the immune response to *A. fumigatus* infection, providing critical insights into the crosstalk between c-MET and lung immunity. Moreover, given the importance of macrophages as preservers of pulmonary homeostasis, first responders and defenders against lung injuries or threats, such as inhalation of infectious pathogens, in this Doctoral Thesis, we intend to emphasize the role of c-MET in pulmonary macrophage populations.

Taking this into consideration, this Doctoral Thesis had the following aims:

**Aim 1: To elucidate the involvement of the different macrophage populations in the pathogenesis of pulmonary fibrosis.** Previous studies have suggested that macrophages are present and adapt their phenotype and function when fibrogenesis is dominant. However, the individual contribution of macrophages from alveolar and interstitial compartments in the early stages of the BLM-induced pulmonary fibrosis mouse model is not clearly understood. Thus, the first aim was to characterize these macrophage populations and their paracrine effect on the progression of pulmonary fibrosis.

**Aim 2: To determine the role of c-MET in immune cells in BLM-induced pulmonary fibrosis progression and explore the potential of c-MET expression as a biomarker for distinct interstitial lung diseases.** Although the c-MET signaling pathway has been described in other inflammatory conditions as a potentiator of the proinflammatory activation of immune cells, its influence on the pulmonary fibrosis progression remains unexplored. A similar role for this signaling pathway would presuppose that its inhibition in immune cells could be useful in preventing lung injury caused by excessive proinflammatory milieu that culminates in lung fibrosis, which in the clinic would prevent fibrotic outcomes in ILD patients.

**Aim 3: To elucidate the role of c-MET in the antifungal immune response to *A. fumigatus* infection and in the susceptibility to invasive pulmonary aspergillosis.** Despite the role of the c-MET signaling pathway in the recognition and internalization of invading pathogens by epithelial cells and in the proinflammatory activation of immune cells, its role in the recognition and antifungal immune response to *A. fumigatus* infection and subsequent impact on the susceptibility to pulmonary aspergillosis remains unexplored. A similar role for this signaling pathway in the recognition and enhancement of the proinflammatory immune response to *A. fumigatus* infection would suggest that its over-activation in immune cells could be useful in fighting fungal infections.

## 4. References


1. Bladt, F., Riethmacher, D., Isenmann, S., Aguzzi, A. & Birchmeier, C. Essential role for the c-met receptor in the migration of myogenic precursor cells into the limb bud. *Nature* **376,** 768–771 (1995).
2. Dietrich, S. *et al.* The role of SF/HGF and c-Met in the development of skeletal muscle. *Development* **126,** 1621–1629 (1999).
3. Schmidt, C. *et al.* Scatter factor/hepatocyte growth factor is essential for liver development. *Nature* **373,** 699–702 (1995).
4. Uehara, Y. *et al.* Placental defect and embryonic lethality in mice lacking hepatocyte growth factor/scatter factor. *Nature* **373,** 702–705 (1995).
5. Birchmeier, C. & Gherardi, E. Developmental roles of HGF/SF and its receptor, the c-Met tyrosine kinase. *Trends Cell Biol.* **8,** 404–410 (1998).
6. Bussolino, F. *et al.* Hepatocyte growth factor is a potent angiogenic factor which stimulates endothelial cell motility and growth. *J. Cell Biol.* **119,** 629–641 (1992).
7. Takayama, H., La Rochelle, W. J., Anver, M., Bockman, D. E. & Merlino, G. Scatter factor/hepatocyte growth factor as a regulator of skeletal muscle and neural crest development. *Proc. Natl. Acad. Sci.* **93,** 5866–5871 (1996).
8. Andermarcher, E., Surani, M. A. & Gherardi, E. Co-expression of theHGF/SF andc-met genes during early mouse embryogenesis precedes reciprocal expression in adjacent tissues during organogenesis. *Dev. Genet.* **18,** 254–266 (1996).
9. Comoglio, P. M., Giordano, S. & Trusolino, L. Drug development of MET inhibitors: targeting oncogene addiction and expedience. *Nat. Rev. Drug Discov.* **7,** 504–516 (2008).
10. Okada, H. & Kalluri, R. Cellular and Molecular Pathways that Lead to Progression and Regression of Renal Fibrogenesis. *Curr. Mol. Med.* **5,** 467–474 (2005).
11. Liu, Y. & Yang, J. Hepatocyte growth factor: New arsenal in the fights against renal fibrosis? *Kidney Int.* **70,** 238–240 (2006).
12. Fu, H. *et al.* The hepatocyte growth factor/c-met pathway is a key determinant of the fibrotic kidney local microenvironment. *iScience* **24,** 103112 (2021).
13. Ueki, T. *et al.* Hepatocyte growth factor gene therapy of liver cirrhosis in rats. *Nat. Med.* **5,** 226–230 (1999).
14. Zhao, Y., Ye, W., Wang, Y. D. & Chen, W. D. HGF/c-Met: A Key Promoter in Liver Regeneration. *Front. Pharmacol.* **13,** 1–10 (2022).
15. Watanabe, M. *et al.* Hepatocyte Growth Factor Gene Transfer to Alveolar Septa for Effective Suppression of Lung Fibrosis. *Mol. Ther.* **12,** 58–67 (2005).
16. Nakamura, T. *et al.* Myocardial protection from ischemia/reperfusion injury by endogenous and exogenous HGF. *J. Clin. Invest.* **106,** 1511–1519 (2000).
17. Uchikawa, E., Chen, Z., Xiao, G.-Y., Zhang, X. & Bai, X. Structural basis of the activation of c-MET receptor. *Nat. Commun.* **12,** 4074 (2021).
18. Gherardi, E., Birchmeier, W., Birchmeier, C. & Woude, G. Vande. Targeting MET in cancer: Rationale and progress. *Nat. Rev. Cancer* **12,** 89–103 (2012).
19. Trusolino, L., Bertotti, A. & Comoglio, P. M. MET signalling: principles and functions in development, organ regeneration and cancer. *Nat. Rev. Mol. Cell Biol.* **11,** 834–848 (2010).
20. Imura, Y. *et al.* Functional and therapeutic relevance of hepatocyte growth factor/c-MET signaling in synovial sarcoma. *Cancer Sci.* **107,** 1867–1876 (2016).
21. Pilotto, S. *et al.* Tracking MET de-addiction in lung cancer: A road towards the oncogenic target. *Cancer Treat. Rev.* **60,** 1–11 (2017).
22. Wu, J.-C. *et al.* Heteronemin Is a Novel c-Met/STAT3 Inhibitor Against Advanced Prostate Cancer Cells. *Prostate* **76,** 1469–1483 (2016).

23. Safaie Qamsari, E. *et al.* The c-Met receptor: Implication for targeted therapies in colorectal cancer. *Tumor Biol.* **39,** 101042831769911 (2017).
24. Hughes, P. E. *et al. In vitro* and *In vivo* Activity of AMG 337, a Potent and Selective MET Kinase Inhibitor, in MET-Dependent Cancer Models. *Mol. Cancer Ther.* **15,** 1568–1579 (2016).
25. Kuang, W. *et al.* Hepatocyte growth factor induces breast cancer cell invasion via the PI3K/Akt and p38 MAPK signaling pathways to up-regulate the expression of COX2. *Am. J. Transl. Res.* **9,** 3816–3826 (2017).
26. Leung, E. *et al.* Blood vessel endothelium-directed tumor cell streaming in breast tumors requires the HGF/C-Met signaling pathway. *Oncogene* **36,** 2680–2692 (2017).
27. Goyal, L., Muzumdar, M. D. & Zhu, A. X. Targeting the HGF/c-MET Pathway in Hepatocellular Carcinoma. *Clin. Cancer Res.* **19,** 2310–2318 (2013).
28. Nishikoba, N. *et al.* HGF-MET Signaling Shifts M1 Macrophages Toward an M2-Like Phenotype Through PI3K-Mediated Induction of Arginase-1 Expression. *Front. Immunol.* **11,** 1–10 (2020).
29. Coudriet, G. M., He, J., Trucco, M., Mars, W. M. & Piganelli, J. D. Hepatocyte growth factor modulates interleukin-6 production in bone marrow derived macrophages: Implications for inflammatory mediated diseases. *PLoS One* **5,** 1–7 (2010).
30. Tesio, M. *et al.* Enhanced c-Met activity promotes G-CSF-induced mobilization of hematopoietic progenitor cells via ROS signaling. *Blood* **117,** 419–428 (2011).
31. Glodde, N. *et al.* Reactive Neutrophil Responses Dependent on the Receptor Tyrosine Kinase c-MET Limit Cancer Immunotherapy. *Immunity* **47,** 789-802.e9 (2017).
32. Finisguerra, V. *et al.* MET is required for the recruitment of anti-tumoural neutrophils. *Nature* **522,** 349–353 (2015).
33. Benkhoucha, M. *et al.* Identification of a novel population of highly cytotoxic c-Met-expressing CD8 + T lymphocytes. *EMBO Rep.* **18,** 1545–1558 (2017).
34. Loddo, I. & Romano, C. Inflammatory Bowel Disease: Genetics, Epigenetics, and Pathogenesis. *Front. Immunol.* **6,** 6–11 (2015).
35. Shapiro, J. M., Subedi, S. & LeLeiko, N. S. Inflammatory Bowel Disease. *Pediatr. Rev.* **37,** 337–347 (2016).
36. Shivashankar, R. & Lichtenstein, G. R. Mimics of Inflammatory Bowel Disease. *Inflamm. Bowel Dis.* **24,** 2315–2321 (2018).
37. Liu, Y. *et al.* Therapeutic effects of lentinan on inflammatory bowel disease and colitis-associated cancer. *J. Cell. Mol. Med.* **23,** 750–760 (2019).
38. Bressenot, A. *et al.* Comparing histological activity indexes in UC. *Gut* **64,** 1412–1418 (2015).
39. Geboes, K. A reproducible grading scale for histological assessment of inflammation in ulcerative colitis. *Gut* **47,** 404–409 (2000).
40. Fournier, B. M. & Parkos, C. A. The role of neutrophils during intestinal inflammation. *Mucosal Immunol.* **5,** 354–366 (2012).
41. Dinallo, V. *et al.* Neutrophil extracellulartraps sustain inflammatory signals in ulcerative colitis. *J. Crohn's Colitis* **13,** 772–784 (2019).
42. Stakenborg, M. *et al.* Neutrophilic HGF-MET Signalling Exacerbates Intestinal Inflammation. *J. Crohn's Colitis* **14,** 1748–1758 (2020).
43. Srivastava, M., Zurakowski, D., Cheifetz, P., Leichtner, A. & Bousvaros, A. Elevated serum hepatocyte growth factor in children and young adults with inflammatory bowel disease. *J. Pediatr. Gastroenterol. Nutr.* **33,** 548–553 (2001).
44. Baecher-Allan, C., Kaskow, B. J. & Weiner, H. L. Multiple Sclerosis: Mechanisms and Immunotherapy. *Neuron* **97,** 742–768 (2018).
45. Dendrou, C. A., Fugger, L. & Friese, M. A. Immunopathology of multiple sclerosis. *Nat. Rev. Immunol.* **15,** 545–558 (2015).

46. Glatigny, S. & Bettelli, E. Experimental Autoimmune Encephalomyelitis (EAE) as Animal Models of Multiple Sclerosis (MS). *Cold Spring Harb. Perspect. Med.* **8,** 1–19 (2018).
47. Müller, A. M., Jun, E., Conlon, H. & Sadiq, S. A. Cerebrospinal hepatocyte growth factor levels correlate negatively with disease activity in multiple sclerosis. *J. Neuroimmunol.* **251,** 80–86 (2012).
48. Moransard, M., Sawitzky, M., Fontana, A. & Suter, T. Expression of the HGF receptor c-met by macrophages in experimental autoimmune encephalomyelitis. *Glia* **58,** 559–571 (2010).
49. Bai, L. *et al.* Hepatocyte growth factor mediates mesenchymal stem cell-induced recovery in multiple sclerosis models. *Nat. Neurosci.* **15,** 862–870 (2012).
50. Benkhoucha, M. *et al.* Hepatocyte Growth Factor Limits Autoimmune Neuroinflammation via Glucocorticoid-Induced Leucine Zipper Expression in Dendritic Cells. *J. Immunol.* **193,** 2743–2752 (2014).
51. Benkhoucha, M. *et al.* Hepatocyte growth factor inhibits CNS autoimmunity by inducing tolerogenic dendritic cells and CD25+Foxp3+ regulatory T cells. *Proc. Natl. Acad. Sci. U. S. A.* **107,** 6424–6429 (2010).
52. Benkhoucha, M., Senoner, I. & Lalive, P. H. C-Met is expressed by highly autoreactive encephalitogenic CD8+ cells. *J. Neuroinflammation* **17,** 1–12 (2020).
53. Benkhoucha, M. *et al.* CD4+c-Met+Itgα4+ T cell subset promotes murine neuroinflammation. *J. Neuroinflammation* **19,** 103 (2022).
54. Benkhoucha, M. *et al.* c-Met enforces proinflammatory and migratory features of human activated CD4+ T cells. *Cell. Mol. Immunol.* **18,** 2051–2053 (2021).
55. Choi, W., Lee, J., Lee, J., Lee, S. H. & Kim, S. Hepatocyte Growth Factor Regulates Macrophage Transition to the M2 Phenotype and Promotes Murine Skeletal Muscle Regeneration. *Front. Physiol.* **10,** 914 (2019).
56. FitzGerald, R. & Smith, S. M. *Helicobacter Pylori*. *Methods Mol. Biol.* **2283,** 1–14 (2021).
57. Noto, J. M. & Peek, R. M. *Helicobacter pylori*: An Overview. *Methods Mol. Biol.* **921,** 7–10 (2012).
58. Chmiela, M., Walczak, N. & Rudnicka, K. *Helicobacter pylori* outer membrane vesicles involvement in the infection development and *Helicobacter pylori*-related diseases. *J. Biomed. Sci.* **25,** 78 (2018).
59. Cover, T. L., Lacy, D. B. & Ohi, M. D. The *Helicobacter pylori* Cag Type IV Secretion System. *Trends Microbiol.* **28,** 682–695 (2020).
60. Wang, F., Meng, W., Wang, B. & Qiao, L. *Helicobacter pylori*-induced gastric inflammation and gastric cancer. *Cancer Lett.* **345,** 196–202 (2014).
61. Churin, Y. *et al. Helicobacter pylori* CagA protein targets the c-Met receptor and enhances the motogenic response. *J. Cell Biol.* **161,** 249–255 (2003).
62. Oliveira, M. J. *et al.* CagA associates with c-met, E-cadherin, and p120catenin in a multiproteic complex that suppresses *Helicobacter pylori*-induced cell-invasive phenotype. *J. Infect. Dis.* **200,** 745–755 (2009).
63. Suzuki, M. *et al. Helicobacter pylori* CagA Phosphorylation-Independent Function in Epithelial Proliferation and Inflammation. *Cell Host Microbe* **5,** 23–34 (2009).
64. Li, N. *et al. Helicobacter pylori* CagA protein negatively regulates autophagy and promotes inflammatory response via c-Met-PI3K/Akt-mTOR signaling pathway. *Front. Cell. Infect. Microbiol.* **7,** 1–15 (2017).
65. Oliveira, M. J. *et al. Helicobacter pylori* Induces Gastric Epithelial Cell Invasion in a c-Met and Type IV Secretion System-dependent Manner. *J. Biol. Chem.* **281,** 34888–34896 (2006).
66. Rieke, C. *et al.* Non-T cell activation linker regulates ERK activation in *Helicobacter pylori*-infected epithelial cells. *Cell. Signal.* **22,** 395–403 (2010).
67. de Noordhout, C. M. *et al.* The global burden of listeriosis: a systematic review and meta-analysis.

*Lancet Infect. Dis.* **14,** 1073–1082 (2014).
68. Schlech, W. F. Epidemiology and Clinical Manifestations of *Listeria monocytogenes* Infection. *Microbiol. Spectr.* **7,** 793–802 (2019).
69. Mengaud, J., Ohayon, H., Gounon, P., Mège, R.-M. & Cossart, P. E-Cadherin Is the Receptor for Internalin, a Surface Protein Required for Entry of *L. monocytogenes* into Epithelial Cells. *Cell* **84,** 923–932 (1996).
70. Pentecost, M., Kumaran, J., Ghosh, P. & Amieva, M. R. *Listeria monocytogenes* Internalin B Activates Junctional Endocytosis to Accelerate Intestinal Invasion. *PLoS Pathog.* **6,** e1000900 (2010).
71. Shen, Y., Naujokas, M., Park, M. & Ireton, K. InlB-Dependent Internalization of *Listeria* Is Mediated by the Met Receptor Tyrosine Kinase. *Cell* **103,** 501–510 (2000).
72. Chalenko *et al.* Phylogenetically Defined Isoforms of *Listeria monocytogenes* Invasion Factor InlB Differently Activate Intracellular Signaling Pathways and Interact with the Receptor gC1q-R. *Int. J. Mol. Sci.* **20,** 4138 (2019).
73. Chalenko, Y. M. *et al.* Natural Isoforms of *Listeria monocytogenes* Virulence Factor Inlb Differ in c-Met Binding Efficiency and Differently Affect Uptake and Survival *Listeria* in Macrophage. *Int. J. Mol. Sci.* **24,** 7256 (2023).
74. Niemann, H. H. *et al.* Structure of the Human Receptor Tyrosine Kinase Met in Complex with the *Listeria* Invasion Protein InlB. *Cell* **130,** 235–246 (2007).
75. Spier, A. *et al.* Mitochondrial respiration restricts *Listeria monocytogenes* infection by slowing down host cell receptor recycling. *Cell Rep.* **37,** 109989 (2021).
76. Jiwani, S. *et al.* Identification of components of the host type IA phosphoinositide 3-kinase pathway that promote internalization of *Listeria monocytogenes*. *Infect. Immun.* **80,** 1252–1266 (2012).
77. Gessain, G. *et al.* PI3-kinase activation is critical for host barrier permissiveness to *Listeria monocytogenes*. *J. Exp. Med.* **212,** 165–183 (2015).
78. Mungunsukh, O. *et al.* A tandem repeat of a fragment of *Listeria monocytogenes* internalin B protein induces cell survival and proliferation. *Am. J. Physiol. Cell. Mol. Physiol.* **299,** L905–L914 (2010).
79. Kolditz, F., Krausze, J., Heinz, D. W., Niemann, H. H. & Müller-Goymann, C. C. Wound healing potential of a dimeric InlB variant analyzed by *in vitro* experiments on re-epithelialization of human skin models. *Eur. J. Pharm. Biopharm.* **86,** 277–283 (2014).
80. Chalenko, Y. *et al.* InlB protein secreted by *Listeria monocytogenes* controls the pathogen interaction with macrophages. *Bull. Russ. State Med. Univ.* **3,** 5–10 (2022).
81. Crump, J. A., Sjölund-Karlsson, M., Gordon, M. A. & Parry, C. M. Epidemiology, clinical presentation, laboratory diagnosis, antimicrobial resistance, and antimicrobial management of invasive Salmonella infections. *Clin. Microbiol. Rev.* **28,** 901–937 (2015).
82. Chowdhury, R., Das, S., Ta, A. & Das, S. Epithelial invasion by *Salmonella Typhi* using STIV–Met interaction. *Cell. Microbiol.* **21,** 1–17 (2019).
83. Jiang, X., McClellan, S. A., Barrett, R., Foldenauer, M. & Hazlett, L. D. HGF signaling impacts severity of *Pseudomonas aeruginosa* keratitis. *Investig. Ophthalmol. Vis. Sci.* **55,** 2180–2190 (2014).
84. Carrolo, M. *et al.* Hepatocyte growth factor and its receptor are required for malaria infection. *Nat. Med.* **9,** 1363–1369 (2003).
85. Leirião, P. *et al.* HGF/MET signalling protects *Plasmodium*-infected host cells from apoptosis. *Cell. Microbiol.* **7,** 603–609 (2005).
86. Kaushansky, A. & Kappe, S. H. I. The crucial role of hepatocyte growth factor receptor during liver-stage infection is not conserved among *Plasmodium* species. *Nat. Publ. Gr.* **17,** 1180–1181 (2011).

87. Silvie, O. *et al.* Hepatocyte CD81 is required for *Plasmodium falciparum* and *Plasmodium yoelii* sporozoite infectivity. *Nat. Med.* **9,** 93–96 (2003).
88. Adderley, J. D. *et al.* Analysis of erythrocyte signalling pathways during *Plasmodium falciparum* infection identifies targets for host-directed antimalarial intervention. *Nat. Commun.* **11,** 4015 (2020).
89. Cunha-Rodrigues, M. *et al.* Genistein-Supplemented Diet Decreases Malaria Liver Infection in Mice and Constitutes a Potential Prophylactic Strategy. *PLoS One* **3,** e2732 (2008).
90. Kaye, P. & Scott, P. Leishmaniasis : complexity at the host – pathogen interface. *Nat. Publ. Gr.* **9,** 604–615 (2011).
91. Burza, S., Croft, S. L. & Boelaert, M. Leishmaniasis. *Lancet* **392,** 951–970 (2018).
92. Al-Khalaifah, H. S. Major Molecular Factors Related to *Leishmania* Pathogenicity. *Front. Immunol.* **13,** 1–10 (2022).
93. Scott, P. & Novais, F. O. Cutaneous leishmaniasis: Immune responses in protection and pathogenesis. *Nat. Rev. Immunol.* **16,** 581–592 (2016).
94. Passelli, K. *et al.* The c-MET receptor tyrosine kinase contributes to neutrophil-driven pathology in cutaneous leishmaniasis. *PLoS Pathog.* **18,** 1–24 (2022).
95. Scully, C., El-Kabir, M. & Samaranayake, L. P. *Candida* and Oral Candidosis: A Review. *Crit. Rev. Oral Biol. Med.* **5,** 125–157 (1994).
96. Phan, Q. T. *et al.* Als3 Is a *Candida albicans* Invasin That Binds to Cadherins and Induces Endocytosis by Host Cells. *PLoS Biol.* **5,** e64 (2007).
97. Dwivedi, P. *et al.* Role of Bcr1-Activated Genes Hwp1 and Hyr1 in *Candida albicans* Oral Mucosal Biofilms and Neutrophil Evasion. *PLoS One* **6,** e16218 (2011).
98. Phan, Q. T. *et al. Candida albicans* stimulates formation of a multi-receptor complex that mediates epithelial cell invasion during oropharyngeal infection. *PLOS Pathog.* **19,** e1011579 (2023).
99. Travis, W. D. *et al.* An Official American Thoracic Society/European Respiratory Society Statement: Update of the International Multidisciplinary Classification of the Idiopathic Interstitial Pneumonias. *Am. J. Respir. Crit. Care Med.* **188,** 733–748 (2013).
100. Frank, A. L., Kreuter, M. & Schwarzkopf, L. Economic burden of incident interstitial lung disease (ILD) and the impact of comorbidity on costs of care. *Respir. Med.* **152,** 25–31 (2019).
101. Fan, Y. *et al.* Hospital-Based Resource Use and Costs Among Patients With Idiopathic Pulmonary Fibrosis Enrolled in the Idiopathic Pulmonary Fibrosis Prospective Outcomes (IPF-PRO) Registry. *Chest* **157,** 1522–1530 (2020).
102. Ryerson, C. J. & Collard, H. R. Update on the diagnosis and classification of ILD. *Curr. Opin. Pulm. Med.* **19,** 453–459 (2013).
103. American Thoracic Society & European Respiratory Society. American Thoracic Society/European Respiratory Society International Multidisciplinary Consensus Classification of the Idiopathic Interstitial Pneumonias. This joint statement of the American Thoracic Society (ATS), and the European Respiratory Society (ERS) was adopted by the ATS board of directors, June 2001 and by the ERS Executive Committee, June 2001. *Am. J. Respir. Crit. Care Med.* **165,** 277–304 (2002).
104. Raghu, G. *et al.* Diagnosis of idiopathic pulmonary fibrosis An Official ATS/ERS/JRS/ALAT Clinical practice guideline. *Am. J. Respir. Crit. Care Med.* **198,** e44–e68 (2018).
105. Richeldi, L., Collard, H. R. & Jones, M. G. Idiopathic pulmonary fibrosis. *Lancet* **389,** 1941–1952 (2017).
106. Brown, K. K. *et al.* The natural history of progressive fibrosing interstitial lung diseases. *Eur. Respir. J.* **55,** 1–15 (2020).
107. Nasser, M. *et al.* Estimates of epidemiology, mortality and disease burden associated with progressive fibrosing interstitial lung disease in France (the PROGRESS study). *Respir. Res.* **22,**

162 (2021).
108. Wijsenbeek, M. & Cottin, V. Spectrum of Fibrotic Lung Diseases. *N. Engl. J. Med.* **383,** 958–968 (2020).
109. Guler, S. A. *et al.* Does Systemic Sclerosis–associated Interstitial Lung Disease Burn Out? Specific Phenotypes of Disease Progression. *Ann. Am. Thorac. Soc.* **15,** 1427–1433 (2018).
110. Wijsenbeek, M., Suzuki, A. & Maher, T. M. Interstitial lung diseases. *Lancet* **400,** 769–786 (2022).
111. Wells, A. U., Brown, K. K., Flaherty, K. R., Kolb, M. & Thannickal, V. J. What's in a name? That which we call IPF, by any other name would act the same. *Eur. Respir. J.* **51,** 1800692 (2018).
112. Cottin, V. *et al.* Presentation, diagnosis and clinical course of the spectrum of progressive-fibrosing interstitial lung diseases. *Eur. Respir. Rev.* **27,** 180076 (2018).
113. Wong, A. W., Ryerson, C. J. & Guler, S. A. Progression of fibrosing interstitial lung disease. *Respir. Res.* **21,** 1–10 (2020).
114. Raghu, G. *et al.* Idiopathic Pulmonary Fibrosis (an Update) and Progressive Pulmonary Fibrosis in Adults: An Official ATS/ERS/JRS/ALAT Clinical Practice Guideline. *Am. J. Respir. Crit. Care Med.* **205,** E18–E47 (2022).
115. Fang, W. *et al.* Diagnosis of invasive fungal infections: challenges and recent developments. *J. Biomed. Sci.* **30,** 42 (2023).
116. Benedict, K., Jackson, B. R., Chiller, T. & Beer, K. D. Estimation of Direct Healthcare Costs of Fungal Diseases in the United States. *Clin. Infect. Dis.* **68,** 1791–1797 (2019).
117. Köhler, J. R., Hube, B., Puccia, R., Casadevall, A. & Perfect, J. R. Fungi that Infect Humans. *Microbiol. Spectr.* **5,** 811–843 (2017).
118. Lionakis, M. S., Iliev, I. D. & Hohl, T. M. Immunity against fungi. *JCI insight* **2,** e93156 (2017).
119. Yao, Z. & Liao, W. Fungal respiratory disease. *Curr. Opin. Pulm. Med.* **12,** 222–227 (2006).
120. Limper, A. H. *et al.* An Official American Thoracic Society Statement: Treatment of Fungal Infections in Adult Pulmonary and Critical Care Patients. *Am. J. Respir. Crit. Care Med.* **183,** 96–128 (2011).
121. Pates, K. M., Periselneris, J. N. & Brown, J. S. Opportunistic bacterial, viral and fungal infections of the lung. *Medicine (Baltimore).* **48,** 366–372 (2023).
122. Latgé, J.-P. *Aspergillus fumigatus* and Aspergillosis. *Clin. Microbiol. Rev.* **12,** 310–350 (1999).
123. Carvalho, A. *et al.* Inflammation in aspergillosis: the good, the bad, and the therapeutic. *Ann. N. Y. Acad. Sci.* **1273,** 52–59 (2012).
124. Chayakulkeeree, M. & Perfect, J. R. Cryptococcosis. *Infect. Dis. Clin. North Am.* **20,** 507–544 (2006).
125. Kronstad, J. W. *et al.* Expanding fungal pathogenesis: *Cryptococcus* breaks out of the opportunistic box. *Nat. Rev. Microbiol.* **9,** 193–203 (2011).
126. Mitchell, T. G. & Perfect, J. R. Cryptococcosis in the era of AIDS - 100 years after the discovery of *Crypotcoccus neoformans*. *Clin. Microbiol. Rev.* **8,** 515–548 (1995).
127. Burton, C. & Hanisch, B. Pneumocystis Pneumonia. *N. Engl. J. Med.* **351,** 1262–1263 (2004).
128. Denning, D. W. & Chakrabarti, A. Pulmonary and sinus fungal diseases in non-immunocompromised patients. *Lancet Infect. Dis.* **17,** e357–e366 (2017).
129. Brown, G. D. *et al.* Hidden killers: human fungal infections. *Sci. Transl. Med.* **4,** 165rv13 (2012).
130. Kosmidis, C. & Denning, D. W. The clinical spectrum of pulmonary aspergillosis. *Thorax* **70,** 270–277 (2015).
131. Cottin, V., Teague, R., Nicholson, L., Langham, S. & Baldwin, M. The Burden of Progressive-Fibrosing Interstitial Lung Diseases. *Front. Med.* **9,** 1–12 (2022).
132. Olson, A. *et al.* Estimation of the Prevalence of Progressive Fibrosing Interstitial Lung Diseases: Systematic Literature Review and Data from a Physician Survey. *Adv. Ther.* **38,** 854–867 (2021).
133. Cottin, V. Treatment of progressive fibrosing interstitial lung diseases: a milestone in the

management of interstitial lung diseases. *Eur. Respir. Rev.* **28,** 190109 (2019).
134. Olson, A. L., Gifford, A. H., Inase, N., Fernández Pérez, E. R. & Suda, T. The epidemiology of idiopathic pulmonary fibrosis and interstitial lung diseases at risk of a progressive-fibrosing phenotype. *Eur. Respir. Rev.* **27,** 180077 (2018).
135. King, T. E., Pardo, A. & Selman, M. Idiopathic pulmonary fibrosis. *Lancet* **378,** 1949–1961 (2011).
136. Ley, B., Collard, H. R. & King, T. E. Clinical Course and Prediction of Survival in Idiopathic Pulmonary Fibrosis. *Am. J. Respir. Crit. Care Med.* **183,** 431–440 (2011).
137. Hopkins, R. B., Burke, N., Fell, C., Dion, G. & Kolb, M. Epidemiology and survival of idiopathic pulmonary fibrosis from national data in Canada. *Eur. Respir. J.* **48,** 187–195 (2016).
138. Wijsenbeek, M. *et al.* Progressive fibrosing interstitial lung diseases: current practice in diagnosis and management. *Curr. Med. Res. Opin.* **35,** 2015–2024 (2019).
139. Kolb, M. *et al.* Acute exacerbations of progressive-fibrosing interstitial lung diseases. *Eur. Respir. Rev.* **27,** 180071 (2018).
140. Raghu, G. *et al.* An Official ATS/ERS/JRS/ALAT Statement: Idiopathic pulmonary fibrosis: Evidence-based guidelines for diagnosis and management. *Am. J. Respir. Crit. Care Med.* **183,** 788–824 (2011).
141. Selman, M., Pardo, A. & King, T. E. Hypersensitivity Pneumonitis. *Am. J. Respir. Crit. Care Med.* **186,** 314–324 (2012).
142. Vasakova, M. *et al.* Hypersensitivity Pneumonitis: Current Concepts of Pathogenesis and Potential Targets for Treatment. *Am. J. Respir. Crit. Care Med.* **200,** 301–308 (2019).
143. Costabel, U. *et al.* Hypersensitivity pneumonitis. *Nat. Rev. Dis. Prim.* **6,** 65 (2020).
144. Raghu, G. *et al.* Diagnosis of Hypersensitivity Pneumonitis in Adults: An Official ATS/JRS/ALAT Clinical Practice Guideline. *Am. J. Respir. Crit. Care Med.* **202,** e36–e69 (2020).
145. Spagnolo, P., Lee, J. S., Sverzellati, N., Rossi, G. & Cottin, V. The Lung in Rheumatoid Arthritis. *Arthritis Rheumatol.* **70,** 1544–1554 (2018).
146. Meyer, K. C. Pulmonary fibrosis, part I: epidemiology, pathogenesis, and diagnosis. *Expert Rev. Respir. Med.* **11,** 1–17 (2017).
147. Upagupta, C., Shimbori, C., Alsilmi, R. & Kolb, M. Matrix abnormalities in pulmonary fibrosis. *Eur. Respir. Rev.* **27,** 180033 (2018).
148. Hansell, D. M. *et al.* Fleischner Society: Glossary of Terms for Thoracic Imaging. *Radiology* **246,** 697–722 (2008).
149. Lynch, D. A. *et al.* Diagnostic criteria for idiopathic pulmonary fibrosis: a Fleischner Society White Paper. *Lancet Respir. Med.* **6,** 138–153 (2018).
150. Adderley, N. *et al.* Bronchoalveolar lavage fluid lymphocytosis in chronic hypersensitivity pneumonitis: a systematic review and meta-analysis. *Eur. Respir. J.* **56,** 2000206 (2020).
151. Meyer, K. C. *et al.* An Official American Thoracic Society Clinical Practice Guideline: The Clinical Utility of Bronchoalveolar Lavage Cellular Analysis in Interstitial Lung Disease. *Am. J. Respir. Crit. Care Med.* **185,** 1004–1014 (2012).
152. Hutchinson, J. P., McKeever, T. M., Fogarty, A. W., Navaratnam, V. & Hubbard, R. B. Surgical lung biopsy for the diagnosis of interstitial lung disease in England: 1997–2008. *Eur. Respir. J.* **48,** 1453–1461 (2016).
153. Fisher, J. H. *et al.* Procedure volume and mortality after surgical lung biopsy in interstitial lung disease. *Eur. Respir. J.* **53,** 1801164 (2019).
154. Tomassetti, S. *et al.* Bronchoscopic Lung Cryobiopsy Increases Diagnostic Confidence in the Multidisciplinary Diagnosis of Idiopathic Pulmonary Fibrosis. *Am. J. Respir. Crit. Care Med.* **193,** 745–752 (2016).
155. Troy, L. K. & Hetzel, J. Lung cryobiopsy and interstitial lung disease: What is its role in the era of

multidisciplinary meetings and antifibrotics? *Respirology* **25,** 987–996 (2020).
156. Troy, L. *et al.* Prevalence and prognosis of unclassifiable interstitial lung disease. *Eur. Respir. J.* **43,** 1529–1530 (2014).
157. Ryerson, C. J., Corte, T. J., Myers, J. L., Walsh, S. L. F. & Guler, S. A. A contemporary practical approach to the multidisciplinary management of unclassifiable interstitial lung disease. *Eur. Respir. J.* **58,** 2100276 (2021).
158. Ferreira, A. *et al.* Pulmonary Rehabilitation in Interstitial Lung Disease. *Chest* **135,** 442–447 (2009).
159. Al-Ghimlas, F. & Todd, D. C. Predictors of Success in Pulmonary Rehabilitation for Patients With Interstitial Lung Disease. *Chest* **136,** 1183–1184 (2009).
160. Dowman, L. M. *et al.* The evidence of benefits of exercise training in interstitial lung disease: a randomised controlled trial. *Thorax* **72,** 610–619 (2017).
161. Bell, E. C. *et al.* Oxygen therapy for interstitial lung disease: A systematic review. *Eur. Respir. Rev.* **26,** 1–7 (2017).
162. Idiopathic Pulmonary Fibrosis Clinical Research Network *et al.* Prednisone, azathioprine, and N-acetylcysteine for pulmonary fibrosis. *N. Engl. J. Med.* **366,** 1968–1977 (2012).
163. Morisset, J. *et al.* Use of Mycophenolate Mofetil or Azathioprine for the Management of Chronic Hypersensitivity Pneumonitis. *Chest* **151,** 619–625 (2017).
164. Tashkin, D. P. *et al.* Cyclophosphamide versus Placebo in Scleroderma Lung Disease. *N. Engl. J. Med.* **354,** 2655–2666 (2006).
165. Jee, A. S. & Corte, T. J. Current and Emerging Drug Therapies for Connective Tissue Disease-Interstitial Lung Disease (CTD-ILD). *Drugs* **79,** 1511–1528 (2019).
166. Raghu, G. *et al.* An Official ATS/ERS/JRS/ALAT Clinical Practice Guideline: Treatment of Idiopathic Pulmonary Fibrosis. An Update of the 2011 Clinical Practice Guideline. *Am. J. Respir. Crit. Care Med.* **192,** e3–e19 (2015).
167. Richeldi, L. *et al.* Efficacy and Safety of Nintedanib in Idiopathic Pulmonary Fibrosis. *N. Engl. J. Med.* **370,** 2071–2082 (2014).
168. Wright, W. A. *et al.* Real-world retrospective observational study exploring the effectiveness and safety of antifibrotics in idiopathic pulmonary fibrosis. *BMJ Open Respir. Res.* **8,** 1–8 (2021).
169. Wollin, L. *et al.* Mode of action of nintedanib in the treatment of idiopathic pulmonary fibrosis. *Eur. Respir. J.* **45,** 1434–1445 (2015).
170. Lamb, Y. N. Nintedanib: A Review in Fibrotic Interstitial Lung Diseases. *Drugs* **81,** 575–586 (2021).
171. Saito, S., Alkhatib, A., Kolls, J. K., Kondoh, Y. & Lasky, J. A. Pharmacotherapy and adjunctive treatment for idiopathic pulmonary fibrosis (IPF). *J. Thorac. Dis.* **11,** S1740–S1754 (2019).
172. Collins, B. F. & Raghu, G. Antifibrotic therapy for fibrotic lung disease beyond idiopathic pulmonary fibrosis. *Eur. Respir. Rev.* **28,** 190022 (2019).
173. Glassberg, M. K. Overview of idiopathic pulmonary fibrosis, evidence-based guidelines, and recent developments in the treatment landscape. *Am. J. Manag. Care* **25,** S195–S203 (2019).
174. Weill, D. *et al.* A consensus document for the selection of lung transplant candidates: 2014—An update from the Pulmonary Transplantation Council of the International Society for Heart and Lung Transplantation. *J. Hear. Lung Transplant.* **34,** 1–15 (2015).
175. Somogyi, V. *et al.* The therapy of idiopathic pulmonary fibrosis: what is next? *Eur. Respir. Rev.* **28,** 190021 (2019).
176. Amor, M. S. *et al.* Lung Transplantation in Idiopathic Pulmonary Fibrosis: Risk Factors and Outcome. *Isr. Med. Assoc. J.* **22,** 741–746 (2020).
177. Balestro, E. *et al.* Immune Inflammation and Disease Progression in Idiopathic Pulmonary Fibrosis. *PLoS One* **11,** e0154516 (2016).

178. Schupp, J. C. *et al.* Macrophage Activation in Acute Exacerbation of Idiopathic Pulmonary Fibrosis. *PLoS One* **10,** e0116775 (2015).
179. Le Saux, C. J. & Chapman, H. A. Idiopathic Pulmonary Fibrosis: Cell Death and Inflammation Revisited. *Am. J. Respir. Cell Mol. Biol.* **59,** 137–138 (2018).
180. Freund, A., Orjalo, A. V., Desprez, P.-Y. & Campisi, J. Inflammatory networks during cellular senescence: causes and consequences. *Trends Mol. Med.* **16,** 238–246 (2010).
181. Ryu, C. *et al.* Extracellular Mitochondrial DNA Is Generated by Fibroblasts and Predicts Death in Idiopathic Pulmonary Fibrosis. *Am. J. Respir. Crit. Care Med.* **196,** 1571–1581 (2017).
182. Futosi, K., Fodor, S. & Mócsai, A. Neutrophil cell surface receptors and their intracellular signal transduction pathways. *Int. Immunopharmacol.* **17,** 638–650 (2013).
183. Car, B. D. *et al.* Elevated IL-8 and MCP-1 in the bronchoalveolar lavage fluid of patients with idiopathic pulmonary fibrosis and pulmonary sarcoidosis. *Am. J. Respir. Crit. Care Med.* **149,** 655–659 (1994).
184. Ashitani, J. -i. *et al.* Granulocyte-colony stimulating factor levels in bronchoalveolar lavage fluid from patients with idiopathic pulmonary fibrosis. *Thorax* **54,** 1015–1020 (1999).
185. Guiot, J., Henket, M., Corhay, J. L., Moermans, C. & Louis, R. Sputum biomarkers in IPF: Evidence for raised gene expression and protein level of IGFBP-2, IL-8 and MMP-7. *PLoS One* **12,** e0171344 (2017).
186. Gregory, A. D. *et al.* Neutrophil elastase promotes myofibroblast differentiation in lung fibrosis. *J. Leukoc. Biol.* **98,** 143–152 (2015).
187. Taooka, Y., Maeda, A., Hiyama, K., Ishioka, S. & Yamakido, M. Effects of neutrophil elastase inhibitor on bleomycin-induced pulmonary fibrosis in mice. *Am. J. Respir. Crit. Care Med.* **156,** 260–265 (1997).
188. Takemasa, A., Ishii, Y. & Fukuda, T. A neutrophil elastase inhibitor prevents bleomycin-induced pulmonary fibrosis in mice. *Eur. Respir. J.* **40,** 1475–1482 (2012).
189. Saffarzadeh, M. *et al.* Neutrophil Extracellular Traps Directly Induce Epithelial and Endothelial Cell Death: A Predominant Role of Histones. *PLoS One* **7,** e32366 (2012).
190. Chrysanthopoulou, A. *et al.* Neutrophil extracellular traps promote differentiation and function of fibroblasts. *J. Pathol.* **233,** 294–307 (2014).
191. Ding, L., Yang, J., Zhang, C., Zhang, X. & Gao, P. Neutrophils Modulate Fibrogenesis in Chronic Pulmonary Diseases. *Front. Med.* **8,** 1–9 (2021).
192. Duru, N., Wolfson, B. & Zhou, Q. Mechanisms of the alternative activation of macrophages and non-coding RNAs in the development of radiation-induced lung fibrosis. *World J. Biol. Chem.* **7,** 231 (2016).
193. Song, E. *et al.* Influence of Alternatively and Classically Activated Macrophages on Fibrogenic Activities of Human Fibroblasts. *Cell. Immunol.* **204,** 19–28 (2000).
194. Wang, L. *et al.* Potential role of M2 macrophage polarization in ventilator-induced lung fibrosis. *Int. Immunopharmacol.* **75,** 105795 (2019).
195. Wynn, T. A. & Vannella, K. M. Macrophages in Tissue Repair, Regeneration, and Fibrosis. *Immunity* **44,** 450–462 (2016).
196. Prasse, A. *et al.* A Vicious Circle of Alveolar Macrophages and Fibroblasts Perpetuates Pulmonary Fibrosis via CCL18. *Am. J. Respir. Crit. Care Med.* **173,** 781–792 (2006).
197. Mora, A. L. *et al.* Activation of Alveolar Macrophages via the Alternative Pathway in Herpesvirus-Induced Lung Fibrosis. *Am. J. Respir. Cell Mol. Biol.* **35,** 466–473 (2006).
198. Gibbons, M. A. *et al.* Ly6C hi Monocytes Direct Alternatively Activated Profibrotic Macrophage Regulation of Lung Fibrosis. *Am. J. Respir. Crit. Care Med.* **184,** 569–581 (2011).
199. Wynn, T. & Barron, L. Macrophages: Master Regulators of Inflammation and Fibrosis. *Semin. Liver Dis.* **30,** 245–257 (2010).

200. Chen, X. *et al.* Macrophage polarization and its role in the pathogenesis of acute lung injury/acute respiratory distress syndrome. *Inflamm. Res.* **69,** 883–895 (2020).
201. Gordon, S., Plüddemann, A. & Martinez Estrada, F. Macrophage heterogeneity in tissues: phenotypic diversity and functions. *Immunol. Rev.* **262,** 36–55 (2014).
202. Bronte, V. & Zanovello, P. Regulation of immune responses by L-arginine metabolism. *Nat. Rev. Immunol.* **5,** 641–654 (2005).
203. Marchal-Sommé, J. *et al.* Cutting Edge: Nonproliferating Mature Immune Cells Form a Novel Type of Organized Lymphoid Structure in Idiopathic Pulmonary Fibrosis. *J. Immunol.* **176,** 5735–5739 (2006).
204. Nuovo, G. J. *et al.* The distribution of immunomodulatory cells in the lungs of patients with idiopathic pulmonary fibrosis. *Mod. Pathol.* **25,** 416–433 (2012).
205. Todd, N. *et al.* Lymphocyte aggregates persist and accumulate in the lungs of patients with idiopathic pulmonary fibrosis. *J. Inflamm. Res.* **6,** 63 (2013).
206. Schrier, D. J., Phan, S. H. & McGarry, B. M. The Effects of the Nude (nu/nu) Mutation on Bleomycin-induced Pulmonary Fibrosis. *Am. Rev. Respir. Dis.* **127,** 614–617 (1983).
207. Wynn, T. A. Fibrotic disease and the TH1/TH2 paradigm. *Nat. Rev. Immunol.* **4,** 583–594 (2004).
208. Roderfeld, M. *et al.* Bone marrow transplantation improves hepatic fibrosis in Abcb4 −/− mice via Th1 response and matrix metalloproteinase activity. *Gut* **61,** 907–916 (2012).
209. Keane, M. P., Belperio, J. A., Burdick, M. D. & Strieter, R. M. IL-12 attenuates bleomycin-induced pulmonary fibrosis. *Am. J. Physiol. Cell. Mol. Physiol.* **281,** L92–L97 (2001).
210. Saito, A., Okazaki, H., Sugawara, I., Yamamoto, K. & Takizawa, H. Potential Action of IL-4 and IL-13 as Fibrogenic Factors on Lung Fibroblasts *in vitro*. *Int. Arch. Allergy Immunol.* **132,** 168–176 (2003).
211. Zhu, Z. *et al.* Pulmonary expression of interleukin-13 causes inflammation, mucus hypersecretion, subepithelial fibrosis, physiologic abnormalities, and eotaxin production. *J. Clin. Invest.* **103,** 779–788 (1999).
212. Wynes, M. W., Frankel, S. K. & Riches, D. W. H. IL-4-induced macrophage-derived IGF-I protects myofibroblasts from apoptosis following growth factor withdrawal. *J. Leukoc. Biol.* **76,** 1019–1027 (2004).
213. Huaux, F. *et al.* Eosinophils and T Lymphocytes Possess Distinct Roles in Bleomycin-Induced Lung Injury and Fibrosis. *J. Immunol.* **171,** 5470–5481 (2003).
214. Wilson, M. S. *et al.* Bleomycin and IL-1β-mediated pulmonary fibrosis is IL-17A dependent. *J. Exp. Med.* **207,** 535–552 (2010).
215. Gu, P. *et al.* Protective function of interleukin-22 in pulmonary fibrosis. *Clin. Transl. Med.* **11,** e509 (2021).
216. Gasse, P. *et al.* IL-1 and IL-23 Mediate Early IL-17A Production in Pulmonary Inflammation Leading to Late Fibrosis. *PLoS One* **6,** e23185 (2011).
217. Chen, Y. *et al.* Neutralization of interleukin-17A delays progression of silica-induced lung inflammation and fibrosis in C57BL/6 mice. *Toxicol. Appl. Pharmacol.* **275,** 62–72 (2014).
218. Sonnenberg, G. F. *et al.* Pathological versus protective functions of IL-22 in airway inflammation are regulated by IL-17A. *J. Exp. Med.* **207,** 1293–1305 (2010).
219. Mi, S. *et al.* Blocking IL-17A Promotes the Resolution of Pulmonary Inflammation and Fibrosis Via TGF-β1–Dependent and –Independent Mechanisms. *J. Immunol.* **187,** 3003–3014 (2011).
220. Senoo, S. *et al.* Pulmonary fibrosis and type-17 immunity. *Respir. Investig.* **61,** 553–562 (2023).
221. Hou, Z. *et al.* Increased activated regulatory T cells proportion correlate with the severity of idiopathic pulmonary fibrosis. *Respir. Res.* **18,** 1–9 (2017).
222. Boveda-Ruiz, D. *et al.* Differential role of regulatory T cells in early and late stages of pulmonary fibrosis. *Immunobiology* **218,** 245–254 (2013).

223. Re, S. Lo *et al.* Platelet-derived growth factor-producing CD4 + foxp3 +regulatory T lymphocytes promote lung fibrosis. *Am. J. Respir. Crit. Care Med.* **184,** 1270–1281 (2011).
224. Xiong, S. *et al.* Treg depletion attenuates irradiation-induced pulmonary fibrosis by reducing fibrocyte accumulation, inducing Th17 response, and shifting IFN-γ, IL-12/IL-4, IL-5 balance. *Immunobiology* **220,** 1284–1291 (2015).
225. Birjandi, S. Z. *et al.* CD4+CD25hiFoxp3+ Cells Exacerbate Bleomycin-Induced Pulmonary Fibrosis. *Am. J. Pathol.* **186,** 2008–2020 (2016).
226. Daniil, Z. *et al.* CD8+ T lymphocytes in lung tissue from patients with idiopathic pulmonary fibrosis. *Respir. Res.* **6,** 2–9 (2005).
227. Habiel, D. M. *et al.* Characterization of CD28null T cells in idiopathic pulmonary fibrosis. *Mucosal Immunol.* **12,** 212–222 (2019).
228. Brodeur, T. Y. *et al.* IL-21 Promotes Pulmonary Fibrosis through the Induction of Profibrotic CD8+ T Cells. *J. Immunol.* **195,** 5251–5260 (2015).
229. Houbraken, J. *et al.* Classification of *Aspergillus*, *Penicillium*, *Talaromyces* and related genera (*Eurotiales*): An overview of families, genera, subgenera, sections, series and species. *Stud. Mycol.* **95,** 5–169 (2020).
230. Lamoth, F. *Aspergillus fumigatus*-Related Species in Clinical Practice. *Front. Microbiol.* **7,** 1–8 (2016).
231. Fernandez-Molina, J. V. *et al.* Rapid and specific detection of section *Fumigati* and *Aspergillus fumigatus* in human samples using a new multiplex real-time PCR. *Diagn. Microbiol. Infect. Dis.* **80,** 111–118 (2014).
232. Stemler, J. *et al.* Diagnosis and Treatment of Invasive Aspergillosis Caused by Non-*fumigatus Aspergillus* spp. *J. Fungi* **9,** 500 (2023).
233. Chakrabarti, A., Chatterjee, S. S., Das, A. & Shivaprakash, M. R. Invasive aspergillosis in developing countries. *Med. Mycol.* **49,** S35–S47 (2011).
234. Kwon-Chung, K. J. & Sugui, J. A. *Aspergillus fumigatus*—What Makes the Species a Ubiquitous Human Fungal Pathogen? *PLoS Pathog.* **9,** e1003743 (2013).
235. Van De Veerdonk, F. L., Gresnigt, M. S., Romani, L., Netea, M. G. & Latgé, J. P. *Aspergillus fumigatus* morphology and dynamic host interactions. *Nat. Rev. Microbiol.* **15,** 661–674 (2017).
236. Valsecchi, I. *et al.* The puzzling construction of the conidial outer layer of *Aspergillus fumigatus*. *Cell. Microbiol.* **21,** 1–22 (2019).
237. Kousha, M., Tadi, R. & Soubani, A. O. Pulmonary aspergillosis: a clinical review. *Eur. Respir. Rev.* **20,** 156–174 (2011).
238. Alastruey-Izquierdo, A. *et al.* Treatment of Chronic Pulmonary Aspergillosis: Current Standards and Future Perspectives. *Respiration* **96,** 159–170 (2018).
239. Denning, D. W. *et al.* Chronic pulmonary aspergillosis: rationale and clinical guidelines for diagnosis and management. *Eur. Respir. J.* **47,** 45–68 (2016).
240. Agarwal, R. Allergic Bronchopulmonary Aspergillosis. *Chest* **135,** 805–826 (2009).
241. Shah, A. & Panjabi, C. Allergic Bronchopulmonary Aspergillosis: A Perplexing Clinical Entity. *Allergy. Asthma Immunol. Res.* **8,** 282 (2016).
242. Mir, E. & Shah, A. Allergic bronchopulmonary aspergillosis in a patient with chronic obstructive pulmonary disease. *Prim. Care Respir. J.* **21,** 111–114 (2012).
243. Schweer, K. E., Bangard, C., Hekmat, K. & Cornely, O. A. Chronic pulmonary aspergillosis. *Mycoses* **57,** 257–270 (2014).
244. Baddley, J. W. *et al.* Factors Associated with Mortality in Transplant Patients with Invasive Aspergillosis. *Clin. Infect. Dis.* **50,** 1559–1567 (2010).
245. Humphrey, J. M., Walsh, T. J. & Gulick, R. M. Invasive Aspergillus Sinusitis in Human Immunodeficiency Virus Infection: Case Report and Review of the Literature. *Open forum Infect.*

*Dis.* **3,** ofw135 (2016).
246. Schauwvlieghe, A. F. A. D. *et al.* Invasive aspergillosis in patients admitted to the intensive care unit with severe influenza: a retrospective cohort study. *Lancet Respir. Med.* **6,** 782–792 (2018).
247. Ku, Y.-H. *et al.* Higher mortality of severe influenza patients with probable aspergillosis than those with and without other coinfections. *J. Formos. Med. Assoc.* **116,** 660–670 (2017).
248. Bongomin, F., Gago, S., Oladele, R. & Denning, D. Global and Multi-National Prevalence of Fungal Diseases—Estimate Precision. *J. Fungi* **3,** 57 (2017).
249. Neofytos, D. *et al.* Epidemiology and Outcome of Invasive Fungal Infection in Adult Hematopoietic Stem Cell Transplant Recipients: Analysis of Multicenter Prospective Antifungal Therapy (PATH) Alliance Registry. *Clin. Infect. Dis.* **48,** 265–273 (2009).
250. Patterson, J. E. *et al.* Investigation and control of aspergillosis and other filamentous fungal infections in solid organ transplant recipients. *Transpl. Infect. Dis.* **2,** 22–28 (2000).
251. Singh, N. & Paterson, D. L. *Aspergillus* infections in transplant recipients. *Clin. Microbiol. Rev.* **18,** 44–69 (2005).
252. Denning, D. W. Aspergillosis in "Nonimmunocompromised" Critically Ill Patients. *Am. J. Respir. Crit. Care Med.* **170,** 580–581 (2004).
253. Lat, A., Bhadelia, N., Miko, B., Furuya, E. Y. & Thompson, G. R. Invasive Aspergillosis after Pandemic (H1N1) 2009. *Emerg. Infect. Dis.* **16,** 971–973 (2010).
254. Meersseman, W., Lagrou, K., Maertens, J. & Wijngaerden, E. V. Invasive Aspergillosis in the Intensive Care Unit. *Clin. Infect. Dis.* **45,** 205–216 (2007).
255. Mercier, T. *et al.* Point of care *Aspergillus* testing in intensive care patients. *Crit. Care* **24,** 1–9 (2020).
256. Falcone, M., Massetti, A. P., Russo, A., Vullo, V. & Venditti, M. Invasive aspergillosis in patients with liver disease. *Med. Mycol.* **49,** 406–413 (2011).
257. Bulpa, P., Dive, A. & Sibille, Y. Invasive pulmonary aspergillosis in patients with chronic obstructive pulmonary disease. *Eur. Respir. J.* **30,** 782–800 (2007).
258. Guo, L., Wu, X. & Wu, X. Aspergillus infection in chronic obstructive pulmonary diseases. *Clin. Respir. J.* **17,** 129–138 (2023).
259. Holding, K. J. *et al.* Aspergillosis among people infected with human immunodeficiency virus: Incidence and survival. *Clin. Infect. Dis.* **31,** 1253–1257 (2000).
260. Denning, D. W. & Morgan, E. F. Quantifying Deaths from Aspergillosis in HIV Positive People. *J. Fungi* **8,** 1131 (2022).
261. Gaffney, S., Kelly, D. M., Rameli, P. M., Kelleher, E. & Martin-Loeches, I. Invasive pulmonary aspergillosis in the intensive care unit: current challenges and best practices. *APMIS* **131,** 654–667 (2023).
262. Mitaka, H., Kuno, T., Takagi, H. & Patrawalla, P. Incidence and mortality of COVID-19-associated pulmonary aspergillosis: A systematic review and meta-analysis. *Mycoses* **64,** 993–1001 (2021).
263. Feys, S. *et al.* A Visual and Comprehensive Review on COVID-19-Associated Pulmonary Aspergillosis (CAPA). *J. Fungi* **7,** 1067 (2021).
264. Koehler, P. *et al.* COVID-19 associated pulmonary aspergillosis. *Mycoses* **63,** 528–534 (2020).
265. White, P. L. *et al.* A National Strategy to Diagnose Coronavirus Disease 2019–Associated Invasive Fungal Disease in the Intensive Care Unit. *Clin. Infect. Dis.* **73,** e1634–e1644 (2021).
266. Denning, D. W. Diagnosing pulmonary aspergillosis is much easier than it used to be: a new diagnostic landscape. *Int. J. Tuberc. Lung Dis.* **25,** 525–536 (2021).
267. Denning, D. W. Invasive Aspergillosis. *Clin. Infect. Dis.* **26,** 781–803 (1998).
268. Peter Donnelly, J. *et al.* Revision and update of the consensus definitions of invasive fungal disease from the european organization for research and treatment of cancer and the mycoses study group education and research consortium. *Clin. Infect. Dis.* **71,** 1367–1376 (2020).

269. Kanj, A., Abdallah, N. & Soubani, A. O. The spectrum of pulmonary aspergillosis. *Respir. Med.* **141,** 121–131 (2018).
270. Patterson, T. F. *et al.* Practice Guidelines for the Diagnosis and Management of Aspergillosis: 2016 Update by the Infectious Diseases Society of America. *Clin. Infect. Dis.* **63,** e1–e60 (2016).
271. Ledoux, M. & Herbrecht, R. Invasive Pulmonary Aspergillosis. *J. Fungi* **9,** 131 (2023).
272. Robbins, N., Caplan, T. & Cowen, L. E. Molecular Evolution of Antifungal Drug Resistance. *Annu. Rev. Microbiol.* **71,** 753–775 (2017).
273. Ghannoum, M. A. & Rice, L. B. Antifungal Agents: Mode of Action, Mechanisms of Resistance, and Correlation of These Mechanisms with Bacterial Resistance. *Clin. Microbiol. Rev.* **12,** 501–517 (1999).
274. Patil, A. & Majumdar, S. Echinocandins in antifungal pharmacotherapy. *J. Pharm. Pharmacol.* **69,** 1635–1660 (2017).
275. Aruanno, M., Glampedakis, E. & Lamoth, F. Echinocandins for the Treatment of Invasive Aspergillosis: from Laboratory to Bedside. *Antimicrob. Agents Chemother.* **63,** e00399-19 (2019).
276. Walsh, T. J. *et al.* Treatment of Invasive Aspergillosis with Posaconazole in Patients Who Are Refractory to or Intolerant of Conventional Therapy: An Externally Controlled Trial. *Clin. Infect. Dis.* **44,** 2–12 (2007).
277. Maertens, J. A. *et al.* Isavuconazole versus voriconazole for primary treatment of invasive mould disease caused by *Aspergillus* and other filamentous fungi (SECURE): a phase 3, randomised-controlled, non-inferiority trial. *Lancet* **387,** 760–769 (2016).
278. Driemeyer, C. *et al.* The current state of clinical mycology in Africa: a European Confederation of Medical Mycology and International Society for Human and Animal Mycology survey. *The Lancet Microbe* **3,** e464–e470 (2022).
279. Tissot, F. *et al.* ECIL-6 guidelines for the treatment of invasive candidiasis, aspergillosis and mucormycosis in leukemia and hematopoietic stem cell transplant patients. *Haematologica* **102,** 433–444 (2017).
280. Thompson, G. & Patterson, T. Pulmonary Aspergillosis: Recent Advances. *Semin. Respir. Crit. Care Med.* **32,** 673–681 (2011).
281. Arastehfar, A. *et al. Aspergillus fumigatus* and aspergillosis: From basics to clinics. *Stud. Mycol.* **100,** 100115–100115 (2021).
282. Janeway, C. A. Approaching the Asymptote? Evolution and Revolution in Immunology. *Cold Spring Harb. Symp. Quant. Biol.* **54,** 1–13 (1989).
283. Brubaker, S. W., Bonham, K. S., Zanoni, I. & Kagan, J. C. Innate Immune Pattern Recognition: A Cell Biological Perspective. *Annu. Rev. Immunol.* **33,** 257–290 (2015).
284. Sales-Campos, H., Tonani, L., Cardoso, C. R. B. & Kress, M. R. V. Z. The Immune Interplay between the Host and the Pathogen in *Aspergillus fumigatus* Lung Infection. *Biomed Res. Int.* **2013,** 1–14 (2013).
285. Wong, S. S. W. & Aimanianda, V. Host Soluble Mediators: Defying the Immunological Inertness of *Aspergillus fumigatus* Conidia. *J. Fungi* **4,** 3 (2017).
286. Kagan, J. C. & Medzhitov, R. Phosphoinositide-Mediated Adaptor Recruitment Controls Toll-like Receptor Signaling. *Cell* **125,** 943–955 (2006).
287. Kagan, J. C. *et al.* TRAM couples endocytosis of Toll-like receptor 4 to the induction of interferon-β. *Nat. Immunol.* **9,** 361–368 (2008).
288. Lamoth, F., Rubino, I. & Bochud, P.-Y. Immunogenetics of invasive aspergillosis. *Med. Mycol.* **49,** S125–S136 (2011).
289. Taylor, P. R. *et al.* Dectin-1 is required for β-glucan recognition and control of fungal infection. *Nat. Immunol.* **8,** 31–38 (2007).
290. Werner, J. L. *et al.* Requisite Role for the Dectin-1 β-Glucan Receptor in Pulmonary Defense against

*Aspergillus fumigatus*. *J. Immunol.* **182,** 4938–4946 (2009).
291. Gessner, M. A. *et al.* Dectin-1-Dependent Interleukin-22 Contributes to Early Innate Lung Defense against *Aspergillus fumigatus*. *Infect. Immun.* **80,** 410–417 (2012).
292. Drummond, R. A. & Brown, G. D. The role of Dectin-1 in the host defence against fungal infections. *Curr. Opin. Microbiol.* **14,** 392–399 (2011).
293. Sun, H. *et al.* Activation of NF-κB and respiratory burst following *Aspergillus fumigatus* stimulation of macrophages. *Immunobiology* **219,** 25–36 (2014).
294. Saijo, S. *et al.* Dectin-2 Recognition of α-Mannans and Induction of Th17 Cell Differentiation Is Essential for Host Defense against *Candida albicans*. *Immunity* **32,** 681–691 (2010).
295. Levitz, S. M. Innate Recognition of Fungal Cell Walls. *PLoS Pathog.* **6,** e1000758 (2010).
296. Reedy, J. L. *et al.* The C-Type Lectin Receptor Dectin-2 Is a Receptor for *Aspergillus fumigatus* Galactomannan. *MBio* **14,** 1–14 (2023).
297. Stappers, M. H. T. *et al.* Recognition of DHN-melanin by a C-type lectin receptor is required for immunity to *Aspergillus*. *Nature* **555,** 382–386 (2018).
298. Serrano-Gómez, D., Antonio Leal, J. & Corbí, A. L. DC-SIGN mediates the binding of *Aspergillus fumigatus* and keratinophylic fungi by human dendritic cells. *Immunobiology* **210,** 175–183 (2005).
299. Park, S. J. & Mehrad, B. Innate Immunity to *Aspergillus* Species. *Clin. Microbiol. Rev.* **22,** 535–551 (2009).
300. Puig-Kröger, A. *et al.* Regulated Expression of the Pathogen Receptor Dendritic Cell-specific Intercellular Adhesion Molecule 3 (ICAM-3)-grabbing Nonintegrin in THP-1 Human Leukemic Cells, Monocytes, and Macrophages. *J. Biol. Chem.* **279,** 25680–25688 (2004).
301. Serrano-Gómez, D. *et al.* Dendritic Cell-Specific Intercellular Adhesion Molecule 3-Grabbing Nonintegrin Mediates Binding and Internalization of *Aspergillus fumigatus* Conidia by Dendritic Cells and Macrophages. *J. Immunol.* **173,** 5635–5643 (2004).
302. Lam, J. S., Huang, H. & Levitz, S. M. Effect of Differential N-linked and O-linked Mannosylation on Recognition of Fungal Antigens by Dendritic Cells. *PLoS One* **2,** e1009 (2007).
303. Frison, N. *et al.* Oligolysine-based Oligosaccharide Clusters. *J. Biol. Chem.* **278,** 23922–23929 (2003).
304. Neth, O. *et al.* Mannose-Binding Lectin Binds to a Range of Clinically Relevant Microorganisms and Promotes Complement Deposition. *Infect. Immun.* **68,** 688–693 (2000).
305. Allen, M. J., Harbeck, R., Smith, B., Voelker, D. R. & Mason, R. J. Binding of Rat and Human Surfactant Proteins A and D to *Aspergillus fumigatus* Conidia. *Infect. Immun.* **67,** 4563–4569 (1999).
306. Madan, T. *et al.* Binding of pulmonary surfactant proteins A and D to *Aspergillus fumigatus* conidia enhances phagocytosis and killing by human neutrophils and alveolar macrophages. *Infect. Immun.* **65,** 3171–3179 (1997).
307. Kaur, S., Gupta, V. K., Thiel, S., Sarma, P. U. & Madan, T. Protective role of mannan-binding lectin in a murine model of invasive pulmonary aspergillosis. *Clin. Exp. Immunol.* **148,** 382–389 (2007).
308. Endo, Y., Matsushita, M. & Fujita, T. Role of ficolin in innate immunity and its molecular basis. *Immunobiology* **212,** 371–379 (2007).
309. Li, Z., Tao, L., Zhang, J., Zhang, H. & Qu, J.-M. Role of NOD2 in regulating the immune response to *Aspergillus fumigatus*. *Inflamm. Res.* **61,** 643–648 (2012).
310. Zhang, H. *et al. Aspergillus fumigatus* conidia upregulates NOD2 protein expression both *in vitro* and *in vivo*. *Acta Pharmacol. Sin.* **29,** 1202–1208 (2008).
311. Briard, B. et al. Galactosaminogalactan activates the inflammasome to provide host protection. *Nature* **588**, 688–692 (2020).
312. Saïd-Sadier, N., Padilla, E., Langsley, G. & Ojcius, D. M. *Aspergillus fumigatus* Stimulates the

NLRP3 Inflammasome through a Pathway Requiring ROS Production and the Syk Tyrosine Kinase. *PLoS One* **5**, e10008 (2010).
313. Speth, C., Rambach, G., Würzner, R. & Lass-Flörl, C. Complement and fungal pathogens: an update. *Mycoses* **51**, 477–496 (2008).
314. Reis, E. S., Mastellos, D. C., Hajishengallis, G. & Lambris, J. D. New insights into the immune functions of complement. *Nat. Rev. Immunol.* **19**, 503–516 (2019).
315. Kang, Y., Yu, Y. & Lu, L. The Role of Pentraxin 3 in Aspergillosis: Reality and Prospects. *Mycobiology* **48,** 1–8 (2020).
316. Baruah, P. *et al.* The tissue pentraxin PTX3 limits C1q-mediated complement activation and phagocytosis of apoptotic cells by dendritic cells. *J. Leukoc. Biol.* **80,** 87–95 (2006).
317. Deban, L., Jaillon, S., Garlanda, C., Bottazzi, B. & Mantovani, A. Pentraxins in innate immunity: lessons from PTX3. *Cell Tissue Res.* **343,** 237–249 (2011).
318. Doni, A. *et al.* Serum amyloid P component is an essential element of resistance against *Aspergillus fumigatus*. *Nat. Commun.* **12,** 3739 (2021).
319. Philippe, B. *et al.* Killing of *Aspergillus fumigatus* by Alveolar Macrophages Is Mediated by Reactive Oxidant Intermediates. *Infect. Immun.* **71,** 3034–3042 (2003).
320. Steele, C. *et al.* The Beta-Glucan Receptor Dectin-1 Recognizes Specific Morphologies of *Aspergillus fumigatus*. *PLoS Pathog.* **1,** e42 (2005).
321. Camargo, J. F. & Husain, S. Immune correlates of protection in human invasive aspergillosis. *Clin. Infect. Dis.* **59,** 569–577 (2014).
322. Ibrahim-Granet, O. *et al.* Phagocytosis and Intracellular Fate of *Aspergillus fumigatus* Conidia in Alveolar Macrophages. *Infect. Immun.* **71,** 891–903 (2003).
323. Bonnett, C. R., Cornish, E. J., Harmsen, A. G. & Burritt, J. B. Early Neutrophil Recruitment and Aggregation in the Murine Lung Inhibit Germination of *Aspergillus fumigatus* Conidia. *Infect. Immun.* **74,** 6528–6539 (2006).
324. Feldmesser, M. Role of neutrophils in invasive aspergillosis. *Infect. Immun.* **74,** 6514–6516 (2006).
325. Jaillon, S. *et al.* The humoral pattern recognition receptor PTX3 is stored in neutrophil granules and localizes in extracellular traps. *J. Exp. Med.* **204,** 793–804 (2007).
326. Gazendam, R. P. *et al.* Human Neutrophils Use Different Mechanisms To Kill *Aspergillus fumigatus* Conidia and Hyphae: Evidence from Phagocyte Defects. *J. Immunol.* **196,** 1272–1283 (2016).
327. Leal, S. M. *et al.* Targeting Iron Acquisition Blocks Infection with the Fungal Pathogens *Aspergillus fumigatus* and Fusarium oxysporum. *PLoS Pathog.* **9,** e1003436 (2013).
328. Ramirez-Ortiz, Z. G. & Means, T. K. The role of dendritic cells in the innate recognition of pathogenic fungi (*A. fumigatus*, *C. neoformans* and *C. albicans*). *Virulence* **3,** 635–646 (2012).
329. Reizis, B., Bunin, A., Ghosh, H. S., Lewis, K. L. & Sisirak, V. Plasmacytoid Dendritic Cells: Recent Progress and Open Questions. *Annu. Rev. Immunol.* **29,** 163–183 (2011).
330. Bozza, S. *et al.* Dendritic Cells Transport Conidia and Hyphae of *Aspergillus fumigatus* from the Airways to the Draining Lymph Nodes and Initiate Disparate Th Responses to the Fungus. *J. Immunol.* **168,** 1362–1371 (2002).
331. Lother, J. *et al.* Human dendritic cell subsets display distinct interactions with the pathogenic mould *Aspergillus fumigatus*. *Int. J. Med. Microbiol.* **304,** 1160–1168 (2014).
332. Loures, F. V. *et al.* Recognition of *Aspergillus fumigatus* Hyphae by Human Plasmacytoid Dendritic Cells Is Mediated by Dectin-2 and Results in Formation of Extracellular Traps. *PLOS Pathog.* **11,** e1004643 (2015).
333. Gafa, V. *et al. In vitro* infection of human dendritic cells by *Aspergillus fumigatus* conidia triggers the secretion of chemokines for neutrophil and Th1 lymphocyte recruitment. *Microbes Infect.* **9,** 971–980 (2007).

334. Gafa, V. *et al.* Human Dendritic Cells following *Aspergillus fumigatus* Infection Express the CCR7 Receptor and a Differential Pattern of Interleukin-12 (IL-12), IL-23, and IL-27 Cytokines, Which Lead to a Th1 Response. *Infect. Immun.* **74,** 1480–1489 (2006).
335. Bozza, S. *et al.* Immune Sensing of *Aspergillus fumigatus* Proteins, Glycolipids, and Polysaccharides and the Impact on Th Immunity and Vaccination. *J. Immunol.* **183,** 2407–2414 (2009).
336. Fei, M. *et al.* TNF-α from inflammatory dendritic cells (DCs) regulates lung IL-17A/IL-5 levels and neutrophilia versus eosinophilia during persistent fungal infection. *Proc. Natl. Acad. Sci.* **108,** 5360–5365 (2011).
337. Arias, M. *et al.* Preparations for Invasion: Modulation of Host Lung Immunity During Pulmonary Aspergillosis by Gliotoxin and Other Fungal Secondary Metabolites. *Front. Immunol.* **9,** 1–12 (2018).
338. Bellocchio, S. *et al.* Immunity to *Aspergillus fumigatus*: the basis for immunotherapy and vaccination. *Med. Mycol.* **43,** 181–188 (2005).
339. Cenci, E. *et al.* Cytokine- and T Helper–Dependent Lung Mucosal Immunity in Mice with Invasive Pulmonary Aspergillosis. *J. Infect. Dis.* **178,** 1750–1760 (1998).
340. Nagai, H., Guo, J., Choi, H. & Kurup, V. Interferon- and Tumor Necrosis Factor- Protect Mice from Invasive Aspergillosis. *J. Infect. Dis.* **172,** 1554–1560 (1995).
341. Moss, R. B. Pathophysiology and immunology of allergic bronchopulmonary aspergillosis. *Med. Mycol.* **43,** 203–206 (2005).
342. Cenci, E. *et al.* Interleukin-4 Causes Susceptibility to Invasive Pulmonary Aspergillosis through Suppression of Protective Type I Responses. *J. Infect. Dis.* **180,** 1957–1968 (1999).
343. Cenci, E. *et al.* Th1 and Th2 cytokines in mice with invasive aspergillosis. *Infect. Immun.* **65,** 564–570 (1997).
344. LeibundGut-Landmann, S., Wüthrich, M. & Hohl, T. M. Immunity to fungi. *Curr. Opin. Immunol.* **24,** 449–458 (2012).
345. Kolls, J. K. & Lindén, A. Interleukin-17 Family Members and Inflammation. *Immunity* **21,** 467–476 (2004).
346. Van De Veerdonk, F. L. *et al.* Th17 responses and host defense against microorganisms: an overview. *BMB Rep.* **42,** 776–787 (2009).
347. Way, E. E., Chen, K. & Kolls, J. K. Dysregulation in lung immunity - The protective and pathologic Th17 response in infection. *Eur. J. Immunol.* **43,** 3116–3124 (2013).
348. Zelante, T. *et al.* Th17 cells in the setting of *Aspergillus* infection and pathology. *Med. Mycol.* **47,** S162–S169 (2009).
349. Zelante, T. *et al.* IL-23 and the Th17 pathway promote inflammation and impair antifungal immune resistance. *Eur. J. Immunol.* **37,** 2695–2706 (2007).
350. Montagnoli, C. *et al.* Immunity and Tolerance to *Aspergillus* Involve Functionally Distinct Regulatory T Cells and Tryptophan Catabolism. *J. Immunol.* **176,** 1712–1723 (2006).
351. Wüthrich, M., Deepe, G. S. & Klein, B. Adaptive Immunity to Fungi. *Annu. Rev. Immunol.* **30,** 115–148 (2012).
352. Wang, F. *et al.* Innate and adaptive immune response to chronic pulmonary infection of hyphae of *Aspergillus fumigatus* in a new murine model. *J. Med. Microbiol.* **66,** 1400–1408 (2017).

# CHAPTER II

## Interstitial Macrophages Lead Early Stages of Bleomycin-Induced Lung Fibrosis and Induce Fibroblasts Activation

This chapter was published in:

Libório-Ramos, S., Barbosa-Matos, C., Fernandes, R., Borges-Pereira, C. & Costa, S. Interstitial Macrophages Lead Early Stages of Bleomycin-Induced Lung Fibrosis and Induce Fibroblasts Activation. *Cells* **12,** 402 (2023).

# Interstitial Macrophages Lead Early Stages of Bleomycin-Induced Lung Fibrosis and Induce Fibroblasts Activation

Sofia Libório-Ramos[1,2,†], Catarina Barbosa-Matos[1,2,†], Raquel Fernandes[1,2], Caroline Borges-Pereira[1,2] and Sandra Costa[1,2,*]

[1] Life and Health Sciences Research Institute (ICVS), School of Medicine, University of Minho, Campus Gualtar, 4710-057 Braga, Portugal

[2] ICVS/3B's - PT Government Associate Laboratory, Braga/Guimarães, Portugal

*Correspondence: sandracosta@med.uminho.pt

†These authors contributed equally to this work.

## Abstract

A progressive fibrosing phenotype is critical in several lung diseases. It is irreversible and associated with early patient mortality. Growing evidence has revealed pulmonary macrophages' role as modulators of the fibrotic processes. The proportion, phenotype, and function of alveolar (AMs) and interstitial macrophages (IMs) at the early stages of bleomycin-induced pulmonary fibrosis have not been clearly described. In this way, our study aimed to characterize these macrophage populations and investigate the effect on fibroblast activation. C57BL/6 mice were intratracheally injected with bleomycin and were sacrificed at day 3, 5, and 7 to perform flow cytometry and fluorescent-activated cell sorting analysis for protein and gene expression quantification. After bleomycin administration, the proportion of IMs was significantly higher than that of AMs, which showed a decay during the inflammatory phase, and peaked at day 7. At day 7 of the inflammatory phase, AMs started shifting their phenotype from M1-like towards M2, while IMs showed a M2-like phenotype. Conditioned medium derived from IMs sorted at day 7 induced fibroblast activation and differentiation in myofibroblasts *in vitro*. Our findings indicate that IMs are the largest macrophage population at the early stages of experimental pulmonary fibrosis and secrete mediators able to activate fibroblasts, pointing to macrophage modulation as a potential therapeutic strategy to restrain progressive fibrosing lung disorders.

## Keywords

Pulmonary fibrosis; interstitial macrophages; alveolar macrophages; conditioned medium; fibroblasts; myofibroblasts

## 1. Introduction

Idiopathic pulmonary fibrosis is the most severe and fatal form of fibrosing lung diseases, with a median survival term of only 2 to 3 years after diagnosis (1,2). Even with the poor prognosis of this disease, its etiology remains undetermined. Despite the poorly defined pathophysiology, it is thought to be caused by a chronic injury in the alveolar epithelial cells induced by aberrant wound healing (3). Unfortunately, current therapeutic strategies remain limited and can delay the disease progression rather than provide a cure (4). Therefore, there is an urgent need to develop new and efficient therapeutic strategies.

In addition to occurring in idiopathic pulmonary fibrosis, pulmonary fibrosis is also a common denominator of several lung disorders and is characterized by the accumulation of myofibroblasts and excessive deposition of ECM (1,5,6). These processes culminate in the formation of a fibrotic 'scar' which leads to the irreversible destruction of lung architecture and, ultimately, to death due to respiratory failure (1,5,6). There is increasing evidence that the immune system is involved in the progression of this pathologic condition. Macrophages are particularly prominent at sites of inflammation and fibrosis, rising as a crucial cell population in these processes (7,8).

During adulthood, macrophages are the central innate immune cells in the lung under homeostatic conditions and are known as the first line of defense in many organs (9). Diverse and distinct macrophage populations exist in the lung. Resident alveolar macrophages (AMs) are mainly derived from precursors in the embryo and populate the airway space soon after birth (10–12). In a steady state, this population is capable of self-renewal and persists in the lung, being the most represented macrophage population in normal adult mice lungs (13). Moreover, a population of recruited AMs arises postnatally from circulating bone marrow-derived monocytes (14). AMs are the best studied and understood lung macrophage population. However, interstitial macrophages (IMs), infiltrated within the lung parenchyma, are rising as critical players in murine lung fibrosis (7,13,15). The origin and function of IMs are still not completely clarified, partly due to the difficulties in isolating this population (13,16). It is believed that IMs originate both from embryonic yolk sac origin and postnatal bone marrow (10,17).

There is increasing evidence of the importance of interstitial and alveolar macrophages in pulmonary fibrosis (18–21). However, their role may be controversial due to their heterogeneity and plasticity which confer them the capacity to exert tissue-specific functions according to the stimuli of the microenvironment which can induce, for example, the dichotomic M1/M2 metabolic state (7, 8). In fact, macrophages can switch between these two different activation states, which dictates how they modulate fibroproliferative responses. It has been suggested that classically activated macrophages (M1) maintain

tissue inflammation, while alternatively activated macrophages (M2) play a role in resolving lung inflammation and aberrant wound healing cascade during fibrosis (9,22,23).

Macrophages are present and adapt their phenotype and function when fibrogenesis is dominant. However, the detailed individual contribution of macrophages, both from the alveolar and interstitial compartments, in the early stages of the lung fibrosis progression has not yet been fully evidenced. In this study, we use a bleomycin (BLM)-induced pulmonary fibrosis mouse model to characterize alveolar and interstitial macrophages in the initial stages of disease progression. In addition, we provide *in vitro* data to determine the paracrine effect played by IMs in the advancement of lung fibrosis.

## 2. Materials and Methods

### Mice

Eight-week-old gender- and age-matched C57BL/6 mice were bred under specific pathogen-free conditions and kept at the Life and Health Sciences Research Institute (ICVS) Animal Facility. Mice were fed *ad libitum* and kept under light/dark cycles of 12 h, temperature of 18–25 °C, and humidity of 40-60%.

All procedures *in vivo* followed the EU-adopted regulations (Directive 2010/63/EU). The ethical and regulatory approvals were consented by the Direção Geral de Alimentação e Veterinária (DGAV, ref. 003671) and conducted according to their guidelines.

### Bleomycin-Induced Pulmonary Fibrosis Mouse Model

Male C57BL/6J mice, 10 to 12 week old, were anesthetized with an intraperitoneal injection of ketamine and medetomidine, followed by intratracheal administration of BLM sulphate (BML-AP302-0010, Enzo Life Sciences) as a single dose of 2 mg/kg body weight dissolved in 50 µL saline (treated) or, as control, with saline alone (untreated)—day 0. Weight was measured every single day throughout the experiment. At 3, 5, and 7 days after BLM administration mice were euthanized. Mice were sacrificed by excessive doses of anesthesia to collect bronchoalveolar lavage fluid (BALF) and lung single-cell suspensions. Regarding the number of animals for flow cytometry analysis, 7–10 mice (*per* timepoint) were injected and sacrificed at day 3, 5, and 7. For fluorescence-activated cell sorting, performed at day 7, 15 mice were injected with saline (untreated), and 15 mice were injected with bleomycin.

### Bronchoalveolar Lavage (BAL)

In brief, the trachea was exposed by a midline incision and cannulated. Bilateral BALF was recovered by lavage three times with 1 mL phosphate-buffered saline (PBS) 1x. After collection, BALF cells were maintained on ice to be then added to single-cell suspensions obtained from tissue dissociation.

### Preparation of Lung Single-Cell Suspensions

Briefly, mice were over-anesthetized intraperitoneally and perfused with 20 mL of sterile PBS 1x. After dissection, lungs were placed in dispase (11553550, Corning) while being minced into 2–3 $mm^3$ pieces for 20 min at room temperature. Then, lungs were also digested in Dulbecco's Modified Eagle Medium (DMEM) 1 (21969-035, Gibco) containing 1 mg/mL DNase I (10104159001, Roche) and 5 mg/mL collagenase II (17101-015, Gibco). After an enzymatic digestion period of 10 min at 37 °C, tissue disruption was performed by mechanical titrations with P1000 tip, and then a second incubation period of 10 min was performed at 37 °C. After incubation, the disrupted tissue suspension was collected and

sequentially filtered through 100 µm and 70 µm cell strainers. The pellet was resuspended in ACK lysis buffer (A1049201, Gibco) and incubated for 4 min. Cells were then resuspended in cold PBS 1x containing 4% fetal bovine serum (FBS-10270-106, Gibco). These lung single-cell suspensions were used to analyze the expression of various surface markers for immune cells by flow cytometry and magnetic (MACS)- and fluorescence (FACS)-activated cell-sorting-based separation.

### Flow Cytometry

In brief, lung cells were harvested, washed, and resuspended in cold PBS containing 4% FBS. Then, 1 x $10^6$ cells were preincubated with TruStain FcX anti-mouse CD16/32 antibody (Biolegend, 101320) for 10 min at room temperature. This blocking of non-specific binding was followed by incubation for 30 min on ice, in the dark, with the following anti-mouse antibodies: BV510-conjugated CD45 (1:100—103138, Biolegend), PE-conjugated SiglecF (1:200—552126, BD Biosciences), PE/Cy7-conjugated CD11b (1:100—101216, Biolegend), FITC-conjugated CD64 (1:200—139316, Biolegend), PerCP/Cy5.5-conjugated CD11c (1:100—117328, Biolegend), BV605-conjugated Ly6G (1:100—127639, Biolegend), Alexa Fluor 647-conjugated I-Ab (1:100—115310, Biolegend), APC/Cy7-conjugated CD24 (1:100—47-0242-80, Invitrogen), BV650-conjugated CD80 (1:100—104731, Biolegend), and BV786-conjugated CD206 (1:100—141729, Biolegend). Then, cells were incubated with Viable Dye (VD) eFluor® 450 (65-0863-14, EBioscience) for 30 min at 4 °C in the dark. Cells were resuspended and fixed in 4% paraformaldehyde for 20 min on ice in the dark.

Regarding intracellular staining with PE-Cy7-conjugated TNF-α (1:100—506323, Biolegend), an additional step was added before the membrane staining, namely a preincubation of the cells for 4 h at 37 °C with 10 ng of Phorbol 12-myristate 13-acetate (P8139, Sigma-Aldrich), 100 ng of ionomycin (I0634, Sigma-Aldrich), and 2 µg of brefeldin A (B7651, Sigma-Aldrich) in DMEM 1x supplemented with 10% FBS and 1% penicillin/streptomycin (P4333, Sigma-Aldrich). Then, the staining proceeded as mentioned in the previous paragraph, except for CD11b; in this case, we used APC-conjugated antibody (1:200—553312, BD). After fixation, cells were permeabilized in 0.5% saponin in PBS 1x, and then intracellular staining was performed.

Data were acquired on a LSRII flow cytometer and analyzed using FlowJo Software. For FACS-based separation of IMs and AMs contained in the CD45-positive fraction, the following antibodies were used: anti-mouse PE/Cy7-conjugated CD45 (1:200—552848, BD Biosciences), PE-conjugated SiglecF (1:200—552126, BD Biosciences), APC-conjugated CD11b (1:400—553312, BD Biosciences), FITC-conjugated CD64 (1:300—139316, Biolegend), PerCP/Cy5.5-conjugated CD11c (1:200—560584, BD Biosciences), and APC/Cy7-conjugated Ly6G (1:300—560600, BD Biosciences).

### Reverse Transcription Quantitative PCR

At day 7 after BLM administration, FACS-sorted IMs and AMs were stored in RLT buffer and frozen at -80 °C. Total RNA was isolated from sorted interstitial and alveolar macrophages using RNeasy Plus Micro Kit following the instructions provided by the manufacturer (74034, Qiagen).

First-strand cDNA was synthesized using the Super Script III First-Strand Synthesis Supermix kit, which was used to convert all the extracted RNA following the instructions provided by the manufacturer (18080400, Invitrogen).

Reverse transcription quantitative PCR (RT-qPCR) was conducted using the 7500 Fast Real-Time PCR System (Applied Biosystems, Life Technologies). RT-qPCR was performed using Taqman Universal PCR MasterMix (4304437, Thermo Fisher Scientific) and one TaqMan® Gene Expression assay.

The following probes were used for each target gene: *Gapdh* (Mm99999915_g1), *IL-1β* (Mm00434228_m1), *Tnf-α* (Mm00443258_m1), *Ccl2* (Mm00441242_m1), *Cxcl2* (Mm00436450_m1), *Ccl5* (Mm01302427_m1), Ccl6 (Mm01302419_m1), *Ccl9* (Mm00441260_m1), *Arg1* (Mm00475988_m1), *Tgf-β1* (Mm01178820_m1), *Tgf-bi* (Mm01337605_m1), *Chi3l3/Ym1* (Mm00657889_m1), *Ccl24* (Mm00444701_m1), *Fibronectin 1* (Mm01256744_m1), *Mmp12* (Mm00500554_m1).

Relative expression levels for each target gene were calculated using the $2^{-\Delta\Delta Ct}$ method; Ct values of target genes were normalized to the reference gene *Gapdh*. Data were presented in fold change, which defined the gene's relative expression in the respective vehicle group to 1.

### Interstitial Macrophages Fluorescence-Activated Cell Sorting and Culture

Untreated and treated animals were used to obtain interstitial macrophages for primary culture and to collect conditioned medium (CM).

The lung single-cell suspensions were incubated with anti-CD45 MicroBeads (130-052-301, Miltenyi Biotec) to enrich the populations of interest, which are minor in the lung.

$CD45^+$ cells were collected over MS column separation (130-042-201, Miltenyi Biotec) in the OctoMACS separator (130-042-109, Miltenyi Biotec) magnetic field. Viable cells were counted using trypan blue, and flow cytometry staining was performed to proceed further to the fluorescence-activated cell sorting procedure using BD FACSARIA II cell sorter (BD Bioscience).

Following cell sorting, 2.5 x $10^5$ macrophages in DMEM 1x supplemented with 10% FBS, and 1% penicillin/streptomycin were plated in SterilinTM Square Petri Dishes (Thermo Fisher Scientific) for 24 h at 37 °C in a humidified atmosphere containing 5% $CO_2$. After this time, the CM was collected, centrifuged at 1500 rpm for 5 min, and then stored at −80 °C.

### Culture and Stimulation of MLg Cell Line

MLg (MLg 2908, ATCC® CCL206™), a mouse lung fibroblast cell line, was used in *in vitro* assays. MLg cells were maintained in Minimum Essential Medium (MEM; 31095-029, Gibco) supplemented with 10% FBS, 10 mM HEPES (15630-056, Gibco), and 1% penicillin–streptomycin solution. Cells were maintained at 37 °C in a humidified atmosphere containing 5% $CO_2$. When cells reached 80–90% confluence, they were enzymatically dissociated using TrypLE Express Enzyme (12605-028, Gibco) for 5 min at 37 °C, and the cell suspension was passed to a new flask in a low dilution.

Based on Meziani *et al.* (19), 5 x $10^3$ or 1.5 x $10^5$ MLg cells in DMEM 1x containing 10% FBS, 10 mM HEPES, and 1% penicillin–streptomycin were seeded in a regular 96-well plate (MTS assay), µ-Plates 96 Well Black (immunofluorescence—89626, Ibidi), or in a regular 6-well plate (Western blot), respectively, and were allowed to adhere overnight. Next, these cells were cultured for 48 h with untreated and treated, sorted IMs-derived CM with 10% FBS. In control conditions, MLg cells were cultured in the same medium without contact with IMs. The supplementation with 10% FBS was necessary as MLg cells do not survive when cultured without it, not even in lower percentages.

### Metabolic Activity Assay

MLg proliferation after stimulation with control or CM for 48 h was assessed by MTS assay according to the manufacturer's instructions (CellTiter 96 Aqueous One Solution, PROMEGA). Briefly, MLg were incubated in control medium with 1:10 MTS for 2.5 h at 37 °C. Next, 490 nm absorbances were read using a 96-well plate reader (Varioskan Flash, Thermo Fisher Scientific). All assays were performed in triplicate.

### Immunofluorescence

The proliferative and transdifferentiating state of MLg cells after CM stimulation was assessed by immunofluorescence. Following 48 h of stimulation with IMs-derived conditioned medium, the medium was carefully removed, and cells were washed with PBS 1x. Then, adherent cells were fixed with PFA 4% (proliferation protocol) or methanol 100% (transdifferentiation protocol) for 30 min. Fixed cells were permeabilized in 0.3% Triton-X-100 in PBS 1x for 20 min in the case of the proliferation protocol. Cells were washed twice with PBS Tween 0.5% for 10 min, and blockage of non-specific binding was performed with newborn calf serum (proliferation protocol; 1/10—186427, Biochrom) or normal goat serum (transdifferentiation protocol; 1/10—G9023-0010, Sigma-Aldrich) for 1 h. Next, cells were incubated with a rabbit anti-mouse Ki-67 (1:250 in blocking solution—AB9260, Millipore), or rabbit anti-mouse vimentin (1:150 in blocking solution—#5741, CellSignalling Technology) and mouse anti-mouse α-smooth muscle

actin (SMA, 1:100 in blocking solution—ab32575, Abcam) primary antibodies overnight. Cells were washed and incubated for 2 h with goat anti-rabbit conjugated to Alexa Fluor 568 (1:250 in blocking solution—a11011, Thermo Fisher Scientific) and goat anti-mouse conjugated to Alexa Fluor 488 (1:250 in blocking solution—a11001, Thermo Fisher Scientific) secondary antibodies. Finally, cells were washed and incubated with DAPI for 5 min, mounted in Ibidi Mounting Medium (50001, Ibidi), and images were obtained with an inverted fluorescence microscope (Olympus widefield inverted microscope IX53, Olympus) using the 10x objective. Data were presented as positive cells *per* DAPI-positive cells.

### Protein Extraction

The transdifferentiating state of MLg cells after CM stimulation was assessed by Western blot. Following 48 h of stimulation with IMs-derived conditioned medium, the medium was carefully removed, and cells were washed with PBS 1x. Then, protein was extracted by scraping the cells after adding lysis buffer (50 mM Tris-Base, 150 mM NaCl, 5 mM EDTA, 1% Triton X-100, and 1:7 of cOmplete protease inhibitors cocktail (11697498001, Roche)). Lysed cells were collected, kept on ice for 15 min, and centrifuged at 10000 rpm at 4 °C for 15 min. The supernatant was collected, and protein was quantified using Bradford reagent (B6916, Sigma-Aldrich). For quantification, 2 µL of protein extracts, as well as a BSA standard curve, was added to each well of a 96-well plate, followed by 98 µL of PBS 1x and 200 µL of Bradford reagent. After a 10 min incubation period, absorbance was measured at 590 nm in the microplate reader (Varioskan Flash, Thermo FisherScientific).

### Western Blot Analysis

Aliquots of 20 µg of protein from MLg cells were prepared in the proportion of 1:1 with loading buffer (950 µL of Laemmli Sample Buffer 2x (161-0737, Biorad) and 50 µL 2-mercaptoethanol (63689, Millipore)) and denatured over 5 min at 98 °C. Samples were then loaded onto a 10% sodium dodecyl sulphate–polyacrylamide (SDS-PAGE) gel and transferred to Amersham Protran nitrocellulose membranes (GE10600008, Sigma-Aldrich) using the Trans-Blot Turbo Transfer System (BioRad Laboratories). After, membranes were blocked for 1 h with TBS 0.1% Tween containing 5% of BSA. Membranes were incubated overnight at 4 °C with the primary antibodies for vimentin (1:1000, rabbit—#5741, CellSignalling Technology), α-SMA (1:500, mouse—ab32575, Abcam), and Gapdh (1:2500, rabbit—ab9485, Abcam). After incubation, membranes were washed three times in TBS 0.1% Tween and then incubated with a secondary antibody coupled to horseradish peroxidase (HRP, 1:2000, anti-rabbit—7074P2, CellSignalling Technology and 1:3000, anti-mouse—sc-516102, Santa Cruz Biotechnology) diluted in 5% milk for 1 h at RT. Membranes were washed three times with TBS 0.1% Tween, and signal

was detected in Sapphire Biomolecular Imager (Azure Biosystems) using Western Bright Sirius HRP Substrate Kit (K-12043-D10, Advansta). The bands were quantified in ImageJ software, and quantifications were normalized to GAPDH levels.

### Statistical Analysis

Data were analyzed and plotted using GraphPad Prism 6.00 (GraphPad Software, San Diego, CA). All results were expressed as group mean ± standard error of the mean (SEM). A *p-value* of less than 0.05 was considered a statistically significant difference. For all comparisons, normality was assessed with Shapiro–Wilk test; if normality was not verified, non-parametric tests were used. Comparisons between two groups were performed either with a parametric, unpaired two-tailed Student's t-test or a non-parametric, two-tailed Mann–Whitney test. Comparisons between three groups were performed either with parametric one-way ANOVA or a non-parametric Kruskall–Wallis test.

## 3. Results

### Inflammatory Phase of Bleomycin-Induced Pulmonary Fibrosis is Characterized by a Predominance of Interstitial Macrophages

Intratracheal injection of BLM or saline was performed on day 0. BLM administration was followed by an inflammatory phase with a peak at day 7. So, to elucidate the potential involvement of IMs and AMs throughout the inflammatory phase of the BLM-induced pulmonary fibrosis model, lung macrophage populations at days 3, 5, and 7 were analyzed by flow cytometry (Figure 1A). The gating strategy used, based on Misharin *et al.* (20), is shown in Figure 1B. First, the debris and doublets were excluded using forward vs. side scatter area (FSC-A vs SSC-A) and FSC-A vs. FSC height plot, respectively. Then, live immune cells were identified by negative staining for viable dye and positive staining for CD45. A sequential gating strategy was first used to exclude neutrophil ($CD11b^{+}Ly6G^{+}$) and eosinophil ($CD11c^{-}SiglecF^{+}$) populations, followed by the identification of alveolar macrophages ($MHCII^{+}CD64^{+}SiglecF^{+}$) and interstitial macrophages ($MHCII^{+}CD64^{+}SiglecF^{-}$).

The macrophage populations' abundance is illustrated in Figure 1C. The percentage of AMs ($CD64^{+}SiglecF^{+}$) was reduced in BLM-treated lungs compared with in the saline lungs at days 3, 5, and 7 (Figure 1C). On the other hand, the frequency of IMs ($CD64^{+}SiglecF^{-}$) was higher in BLM-treated mice than in the untreated mice at all time points, being highest at day 7 (Figure 1C).

Moreover, we observed that the most prevalent macrophage population in BLM-treated animals was IMs (Figure 1D). Their percentage duplicated over the days after BLM administration from 7.2 ± 1.9% on day 3 to 13.8 ± 1.5% on day 7. On the contrary, no differences were observed in the population of AMs. In the BLM-treated animals, the proportion of IMs was around 87%, 93%, and 94% higher than that of AMs on days 3, 5, and 7, respectively.

The existence of a monocytic origin was evaluated to explore the difference in the proportions of these macrophage populations. As shown in Figure 1E, almost the entire population of IMs was CD11b positive, while few AMs presented expression on days 5 and 7. These results indicate that, throughout the inflammatory phase of BLM-induced pulmonary fibrosis, macrophage recruitment to the lung is intensified, and IMs are the predominant macrophage population.

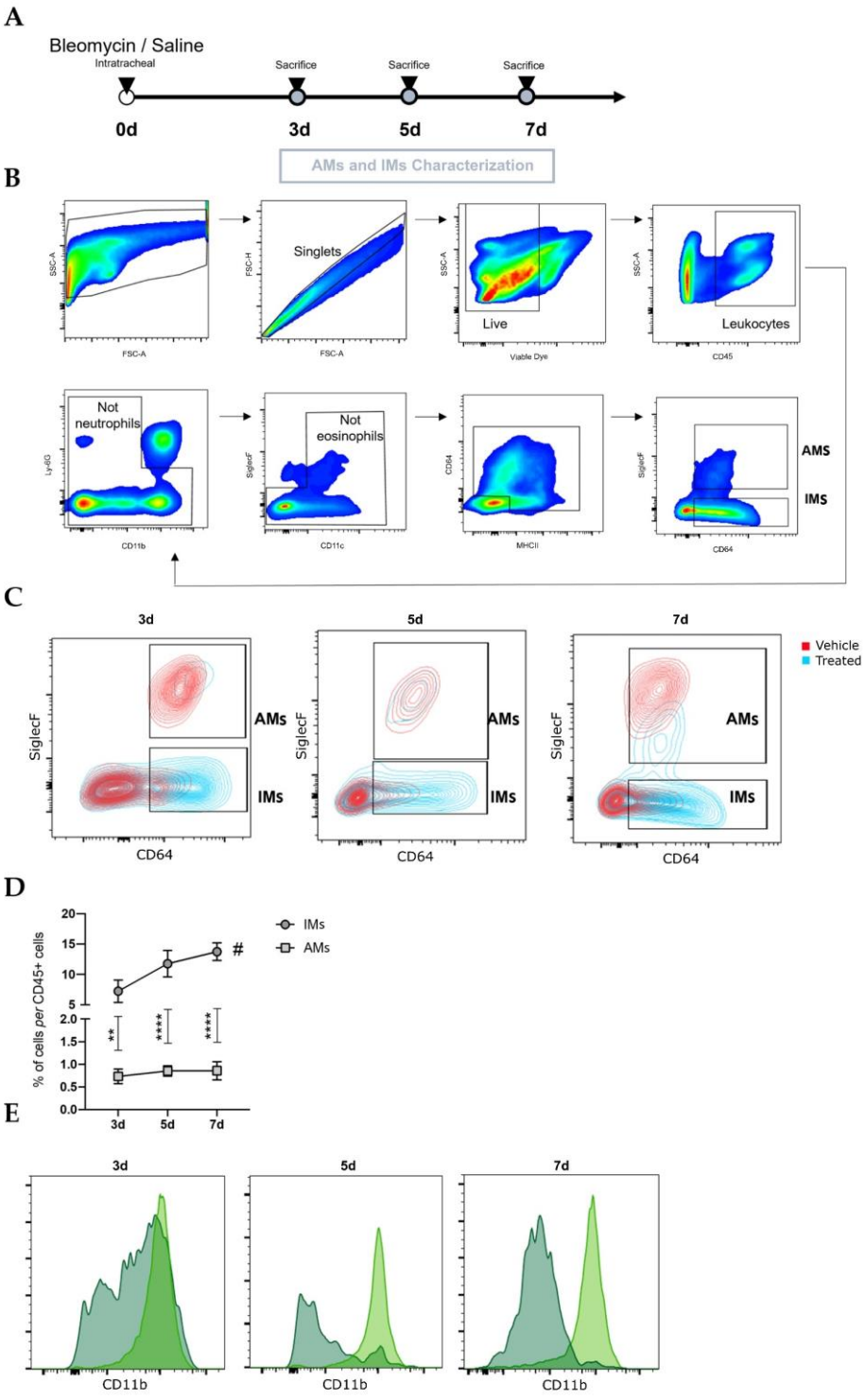



**Figure 1. Macrophage populations in the lung during the inflammatory phase of BLM-induced pulmonary fibrosis mouse model.** (A) Intratracheal injection of BLM or saline was performed on day 0. Animals were sacrificed on days 3, 5, and 7 to quantify macrophage populations. (B) Gating strategy for the identification of AMs and IMs in lung samples by flow cytometry. (C) Representative plots of proportions of AMs and IMs in untreated (red) and BLM-treated (blue) lungs at days 3, 5, and 7. (D) Proportion of IMs and AMs in BLM-treated animals at days 3, 5, and 7. The percentage of cells in live CD45+ is plotted. (E) Profile of CD11b expression in IMs (light green) and AMs (dark green) on BLM-induced PF mice at days 3, 5, and 7. Data are shown as the mean ± SEM of one representative experiment of three independent experiments. ** $p < 0.01$, **** $p < 0.0001$: treated IMs vs. treated AMs. # $p < 0.05$: different time points. IM: interstitial macrophages; AM: alveolar macrophages; d: days post intratracheal BLM administration.

## Inflammatory Phase of BLM-Induced Pulmonary Fibrosis is Associated with a Differential Inflammatory Phenotype in Interstitial and Alveolar Lung Macrophages

Macrophages hold two distinct activation phenotypes (the classically designated M1- and M2-like phenotypes) that impact the fibrotic processes differently (9,22,23). In this way, we next evaluated the profile of lung macrophages during the inflammatory phase of BLM-induced lung fibrosis, studying the cell surface expression of CD80 and MHCII as proinflammatory-associated molecules and CD206 as an anti-inflammatory by flow cytometry.

BLM-treated AMs showed a higher proportion of $CD80^+$ cells than IMs (Figure 2A). The CD80 expression was more pronounced in both lung macrophage populations at day 3 after BLM administration (Figure 2A). Moreover, both IMs and AMs presented decreased $CD80^+$ percentage throughout the disease progression. Interestingly, the levels of CD80 expression in IMs, represented by mean fluorescence intensity (MFI), also decreased after day 3 post BLM (Figure 2A). These data suggest that the number of cells expressing CD80 decreases during the inflammatory phase in both macrophage populations.

IMs from BLM-treated mice presented a statistically significant higher percentage of $MHCII^+$ cells compared with AMs on days 3 and 5 (Figure 2B). Furthermore, these differences were more greatly accentuated regarding the MFI levels of MHCII expression, inclusively, at 7 days after BLM administration (Figure 2B). However, the expression levels were unaltered within each lung macrophage population throughout the inflammatory phase, suggesting that none of the macrophage populations presents a higher number of $MHCII^+$ cells over time.

Regarding the CD206-positive cell percentage, AMs and IMs from BLM-treated mice showed similar proportions at day 3. However, between days 5 and 7, the proportion of $CD206^+$ AMs was increasingly higher than that of $CD206^+$ IMs (Figure 2C). A similar result was observed in CD206 expression levels by MFI (Figure 2C). IMs lost CD206 expression throughout the inflammatory phase, while AMs presented an evident increase. These results indicate that $CD206^+$ AMs increased compared with CD206+ IMs in the later inflammatory phase after BLM administration.

Our flow cytometry data hint that AMs shift from the M1- to M2-like phenotype as CD80 expression levels decrease and CD206 expression levels increase throughout inflammation. On the other hand, these data do not suggest a clearly defined IMs phenotype since CD80, and CD206 expression levels slightly decrease throughout the inflammatory phase of BLM-induced pulmonary fibrosis.

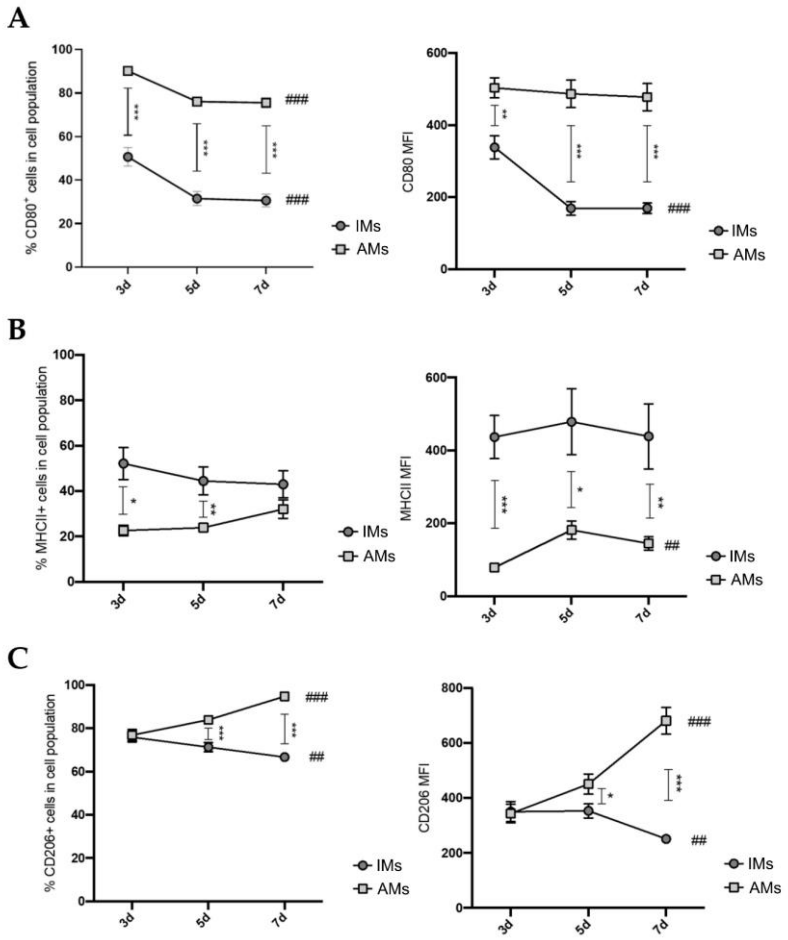



**Figure 2. Macrophage populations phenotype in the lung during the inflammatory phase of BLM-induced pulmonary fibrosis mouse model.** Expression profile of (A) CD80, (B) MHCII, and (C) CD206 in interstitial- and alveolar-macrophage-treated lungs at days 3, 5, and 7 after BLM administration. The percentage of cells was gated in live CD45 cells. The mean fluorescence intensity (MFI) in the respective macrophage population is plotted in the second graph. The data are represented as the mean ± SEM. * $p < 0.05$, ** $p < 0.01$, *** $p < 0.001$: treated IMs vs. treated AMs. ## $p < 0.01$, ### $p < 0.001$: different time points.

Further, a more detailed analysis of the activation profile of the lung macrophage populations at the peak of the inflammatory phase of BLM-induced pulmonary fibrosis was performed (7,8). For that, the macrophages' gene expression of proinflammatory (*Il-1β*, *Tnf-α, Cxcl2*, *Ccl5*, *Ccl9*, *Ccl2*), anti-inflammatory (*Arg1*, *Chi3l3*), and pro-fibrotic (*Tgf-βi*, *Tgf-β1*, *Fn1*, *Mmp12*, *Ccl24*) mediators were evaluated.

Treated IMs displayed a significant decrease in relative expression levels of proinflammatory-related factors compared with both the vehicle (*Il-1β*, *Tnf-α*, *Cxcl2*, *Ccl5*) and with treated AMs (*Il-1β*, *Tnf-α*, *Cxcl2*, *Ccl9*, *Ccl2*) (Figure 3A, 3D and 3E). Moreover, treated IMs presented a significant increase in anti-inflammatory-related factors (*Arg1*, *Chi3l3*) compared with the vehicle control (Figure 3B). Regarding the relative expression levels of pro-fibrotic factors, no differences were found in treated IMs compared with the vehicle. However, there was a decrease compared to AMs (Figure 3C). These results suggest that IMs are activated towards an anti-inflammatory phenotype.

Alveolar macrophages presented a significant increase in proinflammatory (*Il-1β*, *Cxcl2*, *Ccl9*, *Ccl2*), anti-inflammatory (*Arg1*, *Chi3l3*), and pro-fibrotic (*Tgf-βi*, *Fn1*, *Mmp12*, *Ccl24*) factors (Figure 3A, 3B, and 3C, respectively) compared with the vehicle. These results suggest that AMs are in a transient phenotype once they still have a mixed phenotype. The protein expression of TNF-α and IL-1β was analyzed in treated IMs and AMs to validate gene expression levels. In fact, protein expression of both proinflammatory proteins was significantly increased in treated AMs compared with treated IMs (Figure 3D and 3E).

Our results show that BLM impacts differently the phenotype of IMs and AMs since the shift in activation state does not occur simultaneously. At this stage of BLM-induced pulmonary fibrosis, IMs hold an M2-like phenotype, while AMs are in a transient state from an M1- to an M2-like phenotype.

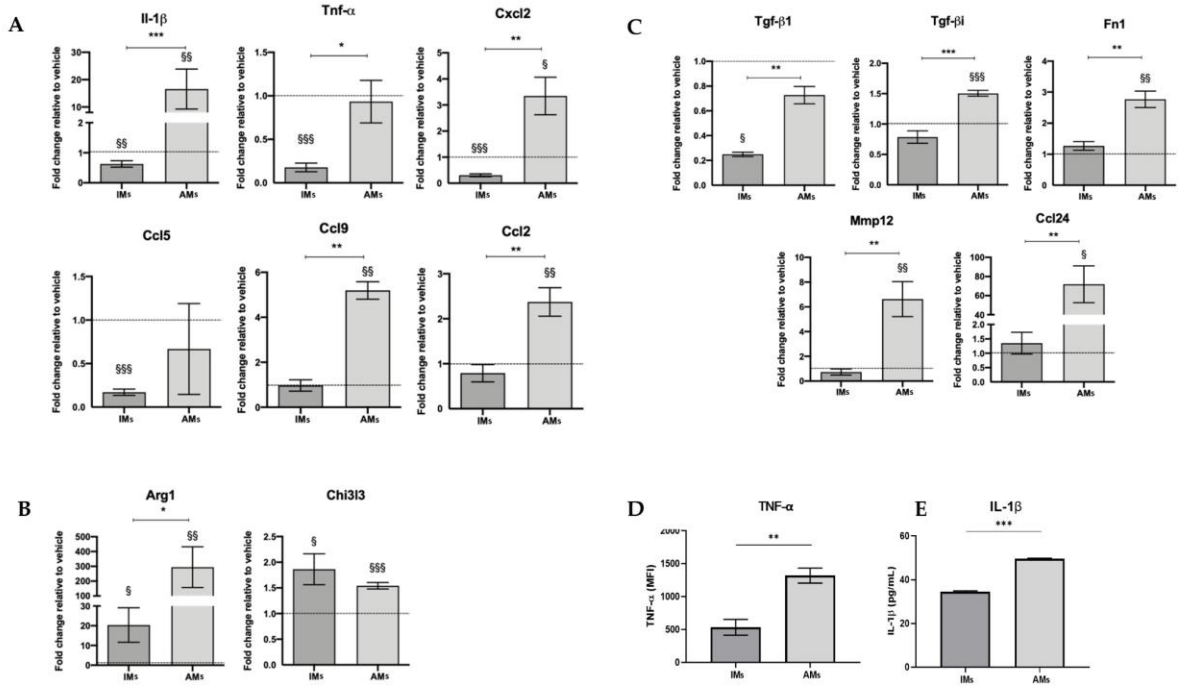



**Figure 3. IMs are activated towards an anti-inflammatory phenotype, and AMs are in a transient activation state at day 7 after BLM-induced pulmonary fibrosis.** Gene expression profile of interstitial and alveolar macrophages sorted from BLM and saline-injected lungs at day 7 of proinflammatory (A), anti-inflammatory (B), and pro-fibrotic factors (C). The fold change of gene relative expression of the respective group vehicle was set to 1. TNF-α protein expression was obtained by the mean fluorescence intensity (MFI) using the flow cytometry gating strategy in Figure 1B (D), and expression of IL-1β was obtained by ELISA assay of IMs-derived and AMs-derived CM after 24 h culture (E). Data are represented as the mean ± SEM. * $p < 0.05$, ** $p < 0.01$, *** $p < 0.001$: treated IMs vs. treated AMs. § $p < 0.05$, §§ $p < 0.01$, §§§ $p < 0.001$: treated vs. vehicle.

## Activated Interstitial Macrophages Promote Fibroblast Proliferation and Differentiation

As the IMs are the most representative lung macrophage population in the early phase of the mouse fibrosis model, next, their effects in fibrogenesis were investigated. Thus, IMs were sorted from the lung at day 7 after BLM or saline administration and subsequently cultured to collect the CM. The lung fibroblast cell line was stimulated with sorted, IMs-derived CM, and proliferation and differentiation were examined using MTS assay and Ki-67 expression and expression of α-SMA and vimentin, respectively

(Figure 4A). α-SMA is the most consistent marker for myofibroblast identification (24). This cell type can also co-express α-SMA and vimentin; however, a single vimentin stain is reliable in distinguishing fibroblasts.

Fibroblasts stimulated with untreated and treated, sorted IMs-derived CM exhibited increased viability and proliferation compared with the control, as shown by MTS assay (Figure 4B). However, no differences were found in MLg to Ki-67 expression by immunofluorescence (Figure 4C and 4D).

After stimulation with sorted IMs-derived CM, single vimentin expression decreased and was mostly co-localized with α-SMA expression (Figure 4E and 4F) in both untreated and treated conditions. A significant increase in single α-SMA expression was observed when fibroblasts were stimulated with CM of IMs sorted from BLM-treated animals (Figure 4E–4H).

These results suggest that activated IMs modulate the proliferation of fibroblasts and promote their differentiation towards myofibroblasts, which are responsible for extracellular matrix production in pulmonary fibrosis.

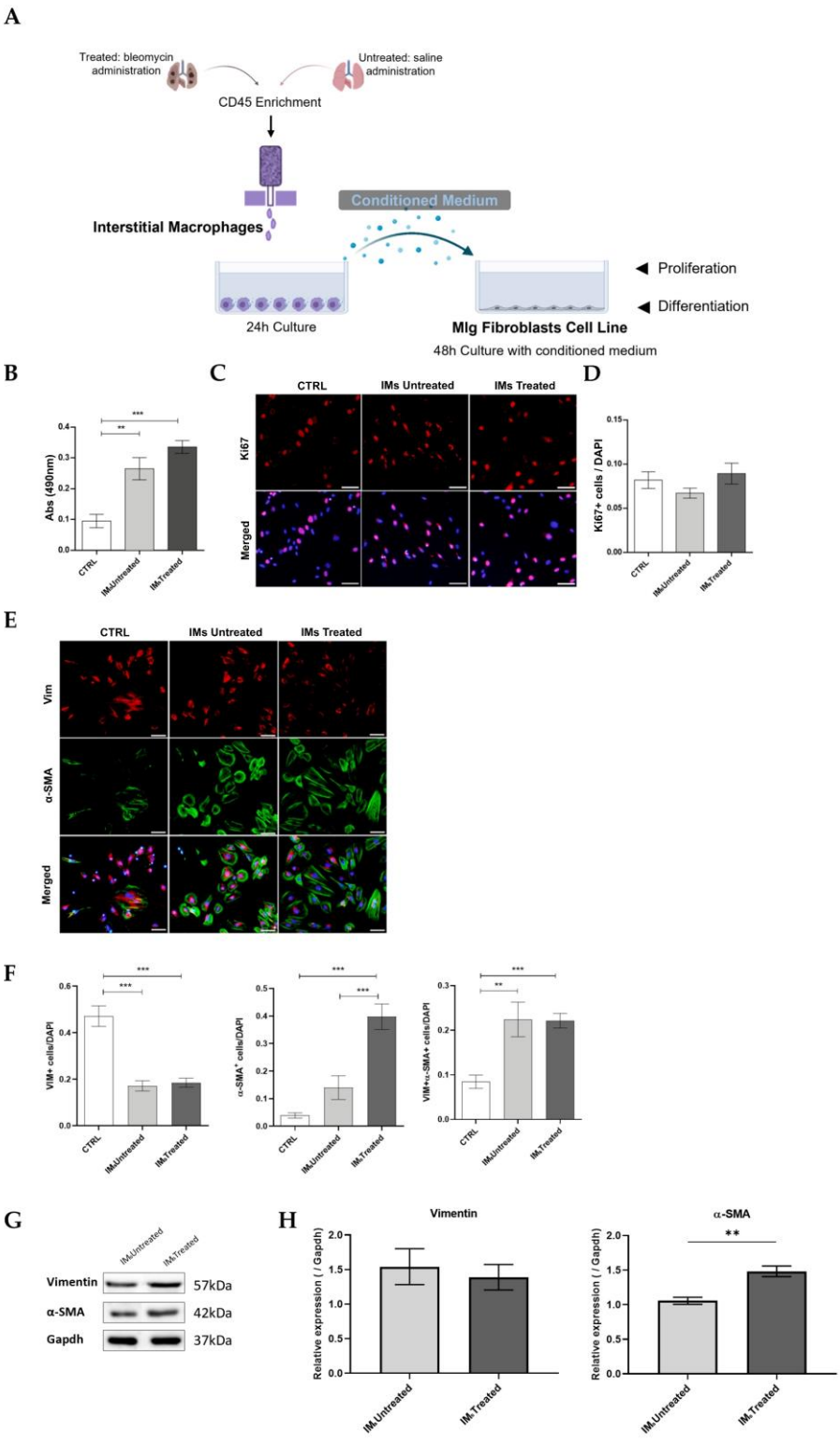



**Figure 4. Conditioned medium from BLM-sorted IMs induced fibroblasts proliferation and differentiation into myofibroblasts.** (A) Experimental design. After CD45 enrichment, IMs were sorted from dissociated lung samples on day 7 after saline (IMs untreated) or BLM (IMs treated) administration and cultured for 24 h to collect the CM. MLg, a fibroblast cell line, was cultured with control medium, conditioned medium from untreated IMs, or treated IMs. After 48 h, the (B) metabolic activity was measured by MTS assay, (C) cell proliferation by Ki-67 staining, and (D) respective quantification was performed. Differentiation state was analyzed by (E) immunofluorescence with vimentin (red) and α-SMA (green), nuclei are stained with DAPI (blue), and (F) respective quantification, also by (G) western blot, and (H) quantification of relative expression. Scale bar = 200 µm. Original magnification, 100×. Data are shown as the mean ± SEM of one representative experiment of three independent experiments. ** $p < 0.01$, *** $p < 0.001$: treated IMs vs. treated AMs.

## 4. Discussion

Pulmonary fibrosis is a common and severe pathological condition, and since there are no effective therapies to halt this condition, the discovery of new treatments is urgently needed. Therefore, a better understanding of macrophages' signature and functionality in this context is critical to unraveling new therapeutic strategies.

Pulmonary fibrosis is a rapidly progressive condition characterized by the activation of fibroblasts and their differentiation into myofibroblasts. These cells are responsible for the excessive production and consequent accumulation of extracellular matrix (1,5,6). In our study, we used the BLM-induced pulmonary fibrosis mouse model. BLM intratracheal administration is one of the best established and most widely used mouse model for studies that mimic human pulmonary fibrosis (25). Intratracheal instillation of BLM is associated with an inflammatory phase during the first week, reaching a peak at day 7, and a subsequent fibroproliferative phase leading to excessive collagen deposition (26). Indeed, several studies demonstrated that this model shares cellular and molecular mechanisms important in the pathogenesis of idiopathic pulmonary fibrosis and other fibrotic interstitial lung human diseases (27–29). We demonstrated in the early stage of this model that IMs accumulate in the lung and become phenotypically activated toward an anti-inflammatory phenotype during the disease progression. *In vitro*, this macrophage population leads to myofibroblast activation by paracrine mechanisms.

Our flow cytometry data in early BLM-induced pulmonary fibrosis showed that the proportion of IMs increased throughout the disease and peaked at day 7. On the other hand, the proportion of AMs decreased drastically and remained unaltered during these periods. These findings suggest the critical involvement of IMs in the fibrogenesis process of the disease and a slightly residual role of the AMs population. Moreover, our results show that the population of IMs is positive for CD11b, while AMs present a low percentage of positive staining. These results indicate that the increase in IMs throughout the inflammatory phase of BLM-induced pulmonary fibrosis is due to their monocytic origin. This intensified recruitment and predominance of IMs in the lung reinforces the potential involvement of this macrophage population rather than AMs in the disease pathogenesis.

Macrophages present a colossal capacity to modulate their phenotype and function according to the tissue microenvironment. In this way, we investigated the respective activation state of AMs and IMs 7 days after BLM administration. Our results demonstrated that, until day 7, AMs presented increasing expression levels of CD206 and decreasing expression levels of CD80. In addition, at the gene relative expression levels, several M1-, M2-like, and pro-fibrotic factors were simultaneously elevated. Other reports presented the same tendency, such as Misharin *et al.* (20), who suggested that, during the early

stages of BLM-induced pulmonary fibrosis mouse model, a mixed phenotype occurs in AMs. Furthermore, this study suggests that M1-like response and M2-like response of AMs are simultaneous in the early stages, and then the M1-like response of AMs ceases at later fibrotic stages. Particularly, showing that in the early stages of BLM-induced pulmonary fibrosis (5 days) AMs express higher levels of CD206 and CD80 than the vehicle control, while, in later stages (21 days), AMs only express higher levels of CD206 than the vehicle control. Zhang *et al.* (30) described that, on day 14 after BLM administration, AMs had higher relative expression levels of *Arg1* and lower expression levels of *Tnf-α* than vehicle control. Furthermore, Zhu *et al.* (31) described that, on day 17 after BLM administration, AMs expressed higher CD206 levels than the control. These data corroborate our results indicating that, at early stages of BLM-induced lung fibrosis, AMs are transient state from an M1-like to an M2-like phenotype.

Regarding IMs, our data showed that IMs have slightly decreased levels of CD206 and CD80 expression during the inflammatory phase. In contrast, Misharin *et al.* (20) showed that, on day 5 after BLM administration, IMs have increased CD80 expression and lower CD206 expression compared with the vehicle control. Additionally, at the gene relative expression levels, several proinflammatory factors were reduced and anti-inflammatory factors were elevated compared with the vehicle control. Concordantly, Ucero *et al.* (32) and Zhang *et al.* (33) described that, at day 10 after BLM administration, IMs have higher relative expression levels of CD206 and *Arg1* compared with the vehicle control, suggesting that, at this phase, IMs are activated towards an M2-like phenotype. In accordance with these findings, our study reveales that, at day 7, IMs were activated towards an M2-like phenotype.

Since M2-activated IMs accumulate in BLM-treated mice lungs and M2-like macrophages are widely described to be associated with aberrant tissue healing and consequent fibrosis through the secretion of anti-inflammatory and pro-fibrotic factors (7,22,23,34), we further investigated the role of IMs in fibrogenesis processes using an *in vitro* approach. In fact, we showed that CM from sorted IMs of BLM-treated mice induced fibroblasts proliferation and differentiation into myofibroblasts. Our findings comply with other studies. For instance, Meziani *et al.* (19) used sorted IMs ($F4/80^{+}Gr1^{-}$) from radiation-induced lung fibrosis and activated them with IFN-γ to induce the M1-like phenotype or IL-13/IL-4 to induce the M2 phenotype. After being co-cultured with M2-activated IMs, normal fibroblasts overproduce extracellular matrix components and increase their α-SMA expression. On the other hand, co-culturing with M1-activated macrophages does not affect either fibroblasts phenotype or function. Hou *et al.* (35) performed co-cultures of lung-resident mesenchymal stem cells (LR-MSCs), with M1- or M2-activated macrophages, using a mouse macrophage cell line, RAW264.7. This study showed that co-culture with M2 macrophages induces LR-MSCs differentiation, evidenced by the increased α-SMA

expression, while M1 macrophages do not alter LR-MSCs. Both studies suggested that M2-like macrophages, rather than M1-like macrophages, induce differentiation into myofibroblasts, which corroborates our results that show IMs activation towards an M2-like phenotype and acted as fibrogenesis promotors in the early stages of BLM-induced pulmonary fibrosis.

## Conclusions

Our study revealed the dynamic profile of AMs and IMs proportions during the early stages of a BLM-induced pulmonary fibrosis mouse model, with IMs being the more numerous lung macrophage population. Additionally, our data confirmed the AMs and IMs activation phenotype in this model, concretely showing that IMs present an M2-like activation phenotype. Importantly, we revealed the influence of IMs at the early stages of BLM-induced pulmonary fibrosis on promoting fibrotic processes by paracrine mechanisms.

**Author Contributions**: S.L.-R.: conception and design of the study, animal experiments, lung cell preparation for flow cytometry and cell sorting, qPCR, primary and cell line culture, MTS assays, immunofluorescence, acquisition of immunofluorescence images data, data analysis and interpretation, revision of the manuscript for important intellectual content, C.B.-M.: animal experiments, lung cell preparation for flow cytometry and cell sorting, flow cytometry, qPCR, data analysis and interpretation, writing of the manuscript for important intellectual content, R.F.: animal experiments, lung cell preparation for flow cytometry and cell sorting, revision of the manuscript for important intellectual content, C.B.-P.: lung cell preparation for flow cytometry and cell sorting, cell line culture, revision of the manuscript for important intellectual content, S.C.: conception and design of the study, animal experiments, cell sorting, data analysis and interpretation, revision and editing of the manuscript for important intellectual content. All authors have read and agreed to the published version of the manuscript.

**Funding**: This research was funded by the Programa Operacional Potencial Humano (POPH) and Programa Investigador Fundação para a Ciência e Tecnologia (FCT) (IF/00959/2014); by Programa Operacional Fatores de Competitividade (COMPETE) and national funds of FCT (POCI-01-0145- FEDER-028113); and by national funds of FCT (UIDB/50026/2020, UIDP/50026/2020).

**Institutional Review Board Statement**: The study was conducted according to the guidelines of European-adopted regulations (Directive 2010/63/EU) and approved and consented to by the ethical and regulatory Portuguese committee for animal experimentation (DGAV) (ref. 003671).

**Data Availability Statement**: The authors will freely release all data supporting the published paper upon direct request to the corresponding author.

**Acknowledgments**: The authors acknowledge the Life and Health Sciences Research Institute (ICVS). The authors also acknowledge Maria José Oliveira for scientific assistance on primary culture and Catarina Meireles for her FACS technical assistance. The authors acknowledge: the Fundação para a Ciência e Tecnologia (FCT) and Stemmatters, Biotecnologia e Medicina Regenerativa SA for PhD fellowship support (PD/BDE/142978/2018); FCT for PhD fellowship support (SFRH/BD/145955/2019); and ICVS Scientific Microscopy Platform, member of the national infrastructure PPBI – Portuguese Platform of Bioimaging (PPBI-POCI-01-0145-FEDER-022122).

**Conflicts of Interest**: The authors declare no conflict of interest.

## 5. References


1. Wynn, T. A. Integrating mechanisms of pulmonary fibrosis. *J. Exp. Med.* **208,** 1339–1350 (2011).
2. Raghu, G. *et al.* An Official ATS/ERS/JRS/ALAT Statement: Idiopathic pulmonary fibrosis: Evidence-based guidelines for diagnosis and management. *Am. J. Respir. Crit. Care Med.* **183,** 788–824 (2011).
3. Wilson, M. S. & Wynn, T. A. Pulmonary fibrosis: pathogenesis, etiology and regulation. *Mucosal Immunol.* **2,** 103–121 (2009).
4. Raghu, G. *et al.* An Official ATS/ERS/JRS/ALAT Clinical Practice Guideline: Treatment of Idiopathic Pulmonary Fibrosis. An Update of the 2011 Clinical Practice Guideline. *Am. J. Respir. Crit. Care Med.* **192,** e3–e19 (2015).
5. Lederer, D. J. & Martinez, F. J. Idiopathic Pulmonary Fibrosis. *N. Engl. J. Med.* **378,** 1811–1823 (2018).
6. King, T. E., Pardo, A. & Selman, M. Idiopathic pulmonary fibrosis. *Lancet* **378,** 1949–1961 (2011).
7. Gu, Y., Lawrence, T., Mohamed, R., Liang, Y. & Yahaya, B. H. The emerging roles of interstitial macrophages in pulmonary fibrosis: A perspective from scRNA-seq analyses. *Front. Immunol.* **13,** 1–11 (2022).
8. Aegerter, H., Lambrecht, B. N. & Jakubzick, C. V. Biology of lung macrophages in health and disease. *Immunity* **55,** 1564–1580 (2022).
9. Shi, T., Denney, L., An, H., Ho, L. & Zheng, Y. Alveolar and lung interstitial macrophages: Definitions, functions, and roles in lung fibrosis. *J. Leukoc. Biol.* **110,** 107–114 (2021).
10. Guilliams, M. *et al.* Alveolar macrophages develop from fetal monocytes that differentiate into long-lived cells in the first week of life via GM-CSF. *J. Exp. Med.* **210,** 1977–92 (2013).
11. Hoeffel, G. *et al.* C-Myb+ Erythro-Myeloid Progenitor-Derived Fetal Monocytes Give Rise to Adult Tissue-Resident Macrophages. *Immunity* **42,** 665–678 (2015).
12. Tan, S. Y. S. & Krasnow, M. A. Developmental origin of lung macrophage diversity. *Development* **143,** 1318–1327 (2016).
13. Gibbings, S. L. *et al.* Three Unique Interstitial Macrophages in the Murine Lung at Steady State. *Am. J. Respir. Cell Mol. Biol.* **57,** 66–76 (2017).
14. Mould, K. J. *et al.* Cell Origin Dictates Programming of Resident versus Recruited Macrophages during Acute Lung Injury. *Am. J. Respir. Cell Mol. Biol.* **57,** 294–306 (2017).
15. Schyns, J., Bureau, F. & Marichal, T. Lung Interstitial Macrophages: Past, Present, and Future. *J. Immunol. Res.* **2018,** 1–10 (2018).
16. Liegeois, M., Legrand, C., Desmet, C. J., Marichal, T. & Bureau, F. The interstitial macrophage: A long-neglected piece in the puzzle of lung immunity. *Cell. Immunol.* **330,** 91–96 (2018).
17. Chakarov, S. *et al.* Two distinct interstitial macrophage populations coexist across tissues in specific subtissular niches. *Science* **363,** eaau0964 (2019).
18. Ji, W.-J. *et al.* Temporal and spatial characterization of mononuclear phagocytes in circulating, lung alveolar and interstitial compartments in a mouse model of bleomycin-induced pulmonary injury. *J. Immunol. Methods* **403,** 7–16 (2014).
19. Meziani, L. *et al.* CSF1R inhibition prevents radiation pulmonary fibrosis by depletion of interstitial macrophages. *Eur. Respir. J.* **51,** 1702120 (2018).
20. Misharin, A. V., Morales-Nebreda, L., Mutlu, G. M., Budinger, G. R. S. & Perlman, H. Flow Cytometric Analysis of Macrophages and Dendritic Cell Subsets in the Mouse Lung. *Am. J. Respir. Cell Mol. Biol.* **49,** 503–510 (2013).
21. Misharin, A. V. *et al.* Monocyte-derived alveolar macrophages drive lung fibrosis and persist in the lung over the life span. *J. Exp. Med.* **214,** 2387–2404 (2017).
22. Murray, P. J. Macrophage Polarization. *Annu. Rev. Physiol.* **79,** 541–566 (2017).

23. Zhang, L. *et al.* Macrophages: friend or foe in idiopathic pulmonary fibrosis? *Respir. Res.* **19,** 170 (2018).
24. Ballester, B., Milara, J. & Cortijo, J. Idiopathic Pulmonary Fibrosis and Lung Cancer: Mechanisms and Molecular Targets. *Int. J. Mol. Sci.* **20,** 593 (2019).
25. Moore, B. B. & Hogaboam, C. M. Murine models of pulmonary fibrosis. *Am. J. Physiol. Cell. Mol. Physiol.* **294,** L152–L160 (2008).
26. Redente, E. F. *et al.* Age and sex dimorphisms contribute to the severity of bleomycin-induced lung injury and fibrosis. *Am. J. Physiol. Cell. Mol. Physiol.* **301,** L510–L518 (2011).
27. Kim, S.-N. *et al.* Dose-response Effects of Bleomycin on Inflammation and Pulmonary Fibrosis in Mice. *Toxicol. Res.* **26,** 217–222 (2010).
28. Kolb, P. *et al.* The importance of interventional timing in the bleomycin model of pulmonary fibrosis. *Eur. Respir. J.* **55,** 1901105 (2020).
29. Moeller, A., Ask, K., Warburton, D., Gauldie, J. & Kolb, M. The bleomycin animal model: A useful tool to investigate treatment options for idiopathic pulmonary fibrosis? *Int. J. Biochem. Cell Biol.* **40,** 362–382 (2008).
30. Zhang, W. *et al.* S100a4 is secreted by alternatively activated alveolar macrophages and promotes activation of lung fibroblasts in pulmonary fibrosis. *Front. Immunol.* **9,** 1–14 (2018).
31. Zhu, L., Fu, X., Chen, X., Han, X. & Dong, P. M2 macrophages induce EMT through the TGF-β/Smad2 signaling pathway. *Cell Biol. Int.* **41,** 960–968 (2017).
32. Ucero, A. C. *et al.* Fra-2–expressing macrophages promote lung fibrosis. *J. Clin. Invest.* **129,** 3293–3309 (2019).
33. Zhang, F. *et al.* Reprogramming of profibrotic macrophages for treatment of bleomycin-induced pulmonary fibrosis. *EMBO Mol. Med.* **12,** 1–15 (2020).
34. Kolahian, S., Fernandez, I. E., Eickelberg, O. & Hartl, D. Immune mechanisms in pulmonary fibrosis. *Am. J. Respir. Cell Mol. Biol.* **55,** 309–322 (2016).
35. Hou, J. *et al.* M2 macrophages promote myofibroblast differentiation of LR-MSCs and are associated with pulmonary fibrogenesis. *Cell Commun. Signal.* **16,** 89 (2018).

**Disclaimer/Publisher's Note**: The statements, opinions and data contained in all publications are solely those of the individual author(s) and contributor(s) and not of MDPI and/or the editor(s). MDPI and/or the editor(s) disclaim responsibility for any injury to people or property resulting from any ideas, methods, instructions or products referred to in the content.

# CHAPTER III

## c-MET Exacerbates Pulmonary Fibrosis via Deregulation of Immune Cell Recruitment and Activation

Manuscript submitted for publication:

Catarina Barbosa-Matos, Caroline Borges-Pereira, Sofia Libório-Ramos, Raquel Fernandes, Marcela Oliveira, Ana Mendes-Frias, Ricardo Silvestre, Nuno S. Osório, Hélder N. Bastos, Rita F. Santos, Susana Guimarães, António Morais, Massimiliano Mazzone, Agostinho Carvalho, Cristina Cunha, Sandra Costa. c-MET Exacerbates Pulmonary Fibrosis via Deregulation of Immune Cell Recruitment and Activation. CB-M contributed to all figures of this work.

## c-MET Exacerbates Pulmonary Fibrosis via Deregulation of Immune Cell Recruitment and Activation

Catarina Barbosa-Matos, Caroline Borges-Pereira, Sofia Libório-Ramos, Raquel Fernandes, Marcela Oliveira, Ana Mendes-Frias, Ricardo Silvestre, Nuno S. Osório, Hélder N. Bastos, Rita F. Santos, Susana Guimarães, António Morais, Massimiliano Mazzone, Agostinho Carvalho, Cristina Cunha, Sandra Costa

### Abstract

Pulmonary fibrosis (PF) represents the pathologic end stage of several interstitial lung diseases (ILDs) associated with high morbidity and mortality rates. However, current treatments can only delay disease progression rather than provide a cure. The role of inflammation in PF progression is well-established, but new insights into immune regulation are fundamental for developing more efficient therapies. c-MET signaling pathway has been implicated in the migratory capacity and effector functions of immune cells. Nevertheless, the role of this signaling pathway in the context of PF-associated lung diseases remains unexplored. We discovered that c-MET expression was induced in lung immune cells, specifically in T cells, interstitial macrophages, and neutrophils, during the inflammatory phase of bleomycin (BLM)-induced PF mouse model. Deletion of *c-Met* in immune cells correlated with earlier weight recovery and improved survival of BLM-treated mice. Moreover, the deletion of *c-Met* in immune cells was associated with early recruitment of the immune cell populations, normally found to express c-MET, leading to a subsequent attenuation of the cytotoxic and proinflammatory environment. Consequently, the less extensive inflammatory response, coupled with tissue repair rather than damage, culminated in less exacerbated fibrotic lesions. Furthermore, c-MET expression was up-regulated in lung T cells from patients with fibrosing ILDs, suggesting a potential involvement of c-MET in the development of fibrosing disease. Together, these data highlight the critical contribution of c-MET signaling pathway in immune cells to their enhanced uncontrolled recruitment and activation toward a proinflammatory and profibrotic phenotype, leading to the exacerbation of lung injury and consequent development of fibrosis.

### Keywords

Bleomycin, c-MET, ILDs, Inflammation, Pulmonary fibrosis

## 1. Introduction

Pulmonary fibrosis is a common denominator in several ILDs, including idiopathic pulmonary fibrosis, and can be triggered by other diseases, such as COVID-19 (1,2). In addition to IPF, other ILDs can develop fibrotic condition, namely patients with HP and CTD-ILD (1). HP is caused by exposure and sensitization to an inhaled antigen and can range from a purely inflammatory disease to a progressive fibrotic disease resembling IPF (3). CTD are systemic autoimmune disorders caused by excessive immune activated inflammation that mediates organ damage (4,5). ILDs occur in approximately 40–50% of patients with CTD and is the main cause of morbidity and mortality (6). IPF is the most severe form of PF and, due to the irreversibility of PF, patients present a poor prognosis and a median survival of only 2-4 years after diagnosis (7). The complex etiology and unclear pathogenesis of IPF result in limited and inefficient therapeutic strategies (8–11). A better understanding of the pathogenesis of IPF is therefore essential to identify new therapeutic targets.

Although the precise trigger-associated mechanisms remain unclear, under certain circumstances, chronic or repetitive injuries can evolve to fibrosis. PF is characterized by a persistent wound repair environment, resulting in the accumulation of ECM proteins such as fibronectin and collagens in the lung, irreversible tissue damage, and loss of pulmonary function (12–15). Wound healing processes can be modulated by several factors, including the recruitment and activation of inflammatory cells. A slight imbalance in these mediators can lead to uncontrolled tissue remodeling and, ultimately, fibrosis. In IPF, the inflammatory response is characterized by excessive amounts of Th2 cytokines, such as interleukin (IL)-4 and IL-13 that are critical mediators of fibrotic lung remodeling (16–19). Likewise, studies in mouse models of PF suggest that Th2 cytokines play a pro-fibrotic role (20).

The role of myeloid cells has long been recognized in lung development, homeostasis, and in the pathogenesis of PF (14). Macrophage populations in the lung are crucial for maintaining homeostasis responding appropriately to insults (21,22). Alveolar macrophages are localized in the alveolar space, contributing to airway homeostasis, pulmonary defense, repair, surfactant processing, and inflammatory responses (23). In contrast, interstitial macrophages (IMs) are present in the interstitial area of the lung, maintaining immune homeostasis and modulating tolerance toward non-threatening antigens (24,25). Macrophages can also modulate the inflammatory recruitment and activate myofibroblasts through the secretion of chemokines and profibrotic cytokines, respectively (13,26,27). Furthermore, the phenotypic activation of macrophages dictates how they modulate fibroproliferative responses. The M1, classically activated macrophages, maintain tissue inflammation, while M2, alternatively activated macrophages, play a role in resolving lung inflammation and the aberrant wound healing cascade during fibrosis (28–

31). Neutrophils are also an important cell population of the innate immune system, which migrate to the sites of infection or tissue injury and exhibit a wide variety of effector functions such as phagocytosis, production of ROS, degranulation, and release of neutrophil extracellular traps (32). Despite their efficient, protective functions, the inflammatory response of neutrophils can be a double-edged sword, as it can also cause severe tissue damage. During PF, neutrophil accumulation appears to amplify uncontrolled tissue repair and fibrosis by secreting elastase, which stimulates proliferation and differentiation of fibroblasts and ECM production (33,34). Furthermore, neutrophil recruitment is a predictor of early mortality in patients with IPF (35).

Recently, the signaling pathway involving HGF and its tyrosine kinase receptor, c-MET, has been described in the modulation of the migratory and functional activity of immune cells. In the tumoral context, c-MET is induced in neutrophils upon inflammatory stimuli, increasing their migratory capacity and reinforcing their nitric oxide release, thereby promoting cancer cell death (36). Moreover, c-MET inhibition decreases the recruitment of neutrophils into the T cell–inflamed tumor microenvironment and draining lymph nodes in response to cytotoxic immunotherapies (37). Also, tumoral cytotoxic T cells that express c-MET have enhanced cytolytic capacities (38). In *Leishmania mexicana* infection, c-MET expression is activated in neutrophils and favors their recruitment to the site of infection (39). Furthermore, in a murine model of intestinal inflammation, c-MET expression is induced mainly in neutrophils and its deletion in neutrophils reduces disease severity (40).

Although inflammation plays a critical role in the progression of PF, the role of c-MET signaling pathway in immune cells remains to be determined. Herein, we demonstrate that c-MET expression is induced in lung immune cells in response to bleomycin (BLM) administration. Moreover, conditional deletion of *c-Met* in immune cells leads to their early recruitment to the lung but, paradoxically, to a less proinflammatory environment. This prevents subsequent uncontrolled cytotoxicity and inflammation, while promoting tissue repair, and attenuates the long-term effects and the histopathological characteristics of BLM-induced lung fibrosis. Together, these data highlight the critical contribution of c-MET signaling pathway in immune cells to their enhanced uncontrolled recruitment and activation towards a proinflammatory and profibrotic phenotype, leading to the exacerbation of lung injury and consequent development of fibrosis. More importantly, we demonstrate that c-MET expression in T cells is increased in fibrosing ILD patients, suggesting a potential involvement of c-MET in the development of the fibrosing condition. In this sense, selective c-MET-targeted therapies might represent an attractive strategy to control tissue damage and inflammation in these patients.

## 2. Materials and Methods

### Mice and Human Samples

All procedures *in vivo* followed the EU-adopted regulations (Directive 2010/63/EU). Ethical and regulatory approvals were consented by Direção Geral de Alimentação e Veterinária (DGAV, 003671) and conducted according to the guidelines sanctioned by the DGAV. Mice were supplied by Professor Massimiliano Mazzone, Center for Cancer Biology, VIB, KU Leuven, Belgium. Eight-week-old gender- and age-matched C57BL/6 mice were bred under specific pathogen-free condition and kept at the Life and Health Sciences Research Institute (ICVS) animal facility. Mice were fed *ad libitum* and kept under light/dark cycles of 12 h, temperature of 18–25°C and humidity of 40–60%. Male, 10 to 12 weeks old, wild-type (WT, Tie2:*c-Met*$^{wt/wt}$) and conditional knockout (cKO, Tie2:*c-Met*$^{fl/fl}$) C57BL/6J mice were used.

This study was reviewed and approved by the Ethics Committee of Hospital de São João (CES 72-12). Transbronchial cryobiopsies and cryopreserved bronchoalveolar lavage (BAL) from ILD patients were obtained. Demographic and clinical features of studied patients are reported in Table 1 and Table 2, respectively.

**Table 1. Demographics of patients who performed lung biopsy.**

| Characteristic \ Disease | IPF | Fibrotic HP | CTD-ILD | Non-fibrotic HP |
|---|---|---|---|---|
| Age, mean ± SD, years | 60.8 ± 11.7 | 69.1 ± 6.3 | 77.0 ± 6.1 | 63.0 ± 0.0 |
| Sex, male/female, number | 6/0 | 2/7 | 2/1 | 0/1 |
| Smoking status, active/never, number | 5/1 | 3/6 | 1/2 | 0/1 |

Definition of abbreviations: IPF = idiopathic pulmonary fibrosis; HP = hypersensitivity pneumonitis; CTD-ILD = Connective tissue disease-associated interstitial lung disease.

Table 2. Demographics of patients who performed bronchoalveolar lavage collection.

| Characteristic \ Disease | IPF | Fibrotic HP | CTD-ILD | Non-fibrotic HP | Others (No ILD) |
|---|---|---|---|---|---|
| Age, mean ± SD, years | 76.8 ± 6.0 | 71.3 ± 7.8 | 59.4 ± 13.0 | 61.9 ± 11.1 | 55.8 ± 11.6 |
| Sex, male/female, number | 6/3 | 7/11 | 2/3 | 3/8 | 5/5 |
| Smoking status, active/former/never, number | 0/8/1 | 1/4/13 | 1/1/3 | 0/10/1 | 3/2/5 |

Definition of abbreviations: IPF, idiopathic pulmonary fibrosis; HP, hypersensitivity pneumonitis; CTD-ILD, Connective tissue disease-associated interstitial lung disease.

### BLM-induced pulmonary fibrosis mouse model

Mice were sedated with ketamine and medetomidine and intratracheally administered with BLM sulphate (BML-AP302-0010, Enzo Life Sciences) as a single dose of 2.5 mg/kg in 50 µL saline.

### BAL collection and preparation of mouse lung single-cell suspensions

Briefly, mice were over anesthetized by intraperitoneal injection, then trachea was exposed by a midline incision and cannulated. Bilateral BAL recovered by a three times lavage with 1 mL of PBS. The supernatant from the BAL was frozen for the LDH assay. Then, animals were perfused with PBS. After dissection, the lungs were placed in dispase (734-1312, Corning) while minced into 2-3 $mm^3$ pieces for 20 min. Then, 1 mg/mL DNase I (10104159001, Roche) and 5 mg/mL collagenase II (17101-015, Gibco) solution in Dulbecco's Modified Eagle Medium (21969-035, Gibco) was added to the sample. After, an enzymatic digestion period of 10 min at 37°C, tissue disruption was performed by mechanical titrations with P1000 tip, and then a second incubation period of 10 min at 37°C was conducted. After incubation, the disrupted tissue suspension was collected and sequentially filtered through 100 µm and 70 µm cell strainers. The supernatant was collected and stored at -80 °C for the LDH assay. BAL cells were added to the lung cell suspension, centrifuged and the pellet was resuspended in ammonium-chloride-potassium lysis buffer (A1049201, Gibco), and incubated for 4 min. Cells were then maintained in cold PBS containing 4% fetal bovine serum (10270-106, Gibco).

### Flow cytometric immunophenotyping analysis of mouse and human samples

Single-cell suspension, 1 x $10^6$ cells were preincubated with TruStain FcX anti-mouse CD16/32 antibody (101320, Biolegend) for 10 min at RT. After the blocking of non-specific binding of immunoglobulin to

the Fc receptors, cells were stained with the membrane antibodies listed in Table 3, for 30 min on ice in the dark. After, cells were fixed by incubation in 4% PFA for 20 min on ice in the dark. In the following day, data were acquired on a LSRII flow cytometer and FlowJo Software was used to analyze the data. Defrosted human BAL cells were preincubated with TruStain FcX anti-human CD16/32 antibody (422301, Biolegend) and then stained for 30 min with the membrane antibodies listed in Table 4. Data were acquired on a LSRII flow cytometer and BD LSRFortessa™ Cell Analyzer, for mouse and human samples data acquisition respectively. FlowJo Software was used to analyze the data. Gating strategy is illustrated in Figure 1A and 1B, for the identification of myeloid and lymphoid cells, respectively, in mouse lung and in Figure 2 for human samples.

**Table 3. Antibodies used for flow cytometry staining of mouse samples.**

| Antibody/Dye | Clone | Isotype | Dilution | Conjugate | Reference |
|---|---|---|---|---|---|
| Fixable Viability Dye | | | 1:1000 | eFluor 450 | 65-0863-14, eBioscience |
| Myeloid Panel | | | | | |
| CD11b | M1/70 | Rat IgG2b, κ | 1:100 | PE-Cy7 | 101216, Biolegend |
| CD11c | N418 | Armenian Hamster IgG | 1:100 | PE | 117308, Biolegend |
| CD24 | M1/69 | Rat IgG2b, κ | 1:100 | APC-Cy7 | 47-0242-82, Invitrogen |
| CD45 | 30-F11 | Rat IgG2b, κ | 1:200 | BV510 | 103138, Biolegend |
| CD64 | X54-5/7.1 | Mouse IgG1, κ | 1:100 | BV711 | 139311, Biolegend |
| F4/80 | BM8 | Rat IgG2a, κ | 1:100 | APC | 17-4801-82, Invitrogen |
| Ly6C | HK1.4 | Rat IgG2c, κ | 1:100 | PerCP-Cy5.5 | 128012, Biolegend |
| Ly6G | 1A8 | Rat IgG2a, κ | 1:100 | BV605 | 127639, Biolegend |
| MHCII | M5/114.15.2 | Rat IgG2b, κ | 1:100 | BV785 | 107645, Biolegend |
| SiglecF | 1RNM44N | Rat IgG2a, κ | 1:100 | Super Bright 645 | 64-1702-82, Invitrogen |
| c-MET | eBioclone 7 | Rat IgG1, κ | 1:50 | FITC | 11-8854-82, Invitrogen |
| Lymphoid Panel | | | | | |
| CD3 | 17A2 | Rat IgG2b, κ | 1:100 | APC | 100236, Biolegend |
| CD19 | 6D5 | Rat IgG2a, κ | 1:100 | APC-Cy7 | 115530, Biolegend |
| CD45 | 30-F11 | Rat IgG2b, κ | 1:200 | PE-Cy7 | 103114, Biolegend |
| c-MET | eBioclone 7 | Rat IgG1, κ | 1:50 | FITC | 11-8854-82, Invitrogen |

**Table 4. Antibodies used for flow cytometry staining of human samples.**

| Antibody | Clone | Isotype | Dilution | Conjugate | Reference |
|---|---|---|---|---|---|
| Lymphoid Panel | | | | | |
| **CD45** | HI30 | Mouse IgG1, κ | 1:400 | FITC | 304006, Biolegend |
| **CD56** | HCD56 | Mouse IgG1, κ | 1:200 | PE | 318305, Biolegend |
| **CD19** | HIB19 | Mouse IgG1, κ | 1:200 | APC-Cy7 | 302217, Biolegend |
| **CD3** | OKT3 | Mouse IgG2a, κ | 1:200 | PE-Cy7 | 317333, Biolegend |
| **c-MET** | 3D6 | Mouse IgG1, κ | 1:50 | APC | 566014, BD |

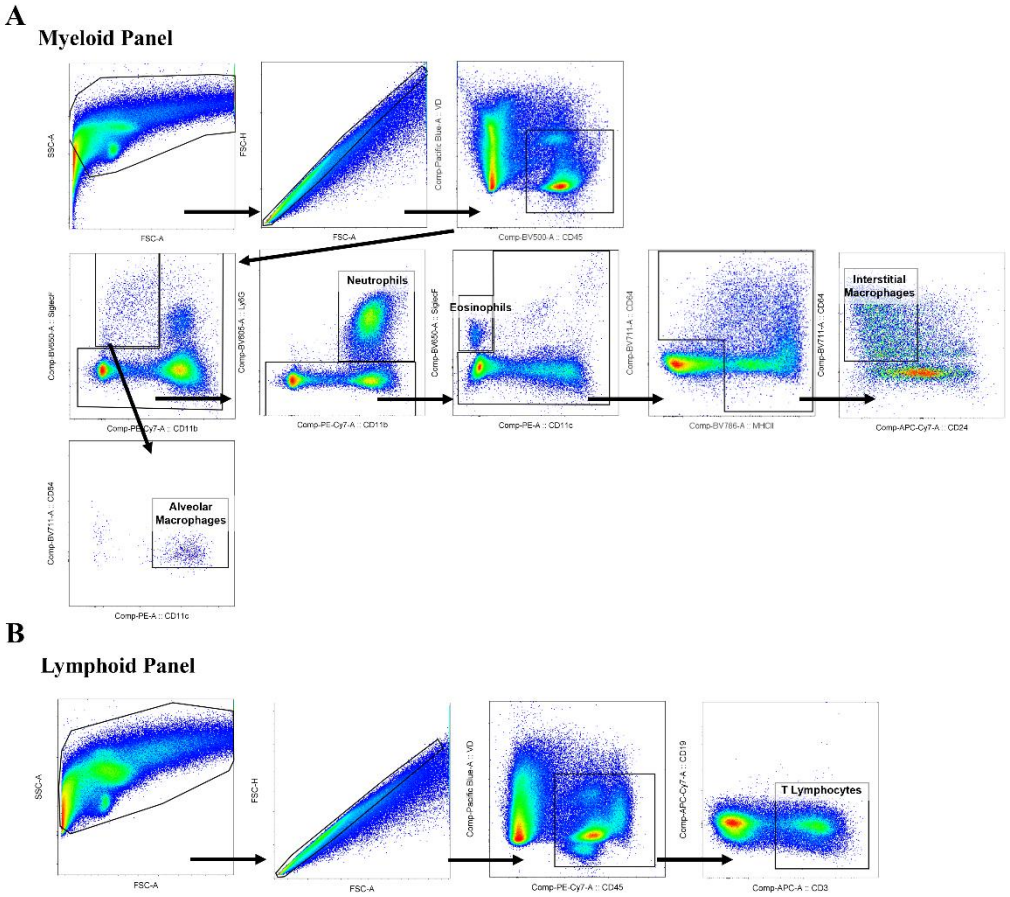



**Figure 1. Gating strategy for the identification of myeloid and lymphoid cell populations in dissociated mice lung by flow cytometry.** Initial exclusion of debris and doublets was performed using forward vs side scatter area (FSC-A vs SSC-A) and FSC-A vs FSC height (FSC-H) plot, respectively. Then live immune cells were identified by CD45 staining and negative for viable dye (VD). (A) A sequential gating strategy was used to identify myeloid populations expressing specific markers: alveolar macrophages ($CD11b^{-}SiglecF^{+}CD11c^{+}CD64^{+}$), neutrophils ($CD11b^{+}Ly\text{-}6G^{+}$), eosinophils ($CD11c^{-}SiglecF^{+}$), interstitial macrophages ($CD11b^{+}MHCII^{+}CD11c^{+}CD64^{+}CD24^{-}$). (B) CD3 status was assessed to identify T cells ($CD3^{+}CD19^{-}$). Afterward, c-MET expression was analyzed within each of the cell population mentioned.

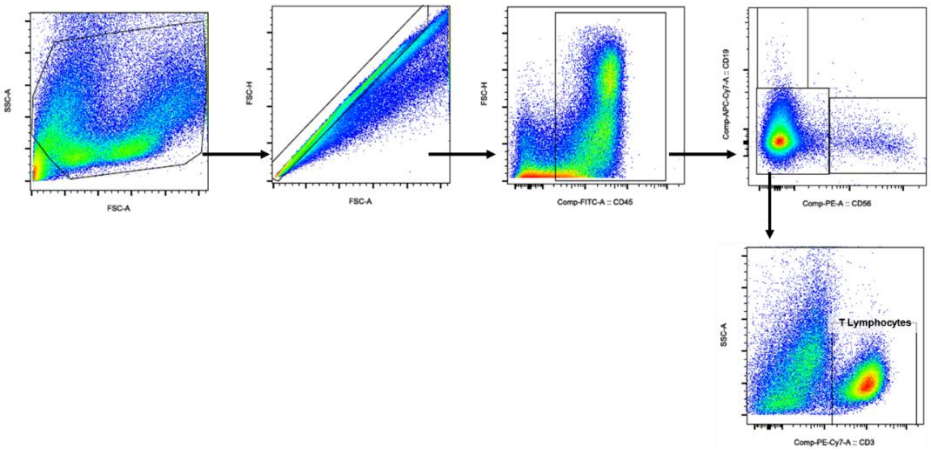



**Figure 2. Gating strategy for the identification of T lymphocytes in dissociated human lung by flow cytometry.** Initial exclusion of debris and doublets was performed FSC-A vs SSC-A and FSC-A vs FSC-H plot, respectively. Then immune cells were identified by CD45 staining. CD3 status was assessed to identify T cells in double negative cells for CD19 and CD56 ($CD3^{+}CD19^{-}CD56^{-}$). Then, c-MET expression was analyzed within this cell population.

### Survival analysis

After BLM administration, animals were followed for 21 days. Animals' weight was monitored every 1-3 days. Mice that reached the humane endpoint were sacrificed, evaluated with a score that accounts for the percentage weight loss, labored breathing, increased respiratory rate, decreased activity, hunched posture and ruffled fur.

### Histological examination

Lungs were perfused with PBS, fixed in 4% paraformaldehyde (PFA) for 24 h, subsequently paraffin-embedded, sectioned and stained with hematoxylin and eosin (H&E) and Masson's trichrome. Histological scoring system for mouse lung inflammation was performed according to Gori *et al.* (41). The fibrotic score was determined according to the modified Aschcroft score (42). Histological scoring system for lesions extension quantification in the lung was randomly performed by blindly score lung lobes, using an ×10 magnification. In both scores, the slides were independently evaluated by two researchers in a double-blind fashion. The average score from all fields was used to reach the inflammatory/fibrotic score of each animal. Representative images from the H&E and Masson's trichrome stained tissue sections were acquired using the Olympus BX61 light microscope equipped with an Olympus DP-70 digital camera in a ×10 or ×20 magnification and processed by cellSens™ software.

### Measurement of lactate dehydrogenase (LDH) activity

The LDH activity in BAL and dissociated tissue supernatants was assayed using the LDH kit (K726, BioVision). Briefly, 2 µL of NADH standards and supernatant samples were transferred to a 96-well plate and 100 µL of LDH substrate mixture were added, the absorbance was measured at the wavelength of

450 nm in a microplate reader Varioskan Flash (Thermo Scientific). Then the plate was incubated for 30 min at 37°C. LDH activity in samples was calculated based on the standard curve, according to the manufacturer instructions, and LDH activity in the samples was expressed in nmol/min (mU) *per* mL.

### RNA isolation and RT-qPCR

On day 7 after BLM administration, single-cell suspensions were frozen at -80 °C and RNA was isolated using ExtractMe total RNA kit (EM09, Blirt) according to the manufacturer instructions. On day 14 after BLM administration, the lungs were flash frozen in liquid nitrogen. For the RNA extraction, the tissue was firstly homogenized in TRIzol reagent (15596-026, Invitrogen), through mechanical disruption using microcentrifuge pestle and then needles with crescent gauge values.

First-strand cDNA was synthesized using the commercial Maxima First Strand cDNA synthesis kit (K1671, Thermo Fisher Scientific), following the manufacturer instructions. Real-time PCR amplifications were performed using commercial 2x Maxima probe/ROX master mix (K0231, Thermo Fisher Scientific), containing a Hot Start Taq DNA Polymerase and TaqMan® gene expression premade assays from Applied Biosystem.

Real-time PCR amplifications were performed using commercial 2x Maxima probe/ROX master mix (K0231, Thermo Fisher Scientific), containing a Hot Start Taq DNA Polymerase and TaqMan® gene expression premade assays from Applied Biosystem. PCR probes. The PCR probes analyzed at 7 days were *Gapdh, (*Mm99999915_g1), *Igf-1* (Mm00439560), *Tgf-β1* (Mm01178820_m1), and *connective tissue growth factor* (*Ctgf*, Mm01192933_g1). The PCR probes assessed at 14 days were *Gapdh* (Mm99999915_g1), *Collagen* (*Col) 1a1* (Mm00801666_g1), *Col1a2* (Mm00483888_m1), *Col3a1* (Mm00802300_m1), *Actin-α 2* (*acta-2,* Mm00725412_s1), *S100a4* (Mm00803372_g1), *Tgf-β1* (Mm01178820_m1), *Ctgf* (Mm01192933_g1), *Elastin* (*Eln,* Mm0051470_m1) and *Igf-1* (Mm00439560_m1). Gene expression levels were normalized to endogenous control *Gapdh* and performed accordingly to the $2^{-\Delta\Delta CT}$ method (43). Gene expression data was presented in relative expression fold-change based on $2^{-\Delta\Delta CT}$ (cKO value) / average ($2^{-\Delta\Delta CT}$ (WT group)).

### LEGENDplex™ (Multi-analyte flow assay kit)

Cell suspensions from dissociated lung tissue were homogenized in 1 mL of PBS with protease inhibitors (cOmplete™, Mini, EDTA-free Protease Inhibitor Cocktail, 04693159001, Roche Diagnostic) and 0.05% Tween 20. The respective supernatants were analyzed with the following Mouse LEGENDplex™ panels. Mouse chemokines were analyzed using a mouse 13-plex multiplex bead-based assay panel, including CXCL1 (KC), Eotaxin (CCL11), MCP-1 (CCL2), IP-10 (CXCL10), MIP-1α (CCL3), MIP-1β (CCL4), RANTES

(CCL5), TARC (CCL17), MIG (CXCL9), MIP-3α (CCL20), LIX (CXCL5), BLC (CXCL13) and MDC (CCL22), according to the manufacturer's instructions (740451, Biolegend). Mouse proinflammatory cytokines, were evaluated using a mouse 8-plex multiplex bead-based assay panel, including IL-18, IL-23, IL-12p70, TNF-α, IL-12p40, IL-1β and IL-6, according to the manufacturer's instructions (740848, Biolegend). Additional mouse cytokines, were quantified using a mouse 12-plex multiplex bead-based assay panel, including, IL-2, IL-4, IL-5, IL-6, IL-9, IL-10, IL-13, IL-17A, IL-17F, IL-22, IFN-γ and TNF-α, according to the manufacturer's instructions (741044, Biolegend). The assays were performed in a V-bottom plate according to the manufacturer's protocol. Data acquisition was done using the LSRII flow cytometer. Data acquisition was done using the LSRII flow cytometer. BioLegend's LEGENDplex™ data analysis software was applied for analysis.

### Measurement of lung hydroxyproline

Hydroxyproline concentration of the lungs was measured to determine the total collagen content in the lung using a colorimetric hydroxyproline assay kit (MAK008, Sigma), according to the manufacturer's instructions. In brief, the lungs were homogenized and then hydrolyzed in 6 N HCl at 120°C for 3 h in a dry block heater. Hydrolyzed samples were transferred to a 96-well plate and evaporated to dryness at 70°C. Then, 100 µL of chloramine T reagent was added to each sample and incubated at room temperature (RT) for 5 min, followed by the addition of 100 µL of 4-(Dimethylamine) benzaldehyde reagent to each sample and standard well and incubated at 60°C for 90 min. Absorbance of oxidized hydroxyproline was read at 560 nm in a microplate reader Varioskan Flash (Thermo Scientific). The amount of hydroxyproline was calculated from the standard curve and its concentration was expressed in micrograms *per* milligram of lung.

### Immunofluorescence

Human lung cryobiopsy slides were incubated for 1 h at 60°C, deparaffinized in xylene and dehydrated in 100% ethanol. Antigen retrieval was performed in 10mM citrate buffer (pH 6.0) heated on microwaved (500 W) during 15 min. Non-specific antibody binding sites in lung tissue sections were blocked for 1 h at RT with blocking solution (BS), 1:20 horse serum in PBS. Slides were incubated at RT overnight with the primary antibody CD3 (ab16669, Abcam) 1:200, CD68 (orb197999, Biorbyt) 1:50 or myeloperoxidase (14569, Cell Signaling Technology) 1:300 in BS. Slides were then stained with the secondary antibody horse anti-rabbit IgG (BA-1100, Vector Labs) 1:150 in BS, for 2 h at RT. Tissue sections were further incubated with Alexa Fluor™ 568 streptavidin (S11226, invitrogen) 1:100 in BS for 1 h at RT. For sequential double staining, non-specific antibody binding sites in lung tissue sections were

blocked for 1 h at RT in BS, PBS with 1:5 donkey serum. Slides were incubated at 4 °C overnight with the primary antibody c-MET (ab51067, Abcam) 1:100 in BS. Slides were then stained with the secondary antibody DyLight™ 488 donkey anti-rabbit IgG (406404, Biolegend) 1:150 in BS for 2 h at RT. Nuclei were counterstained with 0.1 μg/mL DAPI for 5 min at RT. After each mentioned incubation, slides were rinsed with PBS containing 0.02% (v/v) Tween-20. Slides were mounted with PermaFluor Aqueous Mounting Medium (Thermo Fisher) and images acquired using an Olympus BX61 light microscope equipped with an Olympus DP-70 digital camera in a ×20 magnification, processed by cellSens software.

### Single cell RNA-seq analysis

Data from a single cell RNA-seq analysis from eight donor lungs and nine lungs from patients with various forms of pulmonary fibrosis, including IPF, HP and CTD-ILD (44). Raw data were retrieved from GEO with the identifier GSE122960, imported into the R environment (version 3.4), and analyzed with the Seurat package (http://satijalab.org/seurat/, version 2.2). R code used for data analysis is available at https://github.com/NUPulmonary/Reyfman2018.

### Statistical analysis

Data were analyzed and plotted using the GraphPad Prism 6.00 (GraphPad Software, San Diego, CA). All results were expressed as group mean ± SEM. For all comparisons, normality was assessed with Shapiro-Wilk test, if normality is not verified non-parametric tests were used. Comparisons between two groups were performed either with parametric unpaired two-tailed Student's t-test or non-parametric two-tailed Mann-Whitney test. Comparisons between three groups were performed either with parametric one-way ANOVA or non-parametric Kruskall-Wallis test. Survival curves (Kaplan-Meier plots) were compared using the log-rank test. A $p$ value of less than 0.05 was considered a statistically significant difference.

## 3. Results

### c-MET Expression is Induced in Lung Immune Cells during BLM-induced Pulmonary Inflammation

Pulmonary inflammation and fibrosis were induced in mice by intratracheal administration of bleomycin (Figure 3A). This PF mouse model is well-established, characterized by an inflammatory phase peaking on day 7, followed by the fibrotic phase peaking on day 14 (45–47).

To elucidate the potential involvement of c-MET signaling pathway in immune cells during the inflammatory phase of the BLM-induced PF mouse model, we evaluated its expression at different time points of the inflammatory phase (Figure 3A). Flow cytometry analysis revealed a significant increase in both the percentage and MFI of lung c-MET$^+$ T cells, which represent more than 50% of the total T cells, during the inflammatory phase of the disease (Figure 3B and 3G). Both the percentage and the mean fluorescent intensity of c-MET$^+$ interstitial lung macrophages (Figure 3C and 3H) increased after day 3 post BLM administration, representing approximately 60% of total IMs. Both the percentage and MFI of c-MET$^+$ lung neutrophils (Figure 3D and 3I), began to increase from day 3 post-BLM administration, representing around 15% of the total neutrophils. No differences were found in alveolar macrophages (Figure 3E) or in eosinophils (Figure 3F). These results clearly demonstrate that c-MET is induced during the inflammatory phase of BLM-induced PF in immune cells.

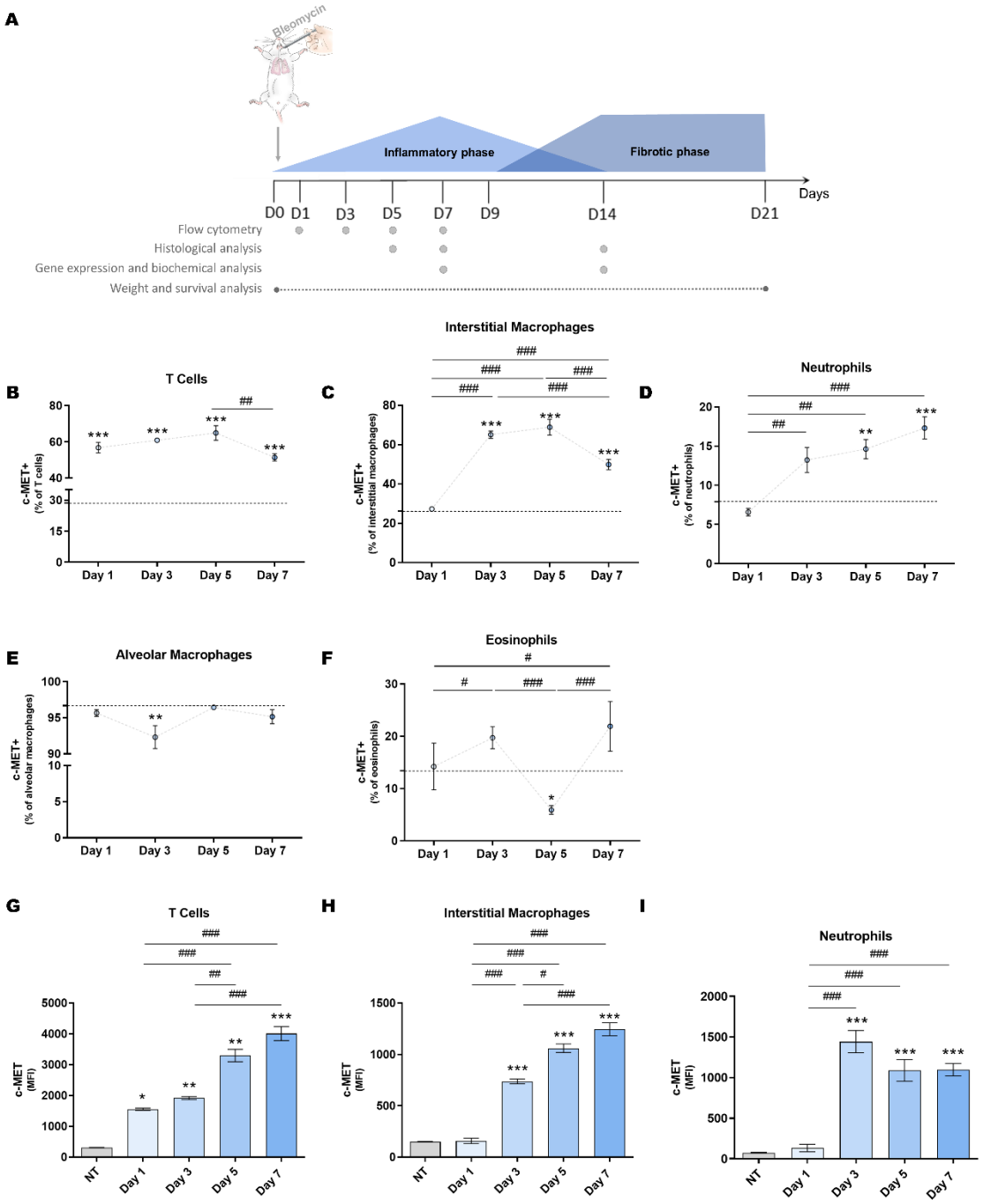



**Figure 3. c-MET expression is enhanced in immune cells during BLM-induced lung inflammation.** (A) Mouse model of pulmonary fibrosis, induced by BLM intratracheal administration. This model comprises an inflammatory reaction which vanishes gradually and it is followed by the fibrotic phase. Several readouts were analyzed at specific time points throughout both phases of disease progression, which are mentioned in the scheme associated with the respective time point. Percentage of c-MET$^+$ among (B) T cells, (C) interstitial macrophages, (D) neutrophils, (E) alveolar macrophages and (F) eosinophils in the dissociated WT mice lung tissues. Horizontal dashed line represents the mean of the vehicle group. MFI of c-MET in lung (G) T cells, (H) interstitial macrophages and (I) neutrophils. Data are expressed as mean ± SEM. Dots and error bars represent mean ± SEM. n = 5–14 per group. $^*p < 0.05$, $^{**}p < 0.01$, $^{***}p < 0.001$, comparison with vehicle. $\#p < 0.05$, $\#\#p < 0.01$, $\#\#\#p < 0.001$, comparison between time points. For all the experiments, similar results were obtained in three independent experiments.

### *c-Met* Deletion in Immune Cells Attenuates Severity and Lung Injury of BLM-induced Pulmonary Fibrosis

To investigate the impact of c-MET signaling pathway in immune cells on the severity of BLM-induced PF, we analyzed the body weight and survival of WT mice and mice with *c-Met* deletion in immune cells, cKO, until day 21 after BLM administration (Figure 3A). While both WT and cKO mice experienced weight lost until day 7 following BLM injection, cKO mice showed a significant recovery in body weight after day 7 (Figure 4A). Survival analysis revealed that only 20% of WT mice survived, with the highest mortality rate on day 5, whereas 60% of cKO mice survived after BLM injection (Figure 4B).

As the most significant differences in survival and weight recovery between animal groups occurred on day 5 and 7, we explored the alterations in BLM-induced inflammation (Figure 3A). On day 5 after BLM administration, cKO mice exhibited slightly more inflammatory infiltration in the lungs compared to WT animals, as confirmed by a significant increase in the inflammatory score displayed by cKO mice (Figure 4C and 4D). Interestingly, on day 7 after BLM administration, cKO mice presented fewer and smaller lung inflammatory infiltrates than WT mice, which had extensive lung inflammation (Figure 4E and 4F). To assess tissue and cell cytotoxicity, we measured LDH activity, which was significantly reduced in dissociated lung and BAL supernatants of cKO mice 7 days after BLM injection (Figure 4G and 4H). Indication of less tissue injury was found in cKO mice, and we examined the influence of c-MET signaling pathway in immune cells on the repair environment. Notably, cKO mice presented significantly increased levels of repair-associated genes, *Igf-1* and *Ctgf,* on day 7 after BLM administration, suggesting a more pro-repair environment (Figure 4I).

Taken together, these results demonstrate that *c-Met* deletion in immune cells leads to an earlier inflammatory cell infiltration but paradoxically results in a less cytotoxic and more proficient pro-repair environment during BLM-induced lung inflammation.

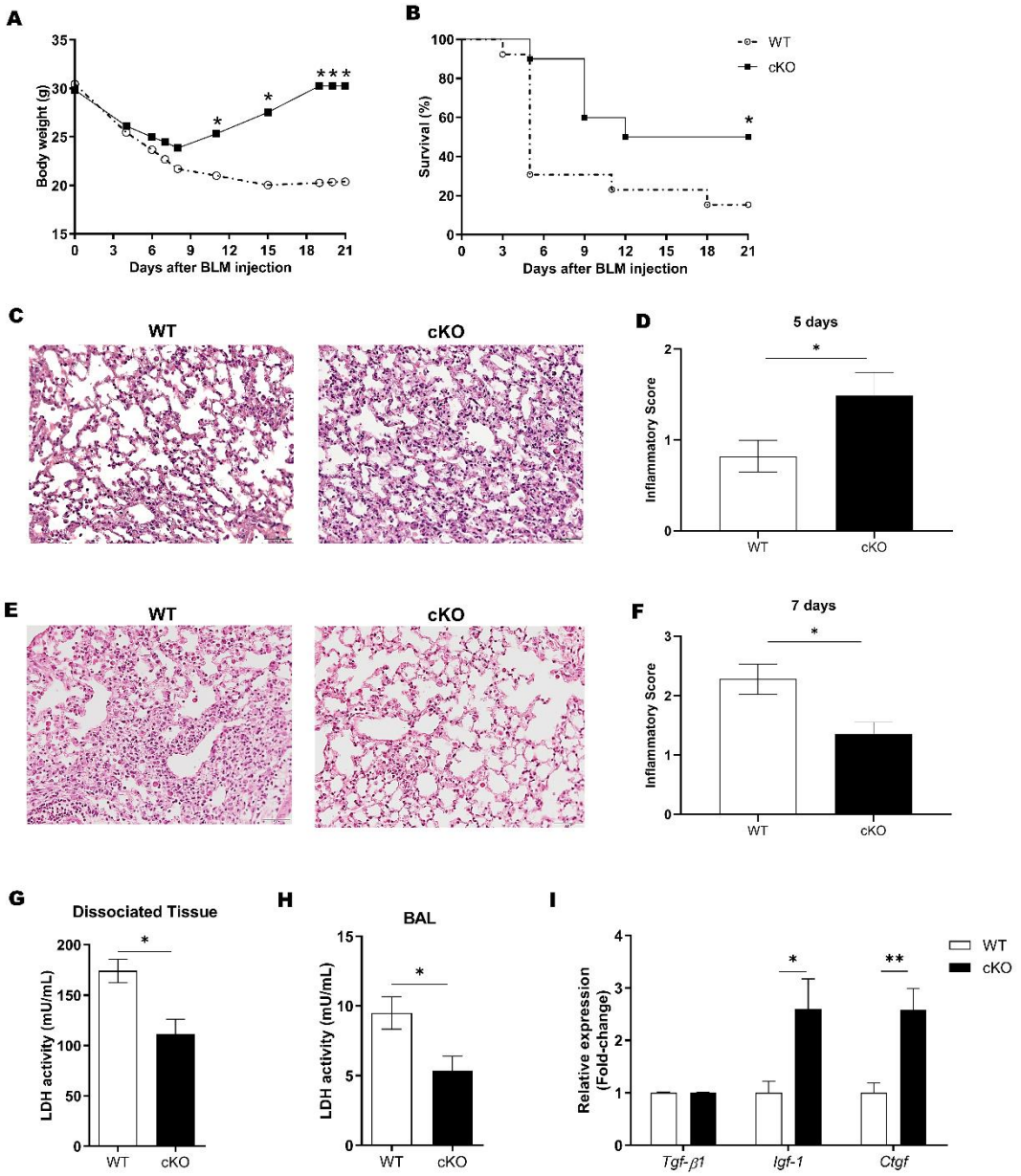



**Figure 4. Deletion of *c-Met* from immune cells attenuates lung injury following BLM administration.** WT and cKO mice administered intratracheally with BLM were followed for (A) weight change and (B) survival. n=10–24 mice per group. (C) Representative images of lung sections stained with H&E at 5 days after BLM injection and (D) respective scoring. (E) Representative images of lung sections stained with H&E at 7 days after BLM injection and (F) respective scoring. Original magnification ×20, scale bar 50 μm. LDH activity in the (G) dissociated tissue and (H) BAL supernatant at 7 days after BLM injection. (I) Gene expression of repair-associated molecules (Tgf-β1, Igf-1, Ctgf) in the lung at 7 days after BLM injection. Columns and error bars represent mean ± SEM. n = 12–14 per group. $*p < 0.05$. Similar results were obtained in three independent experiments.

## Deletion of *c-Met* from Immune Cells Triggers Their Early Accumulation and Restrained the Proinflammatory Environment

To better characterize the kinetics of immune cell populations in the lung, we performed flow cytometry analyses during the BLM-induced inflammatory phase (Figure 3A). Interestingly, in cKO mice, we observed an early accumulation of immune cell populations that exhibited c-MET expression induction. The number

of T cells, interstitial macrophages and eosinophils were significantly increased in the lungs of cKO mice on day 5 after injection of BLM (Figure 5A, 5B and 5E). Of note, the number of neutrophils significantly increased in the lungs of cKO mice at 3 and 5 days after BLM injection (Figure 5C). In contrast, and in accordance with the reduced inflammatory score observed on day 7 after BLM administration, the number of T cells and neutrophils significantly decreased in the lungs of cKO mice (Figure 5A and 5C). No differences were found in the number of alveolar macrophages at any time point (Figure 5D).

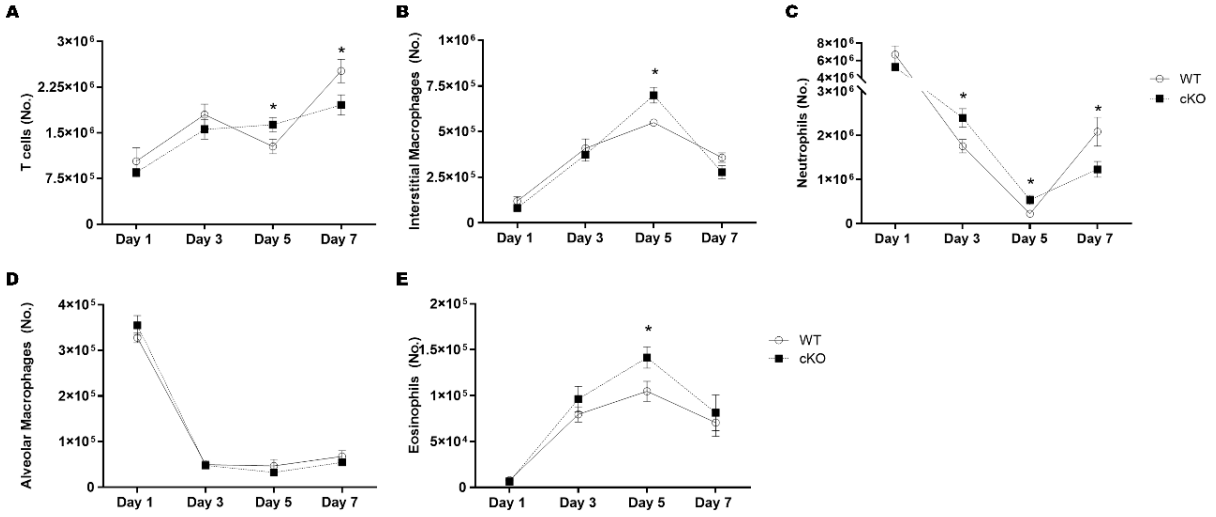



**Figure 5. *c-Met* deletion in immune cells promotes early inflammatory cells recruitment after BLM administration.** Number of (A) T cells, (B) interstitial macrophages, (C) neutrophils, (D) alveolar macrophages and (E) eosinophils. Cell numbers were calculated based on the total number of cells in the dissociated lung. Dots and error bars represent mean ± SEM. n = 8–10 per group. $*p < 0.05$, $**p < 0.01$, $***p < 0.001$. Similar results were obtained in three independent experiments.

To confirm that the accumulation of immune cells was a result of alterations in chemotactic signals, we analyzed lung chemokine levels. Consistent with previous results of immune cell accumulation in the lung, the levels of chemokines for neutrophils, monocytes, macrophages, T cells and eosinophils, namely CXCL1 (KC), MCP-1 (CCL2), eotaxin (CCL11), MIP-1α (CCL3), MIP-1β (CCL4) and IFN-gamma-inducible protein of 10 kDa (IP-10/CXCL10) were significantly increased in the lungs of cKO mice on day 5 post-BLM administration, while some of these chemokines were significantly decreased on day 7 (Figure 6A). The early accumulation of immune cells was concomitant with the paradoxically attenuated proinflammatory environment in cKO mice. Of note, TNF-α, IL-1β, IL-18, IL-23, IL-12p40 and IL-12p70 levels were reduced in cKO mice, mostly on day 5 (Figure 6B). To clarify whether this attenuated proinflammatory environment was associated with changes in immune function related to the respective phenotypic activation of cells, we assessed the levels of cytokines related to immune function, which showed a decrease in cKO mice on day 5 (Figure 6C).

These data highlight the cellular immune alterations related with c-MET signaling pathway in immune cells. Notably, *c-Met* deletion in immune cells leads to a restrained proinflammatory environment, along with a balanced phenotypic activation of inflammatory cells during BLM-induced lung inflammation.

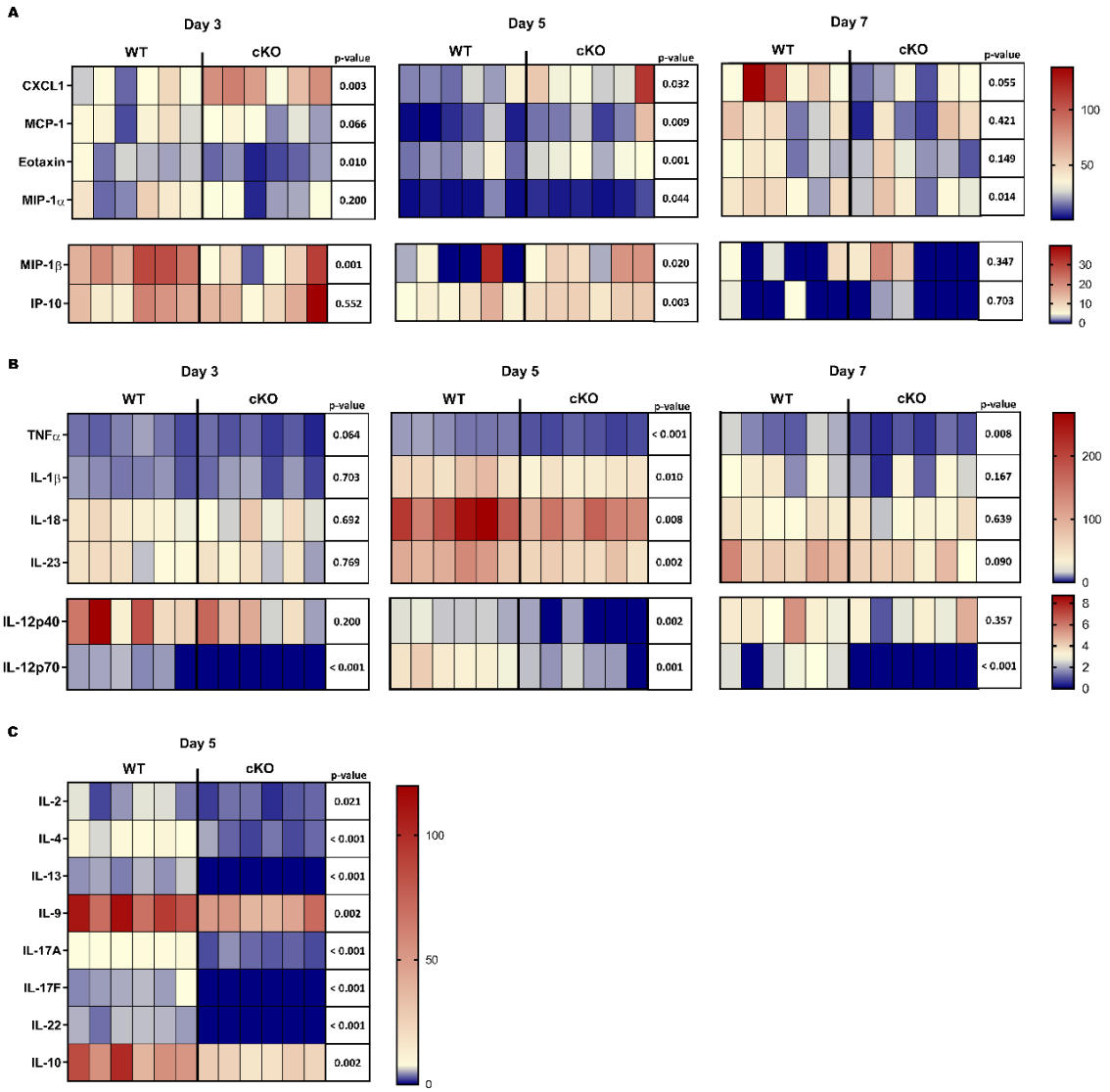



**Figure 6. Boosted leukocyte chemoattraction and restrained proinflammatory milieu in cKO mice lung mainly on day 5 following BLM administration.** Heatmap of the concentration, pg/mL, of (A) chemokines and (B) proinflammatory cytokines in lung on day 3, 5 and 7 and (C) interleukins associated with inflammatory cells phenotypic activation in lung on day 5 after bleomycin administration. *p*-value for each comparation is reported. n = 6 *per* group.

## Lung fibrosis is Attenuated by *c-Met* Deletion in Immune Cells

Then, we decided to clarify whether these alterations impacted the establishment of BLM-induced fibrosis (Figure 3A). Histological analysis on day 14 after BLM administration revealed multifocal fibrotic pulmonary lesions, alveolar architecture destruction and loss of alveolar surface area in WT animals (Figure 7A). In contrast, cKO mice displayed preserved alveolar architecture, alveolar surface area and thinner alveolar walls (Figure 7A). To further assess fibrosis, we analyzed collagen deposition in lung sections using Masson's

trichrome staining. The pulmonary interstitium from cKO mice displayed less collagen fiber deposition compared to WT mice, indicating reduced collagen accumulation in cKO mice (Figure 7A). In accordance with histological evaluation, the Ashcroft score was significantly lower in cKO mice (Figure 7B). Additionally, hydroxyproline levels, a collagen component, were significantly decreased in the lungs of cKO mice at 14 days post-BLM treatment (Figure 7C). Furthermore, cKO mice exhibited significantly lower expression levels of fibrotic markers (*Col1a1*, *Col1a2*, S*100a4* and *Igf-1)* at 14 days after BLM injection (Figure 7D).

Taken together, these data clearly demonstrate that the deletion of *c-Met* in immune cells promotes the attenuation of PF, suggesting that c-MET expression in immune cells boosts the fibrogenesis process.

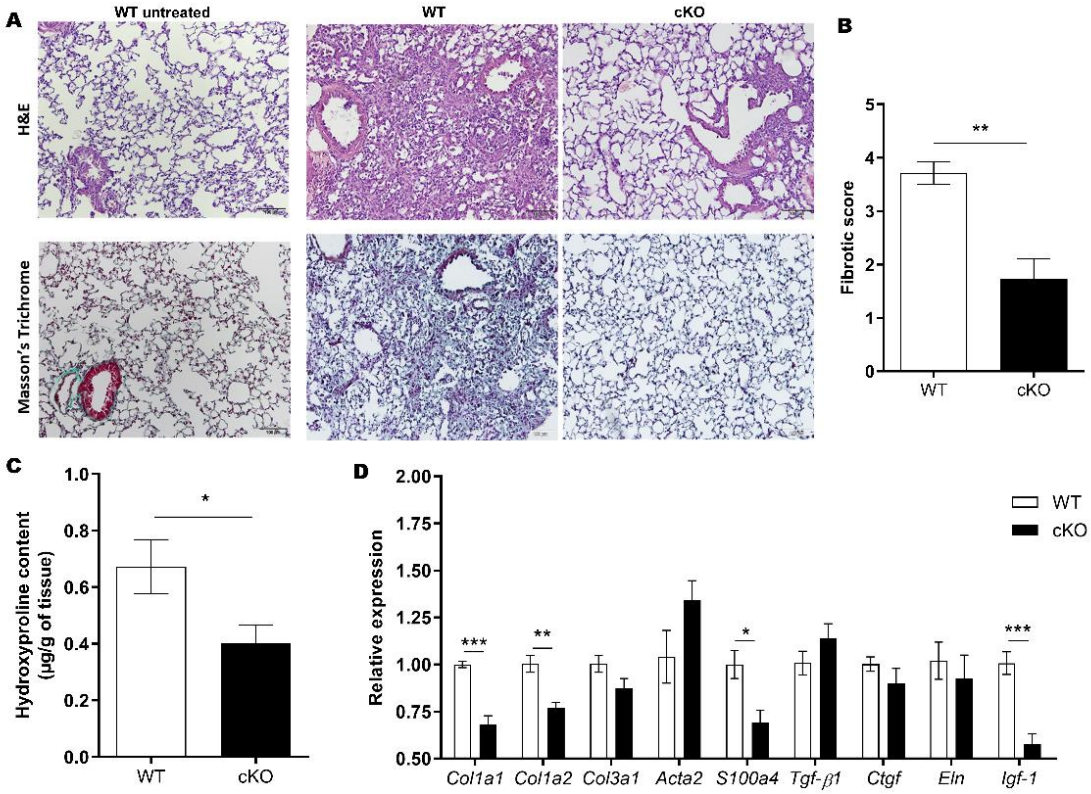



**Figure 7. Attenuated lung fibrosis in cKO mice on day 14 following BLM administration.** (A) Representative images of lung sections stained with H&E and Masson's trichrome. Original magnification ×10, scale bar 100 µm. (B) Ashcroft scoring of lung fibrosis. (C) Hydroxyproline levels in lungs. (D) Gene expression of profibrotic mediators in whole-lung samples. Columns and error bars represent mean ± SEM. n = 12–14 *per* group. **p* < 0.05, ***p* < 0.01, ****p* < 0.001. Similar results were obtained in three independent experiments.

### Lung T cells from Patients with Fibrosing ILDs Show High Expression of c-MET

Finally, to assess the clinical relevance of c-MET signaling pathway in ILDs, we performed immunofluorescence analysis of c-MET on lung cryobiopsies from a patient cohort of Hospital de São João (Table 2). We observed enhanced c-MET expression in T cells from patients with fibrosing conditions, mainly IPF and fibrotic HP, compared to CTD-ILD and non-fibrotic HP patients (Figure 8A and 8B). Furthermore, flow cytometry analysis of cryopreserved BAL samples from an additional cohort of Hospital de São João

patients (Table 3), confirmed elevated c-MET expression in T cells of fibrotic patients (Figure 8C). Of note, a separate group of patients with lung disease other than ILDs exhibited the lowest levels of c-MET expression in T cells (Figure 8C). Bioinformatics analysis of single-cell RNA sequencing data from lung biopsies of healthy donors and ILD patients, including IPF, HP and CTD-ILD (44) further supported our findings. Accordingly, T cells from patients with fibrosing conditions, mainly IPF and HP, presented higher *c-MET* expression levels compared to CTD-ILD patients and healthy donors (Figure 8D).

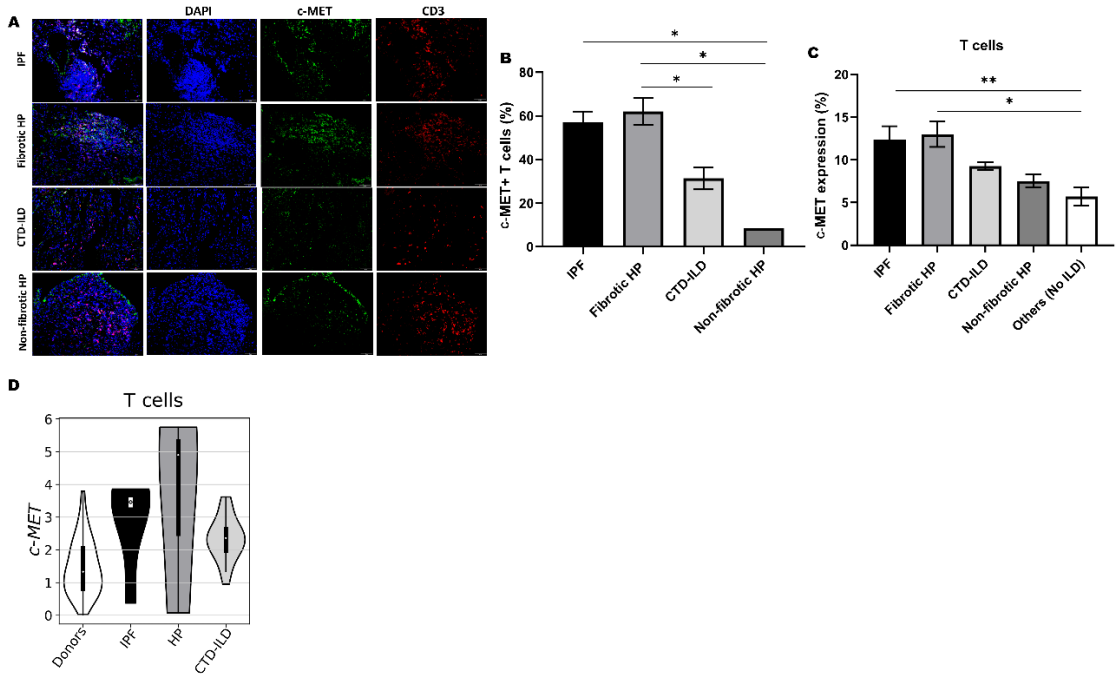



**Figure 8. c-MET expression is augmented in T cells in fibrosis-related ILDs.** (A) Representative images of immunofluorescence on c-MET (green) in T cells (red) and (B) respective expression quantification on human lung sections from a cohort of patients. Original magnification ×20, scale bar 50 μm. (C) Percentage of T cells with c-MET expression, quantified by flow cytometry on cryopreserved BAL samples from a cohort of patients. (D) Plot representing expression of *c-MET* in T cells from donor and ILD patients. Columns and error bars represent mean ± SEM. n = 6 *per* group. $*p < 0.05$, $**p < 0.01$, $***p < 0.001$.

Regarding c-MET expression in other cell populations, such as macrophages and neutrophils, no associations with fibrotic outcome were found (Figure 9). Macrophage c-MET expression was increased in non-HP conditions, including IPF and CTD-ILD (Figure 9A and 9B), while neutrophil c-MET expression levels were higher in IPF patients compared to fibrotic HP and CTD-ILD, with no expression detected in non-fibrotic HP (Figure 9C and 9D).

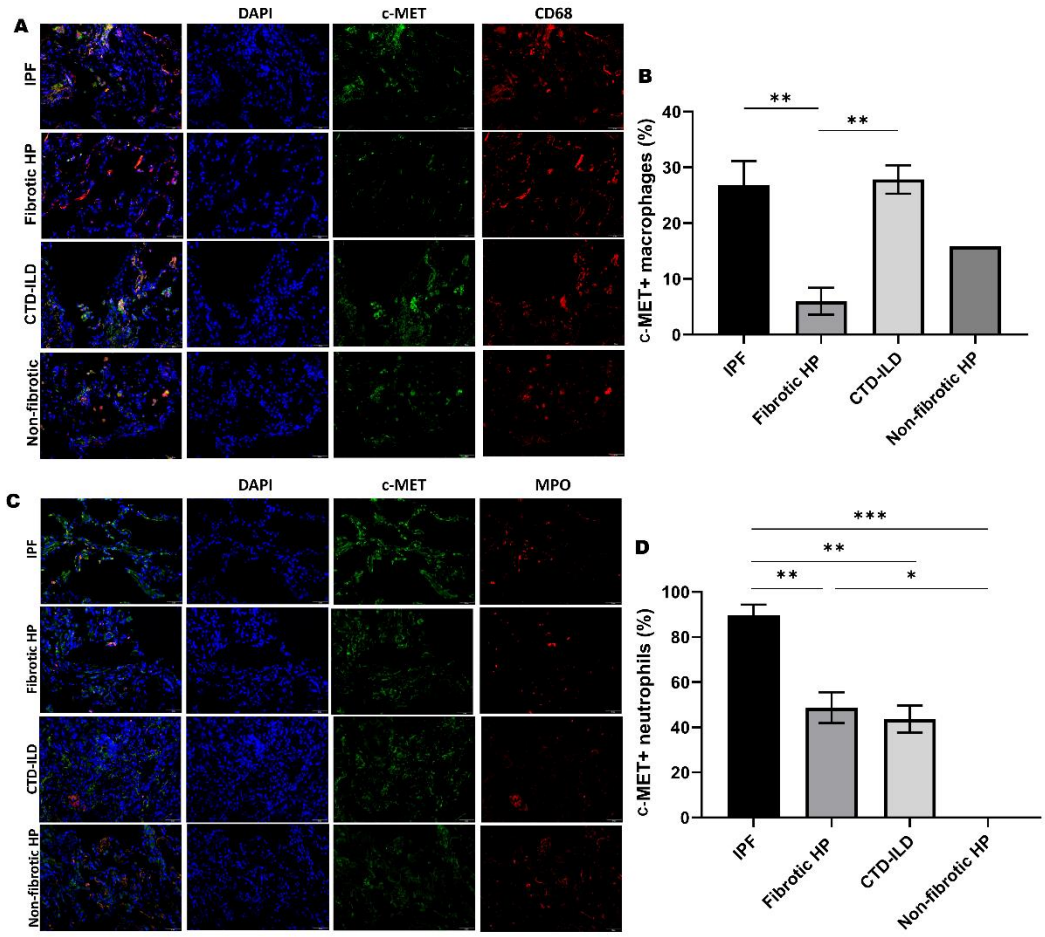



**Figure 9. Profile of c-MET expression in neutrophils and macrophages among distinct interstitial lung diseases.** (A) Representative images of immunofluorescence on lung sections from a cohort of patients confirms c-MET (green) in macrophages (red) and (B) respective expression quantification. (C) Representative images of immunofluorescence on lung sections from a cohort of patients confirms c-MET (green) in neutrophils (red) and (D) respective expression quantification. Original magnification ×20, scale bar 50 µm. Columns and error bars represent mean ± SEM. n = 6 *per* group. $*p < 0.05$, $**p < 0.01$, $***p < 0.001$.

Figure 10 illustrates the variable pattern of c-MET expression among immune cells of ILD patients. Notably, patients with IPF and fibrotic HP present the highest percentages of c-MET$^+$ T cells, IPF patients present the highest percentages of c-MET$^+$ neutrophils and patients with IPF and CTD-ILD present the highest percentages of c-MET$^+$ macrophages.

In summary, these data reveal an association between enhanced c-MET expression in immune cells and interstitial lung diseases, particularly indicating a potential involvement of c-MET expression in T cells underlying the development of the fibrosing condition.

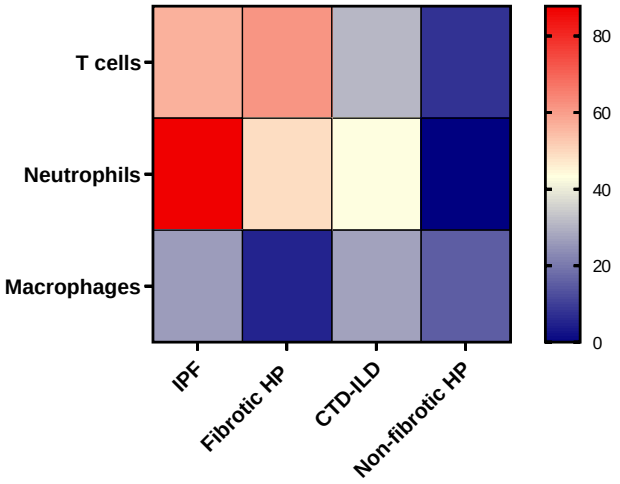



**Figure 10. Profile of c-MET expression in T cells, neutrophils and macrophages among distinct interstitial lung diseases.** Heatmap of the c-MET expression profiles based on mean expression percentages in immune cell populations among distinct interstitial lung diseases.

## 4. Discussion

The current therapies for pulmonary fibrosis primarily slow disease progression rather than reversing it. Previous studies have highlighted the crucial role of c-MET in regulating immune cell recruitment and effector functions in various contexts, such as inflamed tumors, *Leishmania mexicana* infection, and intestinal inflammation. Our study now demonstrates that the immune HGF/c-MET signaling pathway is a novel modulator of the progression of PF. We show that both ILD patients and mice during the acute inflammatory phase of BLM-induced PF have enhanced c-MET expression in lung immune cells. Moreover, we show that the absence of *c-Met* in immune cells reduced the severity of BLM-induced PF. This finding was correlated with an anticipated infiltration of immune cells, namely T cells, IMs, neutrophils, and eosinophils in the lungs, along with a decreased proinflammatory and cytotoxic environment. Accordingly, *c-Met* deletion in immune cells led to more controlled and faster resolution of inflammation than under normal conditions, thereby ameliorating BLM-induced PF.

Previous studies showed induction of c-MET expression in immune cells upon inflammatory stimuli (36–40,48). Particularly, c-MET expression levels were found to be upregulated in circulating human and mouse neutrophils upon inflammatory stimuli (36). In the same line, *L. mexicana* induces c-MET expression predominantly in neutrophils (39). Additionally, in a murine model of intestinal inflammation, c-MET expression was induced in blood and colonic neutrophils (40). Accordingly, we now show that in a well-established murine model of PF induced by BLM, characterized by an early phase of acute lung inflammation and injury (45–47), c-MET expression is upregulated in T cells, interstitial macrophages and neutrophils during this phase.

Furthermore, c-MET exerts an important regulation of immune cell recruitment and functions in various inflammatory contexts. Particularly, c-MET expression in neutrophils has been shown to be required for their transmigration and nitric oxide release in inflamed tumors, which are essential for tumor cell killing (36). Also, c-MET inhibition reduced neutrophil recruitment into T cell–inflamed tumor microenvironment and draining lymph nodes in response to cytotoxic immunotherapies (37). In $CD8^+$ T lymphocytes, c-MET expression enhances their cytolytic capacities ultimately providing greater efficacy in killing melanoma cells (38). Additionally, a mouse model with *c-Met* deleted in neutrophils better controlled the parasite load and the lesion size after *L. mexicana* infection, once *c-Met* deletion reinforced neutrophilic ROS production after infection (39). The same mouse model, with *c-Met* deletion in neutrophils, exhibited reduced disease severity upon induction of intestinal inflammation (40). Furthermore, HGF treatment of c-MET-expressing M1 macrophages shift their phenotype toward M2 (48). To further dissect the role of c-MET in the immune response following BLM administration, we used, in agreement with previous

studies (36), the Tie2-Cre line to specifically delete *c-Met* from bone marrow immune cells, as limited cross-activation of c-MET was detected in endothelial cells in our mouse model of PF. Interestingly, mice with absence of *c-Met* in immune cells exhibited attenuated long-term severity of BLM-induced lung fibrosis, as revealed by the lower weight loss and improved survival. Moreover, mice with deletion of *c-Met* in immune cells presented reduced lung inflammation and injury at the peak of the inflammatory phase of BLM-induced PF. Interestingly, this reduced lung injury was concomitant with higher expression levels of repair-associated growth factors, namely *Igf-1* and *Ctgf*. In fact, previous studies demonstrated that these growth factors could have opposite roles depending on the time course of the disease. Particularly, in the presence of inflammation or without the premature high expression levels of TGF-β, IGF-1 production led to enhanced epithelial cell proliferation and to the absence of chronically denuded alveolar basement membranes, which together result in a constant repair process (49). Furthermore, in skeletal muscle regeneration, IGF-1 produced by monocyte/macrophage has also been described as a potent enhancer of tissue regeneration (50). CTGF is a well-known player downstream TGF-β. However once TGF-β is not altered, an early, transient upregulation of CTGF in the wound repair process promotes normal repair and is necessary to maintain an appropriate angiogenic process within wounds (51). These studies suggest that when expression is confined to early tissue repair, IGF-1 and CTGF serve a pro-reparative role.

Remarkably, during BLM-induced inflammation, an early increase in infiltration of inflammatory cells into the lung of cKO mice was observed, namely the cell populations which were normally found to have induced c-MET expression, T cells, interstitial macrophages, neutrophils, and eosinophils, paradoxically with less simultaneous proinflammatory environment. Overall, *c-Met* deletion associates with lower inflammation, concomitant with a less cytotoxic, less proinflammatory and more repairing environment at the peak of inflammatory phase.

Chemokines are essential players to enhance and properly control the recruitment of inflammatory cells to injury sites. Interestingly, the expression of CXCL1, a potent neutrophil chemoattractant (52,53), was increased in cKO mice on day 3 and 5, which was concomitant with an increased proportion of neutrophils in the lung. Subsequently, on day 7, the proportion of neutrophils in cKO mice lung was drastically decreased compared to WT, as well as the CXCL1 expression. Concomitant with increased MCP-1 expression on day 5, the proportion of macrophages was increased in cKO mice at this time point. MCP-1 is a potent chemoattractant and activator of monocytes/macrophages and is involved in macrophage activation leading to the release of inflammatory mediators and tissue damage (54,55). Eotaxin, known to be a potent chemoattractant for eosinophils (56), showed increased levels in cKO mice on day 5. These

come in accordance with the flow cytometry results, since eosinophils proportion was higher in cKO mice at this time point. MIP-1α (CCL3), MIP-1β (CCL4) and IP-10 (CXCL10) are known chemoattractants for monocytes/macrophages and T cells (57). Expression levels of these chemokines were augmented in cKO mice on day 5. Accordingly, both interstitial macrophages and T lymphocytes were increased in cKO mice at this time point.

The balanced production of proinflammatory cytokines and interleukins associated with the phenotypic activation of inflammatory cells is crucial for controlling inflammation at tissue injury sites. This control prevents exacerbations of damage and favors tissue repair. As so, we evaluated whether the production of proinflammatory cytokines and interleukins was influenced by the c-MET signaling pathway in immune cells. Notably, the analysis of lung proinflammatory cytokines revealed diminished levels in cKO mice compared to WT, mainly on day 5. Furthermore, levels of interleukins produced by inflammatory cells upon activation were lower in the lung of cKO mice. These results suggest that the reduced lung injury in cKO mice is a consequence of more controlled inflammatory recruitment and activation, and diminished proinflammatory environment, which results in lung repair rather than fibrosis progression. In fact, our data at the peak of the fibrotic phase of BLM-induced PF, that occurs on day 14, demonstrated a decrease in fibrotic lesion extension, collagen deposition and in the levels of a profibrotic factor, Igf-1 (58), associated with *c-Met* deletion in the immune cells.

Altogether, our findings reveal that c-MET signaling pathway in immune cells is enhancing their uncontrolled recruitment and activation towards a more proinflammatory and profibrotic phenotype, exacerbating lung injury and ultimately culminating in fibrosis in the BLM-induced PF mouse model.

As illustrated in Figure 11, our results show that *c-Met* deletion in immune cells significantly ameliorated BLM-induced lung fibrosis. The attenuation of lung fibrosis can be attributed to the anticipated inflammatory recruitment and concomitant attenuated proinflammatory environment, ultimately leading to enhanced epithelial repair. Overall, suggesting that c-MET signaling pathway in immune cells deregulates inflammatory recruitment and activation, ultimately leading to pulmonary fibrosis.

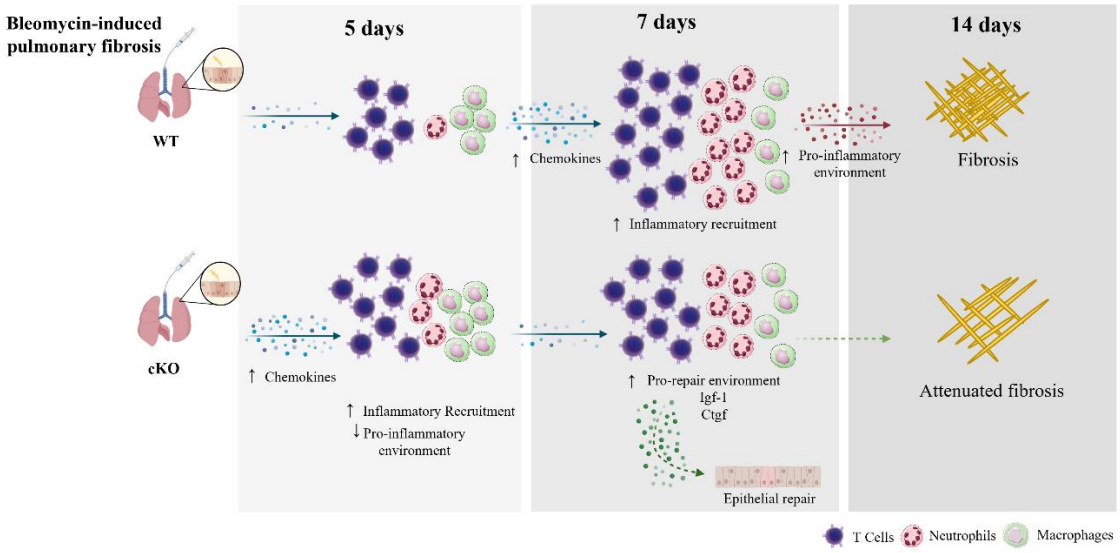



**Figure 11. Schematic illustration of the impact of c-MET in immune cells during BLM-induced PF progression.** Lung injury is induced by BLM leading to uncontrolled inflammatory recruitment, followed by excessive deposition of extracellular matrix proteins, as collagen. Absence of *c-Met* in immune cells resulted in anticipated inflammatory recruitment and attenuated proinflammatory environment, leading to higher epithelial repair, which later culminates in lower collagen deposition and prevents fibrosis.

ILDs include a heterogenous group of parenchyma disorders associated with variable lung inflammatory patterns and fibrosis, being IPF the prototypical fibroproliferative disorder (7). Additionally, other common ILDs can also develop a fibrotic condition, namely HP and CTD-ILD (3,59–62). Although patients with CTD-ILD can be also categorized as non-fibrotic or fibrotic, in our study this distinction was not made. Immune cells have been involved in the pathogenesis of ILDs (63–65), with various populations contributing to the progression of ILDs, particularly macrophages (44,66–68) and lymphoid cells (64,69,70). Interestingly, our results show that T cells, macrophages and neutrophils present enhanced c-MET expression in specific ILDs. Specifically, c-MET expression is higher in T cells from patients with fibrotic conditions, mainly IPF and fibrotic HP. In contrast, macrophages display increased c-MET expression in non-HP conditions, namely IPF and CTD-ILD. Furthermore, neutrophils exhibited elevated c-MET expression in IPF patients compared to those with other fibrotic conditions. These patterns of c-MET expression appear to be associated with the respective ILD. Concordantly, a bioinformatics analysis of single-cell RNA sequencing of biopsies from healthy donors and patients with ILDs, revealed an enrichment of c-MET expressing T cells in patients with fibrosing conditions, mainly IPF and HP. Thus, suggesting a potential involvement of c-MET expression in T cells in the development of the fibrosing condition. Interestingly, in the BAL of patients with IPF, the concentration of HGF was significantly higher than in normal controls (71–74). Since c-MET is classically activated by the binding of its primary ligand, HGF, the receptor and the respective signaling pathway will therefore be overactivated under fibrotic conditions. As such, the expression of c-MET in lung immune cells might be induced by HGF under fibrotic conditions,

reinforcing their proinflammatory and cytotoxic capacities which contributes to the establishment of tissue fibrosis.

Together, both mice and human data highlight the contribution of c-MET-expressing immune cells to the progression of fibrosing condition. Therefore, selective blockage of c-MET pathway in immune cells emerges as an attractive therapeutic strategy to control tissue damage triggered by inflammation.

## 5. References


1. McLean-Tooke, A., Moore, I. & Lake, F. Idiopathic and immune-related pulmonary fibrosis: diagnostic and therapeutic challenges. *Clin. Transl. Immunol.* **8,** 1–15 (2019).
2. Xu, Y. *et al.* Clinical and computed tomographic imaging features of novel coronavirus pneumonia caused by SARS-CoV-2. *J. Infect.* **80,** 394–400 (2020).
3. Salisbury, M. L. *et al.* Diagnosis and Treatment of Fibrotic Hypersensitivity Pneumonia. Where We Stand and Where We Need to Go. *Am. J. Respir. Crit. Care Med.* **196,** 690–699 (2017).
4. Wells, A. U. & Denton, C. P. Interstitial lung disease in connective tissue disease—mechanisms and management. *Nat. Rev. Rheumatol.* **10,** 728–739 (2014).
5. Cottin, V. Idiopathic interstitial pneumonias with connective tissue diseases features: A review. *Respirology* **21,** 245–258 (2016).
6. Mira-Avendano, I. *et al.* Interstitial Lung Disease and Other Pulmonary Manifestations in Connective Tissue Diseases. *Mayo Clin. Proc.* **94,** 309–325 (2019).
7. Ley, B., Collard, H. R. & King, T. E. Clinical Course and Prediction of Survival in Idiopathic Pulmonary Fibrosis. *Am. J. Respir. Crit. Care Med.* **183,** 431–440 (2011).
8. Raghu, G. Treatment of Idiopathic Pulmonary Fibrosis With Ambrisentan. *Ann. Intern. Med.* **158,** 641 (2013).
9. Shulgina, L. *et al.* Treating idiopathic pulmonary fibrosis with the addition of co-trimoxazole: a randomised controlled trial. *Thorax* **68,** 155–162 (2013).
10. Raghu, G. *et al.* An Official ATS/ERS/JRS/ALAT Statement: Idiopathic pulmonary fibrosis: Evidence-based guidelines for diagnosis and management. *Am. J. Respir. Crit. Care Med.* **183,** 788–824 (2011).
11. Raghu, G. *et al.* An Official ATS/ERS/JRS/ALAT Clinical Practice Guideline: Treatment of Idiopathic Pulmonary Fibrosis. An Update of the 2011 Clinical Practice Guideline. *Am. J. Respir. Crit. Care Med.* **192,** e3–e19 (2015).
12. Knudsen, L., Ruppert, C. & Ochs, M. Tissue remodelling in pulmonary fibrosis. *Cell Tissue Res.* **367,** 607–626 (2017).
13. Fernandez, I. E. & Eickelberg, O. New cellular and molecular mechanisms of lung injury and fibrosis in idiopathic pulmonary fibrosis. *Lancet* **380,** 680–688 (2012).
14. Wynn, T. A. Integrating mechanisms of pulmonary fibrosis. *J. Exp. Med.* **208,** 1339–1350 (2011).
15. Ricard-Blum, S., Baffet, G. & Théret, N. Molecular and tissue alterations of collagens in fibrosis. *Matrix Biol.* **68–69,** 122–149 (2018).
16. Furuie, H., Yamasaki, H., Suga, M. & Ando, M. Altered accessory cell function of alveolar macrophages: a possible mechanism for induction of Th2 secretory profile in idiopathic pulmonary fibrosis. *Eur. Respir. J.* **10,** 787–794 (1997).
17. Hancock, A., Armstrong, L., Gama, R. & Millar, A. Production of Interleukin 13 by Alveolar Macrophages from Normal and Fibrotic Lung. *Am. J. Respir. Cell Mol. Biol.* **18,** 60–65 (1998).
18. Jakubzick, C., Kunkel, S. L., Puri, R. K. & Hogaboam, C. M. Therapeutic Targeting of IL-4- and IL-13-Responsive Cells in Pulmonary Fibrosis. *Immunol. Res.* **30,** 339–350 (2004).
19. Wynn, T. A. Type 2 cytokines: mechanisms and therapeutic strategies. *Nat. Rev. Immunol.* **15,** 271–282 (2015).
20. Chung, S. I. *et al.* IL-13 is a therapeutic target in radiation lung injury. *Sci. Rep.* **6,** 39714 (2016).
21. Puttur, F., Gregory, L. G. & Lloyd, C. M. Airway macrophages as the guardians of tissue repair in the lung. *Immunol. Cell Biol.* **97,** 246–257 (2019).
22. Hesketh, M., Sahin, K. B., West, Z. E. & Murray, R. Z. Macrophage Phenotypes Regulate Scar Formation and Chronic Wound Healing. *Int. J. Mol. Sci.* **18,** 1545 (2017).
23. Byrne, A. J., Mathie, S. A., Gregory, L. G. & Lloyd, C. M. Pulmonary macrophages: key players in the innate defence of the airways. *Thorax* **70,** 1189–1196 (2015).

24. Joshi, N., Walter, J. M. & Misharin, A. V. Alveolar Macrophages. *Cell. Immunol.* **330,** 86–90 (2018).
25. Gibbings, S. L. *et al.* Three Unique Interstitial Macrophages in the Murine Lung at Steady State. *Am. J. Respir. Cell Mol. Biol.* **57,** 66–76 (2017).
26. Song, E. *et al.* Influence of alternatively and classically activated macrophages on fibrogenic activities of human fibroblasts. *Cell. Immunol.* **204,** 19–28 (2000).
27. Libório-Ramos, S., Barbosa-Matos, C., Fernandes, R., Borges-Pereira, C. & Costa, S. Interstitial Macrophages Lead Early Stages of Bleomycin-Induced Lung Fibrosis and Induce Fibroblasts Activation. *Cells* **12,** 402 (2023).
28. Murray, P. J. Macrophage Polarization. *Annu. Rev. Physiol.* **79,** 541–566 (2017).
29. Zhang, L. *et al.* Macrophages: friend or foe in idiopathic pulmonary fibrosis? *Respir. Res.* **19,** 170 (2018).
30. Kimura, T. *et al.* Polarization of M2 macrophages requires Lamtor1 that integrates cytokine and amino-acid signals. *Nat. Commun.* **7,** 13130 (2016).
31. Byrne, A. J., Maher, T. M. & Lloyd, C. M. Pulmonary Macrophages: A New Therapeutic Pathway in Fibrosing Lung Disease? *Trends Mol. Med.* **22,** 303–316 (2016).
32. Kolaczkowska, E. & Kubes, P. Neutrophil recruitment and function in health and inflammation. *Nat. Rev. Immunol.* **13,** 159–175 (2013).
33. Gregory, A. D. *et al.* Neutrophil elastase promotes myofibroblast differentiation in lung fibrosis. *J. Leukoc. Biol.* **98,** 143–152 (2015).
34. Takemasa, A., Ishii, Y. & Fukuda, T. A neutrophil elastase inhibitor prevents bleomycin-induced pulmonary fibrosis in mice. *Eur. Respir. J.* **40,** 1475–1482 (2012).
35. Kinder, B. W. *et al.* Baseline BAL Neutrophilia Predicts Early Mortality in Idiopathic Pulmonary Fibrosis. *Chest* **133,** 226–232 (2008).
36. Finisguerra, V. *et al.* MET is required for the recruitment of anti-tumoural neutrophils. *Nature* **522,** 349–353 (2015).
37. Glodde, N. *et al.* Reactive Neutrophil Responses Dependent on the Receptor Tyrosine Kinase c-MET Limit Cancer Immunotherapy. *Immunity* **47,** 789-802.e9 (2017).
38. Benkhoucha, M. *et al.* Identification of a novel population of highly cytotoxic c-Met-expressing CD8 + T lymphocytes. *EMBO Rep.* **18,** 1545–1558 (2017).
39. Passelli, K. *et al.* The c-MET receptor tyrosine kinase contributes to neutrophil-driven pathology in cutaneous leishmaniasis. *PLoS Pathog.* **18,** 1–24 (2022).
40. Stakenborg, M. *et al.* Neutrophilic HGF-MET Signalling Exacerbates Intestinal Inflammation. *J. Crohn's Colitis* **14,** 1748–1758 (2020).
41. Gori, S. *et al.* Acetylcholine-treated murine dendritic cells promote inflammatory lung injury. *PLoS One* **14,** e0212911 (2019).
42. Ashcroft, T., Simpson, J. M. & Timbrell, V. Simple method of estimating severity of pulmonary fibrosis on a numerical scale. *J. Clin. Pathol.* **41,** 467–470 (1988).
43. Livak, K. J. & Schmittgen, T. D. Analysis of Relative Gene Expression Data Using Real-Time Quantitative PCR and the 2−ΔΔCT Method. *Methods* **25,** 402–408 (2001).
44. Reyfman, P. A. *et al.* Single-Cell Transcriptomic Analysis of Human Lung Provides Insights into the Pathobiology of Pulmonary Fibrosis. *Am. J. Respir. Crit. Care Med.* **199,** 1517–1536 (2019).
45. Moeller, A., Ask, K., Warburton, D., Gauldie, J. & Kolb, M. The bleomycin animal model: A useful tool to investigate treatment options for idiopathic pulmonary fibrosis? *Int. J. Biochem. Cell Biol.* **40,** 362–382 (2008).
46. Mouratis, M. A. & Aidinis, V. Modeling pulmonary fibrosis with bleomycin. *Curr. Opin. Pulm. Med.* **17,** 355–361 (2011).
47. Moore, B. B. & Hogaboam, C. M. Murine models of pulmonary fibrosis. *Am. J. Physiol. Cell. Mol.*

*Physiol.* **294,** L152–L160 (2008).
48. Nishikoba, N. *et al.* HGF-MET Signaling Shifts M1 Macrophages Toward an M2-Like Phenotype Through PI3K-Mediated Induction of Arginase-1 Expression. *Front. Immunol.* **11,** 1–10 (2020).
49. Krein, P. M. & Winston, B. W. Roles for Insulin-Like Growth Factor I and Transforming Growth Factor-β in Fibrotic Lung Disease. *Chest* **122,** 289S-293S (2002).
50. Tonkin, J. *et al.* Monocyte/Macrophage-derived IGF-1 Orchestrates Murine Skeletal Muscle Regeneration and Modulates Autocrine Polarization. *Mol. Ther.* **23,** 1189–1200 (2015).
51. Alfaro, M. P. *et al.* A physiological role for connective tissue growth factor in early wound healing. *Lab. Investig.* **93,** 81–95 (2013).
52. Russo, R. C. *et al.* Role of the Chemokine Receptor CXCR2 in Bleomycin-Induced Pulmonary Inflammation and Fibrosis. *Am. J. Respir. Cell Mol. Biol.* **40,** 410–421 (2009).
53. Cheng, I. *et al.* Particulate Matter Increases the Severity of Bleomycin-Induced Pulmonary Fibrosis through KC-Mediated Neutrophil Chemotaxis. *Int. J. Mol. Sci.* **21,** 227 (2019).
54. Baran, C. P. *et al.* Important Roles for Macrophage Colony-stimulating Factor, CC Chemokine Ligand 2, and Mononuclear Phagocytes in the Pathogenesis of Pulmonary Fibrosis. *Am. J. Respir. Crit. Care Med.* **176,** 78–89 (2007).
55. Okuma, T. *et al.* C-C chemokine receptor 2 (CCR2) deficiency improves bleomycin-induced pulmonary fibrosis by attenuation of both macrophage infiltration and production of macrophage-derived matrix metalloproteinases. *J. Pathol.* **204,** 594–604 (2004).
56. Huaux, F. *et al.* Role of Eotaxin-1 (CCL11) and CC Chemokine Receptor 3 (CCR3) in Bleomycin-Induced Lung Injury and Fibrosis. *Am. J. Pathol.* **167,** 1485–1496 (2005).
57. Craig, V. J. *et al.* Profibrotic Activities for Matrix Metalloproteinase-8 during Bleomycin-Mediated Lung Injury. *J. Immunol.* **190,** 4283–4296 (2013).
58. Hung, C. F., Rohani, M. G., Lee, S., Chen, P. & Schnapp, L. M. Role of IGF-1 pathway in lung fibroblast activation. *Respir. Res.* **14,** 102 (2013).
59. Hamblin, M., Prosch, H. & Vašáková, M. Diagnosis, course and management of hypersensitivity pneumonitis. *Eur. Respir. Rev.* **31,** 210169 (2022).
60. Selman, M., Pardo, A. & King, T. E. Hypersensitivity Pneumonitis. *Am. J. Respir. Crit. Care Med.* **186,** 314–324 (2012).
61. Raghu, G. *et al.* Diagnosis of Hypersensitivity Pneumonitis in Adults: An Official ATS/JRS/ALAT Clinical Practice Guideline. *Am. J. Respir. Crit. Care Med.* **202,** e36–e69 (2020).
62. Fernández Pérez, E. R. *et al.* Executive Summary. *Chest* **160,** 595–615 (2021).
63. Yanagihara, T., Sato, S., Upagupta, C. & Kolb, M. What have we learned from basic science studies on idiopathic pulmonary fibrosis? *Eur. Respir. Rev.* **28,** 190029 (2019).
64. Serezani, A. P. M. *et al.* Multiplatform Single-Cell Analysis Identifies Immune Cell Types Enhanced in Pulmonary Fibrosis. *Am. J. Respir. Cell Mol. Biol.* **67,** 50–60 (2022).
65. Yanagihara, T. & Inoue, Y. Insights into pathogenesis and clinical implications in myositis-associated interstitial lung diseases. *Curr. Opin. Pulm. Med.* **26,** 507–517 (2020).
66. Wynn, T. A. & Vannella, K. M. Macrophages in Tissue Repair, Regeneration, and Fibrosis. *Immunity* **44,** 450–462 (2016).
67. Morse, C. *et al.* Proliferating SPP1/MERTK-expressing macrophages in idiopathic pulmonary fibrosis. *Eur. Respir. J.* **54,** 1802441 (2019).
68. Adams, T. S. *et al.* Single-cell RNA-seq reveals ectopic and aberrant lung-resident cell populations in idiopathic pulmonary fibrosis. *Sci. Adv.* **6,** eaba1983 (2020).
69. Celada, L. J. *et al.* PD-1 up-regulation on CD4 + T cells promotes pulmonary fibrosis through STAT3-mediated IL-17A and TGF-β1 production. *Sci. Transl. Med.* **10,** 1–15 (2018).
70. d'Alessandro, M. *et al.* Immunologic responses to antifibrotic treatment in IPF patients. *Int. Immunopharmacol.* **95,** 107525 (2021).

71. Sakai, T. *et al.* Hepatocyte growth factor in bronchoalveolar lavage fluids and cells in patients with inflammatory chest diseases of the lower respiratory tract: detection by RIA and in situ hybridization. *Am. J. Respir. Cell Mol. Biol.* **16,** 388–397 (1997).
72. Przybylski, G. *et al.* Studies of hepatocyte growth factor in bronchoalveolar lavage fluid in chronic interstitial lung diseases. *Pol. Arch. Med. Wewn.* **125,** 260–271 (2015).
73. Hojo, S. *et al.* Hepatocyte growth factor and neutrophil elastase in idiopathic pulmonary fibrosis. *Respir. Med.* **91,** 511–516 (1997).
74. Yamanouchi, H. *et al.* Measurement of hepatocyte growth factor in serum and bronchoalveolar lavage fluid in patients with pulmonary fibrosis. *Respir. Med.* **92,** 273–278 (1998).

# CHAPTER IV

## Recognition of *Aspergillus fumigatus* by c-MET is required for protective immunity against infection

Manuscript in preparation:

Catarina Barbosa-Matos, Cláudio Duarte-Oliveira, Massimiliano Mazzone, Agostinho Carvalho, Sandra Costa, Cristina Cunha. Recognition of *Aspergillus fumigatus* by c-MET is required for protective immunity against infection. CB-M contributed to all figures of this work.

## Recognition of *Aspergillus fumigatus* by c-MET is required for protective immunity against infection

Catarina Barbosa-Matos, Cláudio Duarte-Oliveira, Massimiliano Mazzone, Agostinho Carvalho, Sandra Costa, Cristina Cunha

### Abstract

Invasive pulmonary aspergillosis is the most common fungal pulmonary infection in severely immunocompromised patients, presenting fast-evolving epidemiology and new groups of risk patients, including COVID-19 patients. The pathogenesis of IPA is closely dependent on the immune status of the host. Thus, a better understanding of the molecular and cellular mechanisms involved in fungal recognition and antifungal immune response may facilitate the identification of novel antifungal therapeutic strategies to improve host defense. Interestingly, some pathogens can activate and deregulate host c-MET signaling pathway to favor their internalization and subsequent spread of the infection. In *Leishmania mexicana* infection, activation of c-MET signaling pathway by the parasite not only increased internalization, but also compromised neutrophil ROS production. In this way, to clarify the potential role of c-MET expression in the antifungal immune response to *Aspergillus*, wild-type and *c-Met* conditional knockout mice were intranasally infected with *Aspergillus fumigatus* conidia and sacrificed 3 days post-infection. Interestingly, lung immune cells of infected WT mice displayed higher expression of c-MET compared to uninfected control, mainly in neutrophils, IMs, alveolar macrophages and T cells. Furthermore, cKO mice have increased fungal burden and inflamed area compared to WT mice. Consistently, the lung of infected cKO mice has an increased number of neutrophils and interstitial macrophages, however, these cKO cells display defective ROS production and phagocytic capacity, respectively. In addition, *c-Met* deficient bone marrow-derived macrophages (BMDMs) have restrained antifungal effector functions, namely phagocytosis, killing and proinflammatory cytokines production. Our findings suggest that c-MET could represent a potential target for therapeutic approaches in IPA, due to its crucial role for protective antifungal effector functions in innate immune cells.

### Keywords

*Aspergillus fumigatus*, c-MET, Immunity, Infection, Invasive pulmonary aspergillosis, Macrophage, Neutrophil

## 1. Introduction

Environmental microorganisms such as *Aspergillus fumigatus* are continuously inhaled and may cause IPA in immunocompromised or critically ill patients. IPA is a life-threatening disease and the mortality rate remains high, estimated to be between 30 and 80% (1). Recent studies have reveal an increased incidence of IPA among critically ill patients with viral pneumonia, such as influenza and COVID-19 (2,3). Considering this growing number of patients at risk, there is an urgent need for more effective clinical interventions, which requires a better understanding of pathogen recognition mechanisms and immune response that underlies this severe infection.

Interestingly, the HGF/c-MET signaling pathway has been described to be activated by cell wall components of certain pathogens, namely *Plasmodium* spp., *Listeria monocytogenes, Salmonella typhi, Candida albicans* and *Helicobacter pylori,* which deregulates the signaling pathway through the direct binding to c-MET and enhances pathogen internalization into epithelial cells (4–14). Recently, it has also been reported that expression of c-MET in neutrophils enhances recognition and internalization of *Leishmania mexicana* and inhibits the production of ROS by infected neutrophils, thereby promoting the spread of infection (15). In addition, the role of c-MET in modulating the effector functions of immune cells is transversal to other inflammatory contexts. Indeed, c-MET expression in neutrophils exacerbates intestinal inflammation by intensifying uncontrolled inflammation (16). Also, c-MET signaling pathway induces antitumor immunity by enhancing neutrophil transmigration to inflamed tumors and their nitric oxide release, and by enhancing the cytotoxicity function of CD8 tumor-infiltrating lymphocytes (17,18). Moreover, in BMDMs c-MET activation induces the shift from M1 to M2 phenotype (19).

However, the role of c-MET in the recognition of *Aspergillus fumigatus* and subsequent immune response remains to be explored. In this study, we sought to investigate the role of c-MET signaling pathway to the host immune response against infection with the opportunistic fungal pathogen *Aspergillus fumigatus*. We discovered that mice with *c-Met* deletion in immune cells show increased fungal burden and inflamed area. Consistently, lung of infected cKO mice has an increased number of neutrophils and interstitial macrophages and more importantly, we found that these cells display a deficit in ROS production and phagocytic capacity, respectively. Moreover, *c-Met* deficient BMDMs have a restrained glycolytic capacity, leading to lower mitochondrial ROS production, proinflammatory cytokine secretion and fungal elimination. Therefore, the compromised antifungal effector functions of cKO immune cells in response to *A. fumigatus* conidia and the impaired induction of an inflammatory milieu in the lungs of cKO mice infected with *A. fumigatus* might be a consequence of attenuated activation of immune cells.

Collectively, our results reveal c-MET as an essential pathway in antifungal immunity, due to its possible role in recognition and modulation of antifungal effector functions of macrophages and neutrophils, highlighting the modulation of c-MET activation in immune cells as a potential therapeutic target for IPA.

## 2. Materials and Methods

### Mice

*In vivo* experiments were performed on eight to twelve-weeks old wild-type and conditional knockout (cKO, Tie2:*c-Met*$^{fl/fl}$) C57BL/6J mice were supplied by Professor Massimiliano Mazzone, Center for Cancer Biology, VIB, KU Leuven, Belgium. Animals were housed and bred under specific pathogen-free condition and kept at the Life and Health Sciences Research Institute (ICVS) animal facility, fed *ad libitum* and kept under light/dark cycles of 12 h, temperature of 18–25 °C and humidity of 40–60%.

All animal experimentation was performed following biosafety level 2 protocols approved by the institutional animal care and use committee of University of Minho with ethical and regulatory approvals consented by SECVS (no. 074/016). Furthermore, all experiments followed the EU-adopted regulations (Directive 2010/63/EU) and were conducted according to the guidelines sanctioned by the Direção-Geral de Alimentação e Veterinária (DGAV).

### *Aspergillus* strains and culture conditions

The *A. fumigatus* CEA17 *Δku80* was used as wild-type strains. *A. fumigatus* was grown on 2% malt extract agar for 7 days at 28 °C. The conidia were harvested from agar slants using PBS (Gibco) with 0.05% Tween 20 (Sigma-Aldrich), followed by gentle agitation and subsequent filtration through a 40 μm pore size cell strainer (Falcon). The concentration of conidia/mL was determined by counting in a Neubauer chamber.

Conidia were labeled with fluorescein isothiocyanate (FITC), as described previously (20). Briefly, freshly harvested conidia were incubated with FITC at a final concentration of 0.1 mg/mL at 37°C for 2 h and washed three times in PBS 0.1% Tween 20.

The FLARE conidia was generated as previously described (21). Briefly, Af293-GFP conidia were rotated in 0.5 mg/mL Biotin XX, succinimidyl ester in 50 mM carbonate buffer (pH 8.3) for 2 h at 4°C. Centrifuged at 400 × *g*, followed by neutralization of unbound biotin by suspending the conidial pellet in 0.1 M Tris–HCl, pH 8.0 for 30 min with constant rotation. Then, conidia were labeled with 0.02 mg/ml Alexa Fluor 633 in PBS for 30 min at RT and resuspended in PBS and 0.025% Tween 20 with concentration adjustment for intranasal administration.

### Mouse infection

For the *in vivo* studies, at day 0, mice were anaesthized and administered with 20 μL of 1 x $10^8$ viable conidia of *A. fumigatus* (CEA17 *Δku80*) via noninvasive intranasal route while being maintained in an upright position. Within 1 or 2 h, the mice recovered completely. Clinical manifestations and weight

changes were recorded daily, and mice were euthanized if they lost 20% of their initial weight. At day 3 post-infection, mice were euthanized by $CO_2$ asphyxiation, and the lungs were excised for sample collection and processing.

### Histopathological Analysis

For the histological analysis at 3 days post-infection (dpi), lungs were excised and fixed in buffered formalin solution 10% (Sigma-Aldrich) for 48 h under agitation at room temperature. Lungs were then processed, paraffin-embedded, and lung sections of 5 µm thickness were stained with hematoxylin and eosin (H&E). The images were acquired on a BX61 widefield upright microscope using a DP70 high-resolution camera (Olympus), and the area of inflammation was determined using ImageJ software v1.50i (Fiji).

### Fungal burden quantification

To assess the fungal burden, the right lobes were removed, weighted, and homogenized in 1 mL of sterile PBS with a tissue homogenizer (Glas-Col). The resulting homogenate was serially diluted and plated on solid growth media. The resulting colony-forming units (CFUs) were counted, and the fungal burden was calculated $\log_{10}$ CFUs *per* gram of lung.

### Generation of BMDMs

BMDMs were obtained from femur and tibia bones of male or female 8-week-old WT or cKO. Briefly, bone marrow was harvested and cultured in complete DMEM with 1% penicillin/streptomycin, 1% L-glutamine, 1% HEPES and 10% FBS (Gibco, Thermo Fisher Scientific), supplemented with 20 ng/mL M-CSF (Peprotech) for 7 days at 37 °C and 5% CO2, with the addition of 20 ng/mL of M-CSF at day 3 of differentiation.

### Flow cytometry analysis

After infection, the lungs were excised and collected in incomplete Dulbecco's Modified Eagle Medium (iDMEM) culture medium (Gibco, Thermo Fisher Scientific). Lungs were minced in small fragments and digested at 37 °C for 30 min in iDMEM culture medium containing 1 mg/mL of collagenase D (Sigma-Aldrich). Subsequently, the tissue was forced through a 70 µm cell strainer and contaminating red blood cells were lysed. Leukocytes were isolated by Percoll (GE Healthcare Bio-Sciences Ab) density gradient, and finally resuspended in FACS buffer (PBS containing 2% FBS and 2 mM EDTA). To assess cell viability, cells were stained for 30 min in the dark with the Zombie Green fluorescent dye (BioLegend) and washed with FACS buffer. Single-cell suspensions were preincubated with TruStain FcX anti-mouse CD16/32 antibody (Biolegend) for 10 min at RT. For surface marker staining, cell suspensions were stained for 30

min on ice while protected from light with the indicated antibodies. Samples were washed and resuspended in fresh FACS buffer prior to analysis. Gating for immune cell populations in the lung was performed to analyze the composition of lung-infiltrating cells using a combination of the following antibodies: BV510 CD45 (clone 30-F11), BV605 CD11c (clone N418), PE-Cy7 CD11b (clone M1/70), PerCP-Cy5.5 F4/80 (clone BM8), APC-Cy7 Ly6G (clone 1A8), APC CD3 (Clone 17A2), BV711 CD64 (Clone X54-5/7.1), Pacific Blue Ly6C (HK1.4), BV786 MHCII (Clone M5/114.15.2), PE SiglecF (Clone E50-2440), FITC c-MET (eBioclone 7) (all from BioLegend, except F4/80 and c-MET from Invitrogen, Ly6G and SiglecF from BD). FITC-labeled Abs were omitted in *in vivo* phagocytosis experiment. FITC- and APC-labeled Abs were omitted in *in vivo* FLARE experiments. Gating strategy is illustrated in Figure 1.

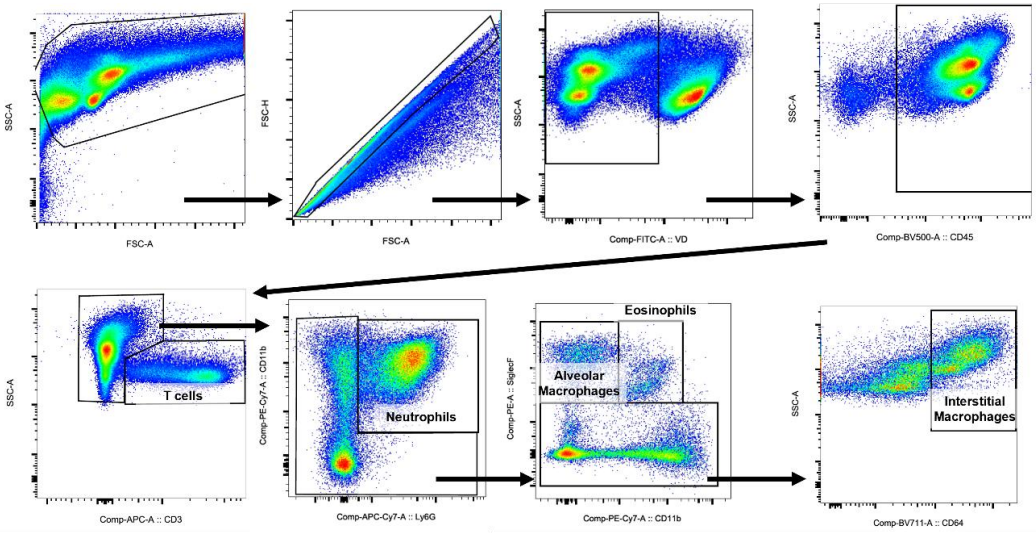



**Figure 1. Gating strategy for the identification of immune cell populations in dissociated mice lung by flow cytometry.** Initial exclusion of debris and doublets was performed using forward vs side scatter area (FSC-A vs SSC-A) and FSC-A vs FSC height (FSC-H) plot, respectively. Then live cells were identified by negative for viability dye (VD). A sequential gating strategy was used to identify immune populations expressing specific markers: T cells ($CD3^{+}CD19^{-}$), neutrophils ($CD11b^{+}Ly\text{-}6G^{+}$), eosinophils ($CD11b^{+}SiglecF^{+}$), alveolar macrophages ($CD11b^{-}SiglecF^{+}$), interstitial macrophages ($CD64^{+}SiglecF^{-}$).

BMDMs ($2.5 \times 10^{5}$/well in 48-well plates) were infected with *A. fumigatus* conidia for the indicated time points at a 1:5 effector-to-target ratio at 37 °C in 5% $CO_2$. Then, the supernatant was removed, and cells were detached with accutase. The cell suspensions were collected, centrifuged for 5 min at 2000 rpm, and then incubated with FITC c-MET (eBioclone 7).

Data were acquired on a LSRII flow cytometer (BD) and processed using FlowJo (Tree Star Inc).

### Phagocytosis assay

Mice were intranasally infected with FITC-labelled *A. fumigatus* conidia and sacrificed 3 dpi. As described previously, lungs were dissociated into single cells suspension and leukocytes were obtained by density gradient centrifugation, then cells were stained with previously mentioned flow cytometry antibodies.

Phagocytosis was presented as the percentage of ingested fluorescent conidia by the immune cells from the dissociated lung.

To determine phagocytosis, BMDMs (5 x $10^5$/well in 24-well plates) were infected with FITC-labeled conidia of *A. fumigatus* at a 1:5 effector-to-target ratio. The infection was synchronized for 30 min at 4°C, and phagocytosis was initiated by shifting the plate to 37°C at 5% $CO_2$ for 1 h. Wells were then washed twice with PBS, and the cells were detached with accutase and resuspended in PBS. The phagocytosis of macrophages was presented as the percentage of ingested fluorescent conidia.

Data were acquired on a LSRII flow cytometer (BD) and analyzed using FlowJo Software (Tree Star Inc.).

### Conidiacidal activity assay

Mice were infected with FLARE conidia intranasally and sacrificed 24 h post-infection. As described previously, lungs were dissociated into single cells suspension and leukocytes were obtained by density gradient centrifugation, then cells were stained with previously mentioned flow cytometry antibodies. Conidiacidal activity of the immune cells from the dissociated lung was analysed as previously described (21). Briefly, infected leukocytes acquire GFP and AF633 fluorescence after engulfing FLARE conidia, subsequently the loss of GFP and retention of AF633 fluorescence coincides with conidia killing.

Following differentiation, 2.5 x $10^5$ BMDMs/well were seeded in 48-well plates in complete DMEM, and a suspension of calcofluor-labelled conidia of *A. fumigatus* was added at a ratio of 10:1 effector-to-target ratio. The cells were then incubated for 1 h at 37°C and 5% $CO_2$ to allow the internalization of conidia. Medium containing the non-ingested conidia was removed, and wells were washed twice with pre-warmed PBS. To measure the conidiacidal ability, BMDMs were allowed to kill the ingested conidia for 2 h at 37°C in 5% $CO_2$. After incubation, culture plates were snap frozen at –80°C and thawed at 37°C to cause cell lysis and release of ingested conidia. Then, the samples were stained with propidium iodide for 10 min. Data were acquired on a LSRII flow cytometer (BD). The percentage of live and dead fluorescent internalized conidia was analysed using FlowJo Software (Tree Star Inc.).

### Measurement of ROS production

To measure cellular ROS production, immune single cell suspensions from dissociated lung were incubated for 1 h with 5 µM CellROX Green (Thermo Fisher) at 37°C, protected from light and then stained with previously mentioned flow cytometry antibodies. ROS production is presented as MFI of CellROX Green within immune cell populations.

BMDMs (2.5 x $10^5$ BMDMs/well) were plated in 48-well plates and infected with *A. fumigatus* conidia at a 1:5 effector-to-target ratio. The cells were then incubated for 2 h or 4 h at 37°C and 5% $CO_2$. Then, the

supernatant was removed, and cells were detached with accutase. The cell suspensions were collected, centrifuged for 5 min at 2000 rpm, and then 10 µM dihydroethidium PE (DHE; Thermo Fisher) or 5 µM Mitosox PE (Thermo Fisher) were added and incubated for 30 min at 37°C, protected from light. Cytosolic and mitochondrial ROS are presented as mean fluorescence intensity of DHE and Mitosox, respectively. Data were acquired on a LSRII flow cytometer (BD) and analyzed using FlowJo v10.5.3 (Tree Star Inc.).

### Cytokine measurements

Lung homogenates were used to quantify TNF, IL-6 and IL-1β by enzyme-linked immunosorbent assay (ELISA) using ELISA MAX Deluxe Set kits (BioLegend), according to the manufacturer's instructions. BMDMs (5 x $10^5$/well in 24-well plates) were infected with *A. fumigatus* conidia at a 1:10 effector-to-target ratio for 24 h at 37°C and 5% $CO_2$. After infection, supernatants were collected and cytokine levels were quantified using ELISA MAX Deluxe Set kits (BioLegend), according to the manufacturer's instructions.

### Quantification of glucose and lactate

Macrophages (5 x $10^5$/well in 24-well plates) infected for 24 h at 37°C in 5% $CO_2$ with *A. fumigatus* conidia at a 1:10 effector-to-target ratio. Then the supernatants were collected and centrifuged, glucose and lactate levels were determined using the enzymatic colorimetric glucose and lactate assay (41011, 10001330, SpinReact), following the manufacturer's instructions.

### Statistical analysis

Statistical analysis was performed using GraphPad Prism 9.0 (GraphPad Software, La Jolla, CA). All data were expressed as mean ± SEM. Prior to comparisons, normality was assessed with Shapiro-Wilk test, if normality is not verified non-parametric tests were used. Comparison between two groups was made either with parametric two-tailed Student's t-test or non-parametric two-tailed Mann-Whitney test. Statistical significance for multiple groups was assessed by one-way ANOVA followed by Tukey's post hoc test or non-parametric Kruskall-Wallis test followed by Dunn's post hoc test for multiple comparisons. $p < 0.05$ was considered statistically significant.

## 3. Results

### c-MET expression is induced in lung immune cells in response to *Aspergillus fumigatus* infection

To elucidate the role of c-MET signaling pathway in response to *A. fumigatus* infection, we started by evaluating the expression of c-MET in immune cells from the lungs of infected mice compared to uninfected control mice. For that, experimental aspergillosis was induced in mice by the intranasal administration of *Aspergillus fumigatus* conidia and c-MET expression was evaluated 3 dpi (Figure 2).

Flow cytometry analysis revealed a significant increase in both the percentage and MFI of c-MET$^+$ lung neutrophils, which represent more than 50% of the total neutrophils (Figure 2A and 2E). Also, the percentage and MFI of c-MET$^+$ lung interstitial and alveolar macrophages were increased 3 dpi, representing approximately 25% and 35% of total IMs (Figure 2B and 2F) and AMs (Figure 2C and 2G), respectively. The percentage and MFI of c-MET$^+$ lung T lymphocytes were also increased at day 3 post-infection, representing around 15% of the total population (Figure 2D and 2H). These results clearly demonstrate that c-MET is induced in lung immune cells in response to *A. fumigatus* infection.

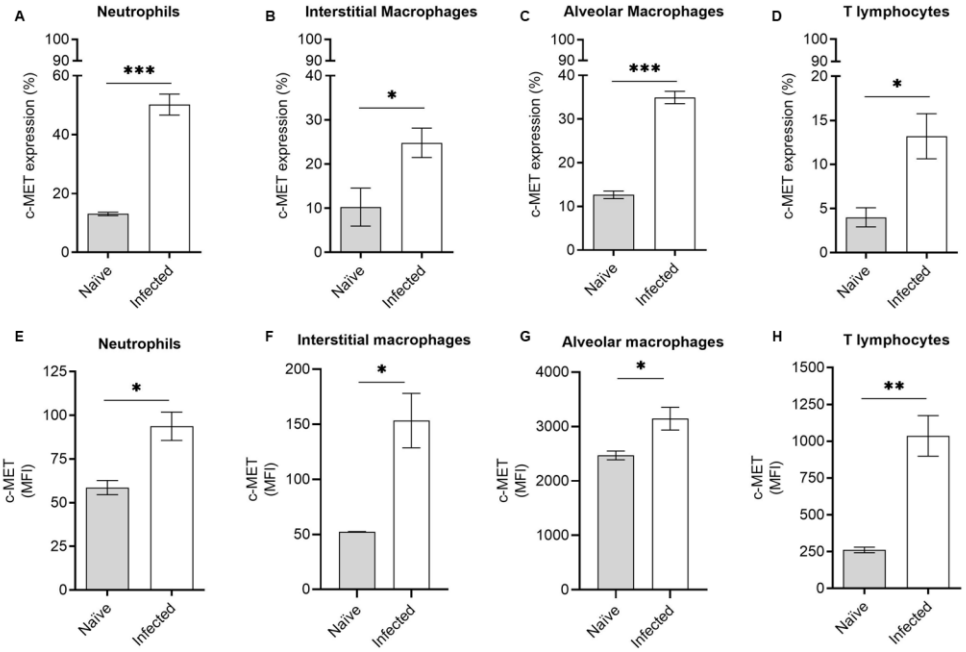



**Figure 2. c-MET expression is induced in immune cells in the lungs of mice infected with *Aspergillus fumigatus*.** Percentage and MFI of c-MET expression in (A and E) neutrophils, (B and F) interstitial macrophages, (C and G) alveolar macrophages and (D and H) T lymphocytes from mice lung uninfected (naïve) or at 3 dpi with *A. fumigatus* (infected). Data represent as mean ± SEM. Data of one independent experiment is shown, n = 3 *per* group. Similar results were obtained in at least two independent experiments. *$p < 0.05$, **$p < 0.01$, ***$p < 0.001$.

### *c-Met* deficiency in immune cells renders mice more susceptible to *A. fumigatus* infection

To assess whether the deficiency of *c-Met* in immune cells is associated with increased susceptibility to experimental aspergillosis, we started by assessing the fungal burden in the lungs. Lung homogenates obtained 3 dpi showed an enhanced fungal burden in the lungs of cKO mice as compared to WT mice

(Figure 3A). Histological analysis of lung sections revealed larger edema and inflammation in cKO mice at day 3 post-infection (Figure 3B). Accordingly, the percentage of lung inflammation area was significantly increased in cKO mice compared to WT mice (Figure 3C). Furthermore, in accordance with increased lung inflammation, the number of lung leukocytes (Figure 3D), particularly neutrophils and interstitial macrophages (Figure 3E and 3F), were increased in the lungs of cKO mice compared to WT mice. Lung homogenates from cKO mice infected with *A. fumigatus* conidia also displayed increased levels of proinflammatory cytokines, such as IL-6 and TNF (Figure 3G and 3H), whereas the levels of IL-1β and IL-10 remained unaltered (Figure 3I and 3J).

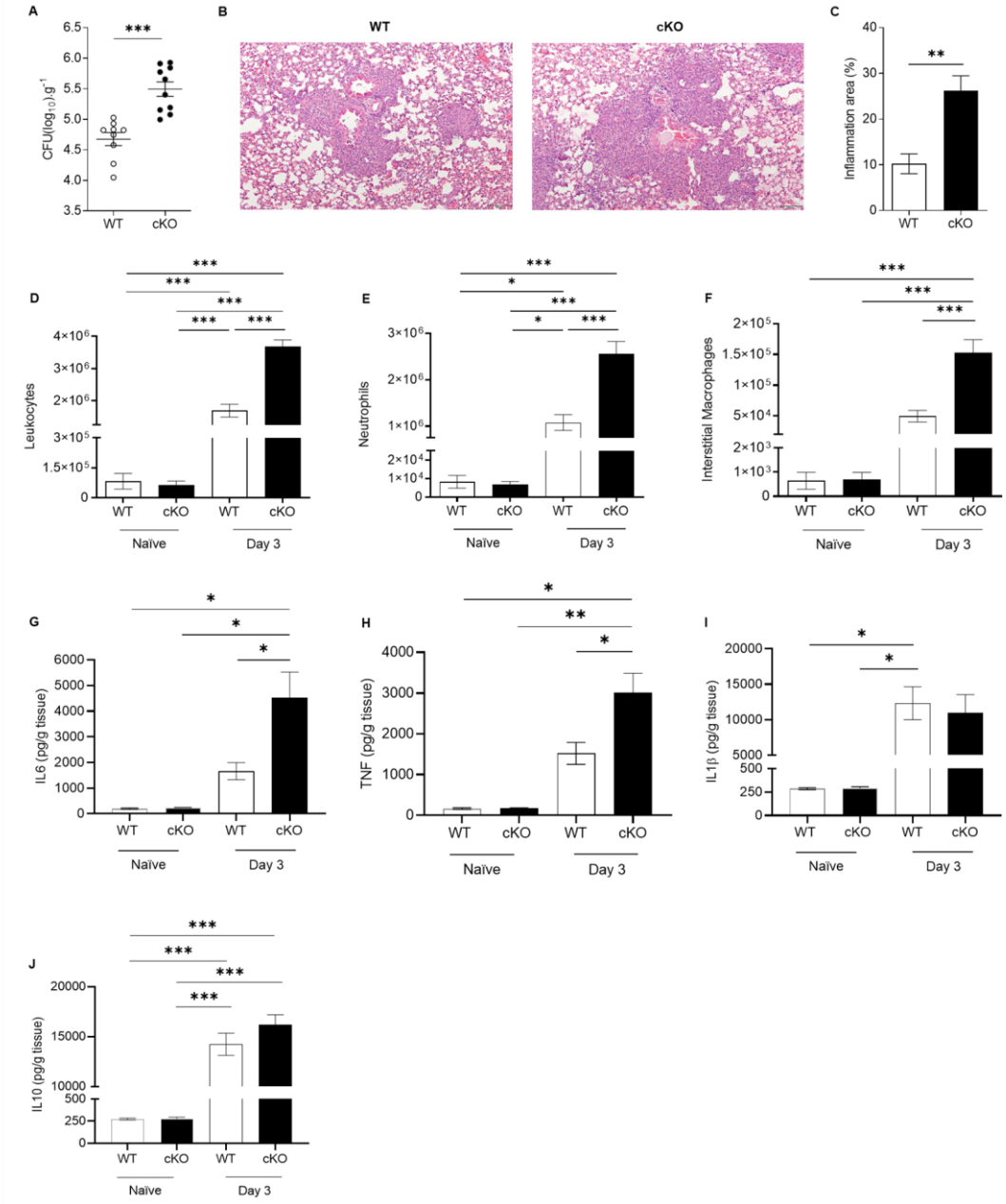



**Figure 3. c-MET expression in immune cells is required to control *A. fumigatus* infection in the lung.** (A) Fungal burden ($log_{10}$) *per* gram of lung tissue was determined 3 days after *A. fumigatus* infection. (B) Representative H&E-stained lung

*(legend continued on the next page)*

sections at 3 dpi and (C) quantification of inflammation area. Total number of (D) leukocytes, (E) neutrophils and (F) interstitial macrophages, in the lung of uninfected (naïve) mice or mice infected for 3 days with *A. fumigatus*. Levels of secreted (G) IL-6, (H) TNF, (I) IL-1β and (J) IL-10 *per* milligram of lung, in lung homogenates of naïve mice or mice infected for 3 days with *A. fumigatus*. Data of one independent experiment is shown, at least, 3 independent experiments were performed (n = 10 mice *per* group). Data represent the mean ± SEM. Groups were compared by unpaired t test and statistically significant differences are indicated as $*p < 0.05$, $**p < 0.01$, $***p < 0.001$.

### *c-Met* deficiency in immune cells compromises their effector functions during *A. fumigatus* infection *in vivo*

Since we found an increased number of immune cells in the lungs of cKO mice concomitant with a paradoxical increase in the fungal load, we wondered if these immune cells could present a defect in their antifungal effector functions. Indeed, the effector functions of both neutrophils and interstitial macrophages were compromised in cKO mice. Particularly, the phagocytic capacity of neutrophils was decreased (Figure 4A), as were the conidiacidal capacity and ROS production by IMs in the lungs of cKO mice compared to WT mice (Figure 4B and 4C). No differences were found in the phagocytic capacity of interstitial macrophages (Figure 4A), conidiacidal capacity and ROS production by neutrophils (Figure 4B and 4C). These results highlight the role of c-MET in antifungal immune response against *A. fumigatus* infection.

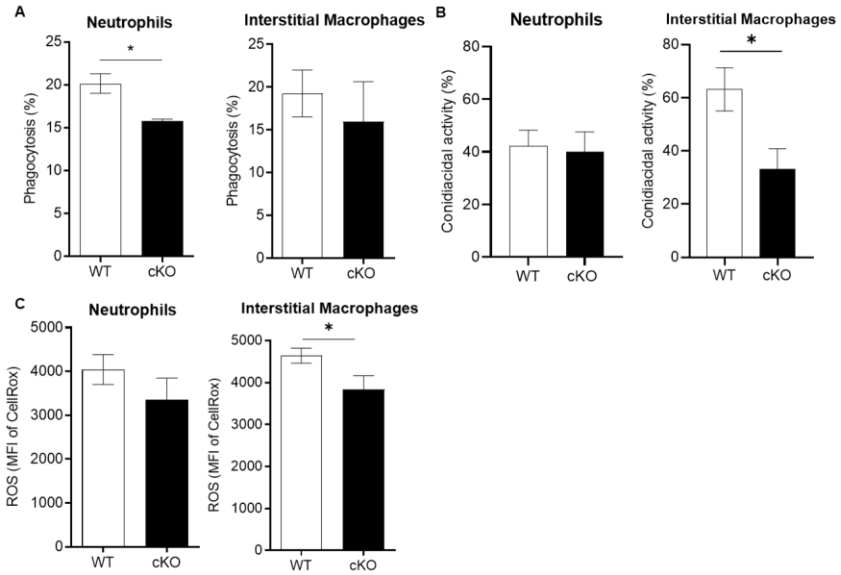



**Figure 4. c-MET expression in immune cells is required for *A. fumigatus*-induced antifungal effector functions.** (A) Phagocytosis of neutrophils and interstitial macrophages, (B) conidiacidal activity of neutrophils and interstitial macrophages and (C) ROS production by neutrophils and interstitial macrophages in lung at 3 dpi with *A. fumigatus*. Data of one independent experiment is shown, at least, 3 independent experiments were performed (n = 10 mice *per* group). Data represent the mean ± SEM. Groups were compared by unpaired t test and statistically significant differences are indicated as $*p < 0.05$, $**p < 0.01$, $***p < 0.001$.

### c-MET regulates the effector functions of macrophages in response to *A. fumigatus* infection

Given the role of c-MET in the activation of protective effector functions of lung immune cells *in vivo*, we sought to dissect the contribution of c-MET signaling pathway in macrophages during *A. fumigatus* infection, *ex vivo.* We found that c-MET expression increased in BMDMs throughout infection with *A.*

*fumigatus* (Figure 5A). Furthermore, both phagocytic and conidiacidal activity were compromised in *c-Met* deficient macrophages (Figure 5B and 5C). Interestingly, despite no differences in the production of cytosolic ROS was observed (Figure 5D), mitochondrial ROS production was instead decreased in *c-Met* deficient macrophages (Figure 5E). In addition, and in contrast to what was observed *in vivo*, the production of proinflammatory cytokines (IL-6 and IL-1β) were decreased in *c-Met* deficient macrophages (Figure 5F and 5G), and no differences were observed in the levels of TNF (Figure 5H). Taken together, these results confirm a key role for c-MET signaling pathway in the regulation of antifungal effector functions of macrophages in response to *A. fumigatus* infection, thereby enabling fungal elimination.

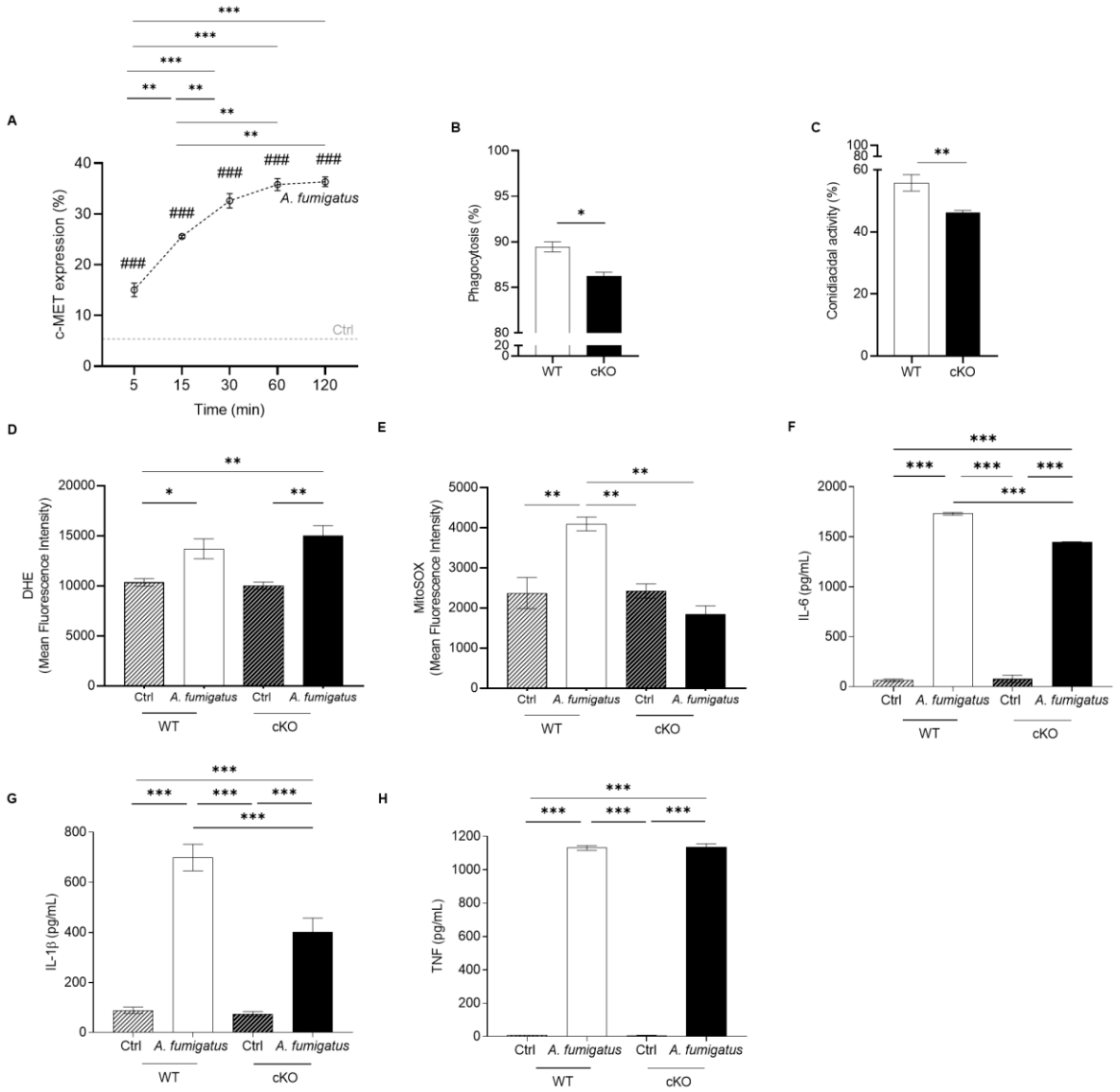



**Figure 5. c-MET is required for effector functions of macrophages after *A. fumigatus* infection.** (A) Expression levels of c-MET, (B) phagocytosis, (C) conidiacidal activity, levels of (D) cytosolic ROS, DHE, (E) mitochondrial ROS, MitoSOX, (F) IL-6, (G) IL-1β and (H) TNF in BMDMs infected with *A. fumigatus* live conidia or uninfected (Ctrl). Data represent as mean ± SEM. Data of one independent experiment is shown, n = 3 per group. Similar results were obtained in at least three independent experiments. *p < 0.05, **p < 0.01, ***p < 0.001; # p < 0.05, ## p < 0.01, ### p < 0.001: infected vs. uninfected control (Ctrl).

## c-MET regulates glucose metabolism of macrophages in response to *A. fumigatus*

Macrophages undergo a metabolic rewiring after infection with *A. fumigatus*, characterized by a boost in glycolysis, which is therefore required for an efficient immune response (22,23). Given that *c-Met* deletion severely compromises the antifungal effector functions of macrophages, we sought to elucidate whether c-MET could modulate the ability of macrophages to induce their metabolic reprograming to combat the infection. As described, fungal infection significantly up-regulated the activity of the glycolytic pathway in WT macrophages (Figure 6A and 6B). However, this activation was compromised in *c-Met* deficient macrophages, presenting decreased glucose uptake and lactate production (Figure 6A and 6B). Taken together, these results confirm a key role for c-MET signaling pathway in the regulation of glucose metabolism of macrophages in response to *A. fumigatus* infection, thereby contributing to an effective antifungal immune response.

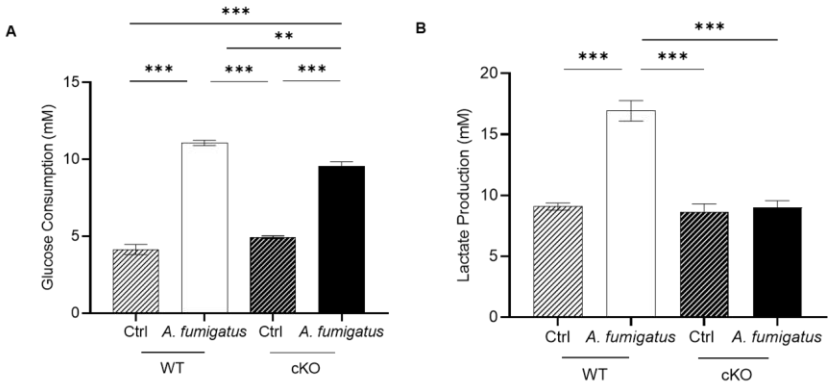



**Figure 6. c-MET is required for the activation of the glycolytic pathway in macrophages after *A. fumigatus* infection.** Levels of (A) glucose consumption and (B) lactate production in BMDMs infected with *A. fumigatus* live conidia or uninfected (Ctrl). Data represent as mean ± SEM. Data of one independent experiment is shown, n = 3 per group. Similar results were obtained in at least three independent experiments. *p < 0.05, **p < 0.01, ***p < 0.001.

## 4. Discussion

The recognition of invading pathogens and the subsequent triggering of an efficient antifungal immune response are crucial for host protection in order to prevent the spread of the infection. The pivotal role of c-MET in the recognition and internalization of invading pathogens has increasingly been recently recognized. Accordingly, several pathogens, namely *Plasmodium* spp., *Listeria monocytogenes, Salmonella typhi, Candida albicans* and *Helicobacter pylori,* are able to directly bind to c-MET enhancing their internalization into epithelial cells (4–14). However, the role of c-MET in the recognition of invading pathogens by immune cells and the subsequent impact on their effector function remains poorly explored. In fact, only a very recent study shows that c-MET expression is induced in neutrophils infected with *Leishmania mexicana* and is required for their recruitment to the site of infection. In this case, c-MET expression in *Leishmania*-infected neutrophils restrained their capacity to produce ROS, which ultimately contributes to an increase in the extension of infection (15). In line with these studies, we now show the crucial role of c-MET in the recognition of *A. fumigatus* in immune cells which in turn enhanced protection against infection. Specifically, we show that in response to *A. fumigatus* infection, both *in vivo* and *in vitro*, c-MET is up-regulated in immune cells compared to uninfected conditions. These results suggest that *A. fumigatus* itself may directly bind to c-MET in immune cells. However, and in contrast to the previous studies, the deletion of *c-Met* in immune cells resulted in an increased recruitment of these cells to *A. fumigatus* infected lungs, namely neutrophils and IMs. Also, in contrast to what has been described for *Leishmania mexicana* infection, the interaction of c-MET with *A. fumigatus* is required for a protective antifungal effector function of immune cells. Accordingly, cKO mice are more susceptible to infection, as confirmed by the increased fungal burden and inflammation observed in the mice lungs. Besides *Leishmania* infection, c-MET expression has also been shown to be required for the recruitment and effector capacities of neutrophils in other contexts of inflammatory conditions, namely in intestinal inflammation and inflamed tumors (16,17). Particularly in inflamed tumors, c-MET was also essential to enhance the cytotoxic capacity of neutrophils, which corroborates our results that show that c-MET potentiated the activation of effector mechanisms of neutrophils and macrophages. Specifically, we found that c-MET enhanced the phagocytic capacity of lung neutrophils, as well as the ROS production and conidiacidal capacity of lung macrophages. In fact, some effector mechanisms for the elimination of fungal pathogens by macrophages depend on ROS production (24–26). In particular, the enhance in mitochondrial ROS production by macrophages after infection with *A. fumigatus* is preceded by the high recruitment of NADPH oxidase (NOX) 2 to the phagosomal membrane, which contributes to the redox signaling required for cytokines secretion and fungal growth inhibition (27,28). In addition, NOX-mediated

ROS production, in turn, regulates the recruitment of autophagy proteins, particularly microtubule-associated protein 1 light chain 3 (LC3)-II, to the phagosomes of macrophages containing *A. fumigatus* (29,30). This process further activates a noncanonical autophagy pathway designated LC3-associated phagocytosis (LAP), facilitating the rapid phagosome maturation upon fusion with lysosomes, effective fungal killing and the subsequent modulation of the inflammatory signaling pathways (29–35). Our results suggest that c-MET may contribute to the macrophages response against *A. fumigatus* infection by modulating these mechanisms, especially NOX accumulation, since mitochondrial ROS levels and cytokine secretion, as well as conidiacidal capacity were compromised in *c-Met* deficient macrophages.

In response to infection, macrophages rapidly adapt their metabolism in favor of glycolysis as a way of rapidly support their specialized antifungal effector functions for host defense against invading pathogens. Our results clearly demonstrate that c-MET compromises the metabolic shift of macrophages, since an impaired induction of glycolysis was found in *c-Met* deficient macrophages. Furthermore, we had previously reported that glucose metabolism during *A. fumigatus* infection of macrophages is crucial for ROS production and consequently fungal elimination (22). In this sense, the decreased glycolytic capacity observed in *c-Met* deficient macrophages could, at least in part, explain their defect in fungal elimination.

Interestingly, HGF-induced activation of c-MET in M1-activated macrophages lead to a reduction in their production of proinflammatory cytokines, namely iNOS, TNF, and IL-6, along with an increase in the production of anti-inflammatory cytokines, IL-10 and TGF-β1, suggesting that c-MET activation by HGF induces a shift from M1 to M2 phenotype (19,36,37). However, in the context of *A. fumigatus* infection, *c-Met* deletion was instead associated with a lower production of proinflammatory cytokines by macrophages, namely IL-6 and IL-1β, suggesting that c-MET activation by *A. fumigatus*, in contrast to HGF, is associated with a proinflammatory phenotype, which is beneficial in the context of infection, since proinflammatory macrophages are widely described to exert antifungal effects in early phase of infection. Overall, the compromised antifungal effector mechanisms observed in both *c-Met*-deleted immune cells and in the lungs of cKO mice infected with *A. fumigatus* could be a consequence of a defective c-MET-mediated *A. fumigatus* recognition, that subsequently contributes to attenuated activation of the immune response and associated metabolic reprogramming.

In conclusion, our study provides mechanistic insights into the interplay between *A. fumigatus* and the c-MET signaling pathway and demonstrates that activation of c-MET in immune cells is crucial for proper immune response to *A. fumigatus* infection. Therefore, the modulation of c-MET expression in immune cells may represent an innovative therapeutic approach to reorient host cells towards immune protection against *A. fumigatus* infection.

## 5. References


1. Bongomin, F., Gago, S., Oladele, R. & Denning, D. Global and Multi-National Prevalence of Fungal Diseases—Estimate Precision. *J. Fungi* **3,** 57 (2017).
2. Mitaka, H., Kuno, T., Takagi, H. & Patrawalla, P. Incidence and mortality of COVID-19-associated pulmonary aspergillosis: A systematic review and meta-analysis. *Mycoses* **64,** 993–1001 (2021).
3. Martin-Loeches, I. *et al.* Increased incidence of co-infection in critically ill patients with influenza. *Intensive Care Med.* **43,** 48–58 (2017).
4. Carrolo, M. *et al.* Hepatocyte growth factor and its receptor are required for malaria infection. *Nat. Med.* **9,** 1363–1369 (2003).
5. Leirião, P. *et al.* HGF/MET signalling protects *Plasmodium*-infected host cells from apoptosis. *Cell. Microbiol.* **7,** 603–609 (2005).
6. Niemann, H. H. *et al.* Structure of the Human Receptor Tyrosine Kinase Met in Complex with the *Listeria* Invasion Protein InlB. *Cell* **130,** 235–246 (2007).
7. Shen, Y., Naujokas, M., Park, M. & Ireton, K. InlB-Dependent Internalization of *Listeria* Is Mediated by the Met Receptor Tyrosine Kinase. *Cell* **103,** 501–510 (2000).
8. Jiwani, S. *et al.* Identification of components of the host type IA phosphoinositide 3-kinase pathway that promote internalization of *Listeria monocytogenes*. *Infect. Immun.* **80,** 1252–1266 (2012).
9. Chowdhury, R., Das, S., Ta, A. & Das, S. Epithelial invasion by *Salmonella Typhi* using STIV–Met interaction. *Cell. Microbiol.* **21,** 1–17 (2019).
10. Phan, Q. T. *et al. Candida albicans* stimulates formation of a multi-receptor complex that mediates epithelial cell invasion during oropharyngeal infection. *PLOS Pathog.* **19,** e1011579 (2023).
11. Churin, Y. *et al. Helicobacter pylori* CagA protein targets the c-Met receptor and enhances the motogenic response. *J. Cell Biol.* **161,** 249–255 (2003).
12. Oliveira, M. J. *et al.* CagA associates with c-met, E-cadherin, and p120catenin in a multiproteic complex that suppresses *Helicobacter pylori*-induced cell-invasive phenotype. *J. Infect. Dis.* **200,** 745–755 (2009).
13. Suzuki, M. *et al. Helicobacter pylori* CagA Phosphorylation-Independent Function in Epithelial Proliferation and Inflammation. *Cell Host Microbe* **5,** 23–34 (2009).
14. Li, N. *et al. Helicobacter pylori* CagA protein negatively regulates autophagy and promotes inflammatory response via c-Met-PI3K/Akt-mTOR signaling pathway. *Front. Cell. Infect. Microbiol.* **7,** 1–15 (2017).
15. Passelli, K. *et al.* The c-MET receptor tyrosine kinase contributes to neutrophil-driven pathology in cutaneous leishmaniasis. *PLoS Pathog.* **18,** 1–24 (2022).
16. Stakenborg, M. *et al.* Neutrophilic HGF-MET Signalling Exacerbates Intestinal Inflammation. *J. Crohn's Colitis* **14,** 1748–1758 (2020).
17. Finisguerra, V. *et al.* MET is required for the recruitment of anti-tumoural neutrophils. *Nature* **522,** 349–353 (2015).
18. Benkhoucha, M. *et al.* Identification of a novel population of highly cytotoxic c-Met-expressing CD8 + T lymphocytes. *EMBO Rep.* **18,** 1545–1558 (2017).
19. Nishikoba, N. *et al.* HGF-MET Signaling Shifts M1 Macrophages Toward an M2-Like Phenotype Through PI3K-Mediated Induction of Arginase-1 Expression. *Front. Immunol.* **11,** 1–10 (2020).
20. Ibrahim-Granet, O. *et al.* Phagocytosis and Intracellular Fate of *Aspergillus fumigatus* Conidia in Alveolar Macrophages. *Infect. Immun.* **71,** 891–903 (2003).
21. Jhingran, A. *et al.* Tracing Conidial Fate and Measuring Host Cell Antifungal Activity Using a Reporter of Microbial Viability in the Lung. *Cell Rep.* **2,** 1762–1773 (2012).
22. Gonçalves, S. M. *et al.* Phagosomal removal of fungal melanin reprograms macrophage metabolism to promote antifungal immunity. *Nat. Commun.* **11,** 1–15 (2020).

23. Gonçalves, S. M. *et al.* Genetic Variation in PFKFB3 Impairs Antifungal Immunometabolic Responses and Predisposes to Invasive Pulmonary Aspergillosis. *MBio* **12,** 1–13 (2021).
24. Grimm, M. J. *et al.* Monocyte- and Macrophage-Targeted NADPH Oxidase Mediates Antifungal Host Defense and Regulation of Acute Inflammation in Mice. *J. Immunol.* **190,** 4175–4184 (2013).
25. Arango Duque, G. & Descoteaux, A. Macrophage Cytokines: Involvement in Immunity and Infectious Diseases. *Front. Immunol.* **5,** 1–12 (2014).
26. Herb, M. & Schramm, M. Functions of ROS in Macrophages and Antimicrobial Immunity. *Antioxidants* **10,** 313 (2021).
27. Hatinguais, R. *et al.* Mitochondrial Reactive Oxygen Species Regulate Immune Responses of Macrophages to *Aspergillus fumigatus*. *Front. Immunol.* **12,** 1–15 (2021).
28. Shlezinger, N. & Hohl, T. M. Mitochondrial Reactive Oxygen Species Enhance Alveolar Macrophage Activity against *Aspergillus fumigatus* but Are Dispensable for Host Protection. *mSphere* **6,** 1–11 (2021).
29. Akoumianaki, T. *et al*. *Aspergillus* Cell Wall Melanin Blocks LC3-Associated Phagocytosis to Promote Pathogenicity. *Cell Host Microbe* **19**, 79–90 (2016).
30. Kyrmizi, I. *et al.* Corticosteroids Block Autophagy Protein Recruitment in *Aspergillus fumigatus* Phagosomes via Targeting Dectin-1/Syk Kinase Signaling. *J. Immunol*. **191**, 1287–1299 (2013).
31. Sanjuan, M. A. *et al.* Toll-like receptor signalling in macrophages links the autophagy pathway to phagocytosis. *Nature* **450**, 1253–1257 (2007).
32. Martinez, J. *et al.* Molecular characterization of LC3-associated phagocytosis reveals distinct roles for Rubicon, NOX2 and autophagy proteins. *Nat. Cell Biol*. **17**, 893–906 (2015).
33. de Luca, A. *et al.* IL-1 receptor blockade restores autophagy and reduces inflammation in chronic granulomatous disease in mice and in humans. *Proc. Natl. Acad. Sci.* **111**, 3526–3531 (2014).
34. Oikonomou, V. *et al.* Noncanonical Fungal Autophagy Inhibits Inflammation in Response to IFN-γ via DAPK1. *Cell Host Microbe* **20**, 744–757 (2016).
35. Latgé, J.-P. & Chamilos, G. *Aspergillus fumigatus* and Aspergillosis in 2019. *Clin. Microbiol. Rev*. **33**, 1–75 (2019).
36. Coudriet, G. M., He, J., Trucco, M., Mars, W. M. & Piganelli, J. D. Hepatocyte growth factor modulates interleukin-6 production in bone marrow derived macrophages: Implications for inflammatory mediated diseases. *PLoS One* **5,** 1–7 (2010).
37. Choi, W., Lee, J., Lee, J., Lee, S. H. & Kim, S. Hepatocyte Growth Factor Regulates Macrophage Transition to the M2 Phenotype and Promotes Murine Skeletal Muscle Regeneration. *Front. Physiol.* **10,** 914 (2019).

# CHAPTER V

General Discussion and Future Perspectives

## 1. General Discussion and Future Perspectives

Immune dysregulation, whether excessive or defective, can cause severe lung diseases such as pulmonary fibrosis and aspergillosis, which are associated with poor prognosis and high mortality rates. These diseases can result from exaggerated chronic inflammatory responses that lead to lung damage or, conversely, from the absence of an immune response that leads to an inability to fight invading pathogens, respectively. Regardless of whether the threat to the lung is initiated by cellular damage or inhaled pathogens, a rapid and properly regulated immune response is required to re-establish lung homeostasis.

Despite the availability of antifibrotic and antifungal treatments and efforts to develop foolproof therapies, mortality rates in patients with IPF and IPA remain high. Unfortunately, the main reason for this is that antifibrotic drugs can only delay, rather than reverse, the progression of pulmonary fibrosis, and antifungal drugs become ineffective due to the inevitable emergence of drug resistance. Thus, there is the need to identify novel effective therapeutic strategies, which requires a deeper understanding of immune mechanisms underlying these diseases, particularly fibrosis-associated lung inflammation and the immune recognition and response to *Aspergillus fumigatus*. Therefore, the focus of this Doctoral Thesis was to investigate the role of c-MET signaling, an immunoregulatory mechanism that underlies the effector immune response, in these inflammatory and infectious lung diseases.

Different macrophage populations can reside in the lung or can be recruited in response to an insult to the lung. These cells are sentinels that rapidly respond and orchestrate host defense mechanisms to re-establish pulmonary homeostasis. AMs and IMs are two populations of lung macrophages located in the airways and within the lung interstitium, respectively (1). Macrophages are a heterogeneous cell population with remarkable phenotypic and functional plasticity, enabling them to adapt in response to microenvironmental signals. In fact, previous studies have suggested that the phenotype acquired by macrophages during fibroproliferative responses to injury will dictate whether their role will contribute to a protective or harmful response (6–8). However, the proportion, phenotype, and individual contribution of AMs and IMs have not been clearly described in fibrosis-associated inflammation. This lack of knowledge prompted us to further investigate the contribution of both these macrophage populations to fibrosis development in a well-established mouse model of lung fibrosis. Bleomycin-induced pulmonary fibrosis is well suited to study fibrosis-associated inflammation because it is known to be characterized by an early phase of acute lung inflammation and injury (2–4). Interestingly, we found that bleomycin administration led to an increase in the proportion of IMs during the inflammatory phase with a peak at day 7, while the proportion of AMs decayed. Notably, at the peak of the inflammatory phase, IMs exhibited

an anti-inflammatory, M2-like, phenotype. Moreover, conditioned medium-derived from these IMs, induce *in vitro* fibroblast activation and differentiation into myofibroblasts. Interestingly, in a previous study in which IMs were isolated from radiation-induced fibrotic lungs and activated *in vitro* into M1-like and M2-like macrophages, showed that only M2-like IMs induce fibroblast differentiation and overproduction of ECM components (5). These results are consistent with previous studies reporting M2-like macrophages to be involved in aberrant tissue healing and consequent fibrosis through the secretion of anti-inflammatory and pro-fibrotic factors (6–8). Overall, our findings show that IMs are the most abundant lung macrophage population at the early stages of experimental pulmonary fibrosis and indicate that these cells promote the progression of lung fibrosis by paracrine activation of fibroblasts.

c-MET signaling pathway has been implicated in the modulation of migratory capacity and effector functions of immune cells. In tumor, c-MET mediates neutrophil transmigration and nitric oxide release, and the cytolytic capacity of tumor-infiltrating CD8+ cytotoxic T lymphocytes (9–11). In addition, in *L. mexicana* infection and intestinal inflammation, c-MET expression also promotes neutrophil migration (12,13). Furthermore, in BMDMs, HGF-induced c-MET activation induces the shift of M1-like macrophages toward a M2-like phenotype (14). Nevertheless, the contribution of c-MET to the effector mechanisms underlying the controlled lung inflammation and the lung antifungal response remains unexplored. Thus, the focus of this Doctoral Thesis was to elucidate the crosstalk between c-MET signaling pathway and lung immunity in the context of inflammatory and infectious lung diseases.

In line with previous studies that showed that c-MET expression triggers immune cell effector functions, we speculated that modulation of c-MET signaling pathway in immune cells might influence PF, and to test this hypothesis we used the well-established murine model of BLM-induced PF. During the early phase of acute lung inflammation and injury of the BLM-induced PF model, c-MET expression was induced in lung immune cells, specifically in T cells, IMs, and neutrophils. Interestingly, our results come in accordance with previous studies showing induction of c-MET expression in immune cells in several inflammatory conditions (9–14). Taking into consideration this result and the fact that myeloid and lymphoid lineage are critical in PF, we took advantage of the conditional knockout mice with *c-Met* deletion in bone marrow hematopoietic cells, to elucidate the role of c-MET in the immune response to BLM. Interestingly, the absence of *c-Met* in immune cells reduces the severity of BLM-induced fibrosis, as revealed by earlier weight recovery and improved survival. Moreover, the attenuation of the disease phenotype in the absence of *c-Met* in immune cells is associated with an early recruitment of immune cell populations normally found to express c-MET. Despite this early accumulation of immune cells, the tissue microenvironment remained paradoxically less proinflammatory and cytotoxic during the

inflammatory phase. Consequently, the less extensive inflammatory response, possibly associated with tissue repair rather than damage, culminated in attenuation of the histopathological characteristics of BLM-induced lung fibrosis and long-term effects. Together, these data highlight the critical contribution of c-MET signaling pathway in immune cells to their enhanced uncontrolled recruitment and activation towards a proinflammatory and profibrotic phenotype, leading to the exacerbation of lung injury and consequent development of fibrosis. Remarkably, our analysis revealed that c-MET expression was up-regulated in lung T cells from patients with fibrosing ILD, suggesting a potential involvement of c-MET in the development of fibrosing disease at the level of inflammatory cells. In this sense, selective immune blockage of the c-MET pathway might represent an attractive strategy to control tissue damage triggered by uncontrolled inflammation and subsequent fibrosing outcome in these patients.

The incidence of invasive fungal infections is estimated to be increasing worldwide, mainly due to an increased number of immunocompromised patients (15). Environmental microorganisms such as *Aspergillus fumigatus* are continuously inhaled and may cause a life-threatening disease, IPA. The effective recognition and elimination of fungal pathogens is facilitated by a competent host immune status. Therefore, modulation of the immune response could be a potential therapeutic strategy for this infection. Innate immune cells recognize and bind to cell wall components potentiating their antifungal effector mechanisms. Undeniably, macrophages are essential cells in the lung for the orchestration of the innate immune response, representing the patrols that first identify and phagocytose inhaled foreign matter, thus maintaining airway clearance. In addition, macrophages are able to process engulfed foreign material and then present it with subsequent activation of the adaptive immune response.

In line with previous studies that reveal c-MET expression as a trigger for immune cell effector functions (9–14), we hypothesize that c-MET signaling pathway could influence antifungal immune response against *A. fumigatus* infection. To test this hypothesis, we used a murine model of experimental aspergillosis by intranasal administration of *Aspergillus fumigatus* conidia. Early after *A. fumigatus* infection, c-MET expression was induced in lung immune cells, specifically in neutrophils, IMs, AMs, and T cells. Considering this result, we took advantage of the previously mentioned conditional knockout mice with *c-Met* deletion in bone marrow hematopoietic cells, to further investigate the role of c-MET in anti-*Aspergillus* lung immunity. Interestingly, the absence of *c-Met* in immune cells increased the extent of *A. fumigatus* infection in the lung, as revealed by increased lung fungal burden and inflamed area. Moreover, the exacerbation of the disease phenotype in the absence of *c-Met* in immune cells is associated with the increased proportion of two immune cell populations normally found to express c-MET, namely neutrophils and IMs. However these lung *c-Met* deficient cells display a deficit in ROS production and

phagocytic capacity, respectively, in response to *A. fumigatus*. In accordance, an *in vitro* culture of *c-Met* deficient BMDMs infected with *A. fumigatus* also showed a defect in their production of ROS and, consequently, fungal elimination. Furthermore, these cells also displayed lower glycolytic capacity and decreased production of proinflammatory cytokines. Taken together, the work presented here identifies for the first-time c-MET as an essential pathway in antifungal immunity through its possible role in recognizing and modulating the antifungal effector functions of macrophages and neutrophils. This study highlights the potential of an innovative therapeutic approach based on the modulation of c-MET activation to redirect host cells toward immune protection against fungal infection. The identification of the *A. fumigatus* cell wall component(s) that can directly interact with the c-MET receptor will be of critical importance to designing novel preventive or therapeutic strategies. In addition, we intend to validate the clinical relevance of these findings by evaluating the signatures of c-MET expression in immune cells in IPA patients and to investigate whether differential c-MET expression in patients could be associated with different risks of infection in patients.

In conclusion, the results and considerations presented in this Doctoral Thesis emphasize the relevance of the c-MET signaling pathway in lung immune responses, either in response to injuries or infectious agents. Particularly the pivotal contribution of this signaling pathway to potentiate the proinflammatory activation of immune cells, with detrimental consequences for lung injury and fibrosis, while providing a protective response to *Aspergillus fumigatus* infection. As such, highlighting the potential of targeted therapies based on redirecting immune cell activation and effector functions by modulating c-MET expression may hold promise for an era of new strategies aimed at improving patient outcomes and reducing mortality.

## 2. References


1. Byrne, A. J., Mathie, S. A., Gregory, L. G. & Lloyd, C. M. Pulmonary macrophages: key players in the innate defence of the airways. *Thorax* **70,** 1189–1196 (2015).
2. Moeller, A., Ask, K., Warburton, D., Gauldie, J. & Kolb, M. The bleomycin animal model: A useful tool to investigate treatment options for idiopathic pulmonary fibrosis? *Int. J. Biochem. Cell Biol.* **40,** 362–382 (2008).
3. Mouratis, M. A. & Aidinis, V. Modeling pulmonary fibrosis with bleomycin. *Curr. Opin. Pulm. Med.* **17,** 355–361 (2011).
4. Moore, B. B. & Hogaboam, C. M. Murine models of pulmonary fibrosis. *Am. J. Physiol. Cell. Mol. Physiol.* **294,** L152–L160 (2008).
5. Meziani, L. *et al.* CSF1R inhibition prevents radiation pulmonary fibrosis by depletion of interstitial macrophages. *Eur. Respir. J.* **51,** 1702120 (2018).
6. Gu, Y., Lawrence, T., Mohamed, R., Liang, Y. & Yahaya, B. H. The emerging roles of interstitial macrophages in pulmonary fibrosis: A perspective from scRNA-seq analyses. *Front. Immunol.* **13,** 1–11 (2022).
7. Zhang, L. *et al.* Macrophages: friend or foe in idiopathic pulmonary fibrosis? *Respir. Res.* **19,** 170 (2018).
8. Murray, P. J. Macrophage Polarization. *Annu. Rev. Physiol.* **79,** 541–566 (2017).
9. Finisguerra, V. *et al.* MET is required for the recruitment of anti-tumoural neutrophils. *Nature* **522,** 349–353 (2015).
10. Glodde, N. *et al.* Reactive Neutrophil Responses Dependent on the Receptor Tyrosine Kinase c-MET Limit Cancer Immunotherapy. *Immunity* **47,** 789-802.e9 (2017).
11. Benkhoucha, M. *et al.* Identification of a novel population of highly cytotoxic c-Met-expressing CD8 + T lymphocytes. *EMBO Rep.* **18,** 1545–1558 (2017).
12. Passelli, K. *et al.* The c-MET receptor tyrosine kinase contributes to neutrophil-driven pathology in cutaneous leishmaniasis. *PLoS Pathog.* **18,** 1–24 (2022).
13. Stakenborg, M. *et al.* Neutrophilic HGF-MET Signalling Exacerbates Intestinal Inflammation. *J. Crohn's Colitis* **14,** 1748–1758 (2020).
14. Nishikoba, N. *et al.* HGF-MET Signaling Shifts M1 Macrophages Toward an M2-Like Phenotype Through PI3K-Mediated Induction of Arginase-1 Expression. *Front. Immunol.* **11,** 1–10 (2020).
15. Enoch, D. A., Yang, H., Aliyu, S. H. & Micallef, C. The Changing Epidemiology of Invasive Fungal Infections. *Methods Mol. Biol.* **1508,** 17–65 (2017).